MASTER

Fluid mould

producing thermoplastic moulds for mass-production of non-repetitive double-curved concrete panels

van Rijbroek, E.J.; Verboord, M.H.W.

Award date:
2015

MASTER THESIS

Fluid Mould

Producing thermoplastic moulds for mass-production of non-repetitive double-curved concrete panels

Authors (student number):
E.J. van Rijbroek, BSc (0654140)
M.H.W. Verboord, BBE (0792817)

Mastertrack:
Building Technology

Department:
Department of the Built Environment
at the Eindhoven University of Technology

Graduation committee:
prof.dr.ing. P.M. Teuffel
ir. A.D.C. Pronk
ir. M.M.T. Dominicus

Date:
05-02-2015

Colophon

Authors	*1	E.J. (Erwin) van Rijbroek Department of the Built Environment at the Eindhoven University of Technology
	*2	M.H.W. (Martijn) Verboord Department of the Built Environment at the Eindhoven University of Technology
Graduation committee		prof.dr.ing. P.M. Teuffel ir. A.D.C. Pronk ir. M.M.T. Dominicus

Made possible by	3TU.Bouw Department of the Built Environment at the Eindhoven University of Technology Pieter van Musschenbroek Laboratory, TU/e Vertigo
Date	February, 2015

Preface

This Master Thesis is written by Erwin van Rijbroek and Martijn Verboord as part of the graduation project for the master track 'Building Technology'. This master track is part of the Master's degree program 'Architecture, Building and Planning' at the Department of Built Environment at the Eindhoven University of Technology. The thesis encompasses our work from the past year as part of the graduation project. We chose to cooperate on this project because both authors had similar interests in the subject of fluid surfaces and the scope of the project could be increased by working together.

Now we can look back at a very interesting, educative, intensive and enjoyable year and we are very pleased with the result of our project. This result could not have been achieved without the assistance of several people.

First of all, we would like to thank our graduation committee, prof.dr.ing. Patrick Teuffel, ir. Arno Pronk and ir. Maurice Dominicus for their coaching and assistance during the course of the project. We would like to thank ir. Arno Pronk in particular, who was intensively involved with this project.

We also would like to thank dr.ir. Lambert van Breemen for his advice in polymeric materials and his assistance with using the FEA software package MSC Marc Mentat. His expertise in simulating the behaviour of polymers was very valuable.

In the fall of 2014 a proposal about flexible moulds for the Lighthouse Project was awarded by the 3TU Federation. The Lighthouse Project is a collaborative research program from all three Universities of Technology in The Netherlands. Lighthouse Projects support innovative high risk projects related to the theme 'Energy Innovation and the Built Environment'. Awarded projects will receive funding in order to be able to build prototypes. We would like to thank 3TU.Bouw and the project team for their input and including us in the project. This has led to interesting insights and a budget to produce a prototype.

Furthermore, we would like to thank Dick Erinkveld from SolidRocks for his practical insights and helping us constructing the Fluid Mould.

Finally, we would like to thank the staff of the Pieter van Musschenbroek Laboratory, Bas van Wezel and Gerard van Rijbroek for their assistance during the executional phase of this project.

Summary

The design of complex geometries has become one of the most striking trends in contemporary architecture. Due to the developments in three-dimensional Computer Aided Design (CAD) software, nowadays all architects have the ability to design complex fluid architectural designs. However, fluid architectural designs are often condemned to only stay digital, because Computer Aided Manufacturing (CAM) did not make the same leap as CAD did. In order to produce large scale buildings with complex fluid geometries, one has to divide the shape of the building design in non-repetitive double-curved panels. Usually the fluid shaped panels are produced with the use of moulds. For complex fluid geometries each panel requires a non-repetitive double-curved mould. The cost of the mould fabrication often dominates the panel cost. To reduce the overall costs, there is a strong desire to reuse the same mould for the production of multiple panels. The most conventionally used moulding technique is the CNC foam milling technique, which very time consuming and leads to a lot of waste material. Therefore this production method is only interesting if repetition in elements is present. If not, this method is too expensive.

Recent developments in flexible moulding show possibilities to produce these panels with the use of selected technology at reasonable costs. However, the investment costs of such moulds are usually high and the production cycle tends to be very slow. Flexible moulds are identified as *"an adjustable formwork consisting of an elastic material that can be formed into the desired curved surface by the use of pistons, actuators, gravity, pin beds or other means".* The 'tensioned flexible layer' flexible moulding method uses a flexible layer that is tensioned and manipulated at its edges to the desired curvature. This is low-cost and low-tech method which is able to produce high quality surfaces.

In this report the 'Fluid Mould' prototype has been developed as a feasible manufacturing method for mass-production of non-repetitive double-curved concrete elements. The 'Fluid Mould' is a flexible mould which uses the tensioned flexible layer method for thermoforming thermoplastic sheets, which then are used as an intermediate thermoplastic mould. The thermoplastic sheet edges are clamped with the use of flexible edges attached to actuators. After heating the thermoplastic polymer above its glass transition temperature, the edge can be deformed by setting the actuators at proper height. The middle section of the sheet is supported by a flexible layer which can be manipulated by applying tension. With the use of an intermediate thermoplastic mould, the concrete casting and curing process is separated from the flexible mould. This leads to a significantly faster production cycle time. With the use of various pendulum rods as actuators, the flexible edges can be accurately set to the required fluid curvatures without an out-of-plane translation leading to high accuracy double-curved thermoplastic sheets.

The height settings for all actuators have been derived with the use of a developed 'Grasshopper' component for the software application 'Rhinoceros'. These settings were also used as input for finite element analysis software application 'MSC Marc Mentat', which has been used to predict the deformation of the silicone rubber flexible layer. Tests are done to deform polycarbonate (PC) and polyethylene terephthalate glycol (PETG) sheets in a large oven with the use of the Fluid Mould. Validations of the deformed thermoplastic sheets are performed with the use of the image-based modelling software application 'Autodesk 123D Catch' and the 3D point cloud processing software application 'CloudCompare'.

The Fluid Mould was able to produce thermoplastic moulds with an absolute deviation for each sheet varying from 11,7mm to 28,1mm. The maximum absolute deviation of 28,1mm occurred in the middle section of the most extremely curved sheet. This sheet has shown the limitations of the Fluid Mould in combination with the dimensions of the used oven. The minimum absolute deviation of 11,7mm occurred near the middle of a flexible edge of a less extremely curved sheet. The flexible edge is a very accurate component of the Fluid Mould and has been validated for the most extremely curved sheet with a maximum absolute deviation of 5,3mm. It can be concluded the composite flexible edge which consists of silicone rubber casted in spring steel mesh is a success factor of the Fluid Mould. Its stiffness and smoothness allows an accurate flexible edge setup. A significant factor of the deviations in the deformed thermoplastic sheets is presumably due to the rapid decrease in temperature when removing the Fluid Mould out of the oven. This had to be done prior to deforming the thermoplastic sheet. Because of this rapid decrease in temperature the viscoelastic material could become too rigid to be properly thermoformed and therefore returns slightly back to its original flat shape after forming. All deformed

thermoplastic sheets obtained fluid shapes. Little imprints at the location of the flexible edges were noticeable in various tests. However, the surface imprints were not always palpable.
A uniformly distributed load is required to provide counter pressure for the casted concrete. For this research fine granules have been used. With the use of thermoplastic moulds aesthetical qualitative non-repetitive double-curved panels can be produced.
It can be concluded that this research contributes to the research in flexible moulds, focussed on cost-effective production of double-curved non-repetitive concrete panels for fluid architectural designs. The Fluid Mould offers great opportunities for the future of fluid architecture because of the low-investment costs and the rapid production of intermediate thermoplastic moulds. The Fluid Mould prototype provides a solid base for many possibilities for further development.

Abbreviations and Symbols

Abbreviations

CAD	Computer aided design.
CAM	Computer aided manufacturing
CNC	Computer numerically controlled
FEA	Finite element analysis
NURBS	Non-uniform rational basis spline
PC	Polycarbonate
PETG	Polyethylene terephthalate glycol
PMMA	Polymethylmethacrylate

Symbols

T_g	Glass transition temperature
T_m	Melting temperature
MPa	Megapascal
psi	Pound-force per square inch
L	Ratio of the deformed gauge length
L_0	Initial gauge length
E	Engineering strain
I_j	Strain energy functions
W	Strain energy density
C_{10}	Experimental determined material constant
C_{01}	Experimental determined material constant
G	Shear modulus
λ	Stretch ratio
ε	Deformation
N	Newton

Table of Contents

1 Introduction

1.1 Background

1.1.1 Trends in architecture

The building industry has a long tradition of Euclidean geometry designs, due to the availability of two-dimensional drawing instruments (Kolarevic, 2004).The replacement of paper drawings by two-dimensional CAD programs has made drawing more efficient, easier to edit and simplified the process. At first, this shift from analogue to digital drawing was not reflected on the building design itself (Iwamoto, 2009), but now the building industry is undergoing a significant shift from the use of two-dimensional CAD programs for design towards semantically-rich three-dimensional CAD models (Steel, et al., 2010) (Becerik-Gerber & Rice, 2009). The development of NURBS modelling in particular allows architects nowadays to design complex three-dimensional geometries.

Due to these developments, complex geometries have become a vast research area in architecture (Brell-Çokcan & Braumann, 2011) and it has become one of the most striking trends in contemporary architecture (Pottmann, et al., 2008). Examples of complex designs which are already built can be seen in Figure 1.1 to Figure 1.4.

Figure 1.1: 'Philips Pavilion' at the World's Fair in Brussels by Le Corbusier and Iannis Xenakis (1958) (adapted from Hagens)

Figure 1.2: BMW pavilion 'The Bubble' in Frankfurt by Bernhard Franken (1999) (adapted from Franken\Architekten)

Figure 1.3: 'The New Zollhof' in Düsseldorf by Frank O. Gehry (1998) (adapted from Salamone)

Figure 1.4: 'Kunsthaus Graz' in Graz by Peter Cook and Colin Fournier (2003) (adapted from austria.info)

There are several terms used for this type of architecture which consists of complex geometries such as blobitecture/blobism, organic architecture/organo tech and free form architecture. These different terms are often described by comparable, but not uniform descriptions:

- Blobism/Blobitecture:
  - *"Late-C20–early-C21 fashion for anti-urban, anti-contextual buildings resembling large blobs with reptile-like carapaces"* (Curl, 2006).
- Organic Architecture/Organo-Tech:
  - *"Style of architecture involving free forms, blob-like shapes, and a highly complex (and expensive) structure. It came into vogue at the beginning of C21"* (Curl, 2006).
  - The conventional description of organic architecture is that it strives to integrate the building into the environment, so that it becomes a unified whole. Frank Lloyd Wright believed that every building should grow naturally from its own environment and was less concerned about the architectural style. (Craven, n.d.)
  - The modernist approach of organic architecture took the term to new heights. These buildings do not have linear or rigidly geometries, but instead they have fluid lines and curved shapes that suggest natural forms. (Craven, n.d.)
- Free Form Architecture:
  - A free form surface is used in modelling and other computer graphics software to describe the skin of a 3D geometric element. Free form surfaces do not have rigid radial dimensions, unlike regular surfaces such as planes, cylinders and conic surfaces. They are used to describe complex building forms (Milev & Gruendig, 2008).

The terms 'Blobism/Blobitecture', 'Organic Architecture/Organo-Tech' and 'Free Form Architecture' do not have a uniform definition. To avoid confusion in this report, the terms 'Fluid Architecture' and 'Fluid surfaces' will consistently be used.

1.1.2 Current situation in CAD and CAM

Due to the developments in three-dimensional CAD software, nowadays all architects have the ability to design complex fluid architectural designs. However, fluid architectural designs are often condemned to only stay digital, because Computer Aided Manufacturing (CAM) did not make the same leap as CAD did. This gap between CAD and CAM causes complexities for manufacturing fluid architectural designs and therefore fluid architectural designs are still rare (Brell-Çokcan & Braumann, 2011).

The developments in CAD and CAM technologies originate from the automotive/airplane industry and animation (Brell-Çokcan & Braumann, 2011) . CAD and CAM technologies developed in these industries have started to transfer to the building industry. New opportunities are created in the building industry by making the production and construction of very complex fluid forms possible. Traditionally, these complex fluid forms were very difficult and expensive to design, produce and assemble (Kolarevic, 2001).

Architect Frank O. Gehry was a pioneer in exploiting CAD and CAM technologies for tasks of the architectural industry. The original target industry differs in many ways from the architectural industry. For example the architectural application differs in aesthetics, statics, scale and manufacturing technologies, which make it a difficult task. (Pottmann, et al., 2008)

In order to produce large scale buildings with complex geometries, one has to divide the shape of the building design in smaller segments, so-called 'panels'. This so-called 'panelisation' is a very important issue (Spuybroek, 2004). Usually the curved panels are produced with the use of moulds. A mould is a form, both two-dimensional as three-dimensional, around or on which a material can achieve a specific form. A mould is usable for multiple cycles and is a counterpart of the cast (Vree, 2014). For complex geometries every panel requires a non-repetitive mould. These unique moulds can be made with the use of CAD and CAM techniques. The developments in CAD and CAM answer the visible trends in the market (Gelderman & Homan, 2009):

- There are becoming less skilled carpenters available for making complex moulds.
- Modern management asks for more efficiency and digital information offers the best guarantee.
- The consumer is aware of the state of the art of technique and wishes products according to that standard.

Example of a CAM development is the use of a Computer Numerically Controlled (CNC) foam milling technique, which allowed Frank O. Gehry to produce moulds for the double curved surfaces of the Zollhof Towers in Düsseldorf (Figure 1.3). The BMW pavilion in Munich (Figure 1.2), designed by Bernhard Franken and Kunsthaus Graz, designed by Cook and Fournier Figure 1.4 are made using the same method. The CNC foam milling technique is used for the fluid shaped façades of these buildings. After panelising the design, the dimensions of each panel is calculated. This data is then transferred to the milling machine which in turn mills an EPS or XPS foam block in the desired shape. The shaped foam could now be used as a mould for double-curved concrete panels (Figure 1.5).

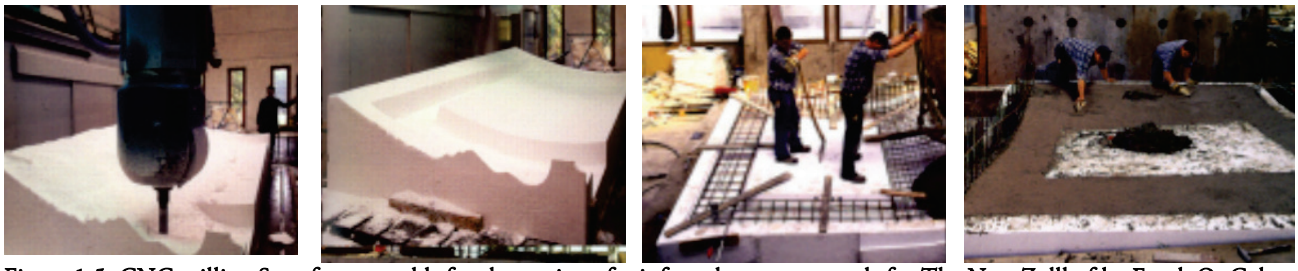

Figure 1.5: CNC milling Styrofoam moulds for the casting of reinforced concrete panels for The New Zollhof by Frank O. Gehry (adapted from Kolarevic)

Before the concrete is casted, the foam block can be finished with wax to close the pores. The use of this wax is expensive, but important to obtain a smooth surface. A disadvantage of applying wax is that the foam cannot be recycled, which leads to a lot of waste material. The density of foam is very low, so there is a risk that the foam will be pushed up in the mortar (Wapperom, 2004).
The use of this CNC foam milling technique is very time consuming and leads to a lot of waste material. Therefore this production method is only interesting if repetition in elements is present. If not, this method will be too expensive. Generally mass production of non-repetitive fluid concrete elements is not feasible with this method. A commercial accepted price range is €500 to €750 per square metre for the investment costs of a double-curved precast fibre-reinforced concrete cladding panel with a thickness of approximately 60mm and reasonable curvature. A foam milled mould cost approximately 60-75% of the mentioned price range (Schipper & Grünewald, 2014).

1.1.3 Recent developments in CAD and CAM

The cost of the mould fabrication often dominates the panel cost. To reduce the overall costs, there is a strong desire to reuse the same mould for the production of multiple panels. This makes complex fluid surfaces of large-scale fluid designs (such as the Philips Pavilion, BMW pavilion and Zollhof Towers) more feasible and affordable to produce. The alternative production of using custom moulds for each individual panel will be too expensive as result the design will never be built (Eigensatz, et al., 2010). Two recent developments in CAD and CAM show possibilities to make these panels by a selected technology at reasonable costs i.e. rationalization and the use of a flexible mould.

Rationalization

The fluid surface of the building can be approximated, within certain boundaries for the desired aesthetic quality of the panels and the smoothness of the surface. The panelising task is actually the rationalization of a building design and reduces the number of required moulds. There are two ways to rationalize the model.

The first method is to allow complex panelising software to deviate from the original surface to achieve a less expensive design, while maintaining the design intent within set divergence and kink angles of the panels. By deviating the original surface, less complex shaped moulds can be required, which reduces the total costs (Figure 1.6).

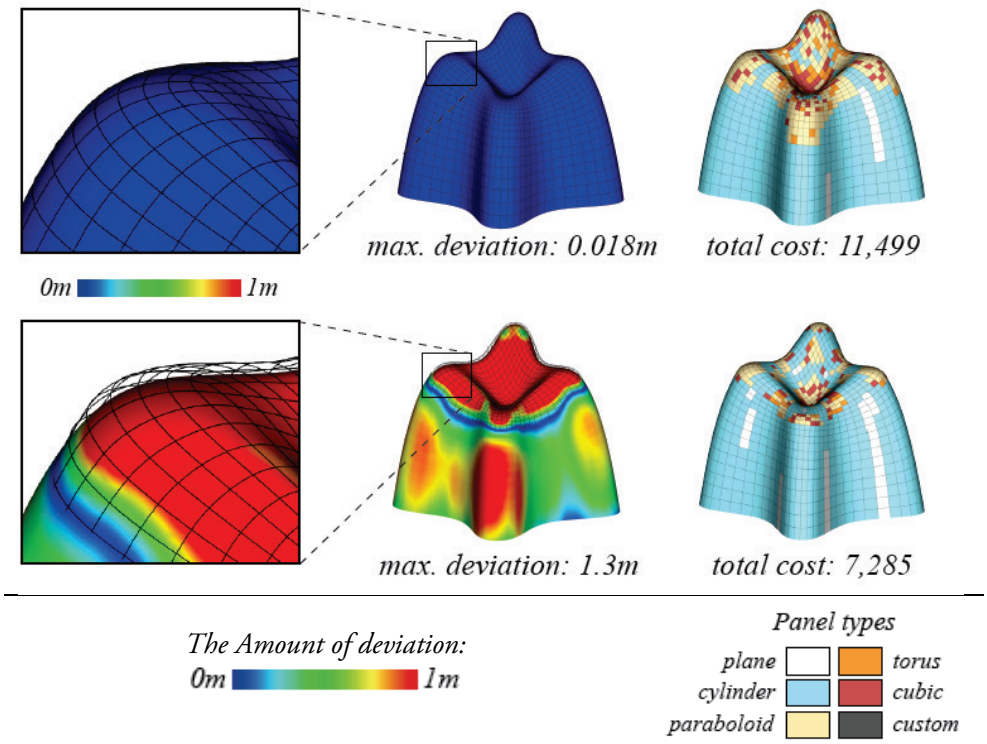

Figure 1.6: Rationalization of the model (adapted from (adapted from Eigensatz)

The second method is to control the tolerance in divergence and kink angles of the panels. The desired quality can be specified by setting thresholds for those two variables (Figure 1.7). By allowing higher kink angle and divergence tolerance less complex shaped moulds can be used which are easier and more affordable to produce.

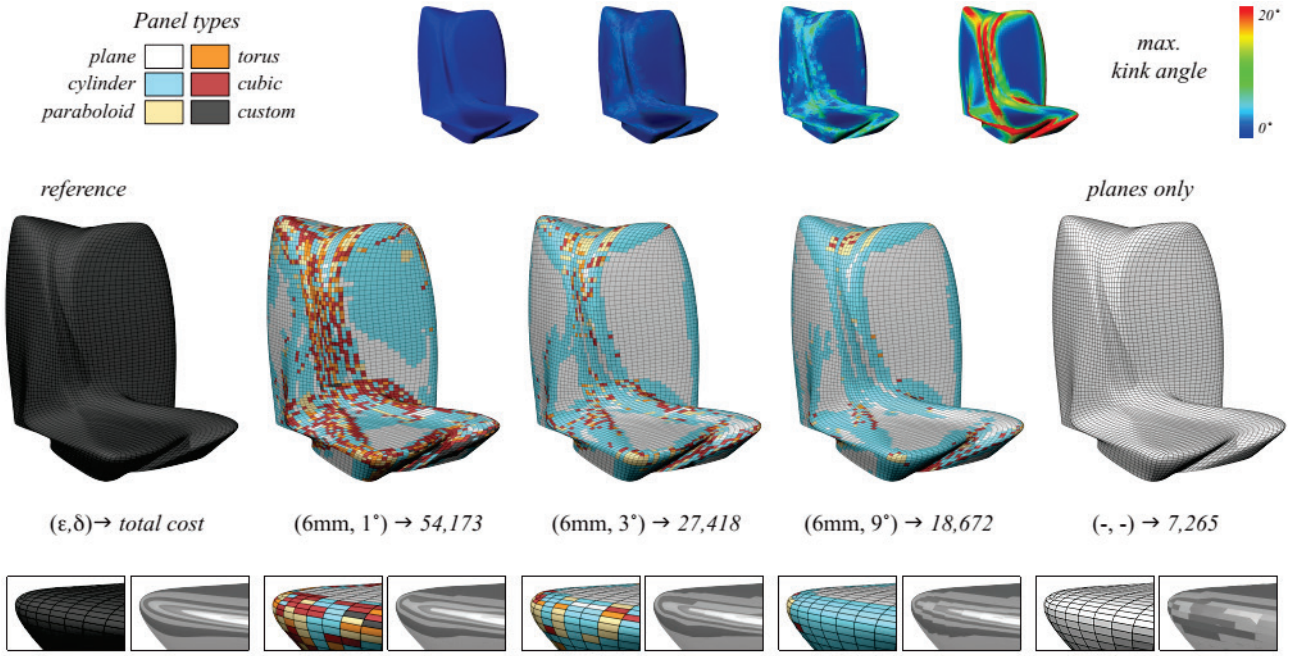

6mm, 1°						
molds	-	263	236	265	551	196
panels	1164	3680	603	526	1096	196

6mm, 3°						
molds	-	312	158	75	243	11
panels	2907	3389	395	142	421	11

6mm, 9°						
molds	-	354	95	18	104	3
panels	3178	3667	228	23	166	3

Figure 1.7: Rationalization of the model (adapted from (adapted from Eigensatz)

Even though this method can decrease the production costs significantly, it results in a less smooth transition between panels and the original design intend will never be achieved. Architects have to compromise to the building geometry and/or kink angle and divergence in order to stay within budget.
In order to achieve the original design intend, non-repetitive moulds are required which produce all individual double-curved panels. In this way, the desired geometry can be realised and smooth transitions between panels can be acquired.

Flexible Mould

Mass production of fluid concrete elements has often been regarded only possible after the realisation of a flexible mould (Schipper & Janssen, 2011). Flexible moulds are adjustable, which allows new shapes to be created with the use of the same mould. The flexibility of the moulding method is a critical success factor for making low-repetitive double-curved concrete elements (Heugten & Huijben, 2012). The flexible mould is defined as follows:

> *"An adjustable formwork consisting of an elastic material that can be formed into the desired curved surface by the use of pistons, actuators, gravity, pin beds or other means"* (Schipper & Janssen, 2011).

Examples of research in flexible moulds are:

1. 'FlexiMold' by Boers (2006)
2. 'Flexible Mold' by Rietbergen & Vollers (2007)
3. 'Zero Waste Free-Form Formwork' by Oesterle (2012)
4. 'Adaptive Mould' by Raun (2010)
5. 'Flexible Mold' by Schipper (2013)
6. 'E-mould' by Van Rooy and Schinkel (2009)

7. 'Flexible Mold' by Gard (2013)
8. 'Vacuumatics' by Huijben (2012)

These recent studies show great potential for flexible moulds. The flexible moulding method demonstrates to be a cost-effective way to produce non-repetitive fluid concrete elements. However, the investment costs of such a mould are usually high and the production cycle tends to be very slow.

1.2 Problem Statement

In order for architects to maintain the intended original design, non-repetitive moulds are required which can produce all the unique double-curved panels. In this way, the architect does not have to compromise on the building geometry and therefore the originally designed geometry can be achieved. The current production methods used to create the non-repetitive fluid building elements are relatively expensive. Every element requires a unique mould which can only be used once, e.g. the CNC milling technique. The cost of the mould fabrication often dominates the panel cost. Therefore, this method is very expensive and only possible for big budget projects. The flexible moulding method could provide a feasible solution to produce non-repetitive fluid concrete elements in a cost-effective way. Unfortunately, the investment costs of flexible moulds are usually high and the production cycle tends to be very slow.

The problem statement is formulated as follows:

> *There is no feasible manufacturing method available for the mass-production of non-repetitive double-curved concrete elements.*

1.3 Purpose

In this research the flexible moulding technique is explored and elaborated in order to contribute to the development of this moulding technique. The aim of this research is to contribute towards closing the gap between CAD and CAM. The purpose of this study is to develop a feasible manufacturing method for mass-production of unique double-curved concrete elements. In this way, this research contributes to the appliance of fluid geometries in lower budget projects without compromising on the design intend.

The focus will be on producing moulds for non-repetitive precast double-curved concrete cladding elements. Concrete has been identified as an ideal material for double-curved elements, because in fluid condition it can take any shape. It has been decided to produce cladding elements, because these elements are less heavy than load-bearing elements. Since the development of the flexible moulding method will be highly experimental it is wisely to start with producing lightweight elements so complexities due to high weight are excluded. Therefore, production of load-bearing elements is outwith the scope of this research.

Figure 1.8 shows the framework of this research.

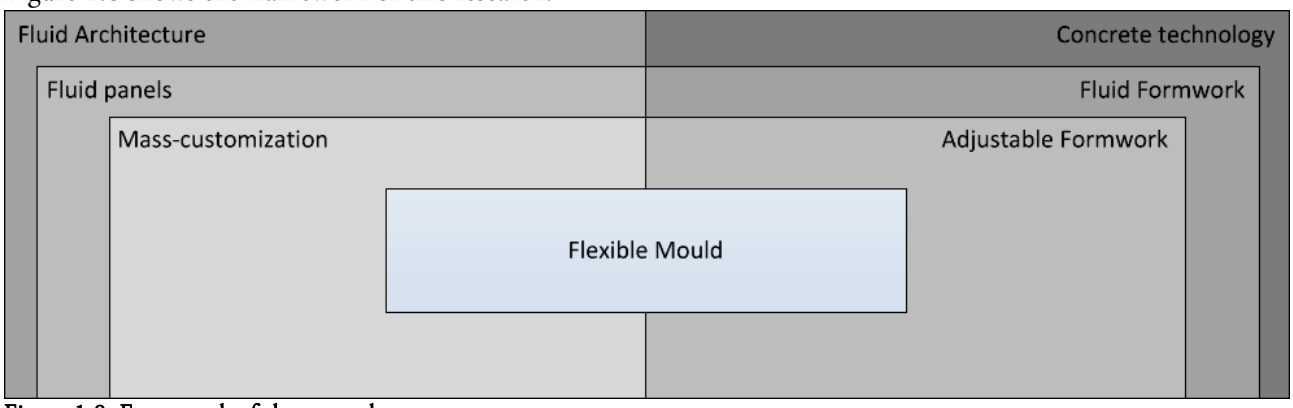

Figure 1.8: Framework of the research

1.4 Research Questions

The main research question is formulated as follows:

> *How can non-repetitive precast double-curved concrete elements be mass-produced with the use of a low-cost flexible mould?*

This main research question is divided in the following five sub-questions:

1. *What are suitable principles of current flexible moulding techniques?*
2. *How can the flexible layer be manipulated?*
3. *Which material is suitable for the flexible layer?*
4. *What are the properties of the flexible layer material?*
5. *How can the manufacturing process be simulated in order to accurately predict the mould geometry?*
6. *How can the mould manufacturing method be designed?*

These questions have led to the following objectives:

- Analyse flexible moulds
- Choose working principles
- Determine manipulation method
- Choose suitable flexible layer material
- Analyse properties of flexible layer material
- Develop manufacturing method
- Simulate manufacturing process
- Test manufacturing process
- Validate correlation between simulations and tests
- Develop flexible mould
- Produce fluid façade

To achieve these objectives, the systematic design process 'Engineering Design: A Systematic Approach' (Pahl & Beitz, 1999) is used. This design process is illustrated in Figure 1.9. The objectives can be found within the various steps of this systematic design process. Firstly, the working principles of flexible moulds will be analysed and working principles will be selected. After combining working principles, material for the flexible layer will be selected. The material properties will be elaborated and preliminary tests will be done during the specification of the product. The materials are evaluated and the most suitable material will be selected and applied in the concept. Following this step, the mould manufacturing method will be developed. Firstly, a preliminary layout will be developed, refined and evaluated. This iterative process will lead to the definitive layout, which then is finalized and all necessary documentation will be produced. Simulations and tests of the manufacturing process will be conducted and the correlation between the simulations and tests will be validated. Finally, the product will be built and tested for its end use, which is the production of fluid concrete panels.

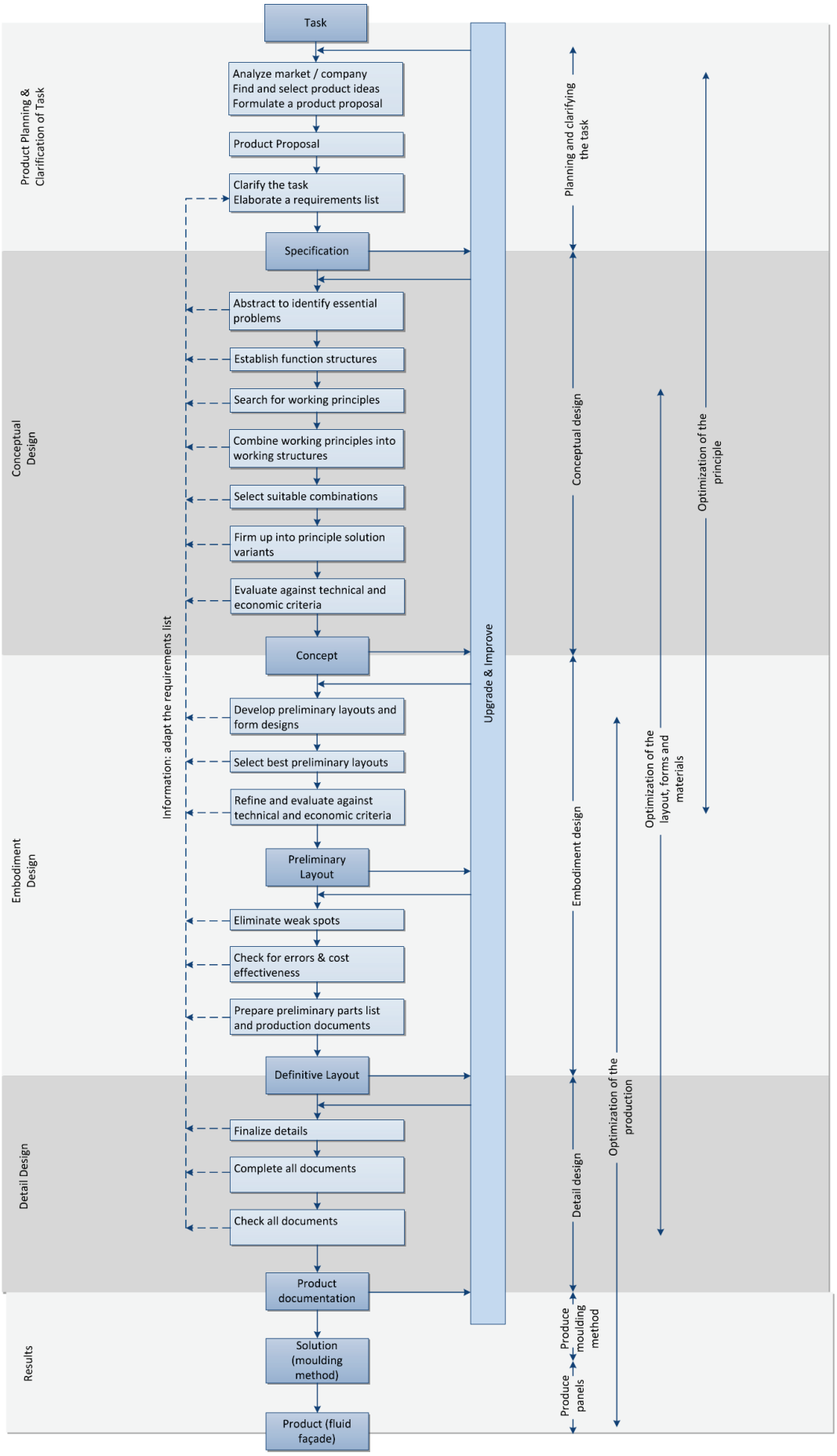

Figure 1.9: Systematic design approach (adapted and reproduced from Pahl)

2 Moulding Techniques

2.1 Current curved moulding techniques

Some large complicated objects cannot be casted at once and sections of the object will be created separately; this is called piece-moulding. In the building industry concrete walls, floors and roofs are components which are often produced by the principle of piece-moulding (e.g. prefabrication, pouring building components separately). The conventional built environment mainly consists of straight shapes and therefore the formworks contains also of straight panels. However, as discussed previously, the trends in architecture show more curved geometry designs which require curved moulds. Several techniques are available for the production of curved moulds:

1. CNC foam milling
2. Wire cutting
3. Timber moulds
4. Steel moulds
5. Vacuum, textile or air pressure forming
6. Rubber moulds
7. Thermoplastic moulds
8. Sand/clay moulds

CNC foam milling

The data of a fluid design CAD model are transferred to a computer numeric controlled (CNC) milling machine. This machine mills an EPS or XPS foam block in the desired shape (Figure 2.5). The top layer of the milled foam block is covered by a harder polymer (synthetic resin). After hardening, the top layer is polished to create a smooth surface. The shaped foam is now ready to be used as a mould for double-curved concrete panels. The foam moulds can be reused several times to reduce the costs. For production of only non-repetitive panels the cost of using this method will be relatively high. After the use of the shaped foam blocks, all blocks will be disposed.

Wire cutting

This method is almost similar to the CNC foam milling method, only a hot wire is used instead of a milling machine (Figure 2.1). However, this method is limited because of the use of a wire. Only surfaces can be produced described by a rotating and translating line, the so-called 'ruled surface' (Figure 2.2).

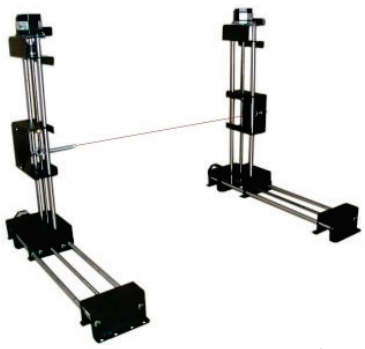

Figure 2.1: Foam wire cutter (adapted from Foamlinx)

Figure 2.2: Lathe work made by a wire cutter (adapted from Foamlinx)

Timber moulds

Projects consisting of repetition of relative complex shapes often use timber moulds (Figure 2.6). The timber mould can be made of plywood or fibreboard. For single curved elements, bending of a board is a relatively easy way to build a mould. It is possible to bend fibreboards into two directions, though only low curves can be achieved. This method is difficult to execute and expertise within this moulding is required. Curved forms can also be made by CNC milling and CNC cutting of timber and board. However, these methods are very expensive and therefore very unusual to see this implemented.

Steel moulds
Steel moulds are similar to timber moulds when it comes to geometrical capabilities (Figure 2.7).
Steel moulds mostly are used when a lot of repetition occurs in a project.

Inflatable, vacuumed foil and textile moulds
A special way to create curved concrete elements is by the use of inflatables, vacuumed foils or textiles (Figure 2.8). These techniques are applied only for specific projects e.g. an inflatable dome (Figure 2.9). The sewing and cutting processes are expensive and the influence of the weight of concrete on textiles is huge. This makes the variety of the geometrical possibilities limited. The thin foils of 'vacuumatics' are fragile, especially when steel rebar are used to increase the strength of the eventually casted structure.

Rubber moulds
The material rubber is flexible and thereby deformable (Figure 2.11). When a rubber is used as a mould, it needs a support material; otherwise the mould can be misshapen. The casting of concrete can be done before or after the rubber mould has obtained its desired shape by deforming the support construction. To avoid outflowing of the concrete, a counter-mould is needed. An alternative to prevent the need for a counter mould is through viscous casting (Figure 2.3) or delayed deforming (Figure 2.4). When using viscous casting, the concrete has already gained some viscous strength when it is casted on a curved mould. This prevents the concrete to flow over the edges of the curved mould. When using delayed deforming, the concrete is cast in a flat position. After a time interval the concrete has gained sufficient viscous strength and is deformed.

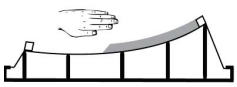

Figure 2.3: Viscous casting (adapted from Gard)

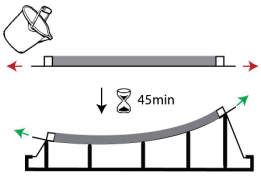

Figure 2.4: Delayed deforming (adapted from Gard)

Plastic moulds
By thermoforming, a thermoplastic sheet can be deformed to a double-curved shape when heated. After cooling down of the thermoplastic sheet, it becomes rigid. In using a foam or rubber strip, an edge support system can be made. The strip is able to absorb torsion. Another method is the use of a closed mould. Two plastic sheets will be clamped in a wooden frame (Figure 2.10).

Sand hill moulding
The Philips pavilion was made by a sand hill mould. Cement stabilized sand hills were shaped in the correct forms (Figure 2.12). The shaped form is subdivided into small elements. After pouring and hardening of the concrete, the elements are ready to be assembled. A concrete element had a thickness of only 50mm. The sand hill mould is a sustainable method because there is no loss of material. A disadvantage of this method is the labour intensity which makes it very expensive nowadays.

2.2 Moulding technique classifications

The previously discussed mould techniques to produce curved concrete surfaces are divided in three classifications according to Van Helvoirt (Helvoirt, 2005):

1. *Static moulds:*
   Statics moulds are permanent. These moulds cannot be reformed without disassembling the moulds. Once the mould is fabricated, it can be reused to multiply the intended product.
2. *Re-formable moulds:*
   The sand hill mould is an example of a re-formable moulding technique, which can be applied for different casted products. This technique is a sustainable method because there is no loss of mould material.

3. *Flexible moulds:*
   Flexible moulds are adjustable formworks consisting of an elastic material. New desired shapes can be created by the same mould by the use of pistons, actuators, gravity, pin beds or other means. The main advantage is the possibility to create fluid shapes with no waste of materials. Unfortunately, the invest cost are usually high.

Table 2.1 shows the classification of the moulding techniques.

Mould technique	Examples		
Static moulds	 Figure 2.5: CNC foam milling (adapted form Nedcam)	 Figure 2.6: Timber mould of a bicycle tunnel in Eindhoven (adapted from Van Hout)	 Figure 2.7: Curved steel formwork (adapted from Van Der Meijden)
	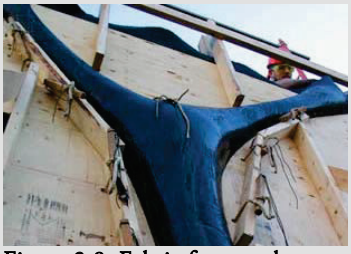 Figure 2.8: Fabric formwork (adapted from University of Manitoba)	 Figure 2.9: Inflatable formwork	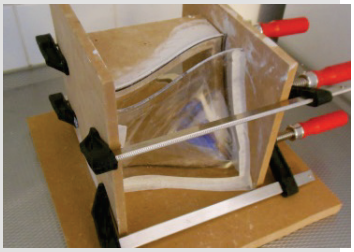 Figure 2.10: Closed plastic mould
Re-formable moulds	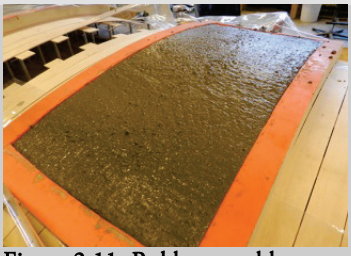 Figure 2.11: Rubber mould using the delayed deforming technique (adapted from Schipper)	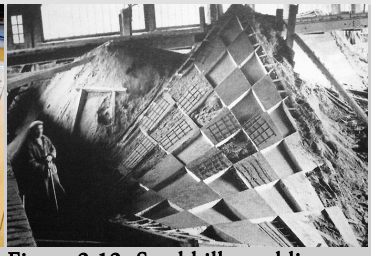 Figure 2.12: Sand hill moulding technique (adapted from arch.mcgill.ca)	
Flexible moulds	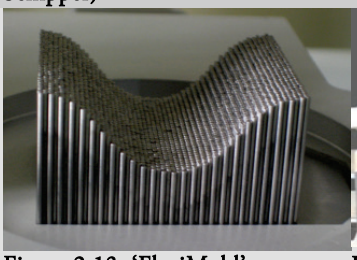 Figure 2.13: 'FlexiMold' (adapted from Boers)	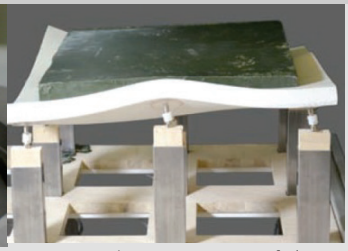 Figure 2.14: Wax on top of the flexible layer (adapted from Oesterle)	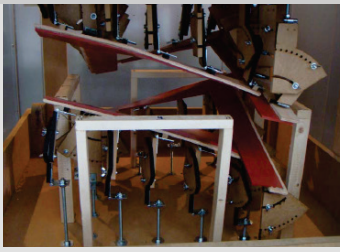 Figure 2.15: Flexible Mold by Gard (adapted from Gard)

Table 2.1: Moulding techniques

Which moulding technique is most suitable is not uniform for all projects. The selection of the mould technique depends on several aspects (Rooy, I. van; Schinkel, P.; Pronk, A., 2009):

- The dimensions of the product
- The quantity of the non-repetitive products
- The costs of the mould material
- The amount of waste
- Production cycle
- The accuracy

Current mould techniques are generally dependent on repetition in order to have a cost-effective production, except for the flexible moulds.

2.3 Flexible moulding techniques

Flexible moulds are adjustable and are thus able to create different shapes with the same mould. The flexibility of the moulding method is the critical success factor for making low-repetitive double-curved concrete elements on large scale (Heugten & Huijben, 2012). However, the investment costs are much higher than the static and re-formable mould techniques. To consider investing in a flexible moulding device depends on the repetitive building elements of a building. When it comes to low-repetitive elements of a building, the investment costs can be worth the effort and lead to lower production costs.

There have been several flexible moulds that have been developed. The eight following flexible moulds are explored and discussed:

1. 'FlexiMold' by Boers (2006)
2. 'Flexible Mold' by Rietbergen & Vollers (2007)
3. 'Zero Waste Free-Form Formwork' by Oesterle (2012)
4. 'Adaptive Mould' by Raun (2010)
5. 'Flexible Mold' by Schipper (2013)
6. 'E-mould' by Van Rooy and Schinkel (2009)
7. 'Flexible Mold' by Gard (2013)
8. 'Vacuumatics' by Huijben (2012)

'FlexiMold' by Boers (2006)

Based on the pin-art design toy, the 'FlexiMold' uses pins to create double-curved shapes (Figure 2.16). The main aim was to develop a reconfigurable mould to create double-curved metal sheets. The first prototype had a working space of 40x50x25mm. The shapes are derived form a CAD design. The use of a high density of pins provides a high resolution which makes the mould more accurate. After the first prototype, further prototypes are developed (Boers, 2009).

'Flexible Mold' by Rietbergen and Vollers (2007)

Rietbergen and Vollers developed a flexible mould consisting of a grid of actuators (Figure 2.17). The actuators are controlled in height by a computer. The mould is used for the production of double-curved glass panels. The flexible mould has been further developed by Huyghe and Schoofs (2009) for the production of concrete and plastic panels. The wooden flexible layer on top of the actuators is used as formwork for concrete panels. The casting takes place in the horizontal position so the thickness of the concrete panels can be controlled and no contra mould is needed. Downward pressure is required to assure that the (loosely resting) flexible layer touches the actuators (Grünewald, et al., n.d.)

'Zero Waste Free-Form Formwork' by Oesterle (2012)

The 'Zero Waste Free-Form Formwork' uses wax as a mould material (Figure 2.18). The defined schape is achieved by a flexible layer resting on controlable actuators. The setings of the actuarors are derived by a digital geometry model. The flexible layer is a sheet of a closed-cell plastic foam. Above the flexible layer a 2mm silicone

layer is applied. The silicone layer allows to easily remove the wax and it prevents traces. After producing the wax formworks through the flexible actuated mould, reinforcement is placed on the wax formwork. When the concrete is cured, the formwork can be removed. The wax elements will be recycled for the production of new moulds. Currently a curvature radius down to 0.6m can be realised for double curvatures (Oesterle, et al., 2012).

'Adaptive Mould' by Raun (2010)

The 'Adaptive Mould' is a flexible formwork system using a non-porous flexible layer which is manipulated by actuators controlled by a computer (Figure 2.19). The flexible layer is used as a mould for creating double-curved concrete panels. The flexible layer exists of a fibre-reinforced plastic laminates. To cast concrete the 'Adaptive Mould' will first positioned horizontal. After a certain curing period, the flat concrete panel can be formed into the desired shape (Raun, 2013).

'Flexible Mold' by Schipper (2013)

A flexble layer is supported by actuators that are placed in a grid. First the flexible layer is positioned horizontally when a rubber frame will be filled with self-compacting concrete (SCC). After a certain period, the yield strength of the concrete increases. The mould will be deformed to the desired shape, this is done by the 'flex-rod system' in combination with weights. The poured concrete follows the deformation and remains stable under a certain curvature (Figure 2.20). After a while the concrete panel can be demoulded. The flexible mould can be reused to create other panels (Schipper, et al., 2014)

'E-mould' by Van Rooy and Schinkel (2009)

The 'E-mould' contains a tensioned flexible layer (Figure 2.21). The flexible layer is manipulated with the use of manualy set actuators, an amount of tension and an inflatable. The actuators are only positioned at the edges and consist of a upper and lower part. The accuracy of the edges is important for the edge transitions of the panels. The surface of the section between the flexible edges is less accurate. The purpose of the E-mould is to produce polyester panels with a low-tech and affordable mould method (Rooy, I. van; Schinkel, P.; Pronk, A., 2009).

'Flexible Mold' by Gard (2013)

The 'Flexible Mold' by Gard (Figure 2.22) is based on the 'E-mould' by Van Rooy and Schinkel. A thermoplastic sheet is used as a flexible layer. Pre-tension is used to manipulate the flexibe layer. The thermoplastic will be heated in a oven and will be deformed by thermoforming. The deformed sheets are used as formwork for casting concrete. The processing time decreases significantly by not casting concrete on the flexible mould itself (Gard, 2013)

'Vacuumatics' by Huijben (2012)

A bag filled with granules is flexible untill the bag will be drawn vacuum, because then the granulates are not able to move along each other. This method achieves ridig forms through the use of vacuum drawing, is called 'Vacuumatics' (Figure 2.23). An arc-shape can easily be formed by hand. Eventually, when the desired shape is achieved, the bag can be rigidized by vacuum drawing. Other forms are more difficult and requires intense labour (Huijben, 2014).

2.4 Flexible moulding methods

The flexible moulds can be divided into four methods (Gard, 2013):

- Pin-bed surface:
  A high density pin-bed on which the desired material can be formed directly and indirectly. This method is suitable for highly shaped non-repetitive objects.
- Supported flexible layer:
  A flexible layer which is supported and adjusted by spaced actuators. The flexible layer has to be flexible enough to be able to deform and stiff enough to avoid sagging.
- Tensioned flexible layer:
  A tensioned flexible layer which is formed by the use of flexible edges. The flexible edges obtains curvatures through actuators. More forms can be obtained by the use of for example inflatables and vacuum techniques.
- Pressurized flexible layer:
  The mould consists of a bag filled with granules which can be formed freely with normal air pressure. Once the bag has been formed in the desired shape, vacuum will be drawn and the form becomes rigid.

In Table 2.2 illustrates an overview of examples of flexible mould methods divided into the four methods.

Flexible mould method	Examples	
Pin-bed surface	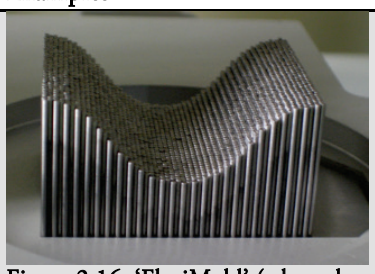 Figure 2.16: 'FlexiMold' (adapted from Boers)	
Supported flexible layer	 Figure 2.17: 'Flexible Mold' (adapted from Rietbergen & Vollers)	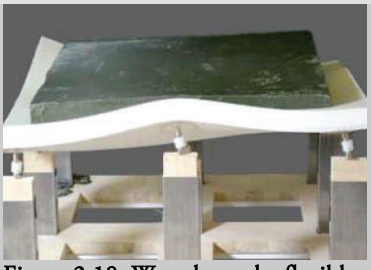 Figure 2.18: Wax above the flexible layer (adapted from Oesterle)
	 Figure 2.19: 'Adaptive Mould' in curved position (adapted from Raun)	 Figure 2.20: 'Flexible Mold' (adapted from Schipper)
Tensioned flexible layer	 Figure 2.21: The 'E-Mould' in flat position (adapted from Van Rooy & Schinkel)	 Figure 2.22: Flexible Mold by Gard (adapted from Gard)
Pressurized flexible layer	 Figure 2.23: Vacuumatic formwork (adapted from Huijben)	

Table 2.2: Flexible moulds

2.5 Tensioned flexible layer

Flexible moulds are not feasible for commercial use because of the relatively high costs (Munro & Walczyk, 2007). In order to produce a low-cost flexible mould method, a faster production cycle is an option. Another option is to make the flexible mould device low-tech. When considering these two aspects, the tensioned flexible layer method is the only method which is low-cost, low-tech and produces high quality surfaces (Gard, 2013). Only two tensioned flexible layer methods are known by the authors: the 'E-mould' by Van Rooy and Schinkel and 'Flexible Mold' by Gard. Therefore, the research of Gard (2013) and Van Rooy and Schinkel (2009) are taken as a starting point for further development.

Form variety

The research of Van Rooy and Schinkel and the research of Gard show that an edge-reconfigurable mould is a feasible and low-tech solution for non-repetitive elements. The use of a minimum of actuators has a great influence on the investment costs (Figure 2.24). However, by minimizing the amount of actuators less extreme curved and complex fluid forms can be produced. Nevertheless, mainly limited curvatures are used in architectural designs. The radius of existing double curved constructions varies between 0,75m and 45m (Schipper, 2015).

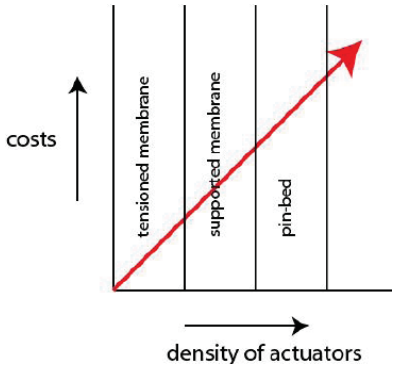

Figure 2.24: Relation between density actuators and costs (Adapted from Gard)

Not all surfaces can be made with the use of a tensioned flexible layer. Surfaces can be categorized with the use of the Gaussian curvature. The Gaussian curvature is explained with the use of Figure 2.25. As can be seen, a normal vector can be found on any given point on a surface. This vector has right angles to the surface. Planes which contain this normal vector are called normal planes. At the intersection of these normal planes with the surface curved can be drawn which are called normal sections. The curvature of these curves is called normal curvature. When using complex surfaces, different sections will have different curvatures. The minimum and maximum of these curvatures are called the principal curvatures (*k1, k2)*. The Gaussian curvature is the product of both principal curvatures (*K=k1 k2*).

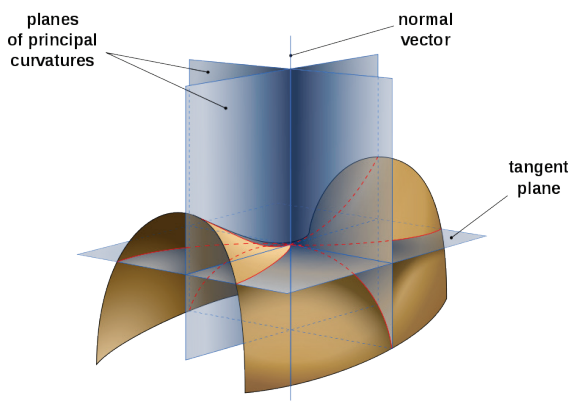

Figure 2.25: View of the planes establishing the main curvatures on a minimal surface (adapted from Gaba)

According to '85 Ways To Make A Membrane Mould' (Pronk & Dominicus, 2011), surface curvatures can be classified in four categories according to its Gaussian curvature i.e. zeroclastic, monoclastic, synclastic and anticlastic (Figure 2.26):

1. If the Gaussian curvature is zero (*k1k2=0*) and both principal curvatures are zero, the surface is said to be zeroclastic at that given point so the surface is flat.
2. If the Gaussian curvature is zero (*k1k2=0*) and only one principal curvature is equal to zero, the surface is said to be monoclastic at that given point. An example of such surface is a cylinder.
3. If the Gaussian curvature is positive (*k1k2>0*), both principal curvatures are the same sign. This means the surface will be synclastic or dome-shaped at that given point.
4. If the Gaussian curvature is negative (*k1k2<0*), the principal curvatures have different signs. This means the surface will be anticlastic or saddle-shaped at that given point.

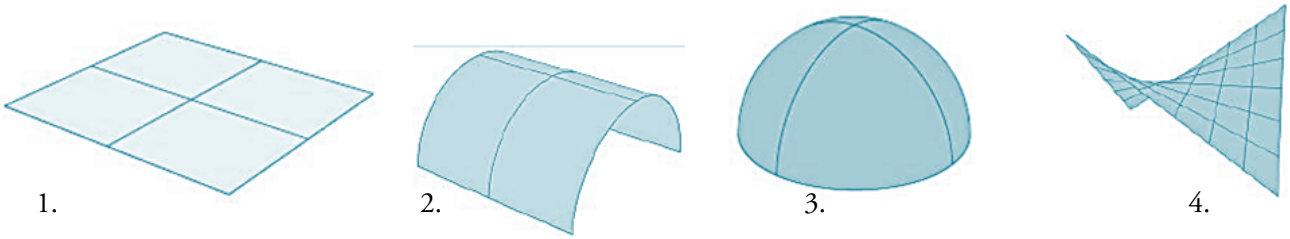

Figure 2.26: Shape classification according to its Gaussian curvature (Adapted from Pronk)

When using a tensioned flexible layer only zeroclastic and anticlastic surfaces can be made. The surface of the flexible layer is formed within a number of high-points, low-points and borders. The surface is not absolutely minimal (Pronk & Dominicus, 2011). The direction and amount of tension in the flexible layer determines its shape. The shape for the same edge settings can be manipulated by varying the direction and/or amount of tension to the flexible layer e.g. less tension leads to more sag. The 'E-mould' by Van Rooy and Schinkel and the 'Flexible Mold' by Gard demonstrates this manipulation method.
Further manipulation methods which can be applied can be found in (Pronk & Dominicus, 2011). The 'E-Mould' uses for example an inflatable to be pressed in the flexible layer in order to enlarge the range of shapes and curvatures.

Intermediate mould

Several flexible mould systems are plotted in Table 2.3 focused on the productivity. The productivity is determined by the configuration time and the production time of one non-repetitive product. The 'Adaptive Mould' uses stepper motors to set the actuators in just one minute. The other methods are taking more time for the configuration. The investment of the stepper motors is costly.

Most systems are able to produce a very small amount of products per day, except for the 'Flexible Mold' by Gard. With the use of an intermediate mould, the process of casting and curing of concrete is separated. As a result, the production cycle time will be significantly decreased (Figure 2.27). The flexible mould method by Gard uses a thermoforming process to produce thermoplastic intermediate moulds. This thermoforming process is applied for the 'tensioned flexible layer'.
The thermoforming procedure is based on the forming of semi-finished polymer products under the influence of heat. This procedure can be devided in following steps: heating, forming and cooling of the thermoplastic material. Thermoforming is a fast production method which is for example used for the production of packagings, drink cups, bathtubs and skylights. Thermoforming represents a group of sheet-forming processes that includes vacuum forming, drape forming, billow of free bubble forming, mechanical bending, matched mold forming, billet molding, pressure forming and twin-sheet forming (Kutz, 2011).
Gards method shows simularities with the free bubble forming thermoforming technique. In both methods a thermoplastic sheet is clamped at the edges and the middle section is free formed. Conventional free forming techniques only forms synclastic shapes with the use of air pressure, while the edges are clamped in a planar

frame. Gard deforms the clamped edges with the use of flexible edges and actuators. Tension is used to manipulate the middle section. This method allows the production of anticlastic shapes. Gard used the thermoplastic sheet itself as a flexible layer, but it is also possible to be place the thermoplastic on a supporting flexible layer.

If other mould methods would use similar intermediate thermoplastic moulds (assuming those methods are able to deform thermoplastics by thermoforming), the productivity of those methods would increase significantly (Table 2.3). It has to be noted that when using an intermediate mould, the total production time also depends on the time which is required to fixate the thermoplastic sheets into a proper formwork and to cast the concrete panels. There has to be found a proper method for doing so. Preliminary experiments have shown an example of how this can be done (Figure 2.10).

	'FlexiMold' by Boers	'Flexible Mold' by Rietbergen & Vollers	'Zero Waste Free-Form Formwork' by Oesterle	'Adaptive Mould' by Raun	'Flexible Mold' by Schipper	'E-mould' by Van Rooy and Schinkel	'Flexible Mold' by Gard
Configuration time [min]	60	15	15	1	15	10	10
Productivity [unique products/day/mould] when using the original mould systems	1	1	3[1]	1	1	1	19[1]
Productivity [unique couples[2] of intermediate thermoplastic sheets/day/mould][3]	4	8	8	11	8	9	9

1) Unique product is in this case one intermediate mould
2) Two thermoplastic sheets are needed for a closed mould
3) Production cycle of producing two intermediate thermoplastic sheets = Configuration time + thermoforming process (2x20 min)

Table 2.3: Comparison productivity of various mould methods (data adapted from Gard)

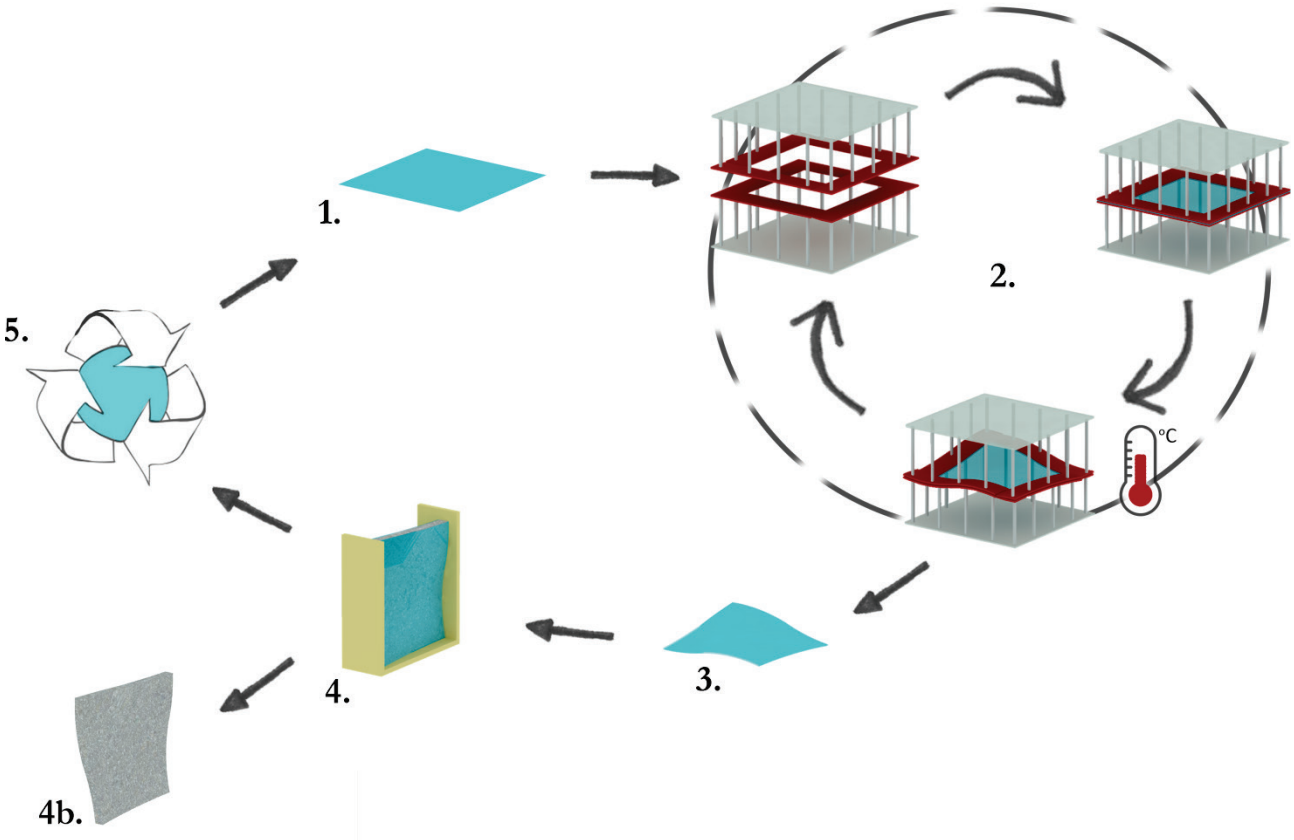

Figure 2.27: Production process of producing double curved concrete panels with the use of intermediate thermoplastic moulds.

2.6 Conclusions

The tensioned flexible layer in combination with an intermediate thermoplastic mould shows great potential for rapid production of double curved concrete panels. The use of stepper motors will lead to a relative high productivity, but the investment cost of such system is high.

Gard was able to apply the thermoforming process to the tensioned flexible layer method, however several issues remained unsolved. The 'Flexible Mold' can be optimized in several aspects to produce more accurate intermediate moulds. The 'Flexible Mold' is for example constructed with wood, which was decided because of the highly experimental approach of that research. However, this has led to high inaccuracies and a difficult production process. Settings have to be manually adjusted, which if far from ideal when using an oven. Also more testing is needed.

To predict the flexible layer deformation and prevent undesirable outcomes, the production process should be simulated. There should also be found a feasible method to validate the geometry of the formed thermoplastic sheets. In order to do so, first a better understanding of the material is required. In the next chapter polymer properties will be elaborated.

3 Materialisation

3.1 Polymers

3.1.1 Main characteristics

The mould material should be low-cost, recyclable and have a high surface quality and fast production cycle. These requirements could be excellently fulfilled in the material group 'polymers'. Polymers consist of many repeating 'monomers', which can be translated to 'one unit'. The name 'polymer' can be translated to 'many units', which refers to the structure of these polymeric materials (Figure 3.1). At structural level two main categories can be distinguished; long (single) chains of repeating molecules, called macromolecules, and large networks of repeating molecules. Usually, the chain or network has a carbon backbone with hydrogen and other elements arranged around it. Covalent bonds act between the molecules of the chains or networks and secondary bonds act between the chains and within the networks (Kaufmyn, n.d.).
A representable scale model for a polymer chain is a human hair of one metre in length. Normally these long and thin chains do not occur in fully stretched form, but in tangles. These tangles determine mainly the specific behaviour of polymers (Vegt, 1999). Polymers can be amorphous or semi-crystalline (Figure 3.2). The amount of crystallinity affects the polymer properties.

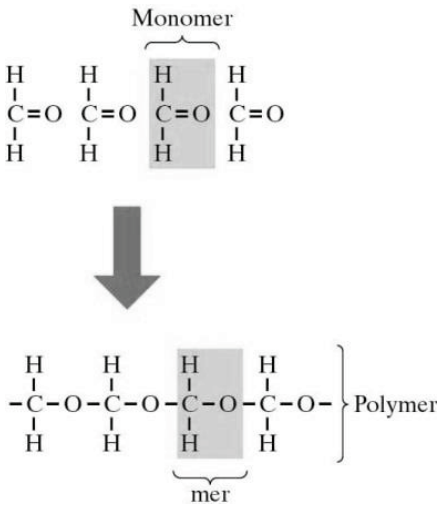

Figure 3.1: Monomer and Polymer (adapted from Kaufmyn)

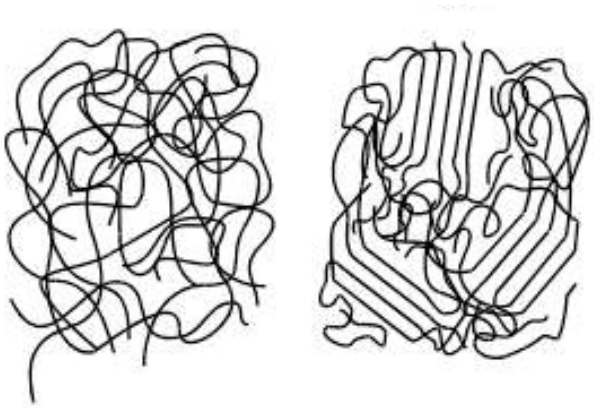

Figure 3.2: Amorphous and semi-crystalline polymer (adapted from Kaufmyn))

3.1.2 Main Classifications of polymeric materials

Polymers can be subdivided in three main classifications; thermoplastic polymers, thermosetting polymers and elastomers. Each classification has its own specific properties and therefore will be briefly discussed.

Thermoplastic polymers

Thermoplastic polymers soften and even liquefy when heated and in contrast when they are cooled, these polymers harden. This is a reversible process which means these materials can be reheated and reformed. Therefore thermoplastic polymers are recyclable. Thermoplastic materials can usually easily be fabricated by heat and pressure.

Thermosetting polymers

Thermosetting polymers become permanently bonded or 'set' by chemical reactions. These reactions either take place when heated or with the use of a catalyst. Thermosetting polymers become more rigid when heated, but they do not soften when they are cooled, which means the process is irreversible and these materials are not recyclable. Thermosetting polymers do not liquefy at higher temperatures, instead they carbonise. Thermosetting polymers are not easily processed.

Elastomers
Elastomers can be elastically deformed for very large percentage, from 200% up to 1000%. These materials could be thermoplastic elastomers or thermosetting elastomers (Kaufmyn, n.d.).

Thermosetting polymers are because of the irreversible process not suitable to be processed with the use of a flexible mould and therefore will not further be discussed.
Thermoplastic polymers are suitable as a mould material. This material can be used in current flexible mould methods when temperatures are elevated. When the temperature is raised, the Young's modulus drops, which means that the material can be deformed. After cooling down, the material becomes rigid and can be used as a mould. Thermoplastic polymers are very easily processed and multiple cycles of heating and cooling down can be repeated without severe damage. This allows reprocessing and recycling (Biron, 2013). It is possible to deform the thermoplastic sheet without using a secondary supporting material, as is done in preliminary experiments (chapter 3.2.3). However, this is a very delicate process. In chapter 3.2 the properties of thermoplastic polymers will be elaborated in order to research the possibilities of this material to be used as a mould and flexible layer.
Elastomeric polymers have excellent properties to be used as a flexible layer. Elastomers can be deformed for a very large percentage and a stable equilibrium occurs after applying tension in the flexible layer. It is possible to use an elastomer as a secondary supporting layer on which a thermoplastic polymer can be thermoformed and then be used as a mould. The properties of elastomeric polymers will be elaborated in Chapter 3.3.

3.2 Thermoplastic polymers

3.2.1 Thermoplastic properties

The thermoplastic properties are elaborated to provide a profound basis to select the most suitable thermoplastic material. Knowledge of these properties is important to accomplish a proper deformation with high surface quality with the use of a fast production cycle. Thermoplastic polymer properties are very dependent of several variables, which will be discussed in this section.

Strain-stress curve
In
Figure 3.3 a typical strain-stress curve of a thermoplastic polymer can be seen. However, this curve will change when other variables are used.

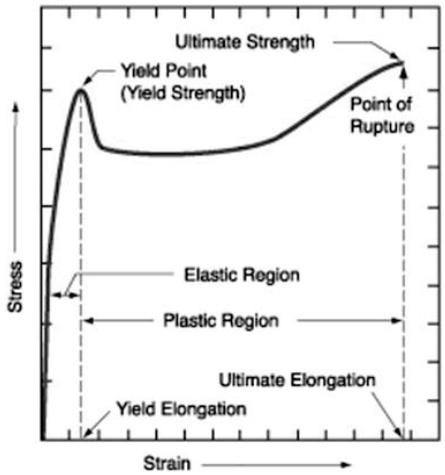

Figure 3.3: Characteristic strain-stress curve for a thermoplastic polymer (adapted from Kazuli)

In the elastic region Hooke's law is obeyed i.e. the stress is proportional to strain. This gradient provides the material's Young's modulus and in this region elastic deformation occurs. Elastic deformations in thermoplastics come from chains uncoiling and stretching. This is reversible, so when forces are removed, the chains revert to their original conformations. On the atomic level the primary bonds are being stretched but not broken

(Kaufmyn, n.d.). The yield point is the point in the strain-stress curve at which the curve levels off and plastic deformation begins to occur. At the yield point a local decrease in cross-sectional area, called 'necking', occurs (University of Cambridge, 2008). Plastic deformations occur because of the chains moving past each other and on the atomic level the secondary bonds are being broken and reformed (Kaufmyn, n.d.). After the yield point the true stress decreases with increasing deformation, which is called 'strain softening'.

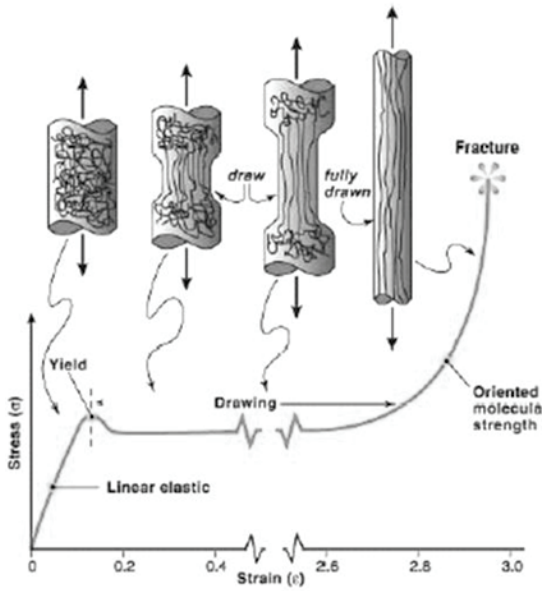

Figure 3.4: Characteristic strain-stress curve for an amorphous polymer (adapted from Kazuli)

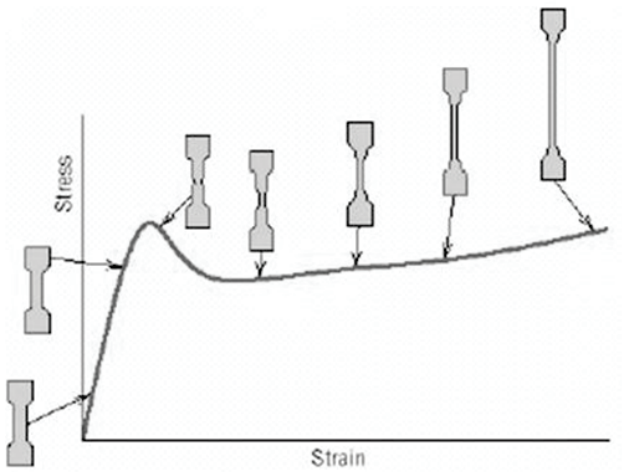

Figure 3.5: Characteristic strain-stress curve for a semi-crystalline polymer (adapted from Schultz)

An amorphous polymeric tensile specimen develops a neck, like metals do, but the necking extends to the entire length of the specimen. This phenomenon is called 'drawing'. In the neck region molecular chains are oriented in the direction of stress, which means that the material has become stronger in that direction and properties of the material become highly anisotropic (Figure 3.4). This phenomenon is called 'strain hardening'. The Young's modulus in the neck of the tensile specimen in the direction of drawing can increase by three times to the original value and the resulting tensile strength in the direction of drawing can be two to five times the original tensile strength. However, at 45° to drawing the Young's modulus can decrease to one fifth of the original value. In the direction perpendicular to drawing the tensile strength can be reduced by one third or a half. If drawing is done to an amorphous polymer, the temperature must quickly be brought to ambient temperature; otherwise the effects will be lost. (Kaufmyn, n.d.). Finally, with enough stress, the primary covalent bonds within the chains are broken. In Figure 3.5 the characteristic strain-stress curve for a semi-crystalline polymer can be seen. It is different from an amorphous strain-stress curve in that it lacks the drawing region (Kazuli, 2003). The strain occurs in the necking area and does not extend to the entire length of the specimen.
The intrinsic deformation behaviour strongly depends on the strain rate and the temperature. An increased strain rate leads to a higher yield stress, whilst an increased temperature has the opposite effect. Strain softening and hardening are less influenced by these variables, but in general can be said that both strain softening and hardening increases with increasing strain rate and/or decreasing temperature (Vegt & Govaert, 2003), as can be seen in Figure 3.6.

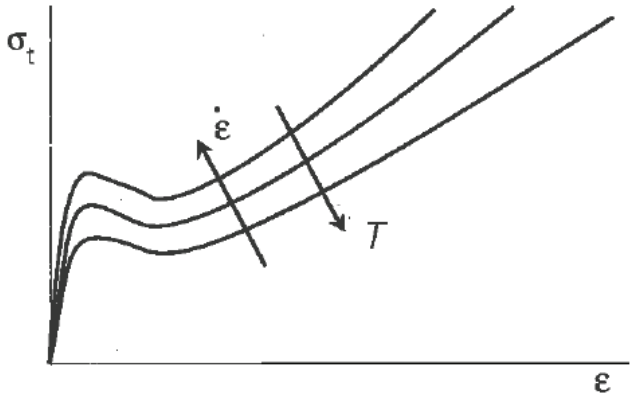

Figure 3.6: Effect strain rate and temperature (adapted from Vegt)

Glass transition temperature (T_g)

The glass transition temperature (T_g) of thermoplastic polymers is the point at which a reversible transition from a hard brittle condition to a viscoelastic or rubber-elastic condition occurs. Below its T_g the Young's modulus is relatively constant with a value close to 2.8 GPa. If temperatures above T_g are reached and the polymer becomes rubbery, the modulus drops about three orders of magnitude to 2.8 MPa. If the molecular weight of the polymer is high, the polymer becomes a viscoelastic fluid at about 100°C above its glass transition temperature. At this temperature the polymer can be processed as a melt, as can be seen in Figure 3.7 (Muzzy, n.d.).
For the application of a thermoplastic for a flexible mould a T_g is preferred within the range of 70 to 150 degrees Celsius. The minimum is set to 70 degrees Celsius in order for the mould user temperature not to exceed T_g. The maximum is set to 150 degrees Celsius to allow for conventional ovens to be used in tests.

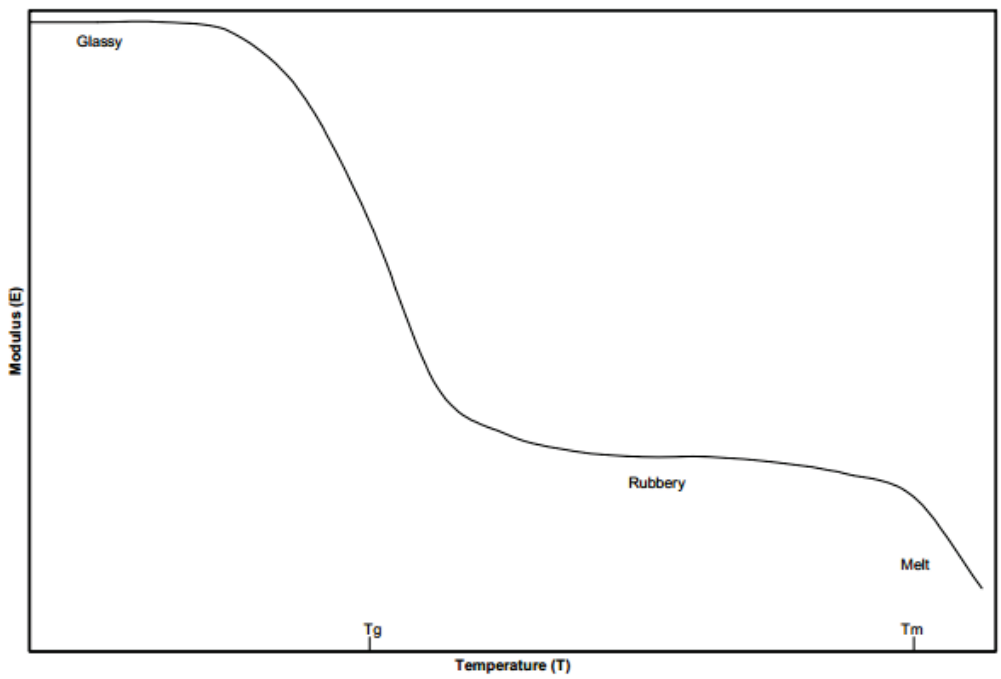

Figure 3.7: Rubber-plateau (adapted from Muzzy)

Melting temperature (T_m)

The melting temperature of a solid is the temperature at which it changes state from solid to liquid at atmospheric pressure. Amorphous thermoplastics do not have a sharp melt point; instead amorphous thermoplastics soften gradually as the temperature rises (RTP Company, n.d.). Below its T_g a semi-crystalline thermoplastic polymer has a similar Young's modulus to an amorphous thermoplastic polymer. However, above T_g a crystalline thermoplastic polymer has an intermediate Young's modulus which depends on its degree of crystallinity. This crystallinity disappears during melting, which leads to a rapid drop in Young's modulus and at

this point the polymer becomes a viscoelastic fluid (Figure 3.8). Semi-crystalline thermoplastic polymers therefore do have an exact melting temperature.

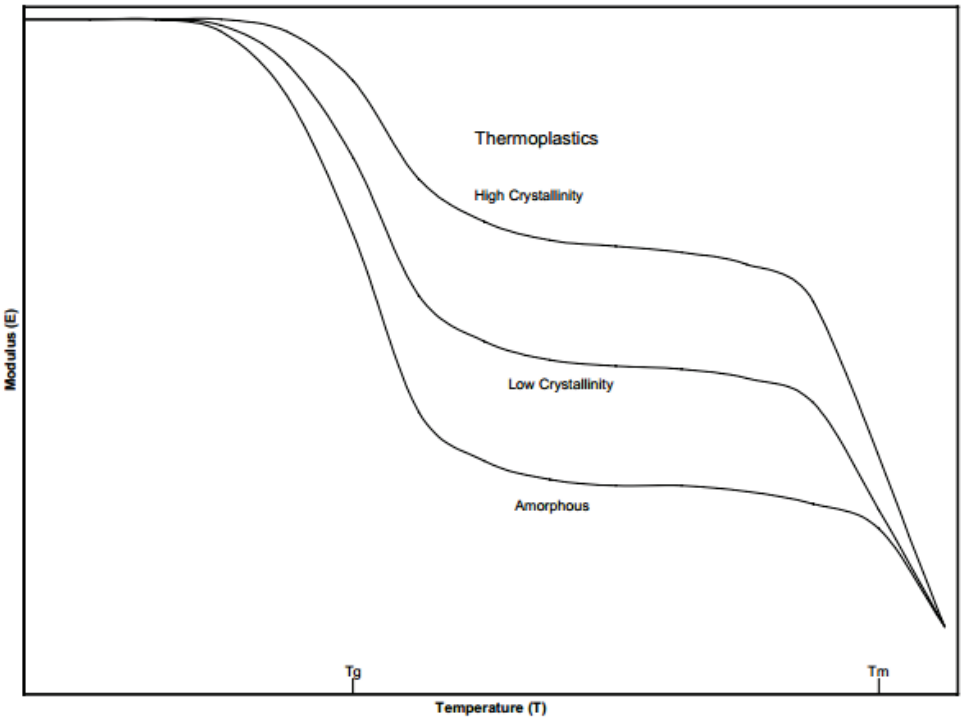

Figure 3.8: Rubber-plateau at different degrees of crystallinity (adapted from Muzzy)

A semi-crystalline thermoplastic polymer with high crystallinity is not desired to be applied for the flexible mould concept, because the rubbery state is masked by the crystallinity (Vegt & Govaert, 2003). This leads to a very small temperature region in which these polymers can be processed. However, low-crystalline thermoplastic polymers with a large region between T_g and T_m should be considered. For these materials the secondary crystallisation occurs slowly just above its glass transition temperature and thereby the crystallinity only has a marginal effect.
A flat rubber-plateau leads to a more uniform deformation, because the Young's modulus only changes marginal if temperature variations occur. Therefore a flat rubber-plateau is an additional requirement for the application in a flexible mould.

Viscoelastic behaviour

Polymers respond very different to applied loads than metals. This makes direct comparisons of strength and stiffness of limited use. Standard formulae rely on the elastic modulus as a fundamental measure of the response of the material to stress, assuming the material behaves in a linear, elastic manner until yielding. Whilst this is true for most metals, for polymers the strain-stress curve is rarely linear, there is no true proportional limit and the behaviour is significantly affected by strain rate and temperature (Way & Regis, 2001).
Polymers exhibit both an elastic component and a viscous component. They are viscoelastic and the behaviour is called viscoelasticity (Fimmtech inc., 2007). Viscosity is an indicator of a fluid's resistance to flow and describes the internal friction of a moving fluid. A highly viscous fluid provides more resistance to flow because its molecular makeup gives it a lot of internal friction (Princeton University, n.d.). The viscoelastic behaviour can be described with the use of basic mechanical models, characterized by a number of parameters. In order to gain a better understanding of linear viscoelastic behaviour, the basic behaviour of these mechanical models constructed from linear springs and dashpots should be observed. (Vegt, 1999).

The spring element can be seen in Figure 3.9. When a constant force is applied instantaneous deformation occurs. When the force is removed, the material instantly and entirely springs back in its original shape.

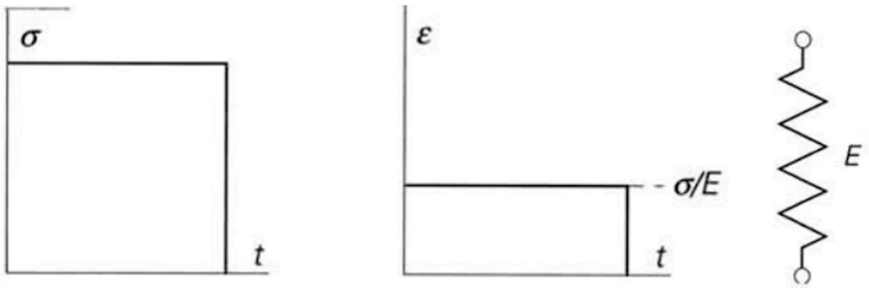

Figure 3.9: Response of an ideal spring (adapted from Vegt)

The dashpot element can be seen in Figure 3.10. For a Newtonian fluid the viscous stresses arising from its flow are linear proportional to the local strain rate. There is no instantaneous response, the deformation is linear proportional in time and there is no shape recovery.

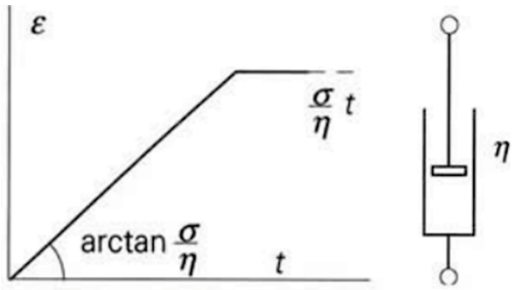

Figure 3.10: Response of an ideal liquid (adapted from Vegt)

The Maxwell model consists of a spring and a dashpot element in series (Figure 3.11). The Maxwell model can be used to very roughly describe the deformation behaviour of liquid viscoelastic polymers. The permanent flow predominates in the long term, while in the short term the response is elastic. In Figure 3.11 can be seen that stress relaxation and irreversible flow occurs.

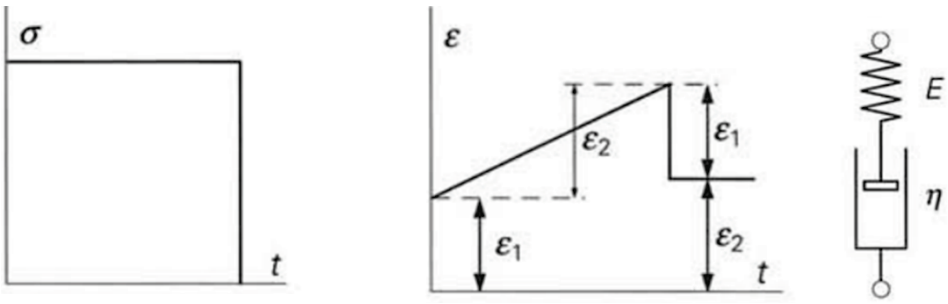

Figure 3.11: Response of a Maxwell element (adapted from Vegt)

The Maxwell element does not provide a realistic representation of the actual viscoelastic behaviour. For a more realistic viscoelastic rheological model a generalized Maxwell model can be used. This model shows a dashpot and spring component in series and a spring component in parallel (Figure 3.12). Figure 3.12 shows the strain stress curve for this generalized Maxwell model. It illustrates the strain stress curve consists of an elastic element and a viscous element. This viscous element ensures the material behaviour is time dependant. It has to be noted the reality is better approximated with the use of a more complex generalized Maxwell model, with a higher number of Maxwell components in parallel. Each component has its own relaxation time, τ_i and its own contribution to the material stiffness E_i. In general, the more elements the generalized Maxwell model has, the more accurate a model will be in describing the response of real materials. The more complex the model, the more material parameters there are which need to be evaluated by experiment. The determination of a large number of material parameters might be a difficult task. (Kelly, 2013)

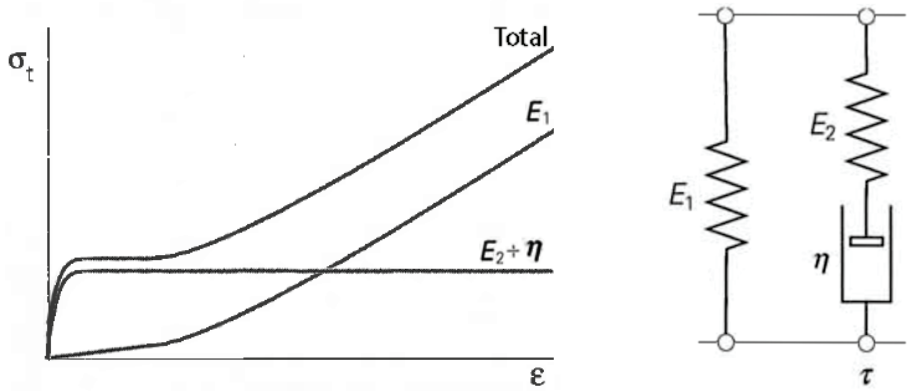

Figure 3.12: Strain stress curve for a generalized Maxwell element

In the next paragraphs suitable thermoplastic materials will be elaborated and tested. The thermoplastic deformation behaviour will be predicted with the use of simulation software. For these simulations a suitable mechanical model will be selected.

3.2.2 Material Selection

In previous paragraphs polymer properties were discussed. This has led to the following list of requirements and wishes for the properties and characteristics of the polymeric material:

- An amorphous or low-crystalline thermoplastic polymer
- A flat rubber plateau
- Glass transition temperature between 70-150 degrees Celsius

In the paper 'Thermoplastics Properties' (Muzzy, n.d.) a selection of forty thermoplastic polymers with their properties were presented. Based on the requirements above, from the forty materials three suitable thermoplastic polymers are shortlisted i.e. polyethylene terephthalate glycol (PETG), polymethylmethacrylate (PMMA) and polycarbonate (PC). In Table 3.1 material properties of these materials are compared in order to select the most suitable material for a flexible mould.

	Polyethylene Terephthalate Glycol (PETG)	Polymethylmethacrylate (PMMA)	Polycarbonate (PC)
Glass transition temperature [°C]	80	100	150
Density ISO 1183 [g/cm^3]	1,27	1,2	1,2
Flexural modulus [psi]	310000	480000	345000
Tensile strength at yield ISO 527 [MPa]	53	42	60
Tensile strength at break ISO 527 [MPa]	26	83	72
Elongation at break ISO 527 [%]	>200	5	150
Tensile modulus of elasticity ISO 527 [MPa]	2200	3200	2300
Flexural strength ISO 178 [Mpa]	79	120	97
Charpy notched impact strength (23°C) ISO 179 [kJ/m^2]	10	-	55
Charpy unnotched ISO 179 [kJ/m^2]	No break	20	-
Coefficient of linear thermal expansion [x10^5/°C]	6,8	7	6,8
Drying time [hours]	0	2-4	3-4

Table 3.1: Material properties of PETG, PMMA and PC (data adapted from Eriks)

Although PETG is a semi-crystalline thermoplastic polymer, it has been selected as a suitable mould material. It is very low-crystalline and has a large region between its glass transition temperature and its melting temperature. In this region the material can be processed for this concept. The thermoplastic polymers are not far heated above the glass transition temperature; therefore the effect of the crystallinity will be barely noticeable. PETG has the lowest glass transition temperature of all three materials, which means that a lower thermoforming temperature can be used. This will have a positive effect on the thermal expansion of the mould device and therefore lead to higher accuracies of the mould settings. It is also safer to work with lower temperatures and it requires a less powerful oven.
As can be seen in Table 3.1, PETG has the lowest flexural modulus, which means that this material will bend most when pouring the concrete in the formwork. PMMA has the highest flexural modulus. PC has the highest impact strength, followed by PETG. PMMA has a very low impact strength, which makes modifying this material by drilling or sawing very risky.
Some thermoplastic polymers are hygroscopic and require a drying period. If drying is not applied, gas bubbles occur during heating which lead to undesired bumps in the material's surface. PETG does not require a drying period, while this is the case for PMMA and PC. The drying period depends on the material thickness, temperature and air pressure.
Modifications of the thermoplastic sheets will be necessary to produce a proper formwork. PMMA is a less suitable material to modify and is therefore not used for the flexible mould. When comparing the glass transition temperatures and drying time, PETG seems to be the most suitable material. However, PC is an amorphous thermoplastic polymer which means it can be tested within a larger temperature region. Both materials have both advantages and disadvantages and therefore both materials will be tested to determine the feasibility of these materials for the flexible mould.

3.2.3 Preliminary tests

Experiments were performed to analyse the deformation behaviour of PC and PETG. This is done by the method of using a static (non-deformable) edge as a mould. For the experiments, heated thermoplastic sheets of 250x250x3mm were deformed through static wooden moulds. This method is called 'static edge mould method'. First, a double curved geometry of 150x150mm was drawn in the software application 'Rhinoceros' (Figure 3.13 and Figure 3.14). The edges of the geometry were transferred to the static edge mould, as can be seen in Figure 3.15. The thermoplastic sheet is pressed between the static edge moulds. This mould method is a simplified representation of the edge manipulation of the flexible mould. Figure 3.17 to Figure 3.26 show the material tests with the use of the static edge mould. Multiple tests above the glass temperature were done to determine a suitable temperature and heating time. These tests were done for both selected thermoplastic materials.

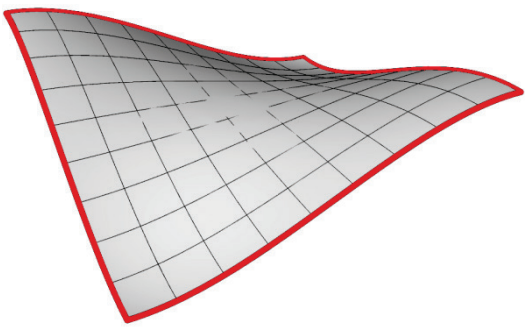

Figure 3.13: Double-curved geometry in Rhinoceros. The red edges represent the static edge mould.

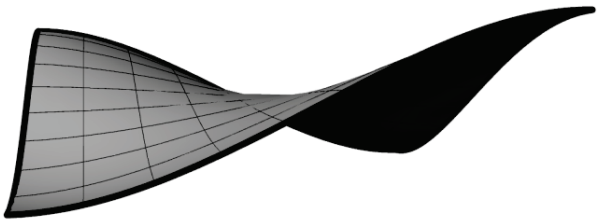

Figure 3.14: Double-curved geometry in Rhinoceros [2]

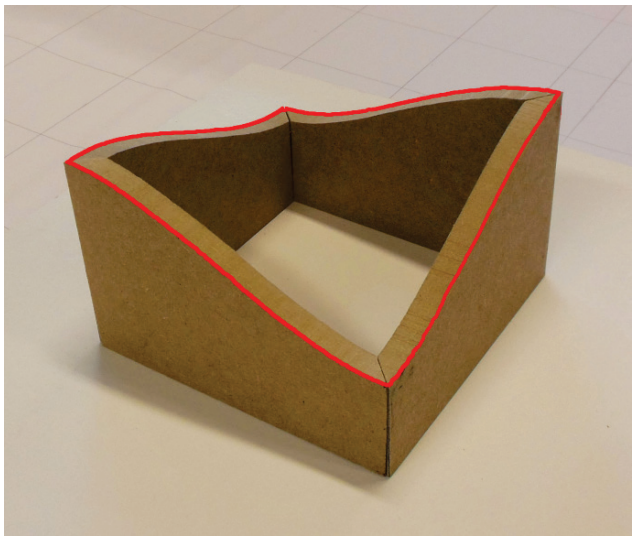

Figure 3.15: Lower part of the static edge mould; the red edges are derived from the Rhinoceros model. The upper part is a counter version of the lower part

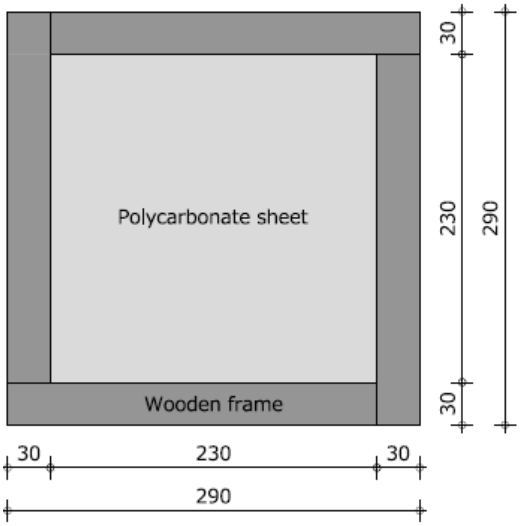

Figure 3.16: Dimensions thermoplastic sheet in fixation frame

Figure 3.17: Thermoplastic sheet of 250x250x3mm clamped in wooden slats

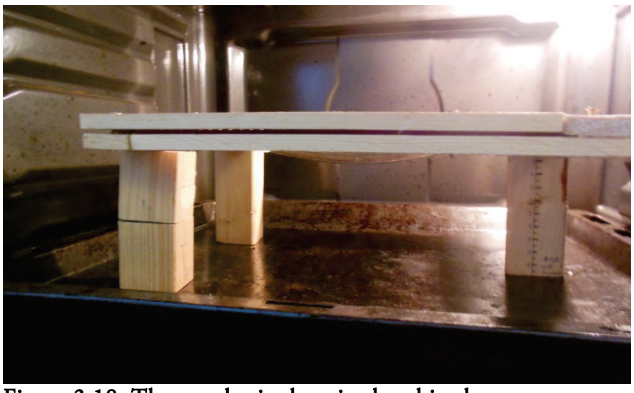

Figure 3.18: Thermoplastic sheet is placed in the oven

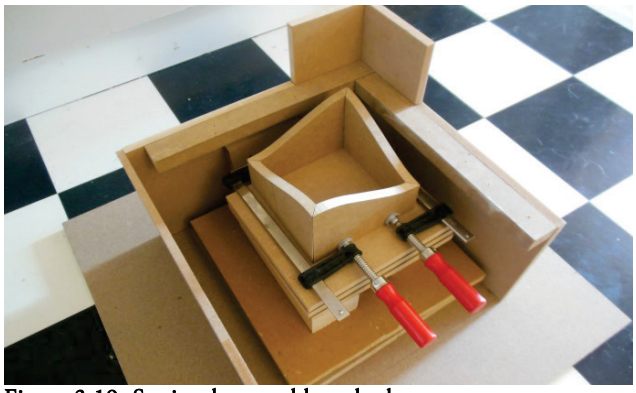

Figure 3.19: Static edge mould method setup

Figure 3.20: Heated thermoplastic sheet between static edge moulds

Figure 3.21: Formed thermoplastic sheet

Figure 3.22: Sawing thermoplastic sheet of 250x250x3mm to a sheet of 150x150x3mm

Figure 3.23: A closed mould is created through clamping two sheets between wooden boards.

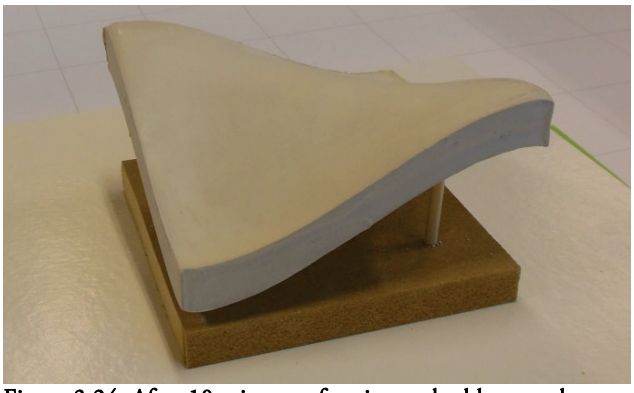

Figure 3.24: After 10 minutes of curing, a double curved gypsum panel is the result. This process is repeated four times.

Figure 3.25: End result (1)

Figure 3.26: End result (2)

The first material to be tested is polycarbonate. During heating the formation of gas bubbles could be observed. Several setups of the oven were used and tested in order to find the optimum settings for the thermoforming process. The test can be seen in Figure 3.27 to Figure 3.31. In the parentheses the amount of time to heat the material from 120°C to the desired temperature can be seen. The most suitable setup for the thermoforming of polycarbonate is a drying time of 45 minutes at a temperature of 120°C followed with a heating time of 20 minutes at 170°C (Figure 3.30).

Similar tests are performed for the thermoforming of PETG. From these tests a suitable thermoforming procedure of 15 minutes heating at 90°C is derived. For all PETG tests no gas bubbles could be observed.

Dimensions	250x250x3	mm
Drying temperature	N.A.	
Drying time	N.A.	
Heating temperature	180	°C
Heating time	16	min.

Figure 3.27: Test 1

Dimensions	250x250x3	mm
Drying temperature	80→120	°C
Drying time	12	min.
Heating temperature	180	°C
Heating time	16(+4)	min.

Figure 3.28: Test 2

Dimensions	250x250x3	mm
Drying temperature	80→120	°C
Drying time	30	min.
Heating temperature	190	°C
Heating time	17(+4)	min.

Figure 3.29: Test 3

Dimensions	250x250x3	mm
Drying temperature	80→120	°C
Drying time	45	min.
Heating temperature	170	°C
Heating time	20(+5)	min.

Figure 3.30: Test 4

Dimensions	250x250x3	mm
Drying temperature	80→120	°C
Drying time	45	min.
Heating temperature	180	°C
Heating time	20(+5)	min.

Figure 3.31: Test 5

3.2.4 Simulations preliminary tests

In order to produce accurately formed thermoplastic sheets, the material behaviour must be predicted. In this paragraph the correlation between simulations and tests is validated. The simulations are done with the use of 'nonlinear finite element' software.

Nonlinear finite element software

The finite element analysis (FEA) program 'Marc Mentat' is used to simulate the deformation behaviour of the thermoplastic sheet. More information about this software can be found in chapter 6. Dr.ir. L.C.A. (Lambert) van Breemen from the 'Department of Mechanical Engineering' at the Eindhoven University of Technology assisted the simulation process.

Simulation 'static edge mould method'

The deformation process of the polycarbonate sheet of the 'static edge mould method' is simulated in 'Marc Mentat'. The edges of the static mould are defined as rigid surfaces. These rigid surfaces are pressed into a deformable polycarbonate sheet, as can be seen in Figure 3.32.

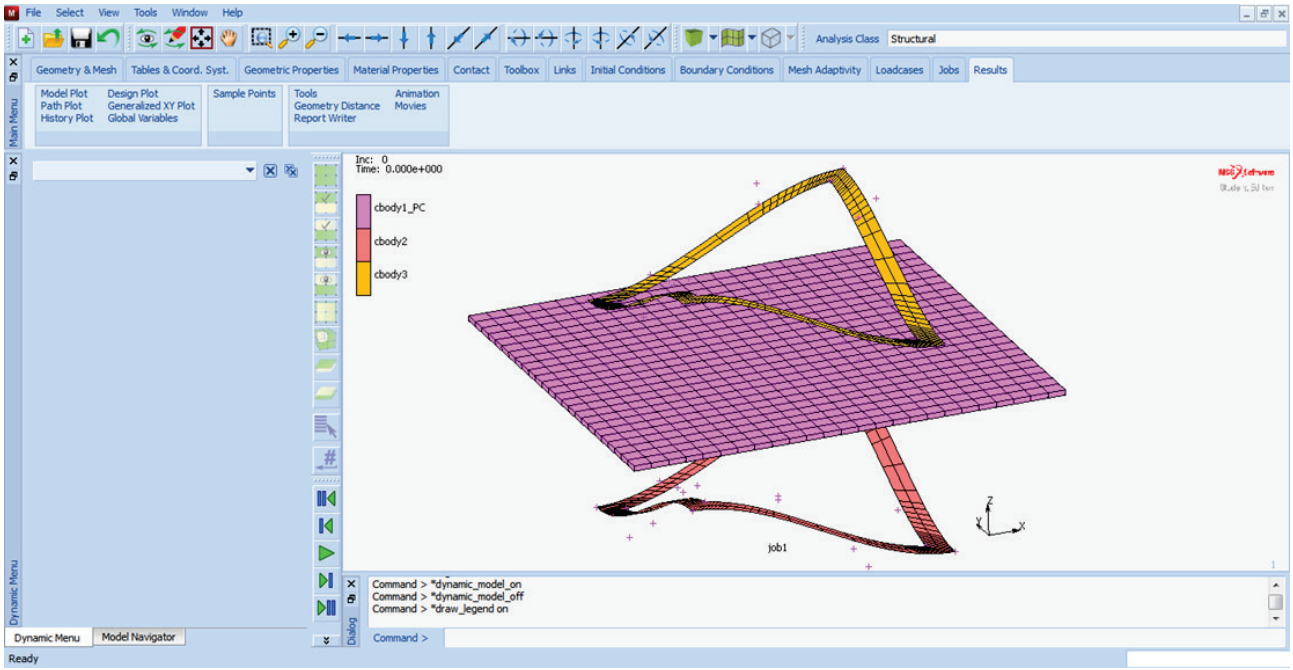

Figure 3.32: Marc Mentat interface: The static edge mould method simulation

After discussions with dr.ir. Lambert van Breemen it was concluded to simplify the material properties of polycarbonate. A Young's modulus is entered for linear elastic behaviour instead of non-linear viscoelastic behaviour. Simulating non-linear viscoelastic behaviour was found to be too complex for the purpose of this research. The large amount of parameters makes this behaviour too complex to be realistically simulated (chapter 3.2.1).

The Young's modulus is determined with the use of the graph in Figure 3.33. The graph shows the stress-strain curves at different temperatures at the strain rate of 0,01 s-1. The curve is fairly linear around the glass transition temperature (T_g) of 150°C and at this temperature the yield point disappears. An approximation of the Young's modulus can be derived at T_g for polycarbonate. With the use of Hooke's law method the Young's modulus can be approximated, which is around 18 MPa.

It has to be noted this method does not simulate the actual viscoelastic behaviour. However, in chapter 3.2.1 has been discussed that the deformation behaviour in the short term is mainly elastic. A Young's modulus of 18 MPa is therefore used to represent the short term elastic behaviour. All significant input values for Marc Mentat can be found in Table 3.2.

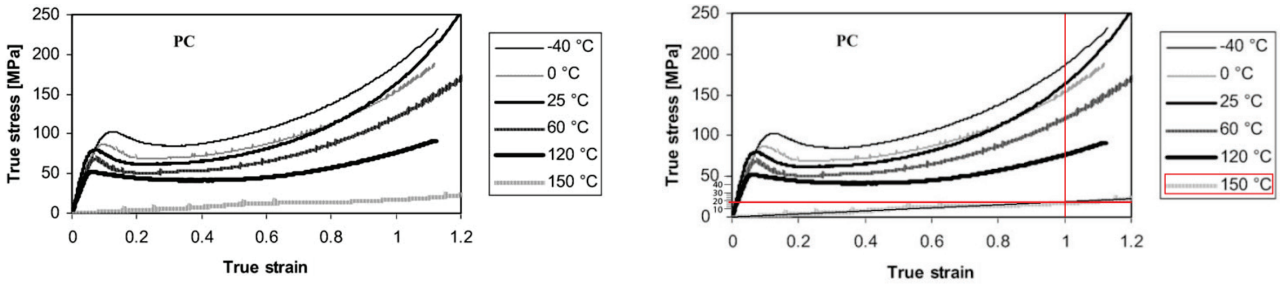

Figure 3.33: Experimental uniaxial compression stress-strain curves for PC, at the strain rate of 0,01s^{-1} over a wide range of temperature (adapted from Richeton).

Options	*Selections*	*Specifications*	*Additional specifications*
Geometry & Mesh:	• Elements: • Surfaces:	Polycarbonate sheet Wooden frames	250x250x3mm 150x150mm
Material properties (polycarbonate)	• Mass density: • Young's modulus: • Poisson's ratio:	1,2 g/cm^3 18 Mpa (N/mm^2) 0,38	
Boundary conditions:	• Gravity load: • Fixed displacement:	-9,81 N 0mm in all directions	Z-direction Edges PC sheet
Contact bodies:	• Deformable cbody: • Rigid contact body: • Rigid contact body:	Polycarbonate sheet Upper wooden frame Lower wooden frame	 Displacement Z = -60 Displacement Z = 57
Element type	• Full integration	80	
Tables	• Time table	Formule: v1	

Table 3.2: Input values Marc Mentat

Results of the mechanical behaviour calculated by Marc Mentat such as the stretching and stress values are false in this case, because realistically a viscoelastic material is deformed instead of a solely elastic material which excludes phenomena such as stress-relaxation and creep. The accuracy of the deformation behaviour is validated in the following paragraph.

3.2.5 Validation preliminary tests

A 3D scan is made of the deformed polycarbonate sheet (Figure 3.21) in order to determine the correlation between the Marc Mentat model and the scanned polycarbonate sheet. The Marc Mentat model and the scanned polycarbonate sheet are validated with the Rhinoceros model (Figure 3.34 to Figure 3.36).
The 3D scanning is done with the use of the software application 'Autodesk 123D Catch' (appendix A) and the validation is done with the use of the software application 'CloudCompare' (appendix B).

Figure 3.34: Rhinoceros model

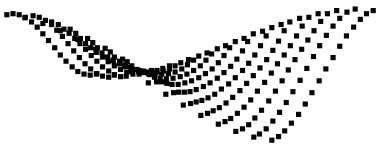

Figure 3.35: Marc Mentat model

Figure 3.36: Polycarbonate sheet

The edges of the sheet are very accurate because of the use of the static edge method. The edges of the Marc Mentat model and scanned sheet have been aligned with the reference geometry (designed Rhinoceros surface) in order to calculate the larger inaccuracies in the middle part of the sheet. The preliminary test sheet and Marc Mentat simulation are validated with the use of the method described in chapter 8. With the use of these results, the cloud to mesh distance is computed on the geometry. In Figure 3.37 and Figure 3.38 these results are shown.

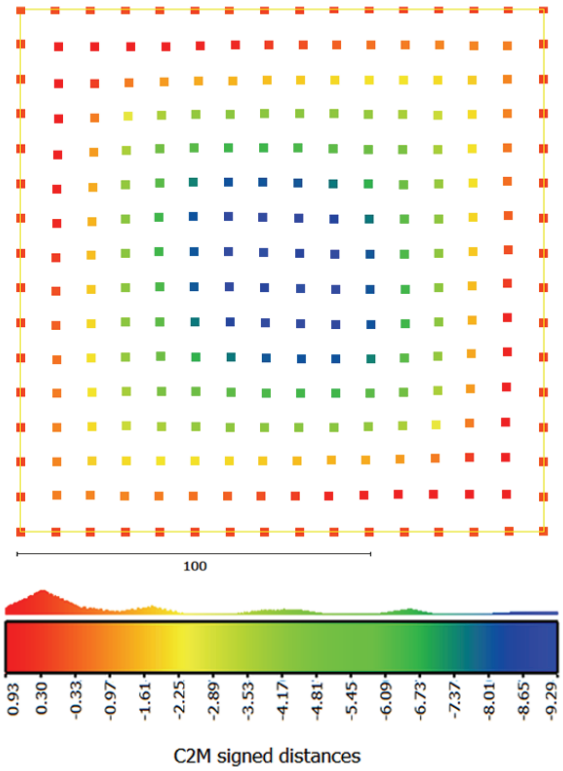

Figure 3.37: Validation Rhinoceros model and Marc Mentat

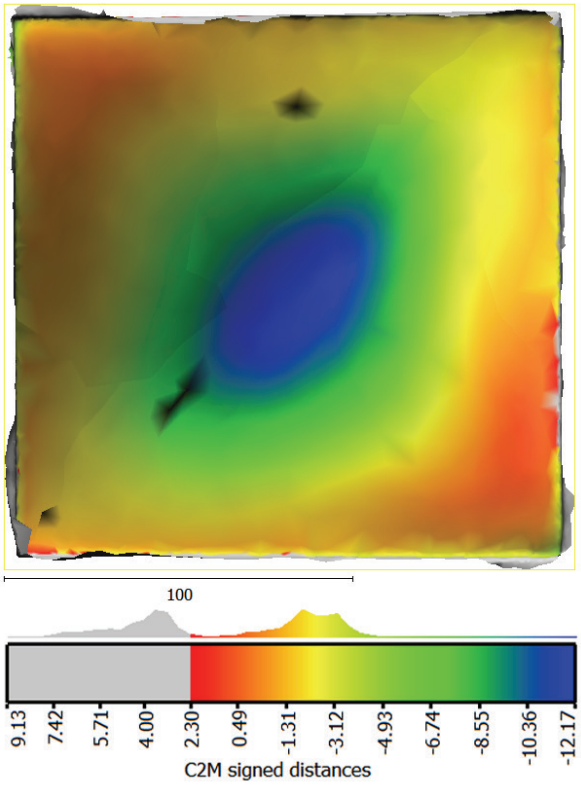

Figure 3.38: Validation Rhinoceros model and PC sheet

The Marc Mentat geometry is created as a point cloud and therefore the distances are computed to points. The edge of the geometry is very accurate, since all the edge points from the designed geometry have been used as input in the Marc Mentat model. This means that the mesh distance at the edge points will approximately be zero. As can be seen in Figure 3.37, the maximum sag occurs in the centre of the sheet. The Marc Mentat simulation shows that the sag is likely to be about 9,3mm compared to the originally designed geometry.

Figure 3.38 shows the deformation of the sheet is less uniform as in the Marc Mentat validation, however still symmetry in two axes can still be observed. This difference could be explained by possible errors during the production process e.g. a non-uniform heat distribution or the sheet has touched the lower mould too soon or the sheet was not one hundred percent horizontal.

The validation shows a similar deforming of the Marc Mentat model and the polycarbonate sheet. The course of the positive and negative deflection is comparable (Figure 3.39). The maximum absolute deflection is 3,44mm.

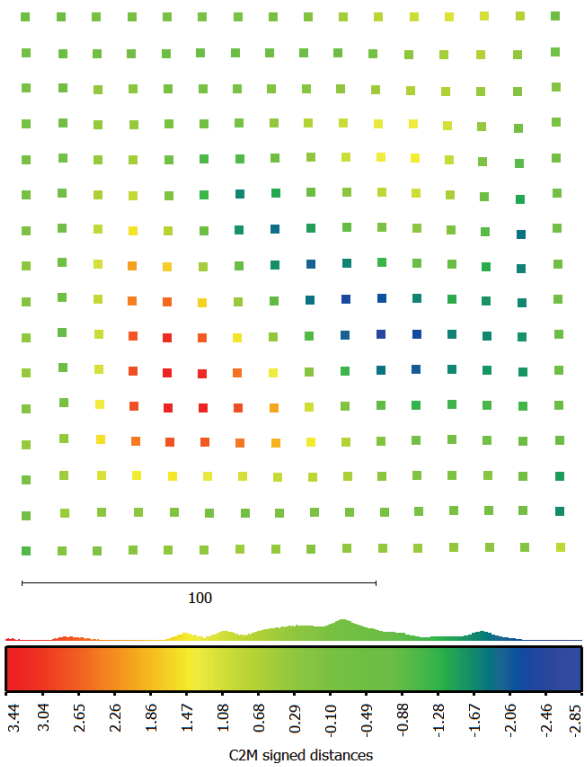

Figure 3.39: Validation Marc Mentat model and PC sheet

3.2.6 Conclusions

The mechanical model of the viscoelastic behaviour is very complex. Viscoelastic properties of the thermoplastic ensure the deformation of the material is time-dependent. The simulation of the deformation behaviour with the use of the static edge mould method has been simplified (after consultation with the supervisor) with the use of a Young's modulus for the viscoelastic region. This method has provided a reasonably accurate prediction for the deformation just above the glass transition temperature for a short period (Figure 3.39), which in turn can be used to gain insight of the correlation between the thermoplastic sheets and the designed geometry. However, this approach is no longer sufficient when stress is applied to manipulate the shape. Stress relaxation and creep occur when tension is applied (as discussed in paragraph 3.2.1). These time-dependant phenomena are very complex to simulate. It has to be noted that even if the viscoelastic behaviour can be accurately simulated, time is needed to set the mould in the proper settings, which can differ for each sheet. Every variation in the thermoforming procedure will have a significant effect on the accuracy of a formed sheet because of its time dependency. Also after deforming the material should be cooled as fast as possible to prevent further sag.
There can be concluded this method because of its time dependency is not feasible and a supporting layer is required, of which its behaviour is not time dependent. As is discussed in chapter 3.1.2, an elastomer can be a suitable flexible layer material. This option is explored in chapter 3.3.

3.3 Elastomers

3.3.1 Elastomer Properties

As described in chapter 0, polymers can be subdivided in three main classifications; thermoplastic polymers, thermosetting polymers and elastomers. In this chapter, the use of elastomers as a manipulable flexible layer will be elaborated.
Elastomers can be elastically deformed by a very large percentage, from 200% up to 1000%. These materials could be both thermoplastic elastomers and thermosetting elastomers (Kaufmyn, n.d.). The most important aspect about elastomers is that they exhibit 'nonlinear' behaviour, which means that the deformation is not directly proportional to the applied load. Elastomers are called to be 'hyperelastic' materials. Figure 3.40 shows a typical strain-stress curve for an elastomer tensile specimen. This figure shows there is no constant value for the

Young's modulus (Bauman, 2008). The stress-strain properties of elastomers typically change with temperature. As was discussed in chapter 3.2.6, property changes with temperature are not desired.

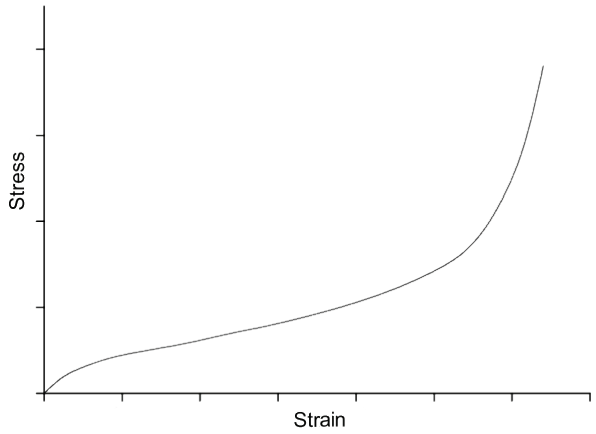

Figure 3.40: Characteristic strain-stress curve of an elastomer tensile specimen (adapted from Bauman)

To gain a better understanding of the behaviour of rubbers, the results of a tensile test performed on a synthetic rubber EPDM are used. The test has been cycled to 10%, 20%, 50% and 100% strain with each cycle repeated twice. The stress-strain behaviour of rubber is very different from Hooke's Law in four basic areas (MSC Software, 2010):

- Initially, the rubber is deformed into a larger strain territory for the first time and it is very stiff. After recycling the same strain territory, the rubber softens dramatically. This phenomenon is often referred to as the Mullins' effect (see Figure 3.41). In most applications this one-off very stiff event is usually discarded where it is assumed in these applications repetitive behaviour will dominate.
- There is always a viscoelastic effect present in rubber which leads to a stable hysteresis loop when cycled over the same strain range (see Figure 3.42). Hysteresis refers to the different stain-stress relationship during unloading (as compared to the loading process) in such materials when the material is subjected to cyclic loading. For the simulations only the loading process is important.
- Another difference between hyperelastic laws and Hooke's law, is the enormous difference between tension and compression of hyperelastic materials (see Figure 3.41). In the flexible layer solely tension is applied.
- The hyperelastic constants are sensitive to the deformation states. Various deformation states show different curves (see Figure 3.44).

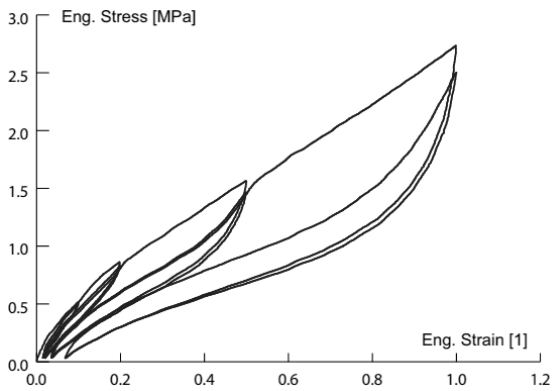

Figure 3.41: Tensile tests performed on an elastomer (adapted from MSC Software)

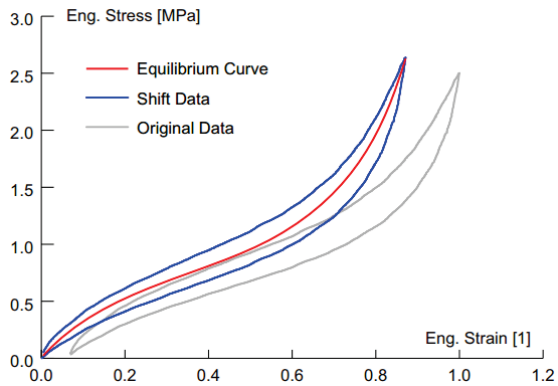

Figure 3.42: Stable hysteresis loop (adapted from MSC Software)

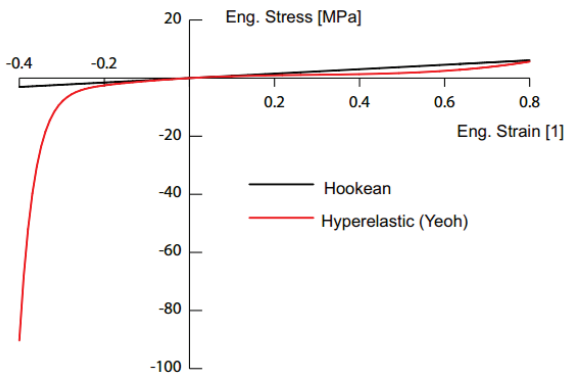

Figure 3.43: Strain-stress curve for compression and tension of an hyperelastic material (adapted from MSC Software)

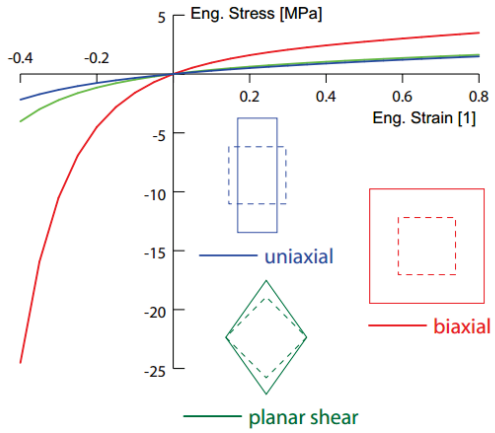

Figure 3.44: Strain-stress curves for various deformation states (adapted from MSC Software)

3.3.2 Material Selection

As described in the previous chapter, rubbers can be elastically deformed to a very large percentage. In order to make a manipulable flexible layer which can assure high accuracy form-finding, a rubbery material is needed which has stable properties at high temperatures for multiple load cycles. A material which exhibits these properties is silicone rubber.

Experimental research results show that the Mullins' effects and hysteresis, as well as strain rate sensitivity, can be considered as negligible for silicone rubber. However, different stress states could be measured for different homogeneous load cases. Silicone rubber has non-linear elastic behaviour and a hyperelastic model can be used to describe its deformation behaviour (Meunier, et al., 2008). The effect of various deformation states on the intrinsic behaviour of silicone rubber can be seen in Figure 3.45.

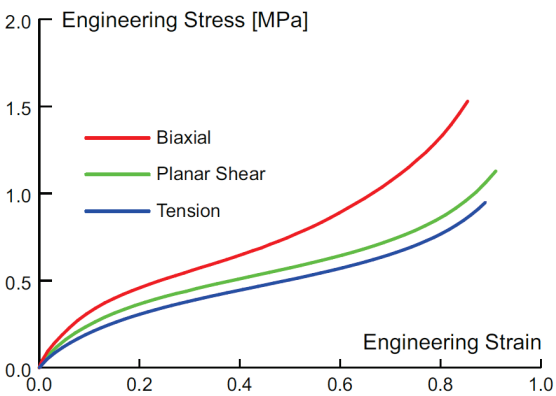

Figure 3.45: Stress-strain curve of a silicone rubber. Each of the three strain states or deformation modes (biaxial, planar shear, and tension) have decreasing stresses for the same strain level (adapted from MSC Software)

Silicone-rubber is an inorganic synthetic elastomer made from a cross-linked silicon-based polymer reinforced with filler. Silicone-rubbers have a backbone which consists of silica and oxygen atoms instead of a carbon backbone like most polymers. They offer a unique combination of chemical and mechanical properties (Dow Corning Corporation, n.d.). Silicone-rubbers have a long service life in adverse environments as they are virtually unaffected by weather and highly resistant to aging. In contrast organic elastomers may become brittle and crack under prolonged exposure to the environment.

Silicone rubbers have a wide operating temperature range from -100 °C to 316 °C. Within this range silicone-rubbers can retain their natural flexibility and resilience, while many organic elastomers soften and deform irreversibly at temperatures above 100 °C and become brittle at temperatures below -25 °C. Silicone-rubbers are

inert materials without taste and smell. Contact with other materials will not lead to degradation of these materials. Because of these properties silicone-rubber is, despite of its high costs, frequently used in many critical applications and in many extreme environments (Vegt, 1999) (HRS Silicone Corporation, n.d.).
Furthermore, there are many special grades and forms of silicone-rubbers available e.g. steam resistant, metal detectable, high tear strength, extreme high temperature, extreme low temperature, electrically conductive, chemical/oil/acid/gas resistant, low smoke emitting, and flame-retardant (Hamilton, 2003). The properties of silicone rubber can be changed with the use of fillers. Various types of fillers can be used (Eriks, n.d.):

- Reinforcing fillers e.g. quartz
- Vulcanization fillers e.g. peroxides
- Thermal stabilizers to improve the temperature resistance e.g. iron-oxides and organic minerals
- Extending fillers to reduce material costs
- Pigment to add color

Silicone rubber is available in a wide range in hardness. Standard hardness ranges from 30 to 80 Shore A. The commercial grade silicon-rubber sheet with hardness of Shore A 60 has suitable properties for the application in the tensioned flexible layer method. Other material properties of this silicone rubber can be seen in Table 3.3.

Silicone rubber properties	
Material	Si MVQ
Colour	Transparant
Density [g/cm^3]	+/- 1,15
Hardness [Shore A]	60 +/- 5
Tensile strength [N/mm^2]	6
Elongation at break [%]	350
Temperature range [°C]	-50/max +200

Table 3.3: Silicone rubber properties (adapted from Eriks)

3.3.3 Preliminary test

A silicone sheet is deformed with the use of the 'static edge mould method', which is similar to the tests that have been done for the polycarbonate sheet. In this case a silicone rubber ('RX® Silicone (Si MVQ)') sheet of 1,5mm thickness is clamped between the static edge moulds. The silicone rubber sheet is tensioned through wooden slats which are attached to the silicone rubber sheet and pressed against the static edge moulds, see Figure 3.46.

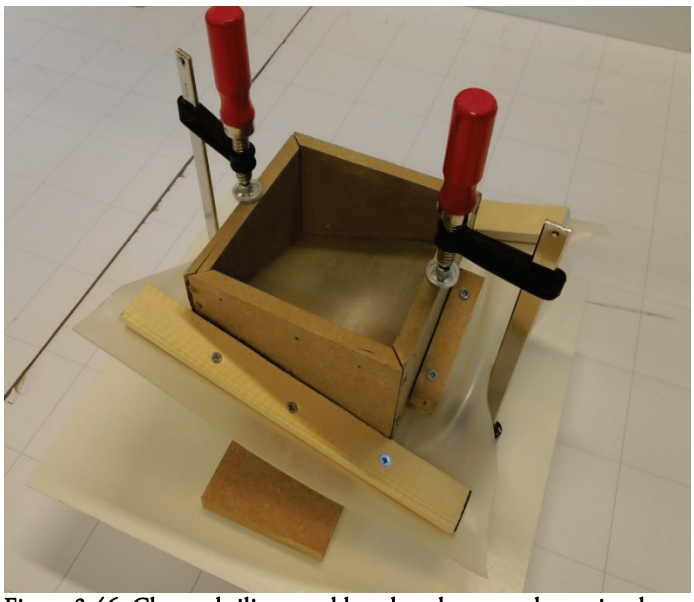

Figure 3.46: Clamped silicone rubber sheet between the static edge moulds

This method has resulted in a smooth and stable flexible layer on which a thermoplastic sheet can be thermoformed. Despite large deformation at the mould edges no wrinkling occurred. However, the required amount of force to deform the silicone rubber sheet was too high and therefore in further research a thinner silicone rubber sheet ('RX® Silicone (Si MVQ)') of 0,5mm will be used (see Table 3.3 for the material properties).

3.3.4 Simulation preliminary test

The relatively constant behaviour of silicone rubber at high temperatures is an ideal property for the simulation of this material. The controllability of the flexible layer could be improved when a silicone rubber sheet is used as the flexible layer.
To model an elastomer using nonlinear finite element analyses, special material modelling and nonlinear finite element analysis tools are required. This paragraph explores on how the aspects of nonlinear elasticity of elastomers can be modelled with the use of these tools. This information has been taken from the paper 'Nonlinear Finite Element Analysis of Elastomers' (MSC.Software, 2010).

Time-independent Nonlinear Elasticity

Nonlinear elasticity consists of the aspects strain energy density functions and incompressibility constraint. The strain energy density describes two parameters. The first parameter is depending on strain (or stretch ratio) and the second parameter is depending on time.

Stretch Ratio

Strain represents the intensity of deformation. For example, the stretch ratio 'λ' (or stretch) of pulled rubber bar along its length, is defined as the ratio of the deformed gauge length L divided by the initial gauge length L_0, namely,

$\lambda = L / L_0 = (L_0 + L - L_0) / L_0 = 1 + (L - L_0) / L_0 = 1 + e$, where e is the engineering strain.

Three different stretch ratios can be described in the three directions (x,y,z) if an in-plane, biaxial load is applied to a rubber material. In an analysis of a large deformed elastomer, the stretch ratios are suitable measures of deformation and are used to describe the strain invariants, I_j for j = 1, 3. These functions can be found in several strain energy functions.

Strain Energy Density Functions

Materials which are represented by different forms of strain energy (density) functions are called 'hyperelastic materials'. Those materials, such as a silicone rubber, are assumed they are isotropic and elastic. These functions are represented by 'W' and stress is the derivative of W (with respect to strain).

The three strain energy functions (I_1, I_2, I_3) represents either in terms of the strain invariants or directly in terms of the stretch ratios themselves. The three strain invariants can be expressed as:

$$I_1 = \lambda_1^2 + \lambda_2^2 + \lambda_3^2$$
$$I_2 = \lambda_1^2\lambda_2^2 + \lambda_2^2\lambda_3^2 + \lambda_3^2\lambda_1^2$$
$$I_3 = \lambda_1^2\lambda_2^2\lambda_3^2$$

When I_3 is described as '1', the material will be incompressible. The strains energy function in Marc Mentat consists of a deviatoric (shear) and dilitational (volumetric) component as:

$W_{total} = W + W_{dilitation}$
W : dilitational part, most concern for elastomer
$W_{dilitation}$ *: dilitation part, most concern for foams*

Only the deviatoric component will be discussed.

The Neo-Hookean model is the simplest model of rubber elasticity. This model is represented by a strain energy density of 'W = $C_{10}(I_1 - 3)$'. The model consist of one modulus ($2C_{10}$ represents the shear modulus (G)). The model obtains a proper correlation with the experimental data up to 40% strain in uniaxial tension and up to 90% strains in simple shear.

Mooney-Rivlin model

In the rubber industrial development, the Mooney-Rivlin model is the most commonly used model because of its simplicity and its suitable representation to a certain amount of deformations (Meunier, et al., 2008). The model is based on two constants C_{10} and C_{01}. With the use of experimental data, these constants are determined by fitting predicted stress. The experimental data can be obtained with the use of various tests: uniaxial tension, equibiaxial compression, equibiaxial tension, uniaxial compression, and for shear, planar tension and planar compression. The Mooney-Rivlin model is described as follows:

Mooney-Rivlin:

$$W = C_{10}(I_1-3) + C_{01}(I_2-3)$$

With the use of the two parameters, the Mooney–Rivlin model shows a valid agreement for strains less than 100%. The model eventually fails at larger strains and in addition the compression mode of deformation is inadequate. The silicone rubber sheet in the tensioned flexible layer method will not be compressed and no strains above 100% occur. Eventually the maximum occurred strain will be checked in the results of the Marc Mentat model. With this knowledge, the Mooney-Rivlin will be used for the simulation.

Incompressible behaviour

One of the unique properties of rubber is its nearly incompressibility. Exact/total incompressibility means that a material shows zero volumetric change (isochoric) under hydrostatic pressure.
The pressure and strain in the material do not have a correlation. It is an unspecified quantity.as far as the stress-strain relationship is applicable. When the bulk modulus is infinite, the Poisson's ratio is exactly 0,5. This incompressibility of the material can be represented as follows:

$$I_3 = 1$$
$$\lambda_1\lambda_2\lambda_3 = 1$$

Herrmann (1965) was the first who applied the incompressibility phenomena in FEA. In the real world rubbers are slightly compressible. This implies the Poisson's ratio is not exactly 0,5, but is 0,49+. For FEA, algorithms with greater numerical stability were developed. Through the use of the correct 'element types' in Marc Mentat, the proper algorithms for modelling of rubbers can be used.

Data of the constants C_{10} and C_{01}

The data of the constants of the silicone rubbers used in the simulations are adapted from a datasheet of 'Impact Engineering Solutions, Inc' (Altidis, et al., 2005). Generally it is recommended to use own experimental data. Because of time constraints, it has been chosen to use the datasheets. See chapter 6 for the specific material properties.

Simulation preliminary test

In Figure 3.47 a simulation of the preliminary test can be seen. This simulation successfully applied the Mooney-Rivlin hyperelasticity model. Unfortunately, due to scanning errors validation of the preliminary test and simulation was not possible.

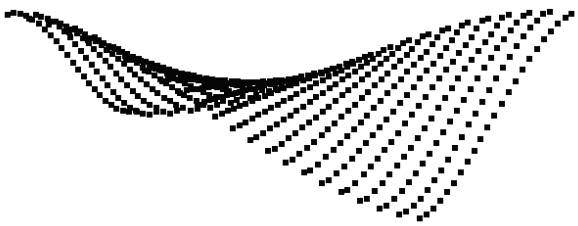

Figure 3.47: Simulation preliminary test

3.3.5 Conclusions

Silicone rubber proves to be a suitable flexible layer material. It can be elastically deformed for a very large percentage and has excellent stable properties, even at elevated temperatures, which makes the use of FEA software to predict the flexible layer deformation possible. The simulations are successfully performed by applying the Mooney-Rivlin hyper elasticity model.
In the next chapter a flexible mould prototype will be designed. This design eventually has to be implemented in the simulations.

4 Concept Development

4.1 Morphological matrix

As is previously discussed, the 'tensioned flexible layer' shows great potential for a feasible flexible moulding method. Nonetheless, the concept shows plenty room for improvement. The edge controllability and the concept of producing rigid thermoplastic moulds in a rapid production cycle are main aspects which make the 'Flexible Mold' by Gard interesting for the purpose of making double-curved concrete elements.
The flexible mould prototype designed by the authors is called the 'Fluid Mould'. This name refers to the type of architecture for which the moulds will be used.
A morphological matrix is used to evaluate various possible solutions per parameter. A high qualitative basis input is needed to gain a qualitative high end result (Utrecht University, 2014). The majority of the input parameters are derived from the literature. This chapter elaborates variables of the mould design. All variables are evaluated and thereafter suitable combinations of working principles have been firmed up into solution variants. The most suitable principle will be elaborated. The morphological matrix can be found in the appendix C.

Analyse and evaluation of working principles
The parameters are indicated by a capital letter and the components are divided by a number (e.g. 'A1').
Some of the components are subdivided in subcomponents (e.g. A.1.1). The used parameters are:

A. Mould Technique
B. Flexible mould method
C. Tensioned flexible layer
D. Actuators
E. Flexible edge
F. Flexible layer
G. Thermoforming procedure
H. Customize the thermoplastic sheet
I. Casting concrete panel

The first parameters have already been decided in previous chapters. However, these parameters are taken into account in order to extend the matrix to the complete scope of this research.

Parameter: **A. Mould Technique**	
Component: A1. Static mould A2. Re-formable mould A3. Flexible mould	*Sub-component:*

The first parameter shows the different mould techniques. These mould techniques have been elaborated in chapter 2. The selection of '*A3. Flexible mould*' is based on the fact the flexible mould technique is an outcome for realizing fluid buildings consisting of non-repetitive double-curved panels.

Parameter: **B. Flexible mould method**	
Component: B1. Pin-bed surface B2. Supported flexible layer B3. Tensioned flexible layer B4. Pressurized flexible layer	*Sub-component:*

Most flexible moulds are not feasible for commercial use because of the relatively high costs. The tensioned flexible layer method which uses reconfigurable edges (B3) is a method which is low-cost, low-tech and produces high quality surfaces. Nevertheless, components and subcomponents of the pin-bed surface and supported mould methods will be taken in account in the morphological matrix.

Parameter: **C. Tensioned flexible layer**	
Component: C1. Thermoplastic layer C2. Elastomer support layer for the thermoplastic sheet	*Sub-component:*

The mechanical model of the viscoelastic behaviour of thermoplastic materials is very complex (chapter 3). Viscoelastic properties of the polymer ensure the deformation of the material is time-dependent. The use of a thermoplastic layer is too complex to predict and too difficult to control. An elastomer layer (C2) has a relatively constant behaviour at high temperatures which is an ideal property for the simulation of this material and the controllability during the manufacturing process. A silicone rubber layer will function as an under laying support layer for the thermoplastic sheet.

The parameters below have not been determined in the previous chapters. Most components of the parameters are derived of the current flexible moulds. These components will be referenced to the following original flexible mould techniques:

1. 'FlexiMold' by Boers (2006)
2. 'Flexible Mold' by Rietbergen & Vollers (2007)
3. 'Zero Waste Free-Form Formwork' by Oesterle (2012)
4. 'Adaptive Mould' by Raun (2010)
5. 'Flexible Mold' by Schipper (2013)
6. 'E-mould' by Van Rooy and Schinkel (2009)
7. 'Flexible Mold' by Gard (2013)

The 'Vacuumatics' by Huijben (2012) is omitted. No components are used from this technique.

Parameter: **D. Actuators**	
Component	Subcomponent
D1 Amount of actuators	D11 4x3
	D12 4x4
	D13 4x5
	D14 4x6
	D15 Pin-bed edge
D2 Determine actuators heights	D21 Analytical determination
	D22 Experimental determination
D3 Set actuator height	D31 Nuts
	D32 Clamping the actuators
	D33 Stepper motor
D4 Set actuator angle	D41 Rotation plate
	D42 Use of two actuators
	D43 Use of rotation plate and two actuators
D5 Lowering of actuators	D51 Use of rods and weights
	D52 Use of a lifting jack
	D53 Use of stepper motor
D6 Allow length variations in flexible edge	D61 Roller support
	D62 Pendulum rod
	D63 Allow strain in flexible layer
D7 Prevent axial rotation actuators	D71 Squared actuator
	D72 Modified threaded rods
	D73 Support actuator

D1. Amount of actuators

The amount of actuators varies in the current flexible mould methods. For example, the 'Zero Waste Free-Form Formwork'[3] uses a minimum of 9 actuators. The pin-bed method[1] uses a maximum density of the actuators in the used surface.

For modelling smooth curves and surfaces often 'Non-Uniform Rational Basis- Splines' (NURBS) are used. Non-uniform means that the portions of a curve, which are affected by individual control points, are not necessarily uniformly distributed along the curve. Rational means that the pull of each control point can be adjusted. Basis-Spline functions define how much each control point influences the curve at any given parameter value. The degree of a curve determines the influence each control point has on the curve. For drawing fluid curves typically degree 3 to 5 NURBS are used. Curves with a degree higher than five are usually not practical or necessary to use (Wenstop, 2008).

To create a desired curve a certain number of control points are required. The minimum number of control points a certain curve degree must have is one number higher than the degree number. The amount of three up to six actuators is elaborated in the Figure 4.1 up to Figure 4.4.

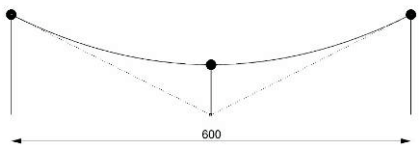

Figure 4.1: Achievable curve with the use of three actuators. With the use of three actuators, only degree two curves can be made. With the use of three actuators per edge only arcs can be made which have a single curve direction. Therefore, three actuators do not provide sufficient design freedom.

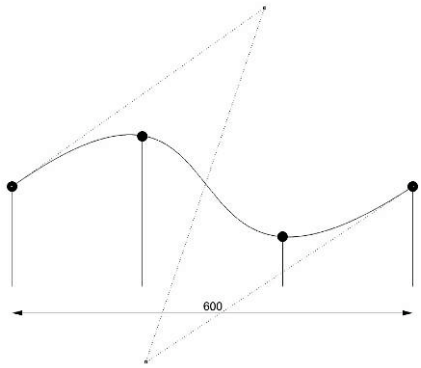

Figure 4.2: Achievable curve by the use of four actuators. A degree three requires a minimal amount of four actuators. With the use of four actuators, shapes such as a one period of a sinusoidal curve can be made.

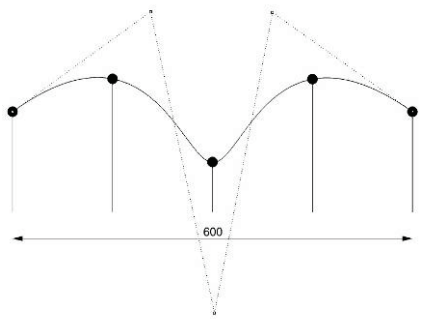

Figure 4.3: Achievable curve by the use of five actuators. A degree four curve requires a minimal amount of five actuators. Shapes such as one and a half period of a sinusoidal curve can be made

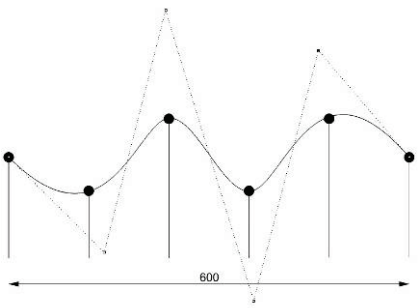

Figure 4.4: Achievable curve by the use of six actuators. A degree five curve requires a minimal amount of six actuators. Shapes such as a two period of a sinusoidal curve can be made.

The radius of existing double curved constructions varies between 0,75m and 45m (Schipper, 2015). This implies the use of many actuators is unnecessary. Therefore, every flexible edge of the Fluid Mould features four actuators by which curved with sufficient complexity can be made.

D2. Determine actuator heights

The actuator heights will be set with the use of input parameters derived from analytical calculations[1,2,3,4,5,6,7] with the use of a computer model. Main advantage is the settings can be calculated in advance by software (e.g. Grasshopper). However, the analytical calculations do not include a structural analysis of the Fluid Mould. This means inaccuracies caused by load forces are not included.
Another method is to continuously monitor the height of the actuators and correct the height until the desired shape is obtained[4]. Main disadvantage is the high investment which is needed for the monitoring equipment such as a laser scanner. Main advantage is that inaccuracies in the height settings due to the forces can be corrected with the use of an iterative process. This leads to a higher accuracy.
For the Fluid Mould method, the actuator heights will be derived from analytical calculations to keep this mould method low-cost.

D3. Set actuator heights

Various ways of pre-setting of the heights are presented in current techniques: manually[5,6,7] or automatically[1,2,3,4]. The most simplistic manually way is to use threaded rods as actuators and nuts to set the proper height. A disadvantage is the thread can falter while setting the proper height. This can make lead to a problematic production process. To smoothen this, steel pipes can be used to guide the threaded rod. Various products can be used to set the proper height e.g. a steel ring and a bolt which clamps the pipe or a hose clamp. Unfortunately, it is more difficult to attach other attributes to these actuators.
The height can also be set by clamping the actuators when they are brought to the proper height. This is however difficult to achieve for all actuators simultaneously.
Ideally, each actuator can be set with the use of stepper motors. All actuators can gradually be set to the proper heights.
The concept of the Fluid Mould has yet to be proven and the result of this thesis is a prototype. Therefore the investment of these stepper motors is not a necessity. The use of threaded rods and nuts is chosen because of the low costs and the availability of many attributes.

D4. Set actuator angle

Rotation disks are applied in previous tensioned moulds[6,7] and are pre-set in the proper angles before the production process. By this method, the risk of imprints in a thermoplastic sheet is greater (Figure 4.1). To reduce the chance on imprints, the flexible edges have to obtain the right angle during the thermoforming process. This implies the angles have to manually set after the thermoplastic is heated when rotation disks are used. One should set the proper angles in the oven at elevated temperatures, which is of course far from ideal.

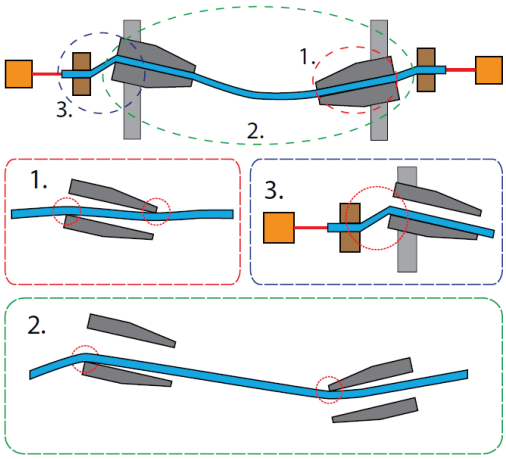

Figure 4.5: Pre-set of the flexible edges in the desired angle causes problems. The risk of imprints is greater.

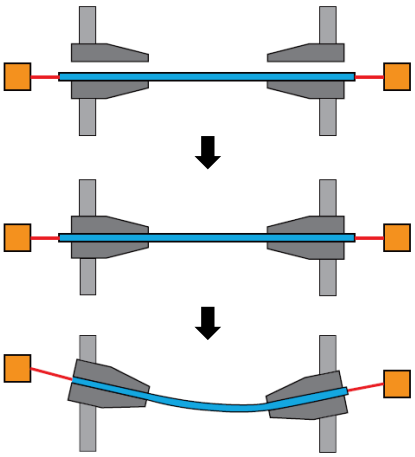

Figure 4.6: The risk of imprints is less by first clamping the flexible layer horizontally.

Supported flexible layers[1,2,3,4,5] achieve curvatures by setting multiple actuators in various heights. Thus with the use of a minimum of two actuators in the width of the flexible edge, the same method can be used for setting

both height and angle. This simplifies the production process and an extra manual operation to set the angle will be avoided.

The rotation disk and the use of the two actuators can be combined. The proper angle of the rotation disk will be obtained by setting the actuators in the proper height. The setting can be obtained with the use of a software application such as 'Grasshopper'. The current rotation disks of the tensioned moulds[6,7] can be improved. The rotation disks of the 'E-mould' has own pivot points, as can be seen in Figure 4.7. Gard's flexible mould has improved this item and converted the two pivot points to one shared pivot point (Figure 4.8). Through this modification it is possible to obtain a smoother transition between two deformed thermoplastic sheets. Furthermore, the thermoplastic sheets will be completely in touch with both flexible edges and one pivot ensures a reduction of friction between the edges. Besides, the exact edge of the thermoplastic sheet is located at the pivot point and is therefore easier to determine with the use of software. When the pivot will be moved to the centre edge of the flexible edge (as can be seen in Figure 4.9), it becomes easier to mark the cutting edges of the thermoplastic sheet.

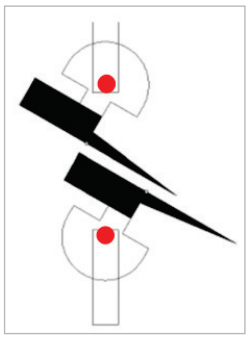

Figure 4.7: Pivot placement of the actuators of the E-Mould (adapted from Gard)

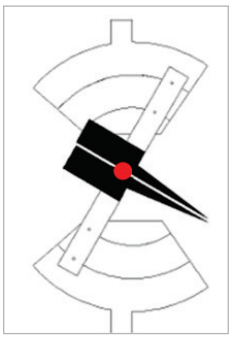

Figure 4.8: Pivot placement of Gard's flexible mould (adapted from Gard)

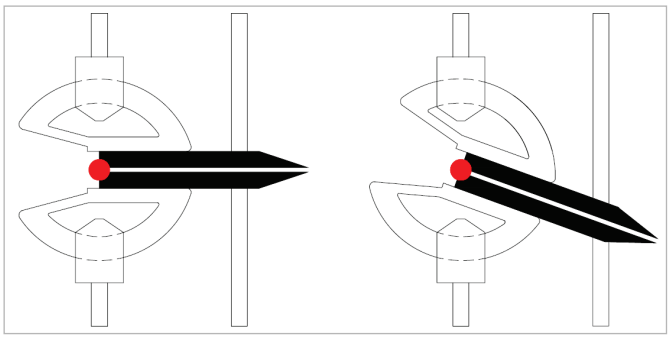

Figure 4.9: Pivot placement at the centre edge of the flexible edge

The use of a rotations disk also has disadvantages. It is more complex to produce than simplified actuator rods. In addition, some play is needed to easily rotate the rotation disk and a hinge is needed for the joint between the rotation disk and flexible edge. It must be emphasized some torque will occur at the hinge.
The method that can be seen in Figure 4.9 is tested (Figure 4.10 and Figure 4.11). The rotation disk in this example is made with the use of a 3D-printer. The rotation disk rotated smoothly while the actuators are varied in height. In order to obtain a higher accuracy, the use of bearings in an option.

Figure 4.10: Testing option 'D53'

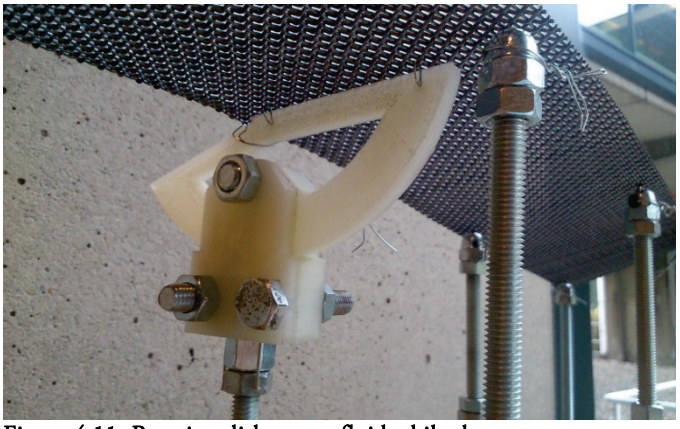

Figure 4.11: Rotation disk moves fluid while the actuators are set in the desired height

The centric alignment of rotation points has been found to be complex for this scale. The use of two actuators without rotation disks (D52) has been chosen. This principle contains two individual eccentric pivot points. Therefore, the aim is to keep the distance between the actuator and the flexible edge as little as possible to match the pivot point as much as possible to the centre. Inaccuracies due to this eccentric pivot points will be included and compromised for in the calculations of the mould settings.

D5. Lowering of actuators

At the start of the production process, the surface of the flexible mould is flat. Eventually, the desired fluid surface can be achieved by changing the heights of the pins/actuators. Depending on the pre-set method (manually or automatically) weights[5], rods[6,7] or stepper motors[1,2,3,4] will set the actuators in the proper height.
For the Fluid Mould prototype the investment in stepper motors is too high. Schipper's flexible mould shows the use of weights and rods is a low-tech and low-cost method to gradually set the actuator heights. Faltering of the actuators is an important aspect to be taken into account. If one lowers the actuators slower than the other, the process jams. This problem can be solved with the use of a lifting jack. A lifting jack is able to lower the actuators with a constant speed. Also, the costs of a lifting jack are very low.

D6. Allow length variations in flexible edge

The change in length of the transforming edge has to be allowed. This can be done by the use of rolls[6], pendulum rods[5,7] or strain in the flexible edge[2]. Allowing strain in the flexible edge can lead to problems such as bending of the actuators due to high stresses and therefore this method has not been chosen.
With the use of rolls the height and angle can be accurately set. It is important the flexible edge is fixated in the vertical direction. Therefore the profile of the flexible edge should be above and below the roll. The E-mould used this method by applying a curtain track which could slide along the actuators. This curtain track however is not suitable to be used in an oven. Another option is to use two rolls, as can be seen in rollercoasters.
Main issue of this method is the flexible edge acts like a track, but still has to allow bending and torsion which deforms the profile. Because of the deformation the amount of friction between the track and roll can become too high and the rail does not slide.
The third option is to apply pendulum rods. Pendulum rods only allow axial forces. With the use of simple calculations there can be determined in which height the actuator should be set to acquire a certain curve. Pendulum rods can be applied in either planar direction (x, z) and in 3D (x, y, z). Pendulum rods have already proven to be a suitable solution in previous studies[5,7].

D7. Prevent axial rotation actuators

Prevention of axial rotation of the actuators is needed. If not prevented, the pendulum rods in planar direction will obtain a certain undesirable degree of freedom in the xy-plane[5,6,7]. This rotation can be prevented by the actuator profile or with the use of a support actuator.
With the use of a square actuator profile instead of a threaded rod, axial rotation can be avoided. However, little deviation in profile dimensions can lead to large axial rotations. If the axial rotation freedom is prevented by connecting one actuator to the other, the arm of the point of engagement is extended. A larger arm means a certain deviation will have a smaller effect on the axial rotation (Figure 4.13).
This can simply be designed with the use of a steel strip with two holes, as can be seen in Figure 4.12. At actuator 'A' this strip should be fixated, so the steel strip cannot torque around the actuator. The steel strip should glide along the opposite actuator 'B' in order to prevent these actuators to torque (Figure 4.12).

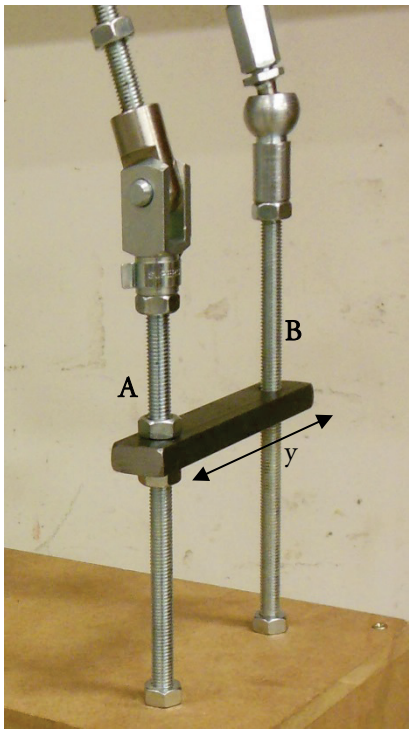

Figure 4.12: Steel strip preventing axial rotation of actuator A

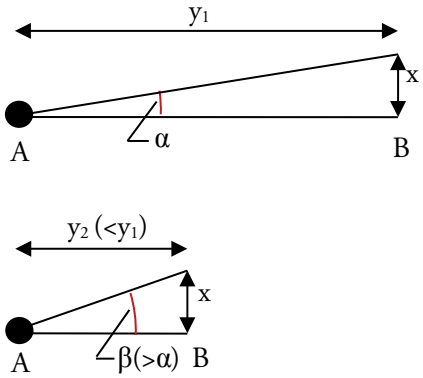

Figure 4.13: Larger arm (y1) leads to a smaller effect (α) on the axial rotation

Parameter:	E. Flexible edge		
Component		Subcomponent	
E1	Material	E11	Silicone rubber
		E12	Silicone rubber stiffened by a thin steel stroke
		E13	Silicone rubber reinforced by glass fibres
		E14	Silicone rubber reinforced by a spring steel wire mesh
E2	Form	E21	Rectangular strip
		E22	Tapered edge
E3	Single / dual flexible edge(s)	E31	Single flexible edge
		E32	Dual flexible edges
E4	Joint actuator and flexible edge	E41	Glue actuator to flexible edge
		E42	Screw actuator to flexible edge
		E43	Attach actuator to reinforcement
E5	Clamping system	E51	Use of weights
		E52	Use of springs
		E53	Use of weights and springs
		E54	Use of nuts
		E55	Screw clamp
E6	Corner solution	E61	Single frame
		E62	Windmill blade formation

E1. Material flexible edge

The material selection (and so the elasticity) of the flexible edges is one of the critical success factors (Schipper & Janssen, 2011). A too flexible or a too stiff material will not lead to a smooth surface. In addition, the actuators will be difficult to adjust in height when a too stiff material is used.

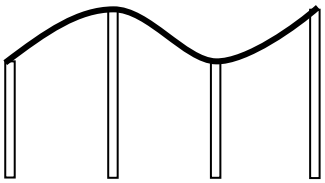

Figure 4.14: Desired flexibility of flexible layer

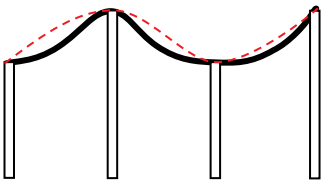

Figure 4.15: Flexible layer too flexible

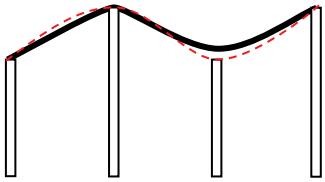

Figure 4.16: Flexible layer too stiff

All materials of the mould have to withstand the high temperatures. Silicone rubber[7] properties are relatively little affected by high temperatures (up to 200-300 degrees Celsius). To prevent the flexible edge to sag between the actuators, the silicone-rubber has to be stiffened. An option to stiffen the flexible edge is to reinforce the silicone strips[7].

The silicone rubber edge can either be produced from standard industrial sheets or liquid silicone rubber for custom casting. Industrial sheets can be cut to the desired shape and glued with high temperature silicone glue, which remains its strength at elevated temperatures. The possibility of the glue to loosen remains and is therefore a risk. If liquid silicone rubber is used, the silicone-rubber and reinforcement can become one unified composite. A mould for the flexible edge can be made in the desired shape and the reinforcement can be cast in the silicone rubber.

The reinforcement can be placed below the silicone rubber or inside the silicone rubber. When using steel, the actuators can be fixated on this reinforcement. It is very important the flexible edge only deforms elastically, therefore spring steel will be used. Spring steel can obtain large deformations in the elastic zone and therefore will spring back to its original flat shape when the mould is brought back into its flat position.

E2. Form

The flexible edge only sets the outer edge of the mould surface[6,7]. The centre of the surface has to be a smooth unified whole with the edge of the surface. When a rectangular shape is used, a very abrupt transition can occur which can lead to a sharp angle in the mould and even imprints.

To prevent this abrupt transition, the profile of the flexible edge should gradually decrease towards the centre of the surface[6]. In other words, the edge should be tapered. A tapered edge however is not available as a form and has to be custom made.

E3. Single/dual flexible edge(s)

An important aspect of the Fluid Mould is the accuracy of the mould edges. This accuracy can be affected with the use of single[1,2,3,4,5] or dual flexible edges[6,7]. If a single flexible edge is used, the flexible layer is not forced in the precise shape defined by the flexible edge. Problems which can occur can be seen in Figure 4.17. To avoid these problems, two flexible edges can be used to force the flexible layer to the desired shape (Figure 4.18).

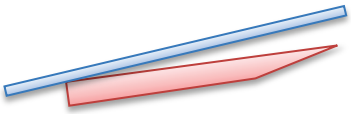

Figure 4.17: Single flexible edge

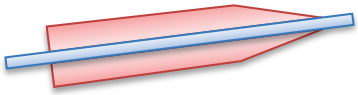

Figure 4.18: Dual flexible edges

E4. Joint actuator and flexible edge

The joint of the actuator and the flexible edge is can be done by glueing[7] or screwing[4,5]. Placement of steel reinforcement below the silicone rubbers allows an easy fixation with the actuators. However, the distance between the centre of the polymer sheet and the rotation point on the actuator will be larger. This distance has to be taken to a minimum and therefore the reinforcement will be placed in the silicone rubber. When using a spring steel wire mesh, the rotation point can be made in the wire mesh itself. This method allows a small distance from the polymer centre to the rotation point and yet is a simple connection.

E5. Clamping system

Several methods are available to clamp the flexible edges like the use of weights[5], tension/compression springs or a combination of these two subcomponents. A manually method is with the use of nuts[6] or a screw clamp method.

It is important all input of the analytical calculations can be pre-set[5,6,7] and as little as possible manual operations are needed during the thermoforming process. With the use of a combination of weights and springs, a clamping force can be obtained while setting the actuators at the desired height. With the use of a nut, the height can be pre-set. When gradually lowering the weight, the actuator will be lowered until the nut touches a steel plate. It is important the weight is sufficient, so the spring will not push the actuators upwards. The length in which the spring is compressed determines the clamping force. To obtain an equal clamping force in all actuators, each spring can be pre-set so all springs are equally compressed in the final deformed situation. Which pre-set is needed can be determined with the use of simple calculations.

In order to provide sufficient force to let the nuts on the actuators sag all the way to the steel plate, weights are used. Approximately 35 Newton is assumed to provide sufficient force by testing the designed flexible edge. This means the spring force in maximum compression cannot exceed this amount of force; otherwise the springs are able to push the actuators upwards. The inside diameter of spring should be slightly larger than 8mm in order to be able to slide over the threaded rods. A maximum spring length of 250mm is designed to fit in the Fluid Mould.

The most suitable spring at 'DTV Springs' has the following properties:

d (mm)	d_m (mm)	L_0 (mm)	L_n (mm)	F_n (N)	R (N/mm)	n (number of windings)	M (gram)
1.00	10.00	1000	310	37.4	0.054	190	37
1.00	10.00	250	77,5	37.4	0.216	47,5	9,25

Table 4.1: Spring type 'DTV art.nr 150015' (data adapted from DTV Springs)

d = Thread diameter (mm)
d_m = Winding diameter axial distance (mm)
L_0 = Spring length unloaded (mm)
L_n = Minimum allowable length when loaded (mm)
F_n = Spring force in at L_n (N)
R = Spring constant (N/mm)
N = Number of windings
M = Mass (gram)

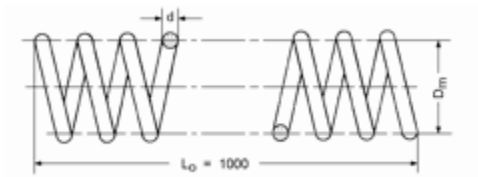

Figure 4.19: Template of a spring (adapted from DTV Springs)

By cutting the spring in pieces of 250mm length, the spring constant *R* becomes 0,216 N/mm (Table 4.1). L_n becomes 77,5mm, so theoretically the maximum compression will be 172,5mm which provides a force of 37,4 Newton. In practice a certain minimum amount of clamping force is required. If for example for all actuators a minimum compression is applied of 20mm, than the overall variation in height cannot exceed 152,5mm. This means the spring selection has a significant effect on which extreme curved surfaces can be made.

E6. Corner solution

The edges can be combined as one; this method is comparable with the supported flexible layers without the middle section. When this frame form is used, the edges will move to the centre during the deforming of the edges, as can be seen in Figure 4.20. To prevent this, separate flexible edges are needed[6,7]. Using four separate edges in a windmill blade formation provides a suitable solution. The windmill blade formation is needed to intercept the change in length in the flexible edges; the deformed position is elongated than the flat position, as can be seen in Figure 4.21.

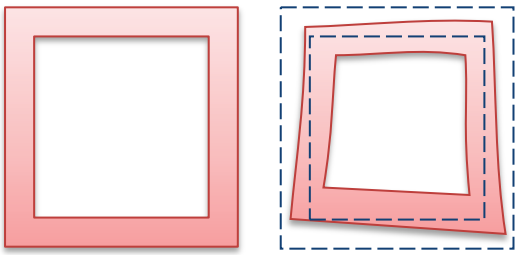

Flat position *Deformed position*

Figure 4.20: Top view frame form. The edges move to the centre during deforming

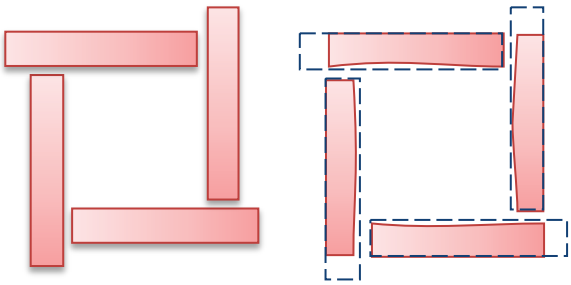

Flat position *Deformed position*

Figure 4.21: Top view windmill blade formation. The edges will stay at the outer edge during deforming

Parameter:	**F. Flexible layer**		
Component		Subcomponent	
F1	Apply tension to flexible layer	F11	Uniform
		F12	Non-uniform
F2	Fixation frame flexible layer	F21	Planar
		F22	Deformable
F3	When to approximate deformation to flexible layer	F31	Before deforming flexible edges
		F32	After deforming flexible edges
		F33	During deforming flexible edges
F4	Move flexible layer edge	F41	Side rod
		F42	Actuators
		F43	Side rod attached to actuators
F5	Fixation flexible layer	F51	Steel cable
		F52	Cable with flexible rod
		F53	Folded flexible layer
		F54	Clamp between profiles
		F55	'Shoelace' with grommets/eyelets
		F56	Steel cables with fixation openings
F6	Apply/adjust tension to the flexible layer	F61	Use 'shoelace'
		F62	Use cables with hooks and eyes
		F63	Use turnbuckles
		F64	Use an inflatable

F1. Apply tension to flexible layer

To obtain stable anti-clastic forms, tension is needed. The 'E-Mould'[6] uses a uniform tension distribution. In order to manipulate the flexible layer in specific directions, non-uniform tension could be applied.

F2. Fixation frame flexible layer

The flexible layer edge can be fixated in a planar frame. To reduce large strain in the flexible layer, the fixation frame must be deformed in approximately the same shape as the desired mould surface[6].

F3. When to approximate deformation to flexible layer

The approximated deformation of the flexible layer can be done in three specific orders: before[6], after and during deforming the flexible edges. To avoid too high tensions in the flexible layer, the flexible layer has to follow the movement of the actuators. When the approximated deformation is done before deforming the edges, complications can occur such as pushing the lower actuators down. When the approximated deformation is done after deforming the flexible edges, the flexible layer can prevent the upper actuators to be lowered. To limit the

stress in the overall process and avoid complications, the approximated deformation by the flexible layer should be done simultaneously with the deformation of the flexible edges.

F4. Move flexible layer edge

The flexible layer can be fixated to actuators or straight side rods. The approximated deformation can be set manually[6] or by the use of actuators. This can be done exactly the same as the method used for the actuators of the flexible edge.

F5. Fixation flexible layer

The fixation of the flexible layer to the rods can be done with the use of standard fixations methods for tensile structures. The flexible layer deforms which means the fixation points must have rotational freedom. If no rotational freedom is applied, wrinkling will occur. The most suitable fixation is the use of grommets/eyelets and hooks.

F6. Apply/adjust tension to the flexible layer

The tension can be applied with the use of various methods. It can be applied by tightening a rope as a shoelace, use cables with hooks and eyes, turnbuckles or an inflatable. Adjusting the tension can for example easily be accomplished with the use of steel hooks and hook them to a side rod. In this side rod, holes can be drilled at various heights; the pre-tension can be varied by hooking at various heights.

Parameter: G. Thermoforming procedure	
Component	Subcomponent
G1 Use of a large oven	
G2 Use of a small oven	
G3 Built-in heater element	
G4 Silicone rubber heater	

G1. Use of a large oven

High temperatures are needed to deform the thermoplastic sheets. The Fluid Mould can be placed in a large oven[7] including the thermoplastic sheet. When a large oven is used, certain dimensional limitations have to be taken into account regarding the design of the Fluid Mould. For example, the size of an available oven in Eindhoven at the foundation 'Beeldenstorm' is 1180x 980x1500mm. The costs of using this oven are approximately 100 euro per day. A disadvantage is that the oven is always closed at three sides; therefore the mould device is difficult to reach.

Figure 4.22: Large oven (1180x 980x1500mm) at the foundation 'Beeldenstorm'

G2. Use of a small oven

To prevent the limitations of the size of the Fluid Mould, a small oven can be used to heat a thermoplastic sheet. Eventually when the thermoplastic is heated it will be transferred to the mould device. This concept is used in the thermoforming industry (Throne, 2011), As can be seen in Figure 4.23 and Figure 4.24.

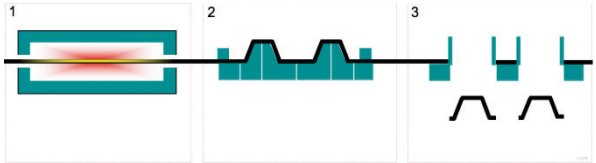

Figure 4.23: Step 1 of a thermoforming procedure: 1. heating; 2. shaping; 3. die cutting (adapted from Van Lieshout)

Figure 4.24: Step 2 of a thermoforming procedure: 1. heating; 2. shaping; 3. die cutting (adapted from Van Lieshout)

There was no suitable small oven available at the department of 'Architecture, Building and Planning', so it is decided to build an oven. Different types of heaters can be used e.g. incandescent lamps. A suitable lamp is a patio heater. Such quartz lamp filled with highly pressurized halogen gas is tested. These heater elements are able to rapidly heat the thermoplastic above its glass temperature. A patio heater costs approximately 25-45 euro. Because the drying time and high glass transition temperature of polycarbonate is an issue it is decided to use PETG for this experiment. PETG has a glass transition temperature of 81 °C. After various tests could be concluded a temperature of approximately 120 °C is a suitable processing temperature.
The oven is built with the use of a patio heater (Figure 4.25) and a wooden box which is coated with aluminium foil (Figure 4.26 and Figure 4.27).The PETG sheet is clamped at two opposite edges. The heater is placed 600mm below the PETG sheet, so the heat is distributed uniformly to the sheet. When the oven is set to its maximum power (1800W), the temperature reaches 120 °C after six minutes. After ten minutes, the PETG is uniformly heated above its glass transition temperature and has become rubbery. Now the PETG sheet is ready to be deformed.

Figure 4.25: Patio heater (1800W)

Figure 4.26: Wooden boards coated with aluminium foil

Figure 4.27: Uniform heat distribution due to reflection of radiation

G3. Built-in heater element

The addition of a built-in heat element to the mould device is alternative option. Vacuum forming is a type of thermoforming which often uses a movable heater element, as can be seen in Figure 4.28 to Figure 4.30. A similar heater element could be integrated in the mould device.

Figure 4.28: A thermoplastic sheet is secured to a vacuum former by pressing down a lever (adapted from National University of Singapore)

Figure 4.29: Once the sheet is secured, the movable red heat panel can be pulled out (adapted from National University of Singapore)

Figure 4.30: After a period of time, the red heat panel can be pulled back and the thermoplastic is ready to be deformed. (adapted from National University of Singapore)

G3. Silicone rubber heater

Silicone rubber sheets with an integrated heater element are available, as can be seen in Figure 4.31. This silicone sheet is able to operate temperatures up to 260 degree Celsius. It is not entirely clear if a silicone rubber sheet can obtain a certain strain without damaging the heater elements.

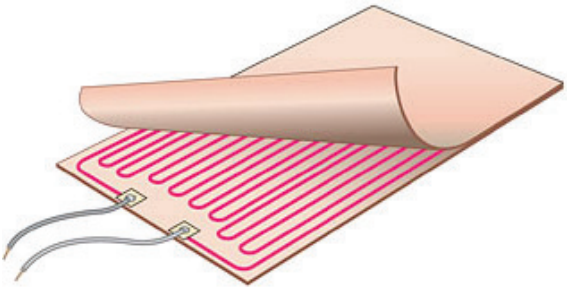

Figure 4.31: Silicone rubber heater (adapted from ABS Heating Element Ltd.)

Parameter:	**H. Customize thermoplastic sheet**
Component	Subcomponent
H1 Band saw	
H2 Hand held cutting	
H3 Hand held router	
H4 CNC cutting	

Due to the deformation of the flexible edges, the thermoplastic sheet can slide of its original position. Therefore the dimensions of the thermoplastic sheet should be larger than the planar dimensions of the flexible edges. Consequence is the thermoplastic sheets need to be cut to size. This can be done by various methods such as a band saw, hand held cutting, hand held router or CNC cutting.

Parameter:	**I. Casting concrete panel**
Component	Subcomponent
I1 Thermoplastic sheets between frames	
I2 Visco casting on open mould	

Two methods can be used for casting the concrete panels with the use of (a) thermoplastic sheet(s) as mould: a closed mould[6,7] and an open mould[7]. A closed mould uses two thermoplastic mould sheets, which are for example clamped between two frames. When pouring concrete, the mould stands vertical.
When an open mould is used, the thermoplastic mould sheet lays horizontal. Viscous casting makes it difficult to achieve a uniformly distributed thickness. Schipper's flexible mould used a method consisting of casting in flat position and deforming after a time interval, which is called 'delayed deforming'. This method is not operational for the Fluid Mould.

Implementation of the solutions

Working principles are combined to solution variants. The most suitable variant is applied for the Fluid Mould and will be elaborated in the next paragraph. It has to be noted all dimensions are designed so the Fluid Mould fits in an oven with dimensions 1180x980x1500mm.

4.2 The Fluid Mould

The steel structure

The structural elements are designed in steel with 4mm thickness. These elements are cut to size by a plasma cutter. After cutting, the profiles have been bended with the use of a press brake. When the steel structure is assembled, it has a height of 1140mm and a width of 900mm.

Figure 4.32: The steel structure

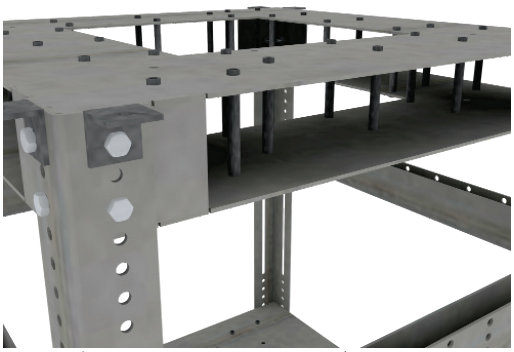

Figure 4.33: Top connections steel structure

Figure 4.34: Side rod of steel structure

The actuators are guided through steel tubes. These tubes are placed through two steel plates and fixated by welding. These plates are used for both upper and lower actuators. The middle sections of the steel plates are cut out to reduce weight and to allow air flow when the device is put in the oven. The steel plates including the steel tubes are equipped with endplates, so they can be fixated with bolts to L-shaped columns.

There are sufficient holes cut in the columns, so the height of the steel plates can be adjusted if necessary. Slices are cut as well to enable the side rods to slide in the desired position. These rods are likewise bended with the use of a press brake. Each rod is attached to the columns with two bolts which can slide through the slice in the column. To allow the length difference, one of the bolts should also be able to move through a slice in the rod. This can be seen in Figure 4.34. The rods are as well lowered with the use of actuators. However, these actuators are guided through holes in an angle steel which are attached on the outside of the column by bolts. The flexible layer can be attached to holes at four different heights, so the applied tension can be varied.

The actuators

Per flexible edge two rows of four actuators are used. The flexible edge is designed in a windmill blade configuration. This leads eventually to more than four control points in the panel edge. This allows the device to produce fluid panels with sufficient complexity.

For the actuators threaded rods are used, which are low-cost and the height can simply be set with the use of a nut. Also low-cost attributes can easily be attached.

To create the pendulum rods, ball joints and clevis eye connections are used. These connections are conventionally used on gas springs for e.g. furniture or a cars tailgate (as can be seen in Figure 4.35 and Figure 4.36). These connections are low-cost. However, the ball joints can obtain a maximum angle of 30°, this limitation must be taken into account.

Figure 4.35: Setup of the pendulum rods. The yellow rod is a non-pendulum rod, the orange rods are clevis eye connections and the red rods are ball joint connections

Figure 4.36: Pendulum rods in operation

The main problem with using these connections is they have some play between the elements. This will lead to inaccuracies in the mould setup. The play in the clevis eye hinges is minimized as much as possible by clamping the clevis with the use of a nut and bolt.
Suitable substitutes for the hinges are universal joints (Figure 4.37). These types of connections are used in e.g. drive shafts and cost approximately 14 euro per piece if applied for the Fluid Mould. Ball joints cost approximately 3 euro per piece. Because of the low costs this connection has been chosen.

Figure 4.37: Universal joint (adapted from Groneman)

The flexible edge

A balance should be found in the stiffness of the flexible edge. The flexible edge should be sufficiently stiff to form a smooth curve. The stiffness should not be too high, because this will lead to high tensions which prevent the actuators to be set to the proper height. The flexible edge should be able to deform back into its original position. A suitable material is spring steel. The used type of mesh is 1,75x0,8, this implies a mesh size of 1,75mm and a wire thickness of 0,8mm (Figure 4.38 to Figure 4.40).

Figure 4.38: Side view of spring steel mesh in flat position

Figure 4.39: Side view of spring steel mesh in curved position

Figure 4.40: Front view of spring steel mesh in curved position

When a spring steel mesh is used, the flexible edge can easily be fixated to the actuators with the use of wires and cap nuts. However, a spring steel mesh is not a smooth material and will not gradually guide the flexible silicone layer to the edge. In order to achieve this, the steel mesh is casted in silicone rubber. The form of the silicone rubber can be tapered, so it will gradually guide the flexible layer to the edge.

Figure 4.41: Casting the silicone rubber into the wooden mould. The spring steel mesh is attached to the mould

Figure 4.42: Result of the silicone rubber reinforced with a spring steel mesh

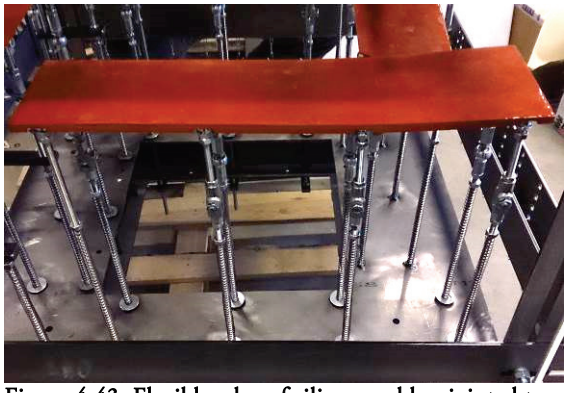

Figure 4.43: Flexible edge of silicone rubber jointed to the pendulum rods

The used silicone rubber is a two component silicone casting rubber which is resistant to high temperatures. It can be continuously loaded to 250°C and a short time to a peak temperature of 350°C. The hardness is shore A50. Mixing ratio of rubber and hardener is 100:2 in parts of weight. The processing time is approximately 30 minutes and the curing time is about 3 hours. The minimum processing temperature is 15°C (Polyservice BV, 2009)). A silicone rubber of a hardness of shore A10 has first been tested. However, the tapered edge of this variant did not provide sufficient stiffness and therefore a more suitable hardness has been chosen.

The flexible layer

The flexible layer consists of a silicone rubber sheet which has 0,5mm thickness. At the edge of the sheet grommets are applied. The sheet is fixated to the steel rod with the use of chains. These chains can easily be hooked in the grommets and holes in the steel rod.

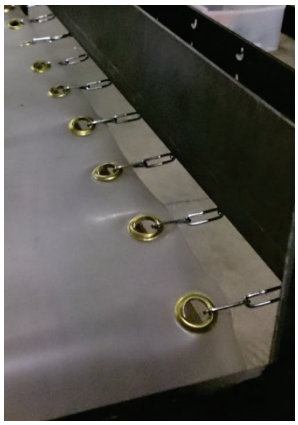

Figure 4.44: The grommets in the flexible layer

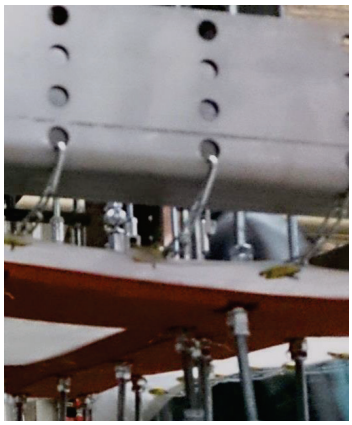

Figure 4.45: Chain hooked in the holes of the side rod

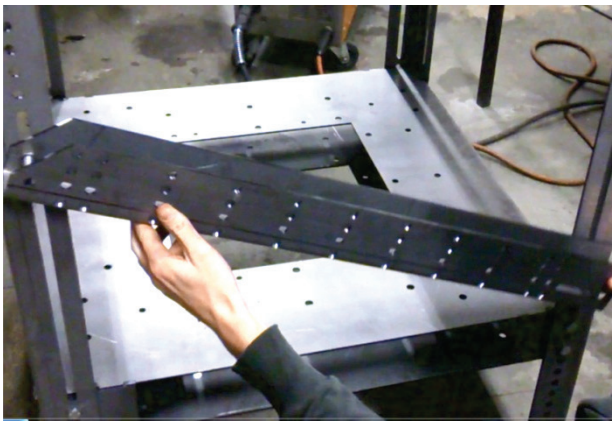

Figure 4.46: Movable side rod

Lowering the actuators

The lowering of the actuators will be done by the use of weights and rods. The lifting plate is holding the weights including the actuators up, as can be seen in Figure 4.47. Four bricks are used as spacers to keep the lifting plate up. After removing those bricks, the actuators can be lowered. Nuts are used to set the actuators in the desired height. After lowering the lifting plate (Figure 4.48), the springs of the lower actuators provide an upward pressure in order to clamp the thermoplastic sheet in between the flexible edges, as can be seen in Figure 4.49.

Figure 4.47: Brick lifted up by lifting plate

Figure 4.48: Lifting plate lowered

Figure 4.49: Springs

Final design

The final design is completed when all implementation of the solutions are integrated to the steel structure, as can be seen in Figure 4.50. The technical drawings of the Fluid Mould are listed in appendix D.

Figure 4.50: The Fluid Mould

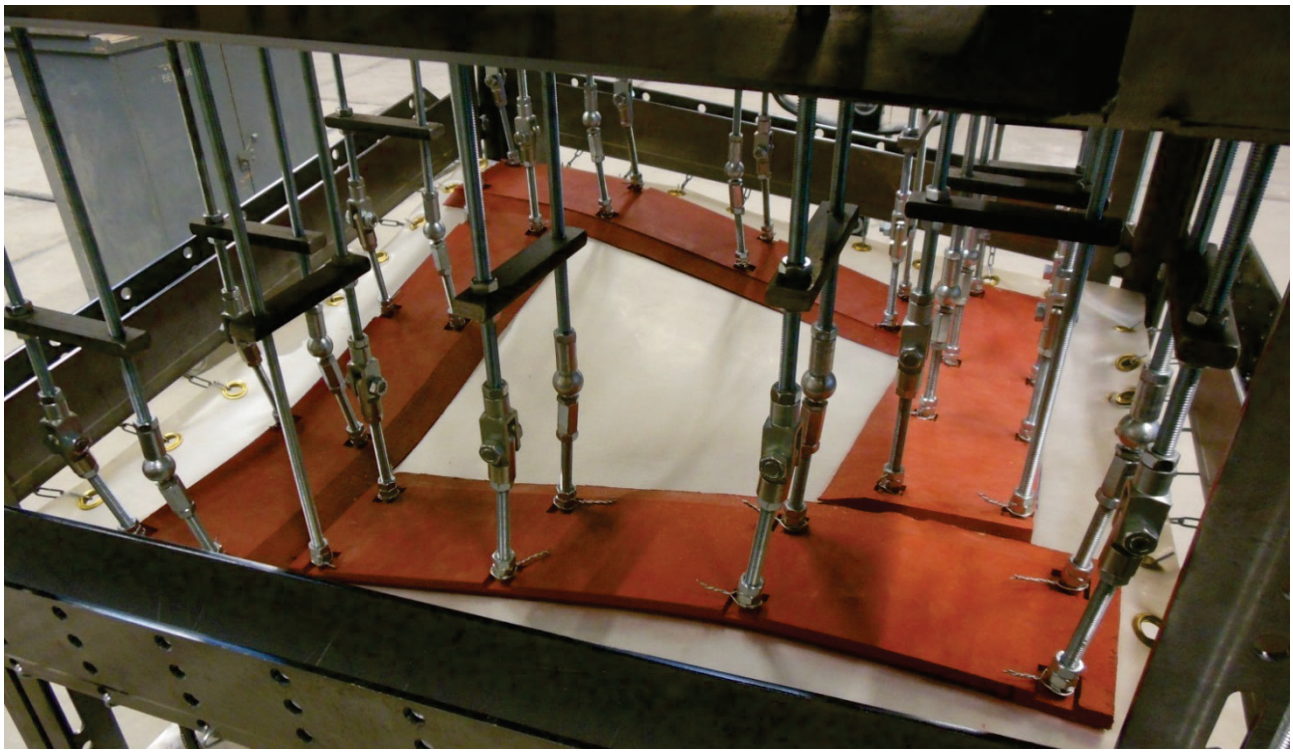

Figure 4.51: Upper actuators of the Fluid Mould

Figure 4.52: Lower actuators of the Fluid Mould

4.3 Production process

After realizing the Fluid Mould, the production of thermoplastic moulds can be started. All thermoplastic sheets will be realized with the use of a specific production process. The production process consists of four steps, as can be seen in Figure 4.53.

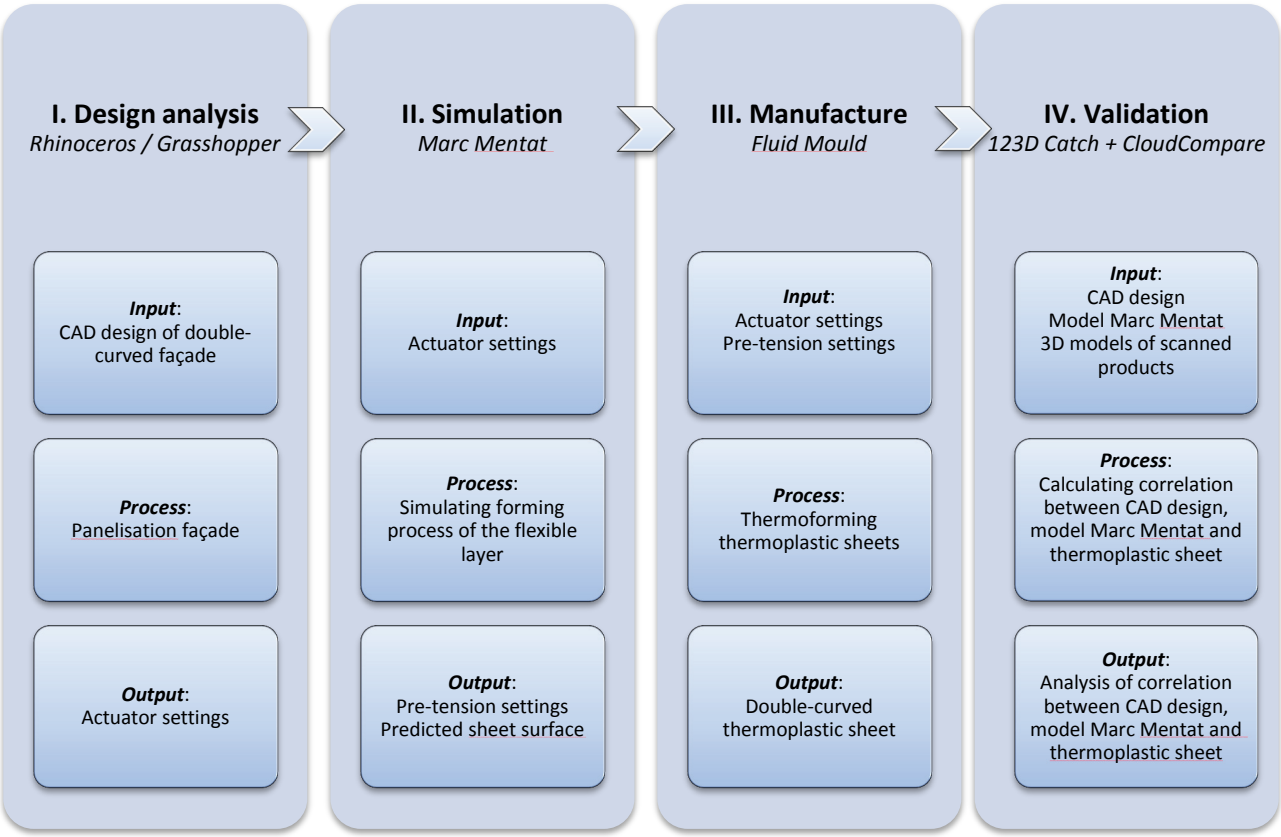

Figure 4.53: Overview of the production process

Descriptions of the process components:

I. Design analysis:
The design is analysed with the use of the software application 'Rhinoceros' in combination with 'Grasshopper'. The analysis includes for example information of the actuators settings which will be used as input for the simulation and production.

II. Simulation
All finite element analyses are done with the use of the software application 'MSc Marc Mentat'. The simulation predicts the final shape of the silicone rubber sheet after a deformation. The shape will be formed by the height settings of the actuators attached to the flexible edges and by the application of pre-tension.

III. Manufacture
After the design analysis and simulations, the actuator settings and amount of pre-tension are known. The Fluid Mould uses this set-up to deform the thermoplastic sheets in the desired shape.

IV. Validation
All produced objects are scanned with the use of the 'Autodesk's 123D Catch' software application. The scanned 3D-models, simulations and the CAD-design are compared with the use of the software application 'CloudCompare'. According to these validations, conclusions can be drawn.

In the following chapters, each process component is elaborated.

5 Design Analysis

5.1 Grasshopper

The development of NURBS modelling in allows architects nowadays to design complex three-dimensional geometries. The software application 'Rhinoceros' is prominent when it comes to NURBS modelling; therefore it has been decided to design a fluid surface with the use of this software. The use of 'Rhinoceros' also allows the use of 'Grasshopper', which is a graphical algorithm editor. 'Grasshopper' is used to analyse the fluid surface for several aspects:

- Panelise the fluid surface
- Curvature analysis
- Required mould offset
- Assembly concrete panels
- Calculate the Fluid Mould settings

All necessary data are automatically transferred to an Excel template, which can be used as an input for the simulations and the Fluid Mould. In the next paragraphs the Grasshopper analysis will be further elaborated with the use of the designed end-product surface and Fluid Mould dimensions as input parameters.

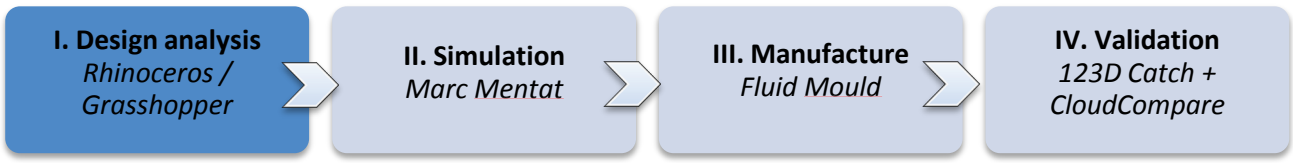

Figure 5.1: Overview of the production process

5.2 Panelising the fluid surface

The end-product is a section of a symmetrical façade (Figure 5.2). This façade has planar dimension is 1800x1800mm and is subdivided in panels by plotting a planar grid with dimensions 600x600mm and applying a seam size of 10mm between the panels. The design consists of nine panels in total. Because of the symmetry, only three panels are unique (Figure 5.3 to Figure 5.6). In addition two other panels have been designed i.e. panel A and panel B (Figure 5.7 and Figure 5.8). With the use of these more extremely curved symmetrical geometries the capabilities of the Fluid Mould can be tested.

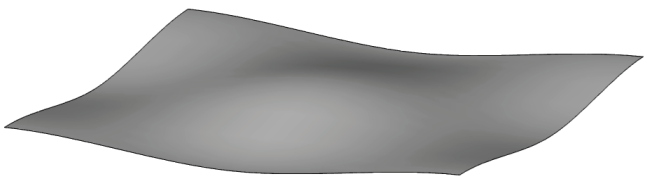

Figure 5.2: Symmetrical section of a double-curved façade

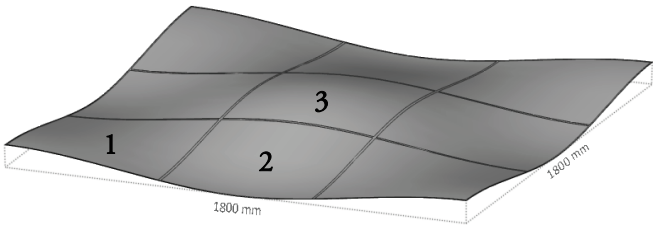

Figure 5.3: Panelisation of double-curved façade

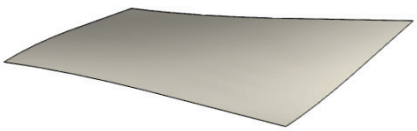

Figure 5.4: Panel 1

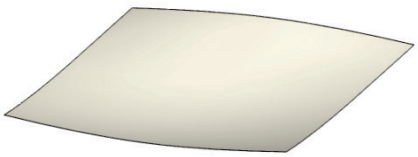

Figure 5.5: Panel 2

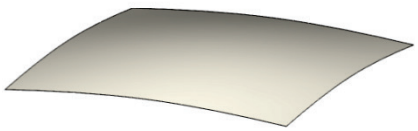

Figure 5.6: Panel 3

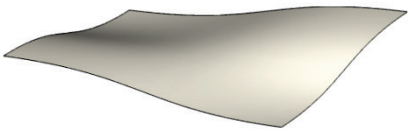

Figure 5.7: Panel A

Figure 5.8: Panel B

It is important the grid and seam offset will take place in planar direction and then will be projected on the fluid surface. This ensures the panels and seams will be of equal size when the façade is viewed from the front. This means all the panels exactly have the dimensions of 600x600mm from the front view, so all the panels can be made with the same mould device (Figure 5.9). When the grid and seam offset would directly occur on the fluid surface, the panels will have different dimensions and the seam size would vary (Figure 5.10).

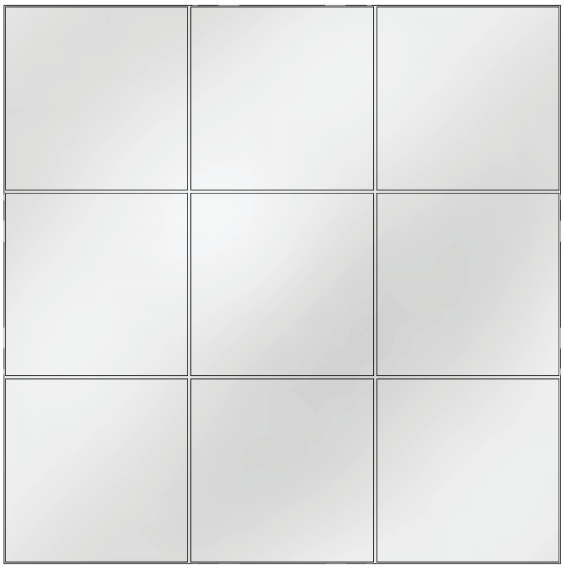

Figure 5.9: Planar grid - top view

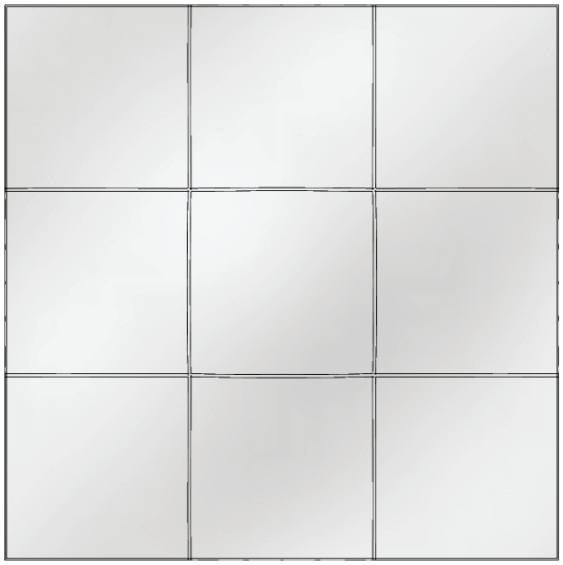

Figure 5.10: Surface grid - top view

5.3 Curvature analysis

Several types of curvatures occur in the panels. A Gaussian curvature analysis can be seen in Figure 5.11. Negative values show anticlastic surface areas and positive values show synclastic areas. There can be noticed panel 1 shows mainly anticlastic areas, panel 2 shows both anticlastic and synclastic areas and panel 3 shows mainly synclastic areas. With these panels as input parameter, the possibility of the Fluid Mould to produce various surface types can be tested. In Figure 5.12 the minimum curvature radius can be seen for each point in the fluid surface. The minimum radius which occurs in the fluid surface is 1145mm.

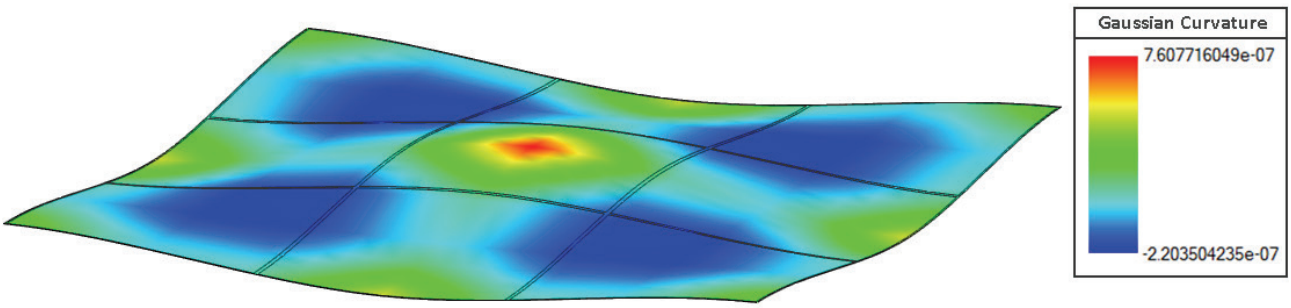

Figure 5.11: Gaussian curvature analysis

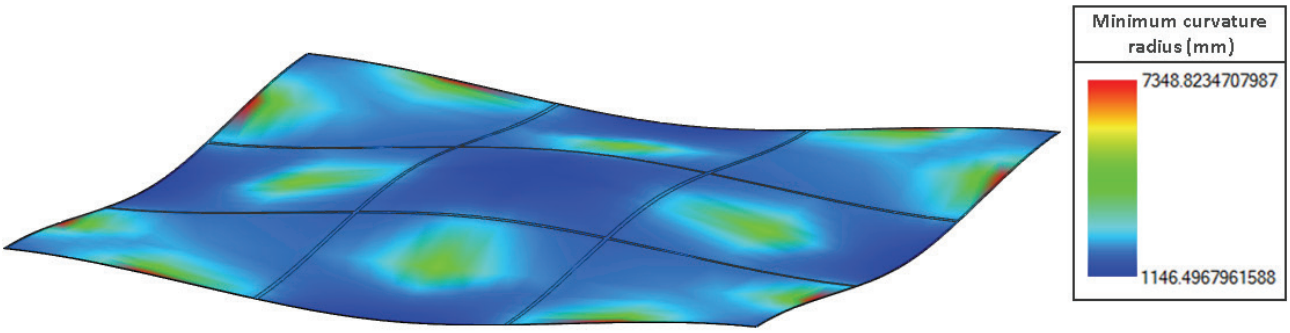

Figure 5.12: Radius of curvature analysis

5.4 Concrete panel analysis

For each concrete panel two thermoplastic sheets are placed in a formwork with a certain offset. The two types of offset, vertex offset and face offset can be seen in Figure 5.13. Each offset has its own effects on the concrete panel geometry and seams. When using a vertex offset, the minimum thickness is always the offset value. However, with the use of a face offset some thickness variations in the concrete panel will occur, as can be seen in Figure 5.14. It has been decided to use a face offset, because then two identical thermoplastic sheets can be used. This only requires one setup for the Fluid Mould per concrete panel instead of two which would have been the case when using a vertex offset.

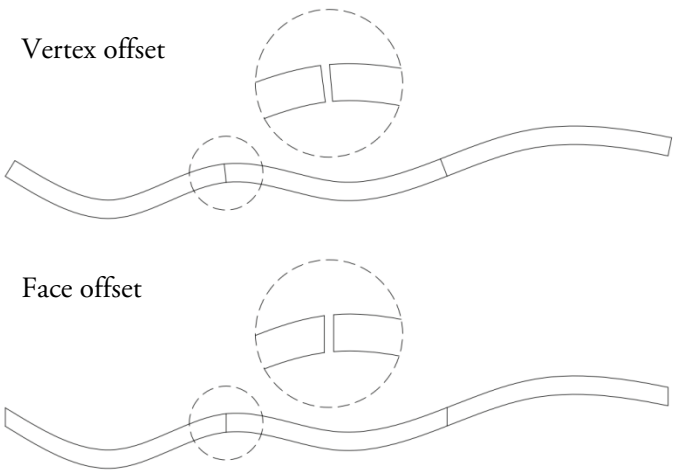

Figure 5.13: Effect offset type on concrete panel geometry and seams

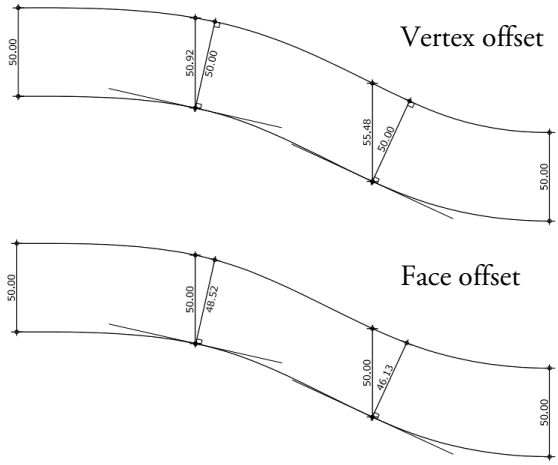

Figure 5.14: Effect offset type on concrete thickness

In the Grasshopper analysis the minimum thickness of the cast concrete panel can be set. The minimum thickness of the concrete panels is in this case set to 50mm. With the use of a Hoopsnake component an analysis is run to determine which face offset is needed in order to achieve this minimum thickness (Figure 5.15). Other output data are as well written to excel such as the volume of the concrete panel and the minimum and maximum curvature (principal and radius).

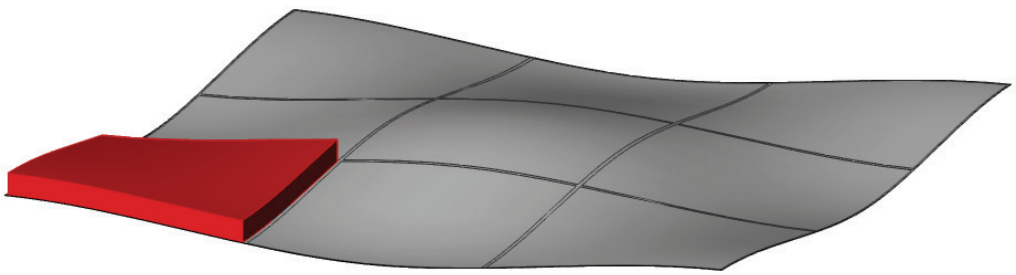

Figure 5.15: Necessary offset calculation for a minimum thickness of 50mm

The concrete panels will eventually be mounted on a planar frame to use the concrete panel as a show model. This means the distance between the frame and the joints on the fluid panel varies. In Grasshopper the location of the joints on the panel can be set with the use of a planar offset from the panel edge. Ideally, these points could be marked on the polymer by a laser. Another input is the minimal distance between the planar steel frame and the joins on the panel. This can be set, so there is some room for adjustments in spacer lengths and there is always a certain workspace available. (Figure 5.16). The Grasshopper component calculates the distance between the frame and the joints on the panel.

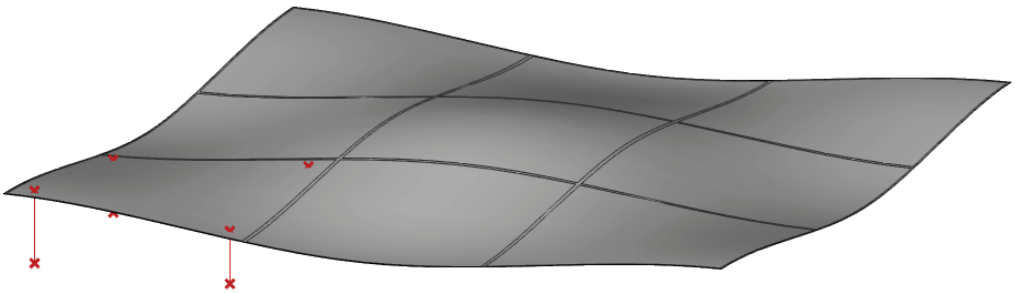

Figure 5.16: Spacer lengths from planar construction frame

5.5 Calculate Fluid Mould settings

The proper Fluid Mould settings have to be acquired for each panel. In the Grasshopper input each panel can be selected for further analysis (Figure 5.17). In order to better illustrate the Fluid Mould Grasshopper model, panel B is henceforth used (Figure 5.8). This surface is a more extremely curved panel. This leads for example to larger angles in the pendulum rods, which makes illustrating how the Fluid Mould settings are derived clearer.

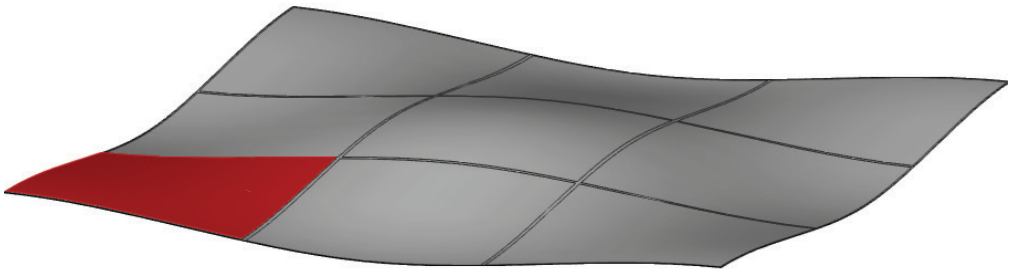

Figure 5.17: Panel selection

For the mould device design, the number of actuators per edge has to be set. For the fluid mould eight actuators per edge are used and labelled. Two rows of actuators (row A and row B) are used. Within these rows the actuators have an equal distance (160mm) between each other. Actuator row B is offset inside by 80mm from actuator row A. The actuator layout can be seen in Figure 5.18.

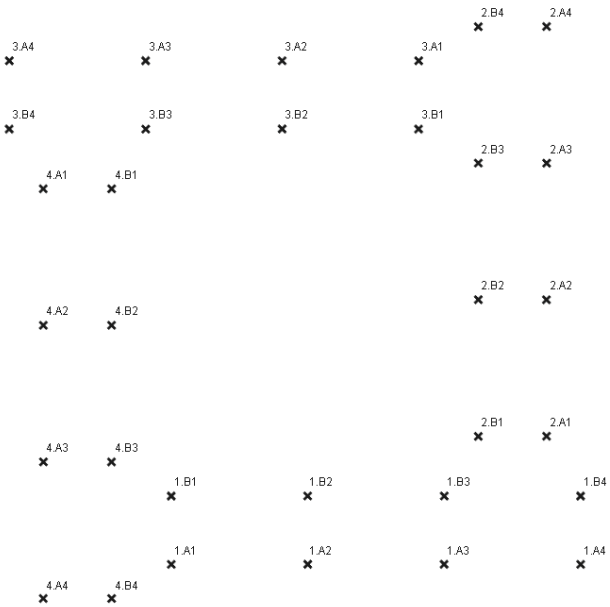

Figure 5.18: Actuator grid labels

The Grasshopper component calculates the height settings for each actuator (Figure 5.20 and Figure 5.21). The settings are acquired by running a geometric analysis, mainly based on the calculation of intersection points between lines, circles and spheres. The proper heights for the side rods are as well calculated based on the tangent of the surface corners (Figure 5.22). A step by step explanation for Fluid Mould settings calculations can be found in appendix E.

Figure 5.19: Selected panel

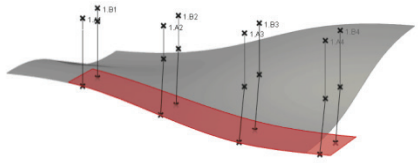

Figure 5.20: Height settings for actuators edge 1

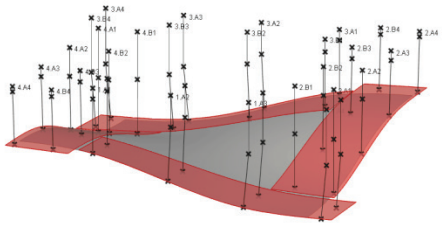

Figure 5.21: Height settings for all edges

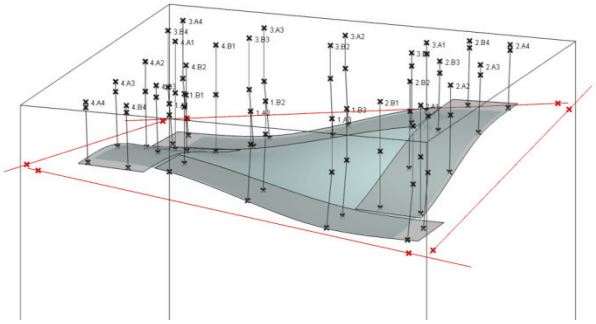

Figure 5.22: Height settings silicone rubber rods

Height correction

The eccentricity of the rotation point leads to a small inaccuracy in the height setting occurs (Figure 5.23 shows a 2D representation of this inaccuracy). This inaccuracy can be determined in 3D with the use of a surface normal vector. The calculation of the height correction can be seen in Figure 5.23. This correction has been applied for the Fluid Mould settings.

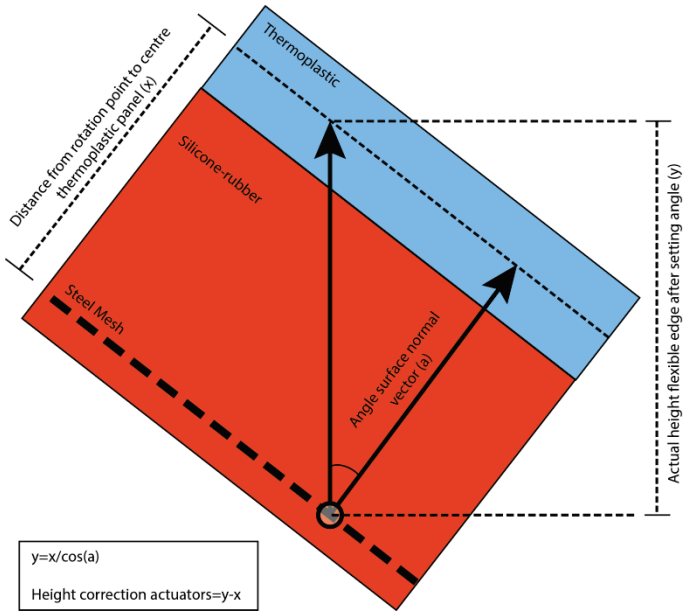

Figure 5.23: 2D representation of height inaccuracy due to eccentric rotation points

Set-up minimal height settings for the production process

A minimum height set-up has to be applied to the actuators in order to acquire sufficient clamping force by the springs by the Fluid Mould. The minimum height settings can be set as an input parameter. To calculate the actuator height settings a Hoopsnake analysis is run. For the first iteration the distance between the surface and the actuator grid is set to 1000mm. The distance between the smallest actuator height and the grid is calculated. Then the grid is moved downwards with this distance minus the minimum height set-up.

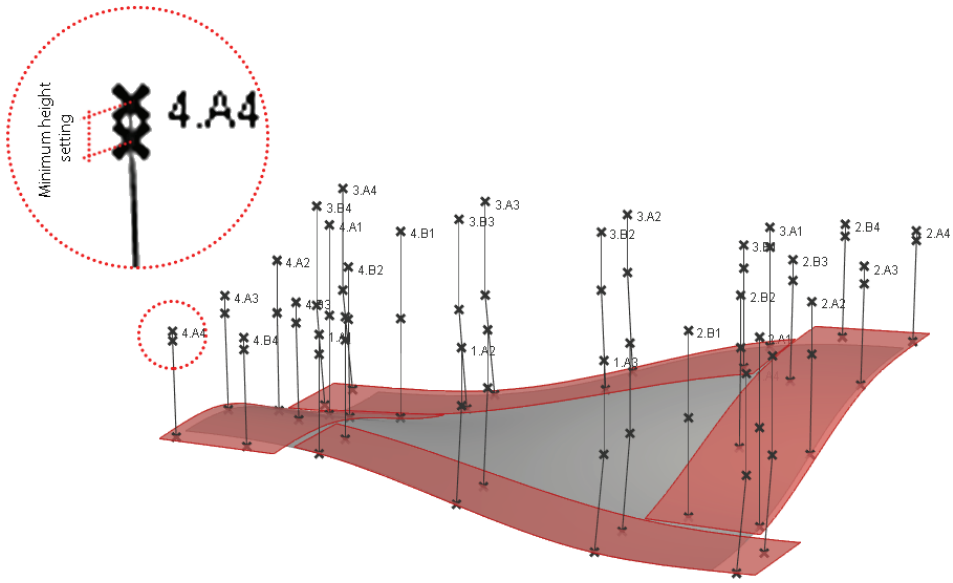

Figure 5.24: Minimum height setting

Maximal angle ball joints

The ball joints which are used have angular limitations. To verify these limitations are not exceeded, the ball joint angles are calculated in Grasshopper. The maximum angle is transferred to the Excel file. When the limitation is exceeded, a warning is given by colouring the Excel cell red.

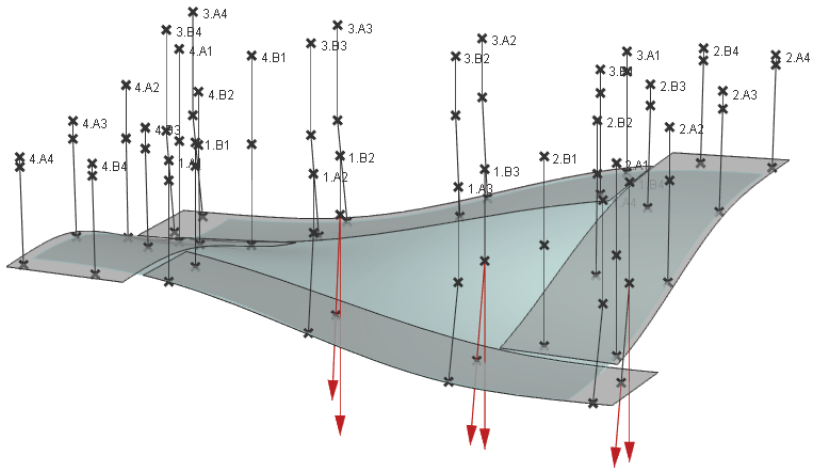

Figure 5.25: Angle ball joints

5.6 Grasshopper component 'Fluid Mould'

The Grasshopper analysis is complex and consists of many components. In order to keep the analysis organized, the components are clustered. In Figure 5.26 the clusters can be seen. The left red frame shows the Fluid Mould component, which is shown in an exploded view in the second red frame. In the Fluid Mould component two large clusters are used, these can be seen in the blue frames.

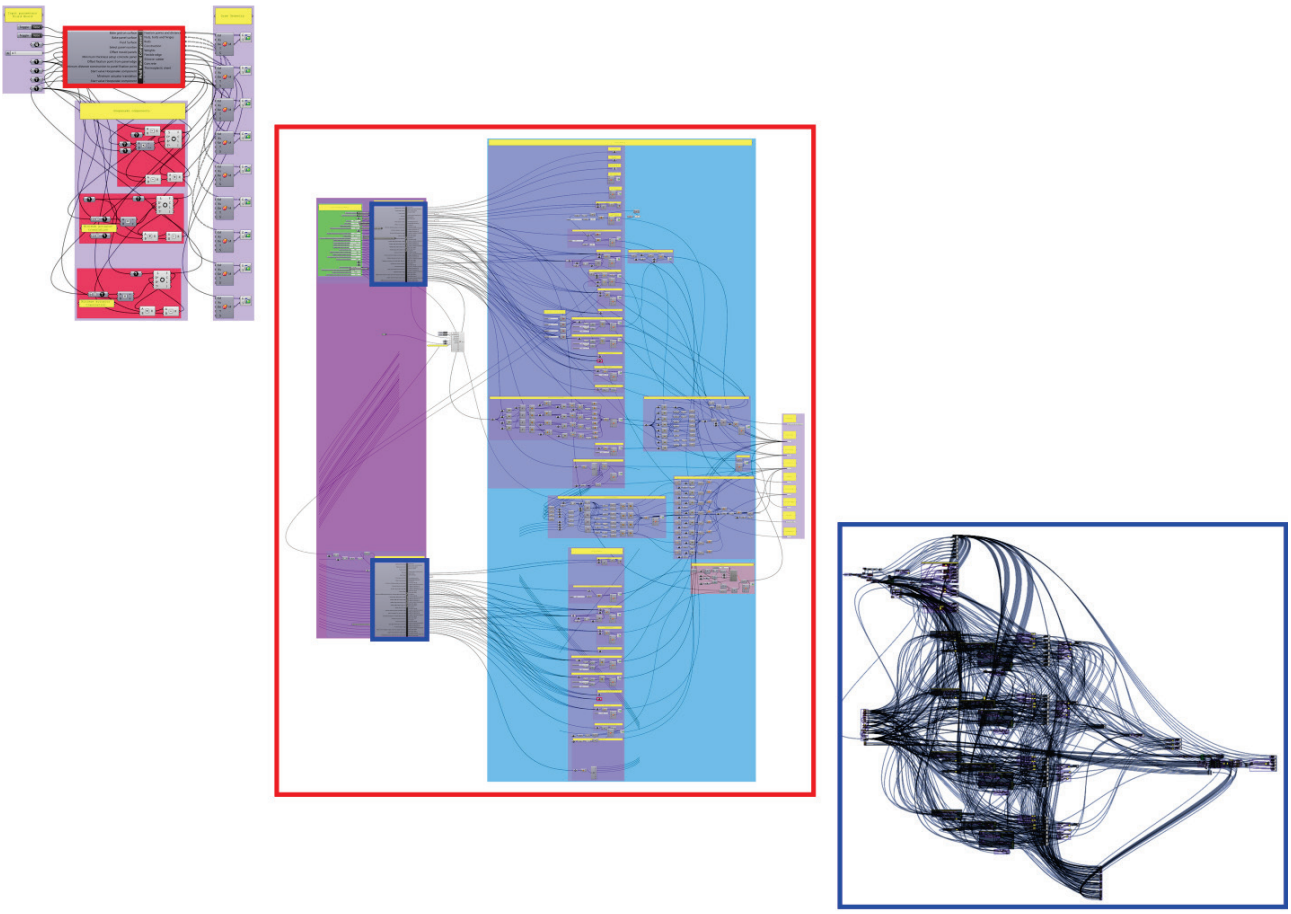

Figure 5.26: Grasshopper clusters

Figure 5.27 shows the Fluid Mould component with its input parameters, Hoopsnake analyses and geometric output. The following input parameters can be set in the Fluid Mould component:

- Fluid surface
- Toggle bake panel grid

- Toggle bake panel surface
- Panel selection
- Minimal thickness concrete panel
- Offset fixation point from panel edge
- Minimal distance between construction and panel fixation
- Minimum actuator translation

The red groups show the Hoopsnake analyses, which can be activated by clicking on 'Auto Loop All'. These analyses have to be run for each panel in order to obtain the proper mould settings. The output data will automatically be transferred to the proper worksheet in the open Excel template (appendix E shows the data of each panel). For a more representative visualization of the Fluid Mould, all points, curves and surfaces have been given a certain geometry, profile and/or thickness. This visualization is done in the group at the right, as can be seen in Figure 5.27. Figure 5.28 illustrates this visualization.
The Grasshopper file can be found in appendix F. To use this component, several Grasshopper plugins have to be installed:

- Lunchbox
- Bowerbird
- Paneling tools
- Geometry Gym
- Kangaroo
- Hoopsnake

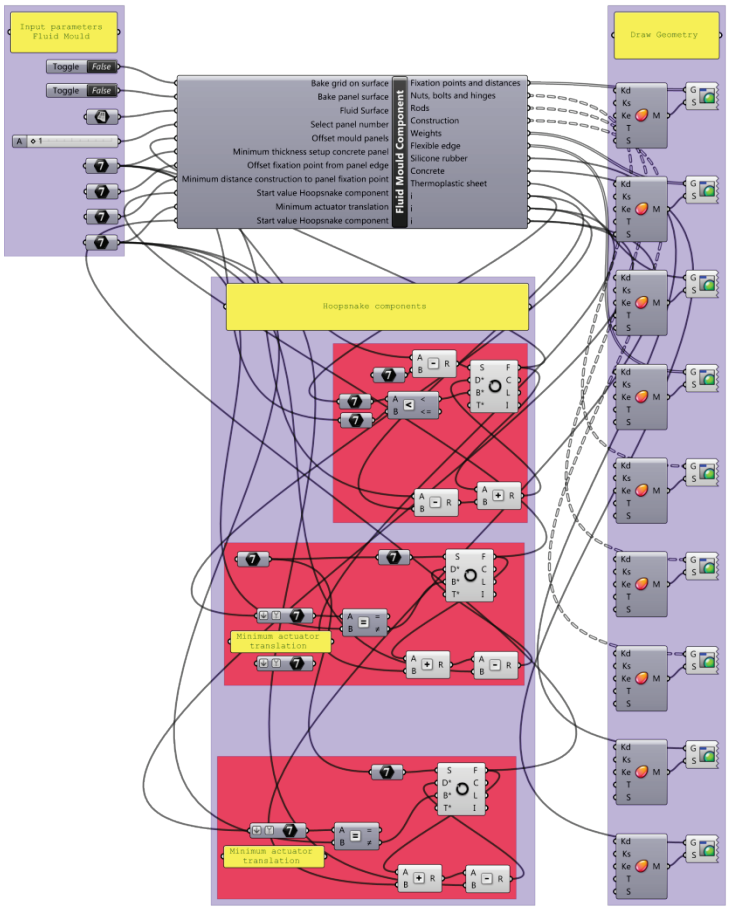

Figure 5.27: Fluid Mould Grasshopper component

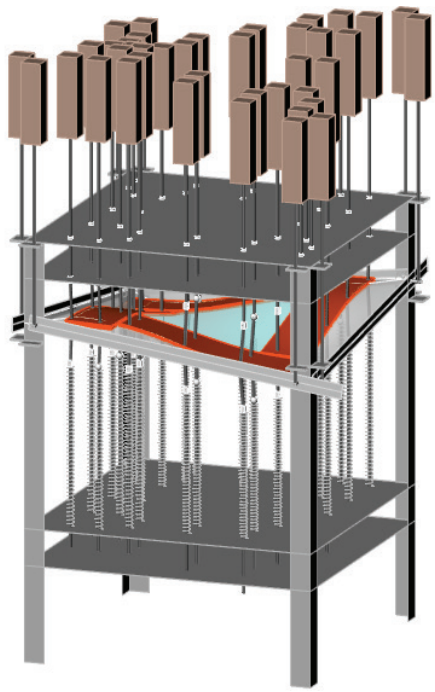

Figure 5.28: Fluid Mould Grasshopper geometry

6 Simulation

6.1 Nonlinear finite analysis software

After analysing the façade design with the use of Grasshopper, the actuator settings can be used as input for the simulations. The simulations are used to predict the deformation behaviour of the silicone rubber sheet and therefore the shape of the thermoplastic sheet. By applying a feedback to the design analysis, it can be checked if the desired shape is achieved. If the desired shape not is achieved, different settings to manipulate the silicone rubber can be used in order to approximate the desired shape.

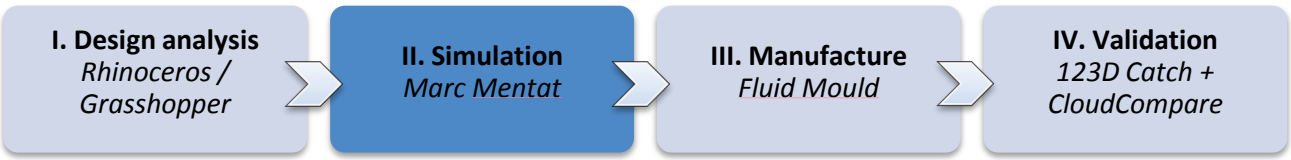

Figure 6.1: Overview of the production process

The finite element analysis (FEA) program 'MSC Marc Mentat' is used to simulate the deformation behaviour of the flexible layer. This software package provides nonlinear analysis capabilities for contact simulations, large deformations / racks or multi physical analyses in static or quasi-static (reversible) domain. The accuracy of the contact simulations determines the accuracy of the deformation behaviour of the flexible layer, therefore the software application 'MSC Marc Mentat' is chosen. In addition, large deformations will occur during these contact simulations. Many other FEA programs are limited to linear material properties and small deformations and/or small rotations. (D2S-International, n.d.).
The FEA program 'MSC Marc Mentat' consists of the parts 'Marc' and 'Mentat'. 'Mentat' is able to generate the data of a model (pre-processing) and is used for the visualization of a model. Once a model is completed in 'Mentat', the data can be exported to 'Marc'. 'Marc' generates the results (post-processing) which can be analysed by 'Mentat', as can be seen in Figure 6.2. The application 'Marc' can be executed in 'Mentat', (Rietbergen, 2011).

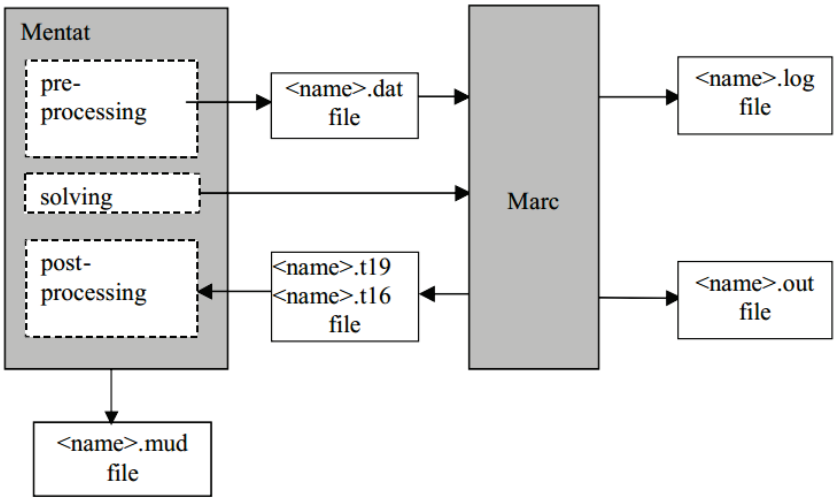

Figure 6.2: Schematic representation of 'Mentat' in combination with 'Marc' (adapted from Rietbergen).

Dr.ir. L.C.A. (Lambert) van Breemen from the 'Department of Mechanical Engineering' at the Eindhoven University of Technology assisted the simulation process. His expertise in simulating the behaviour of polymers by 'Marc Mentat' was found to be very valuable. Much effort was needed to complete the simulation model.

6.2 Structure of the simulations

A simplified representation of the Fluid Mould is modelled in Marc Mentat. The simulation model consists of the flexible layer, flexible edges, and side rods (Figure 6.3). The thermoplastic sheet is not physically modelled in the simulation model in order to simplify the calculations.

All simulations are done with the use of version 'Marc Mentat 2013.0.0'. The used units are [mm] and [N].

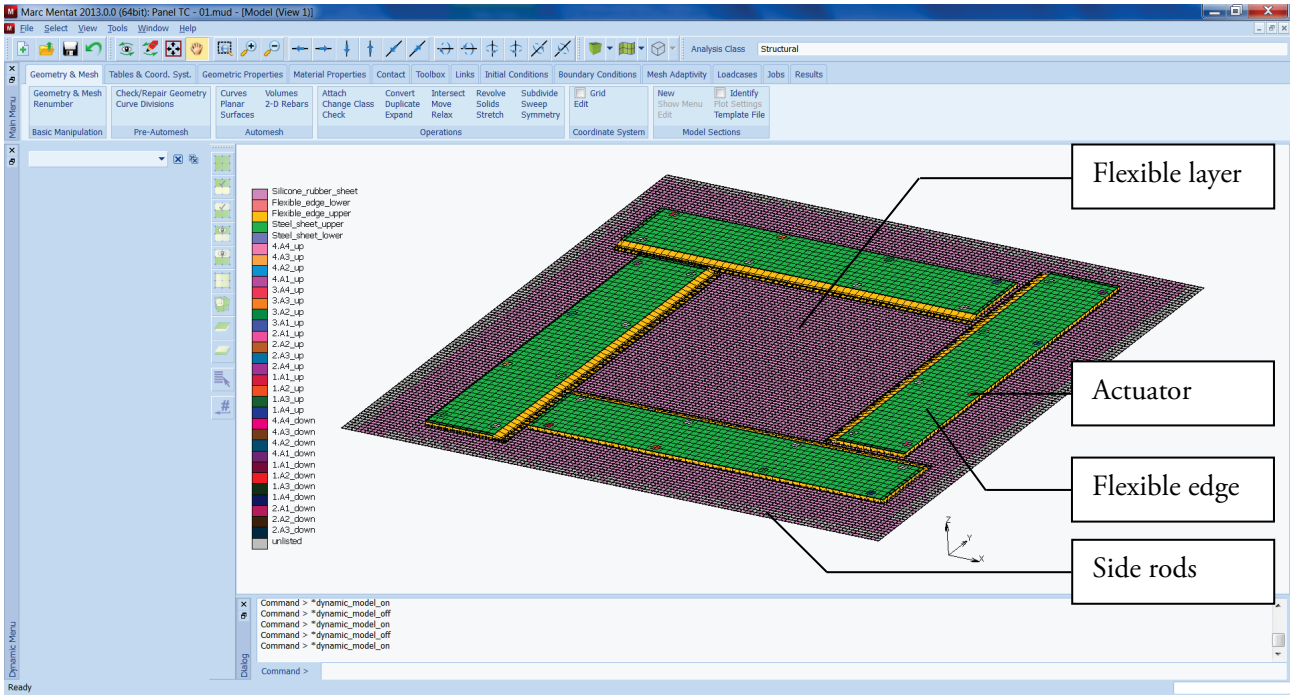

Figure 6.3: Interface of the Fluid Mould simulation model in MSC Marc Mentat,

The flexible layer will be manipulated with the use of face loads, flexible edges and side rods. Two boundary conditions of face loads are applied to the flexible layer. The face loads consists of the own weight of the silicone rubber (replacement of gravity load) and the own weight of the thermoplastic sheet (Table 6.1). The use of solely face loads simplifies the simulation, instead of using a gravity load and a face load. The face loads will be first applied in the simulation process (Table 6.2).

Face load calculation			
Silicone rubber sheet:	Mass density	1,15	g/cm³
	Dimensions	800	mm
		800	mm
		0,5	mm
	Total weight	368	g
		3,61	N
	Face load	5,641E-06	N/mm²
Thermoplastic sheet	Mass density	1,2	g/cm³
	Dimensions	650	mm
		650	mm
		3	mm
	Total weight	1521	g
		14,92	N
	Face load	3,532E-05	N/mm²

Table 6.1: Calculation total face load

The flexible layer is attached to four side rods. In the simulation model the side rods are represented by surfaces and are attached to the flexible layer. The outside movement of the surfaces ensures the amount of tension in the flexible layer and therefore the approximated deformation this layer. The movement of every side rod is entered by x, y and z-directions, a radius in radians and the centre of rotation per side rod. Applying tension by moving

the side rods is the second step in simulation process and will be accomplished in a specific period of time (Table 6.2).
Eight small surfaces are attached per flexible edge. These surfaces represent the top of a pendulum rod and determine the movement of the flexible edges. All positions of the surfaces are retrieved from the Grasshopper analysis. The desired position will be obtained by entering the x, y and z-directions. Applying the tension and obtaining the desired positions will finally be achieved in two different periods of time (Table 6.2).

	Simulation steps									
	1	*2*	*3*	*4*	*5*	*6*	*7*	*8*	*9*	*10*
1. Applying face loads										
2. Applying tension by moving the side rods										
3. Movement side rods										
4. Movement actuators										

Table 6.2: Time lapse simulation model

The processes 'movement side rods' and 'movement actuators' contains the most steps. The flexible edges will deform the flexible layer during this process which is the most critical part of the accuracy of the simulation. These contact simulations are very complex and thereby time-consuming.

6.3 Material properties

Two various types of silicone rubbers are used which each have a specific hardness. A hardness of shore A50 is used for the flexible edges and a hardness of shore A60 is used for the flexible layer. To model the elements with the silicone rubber material properties, the Mooney-Rivlin model is used (chapter 3). The silicone rubber material properties are retrieved from the document 'Analyzing Hyperelastic Materials w/ Some Practical Considerations' (Altidis, et al., 2005).

6.4 Properties simulation model

In Table 6.3, the specific properties of the model are showed.

Marc Mentat input			
Options	*Selections*	*Specifications*	*Additional specifications*
Geometry & Mesh:	• Elements (14400): • Elements (2592): • Elements (2592) • Surfaces (4 pcs) • Surfaces (64 pcs):	Flexible layer Upper flexible edge Lower flexible edge Side rods Actuators	800x800x0.5 [mm] 130x530x10 [mm] 130x530x10 [mm] 740x20 [mm] Every actuator attached to one node of the flexible edge
Material properties (Silicone rubber)	• Mooney-Rivlin (shore A50): o C10: o C01: • Mooney-Rivlin (shore A60): o C10: o C01:	 0,302 MPa [N/mm^2] 0,076 MPa [N/mm^2] 0,474 MPa [N/mm^2] 0,118 MPa [N/mm^2]	Flexible edges Flexible layer
Boundary conditions:	• Face load (applied to 14400 elements): • Face load (applied to 9667 elements):	5.64e-006 [N] 3.53e-005 [N]	Weight flexible layer (800x800mm) Weight PC sheet (650x650mm)

Contact bodies:	Deformable cbody: Rigid contact body: Rigid contact body: Rigid contact body: Rigid contact body: Rigid contact body: Rigid contact body: Rigid contact body: Rigid contact body: Rigid contact body: Rigid contact body: Rigid contact body: Rigid contact body:	Silicone rubber sheet Actuator_1.A1_up (up to……..) Actuator_4.A4_up Actuator_1.B1_up (up to……..) Actuator_4.B4_up Actuator_1.A1_down (up to……..) Actuator_4.A4_down Actuator_1.B1_down (up to……..) Actuator_4.B4_down Side_rod_1 Side_rod_2 Side_rod_3 Side_rod_4	(All settings retrieved from Grasshopper model per panel)
Contact table	• Contact_table_1		
Contact interactions	• Meshed (Deformable) • Meshed (Deformable) • Meshed (Deformable)	Touching Glued (Geometric) Glued	Contact between elements Contact between elements and surfaces Contact between elements
Element types	• 3-D Solid	Full integration (7) Full & Herrmann F. (84)	Steel material Silicone materials
Tables	• Time table 1 (steps: 10) • Time table 2 (steps: 10) • Time table 3 (steps: 10)	Applying faceload Applying tension Movement actuator	Step 0 to 1 Step 1 to 2 Step 2 to 10
Loadcases	Constant time steps	Step interval: 0,005	Total steps: 400

Table 6.3: Model structure Marc Mentat

6.5 Results

A job can be submitted after defining the model parameters. Approximately 7 to 9 hour is needed to complete one job. Eventually, three simulation jobs have been succesfully runned. Panel 3 has been excluded for the simulations, because this panel has not been produced.

6.5.1 Panel 1

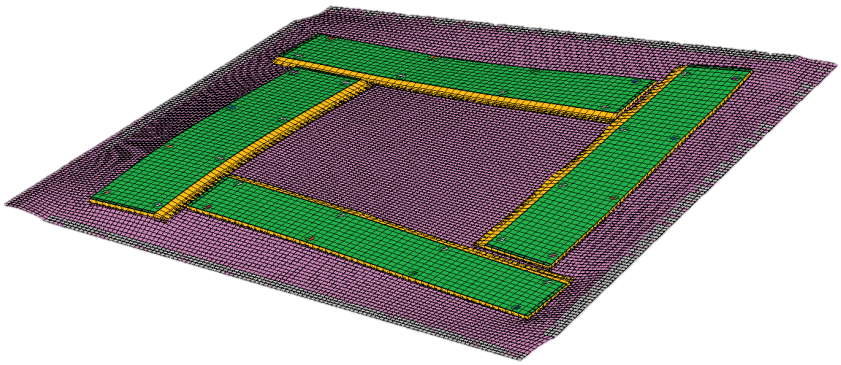

Figure 6.4: Visualization result of the panel 1 simulation by 'Marc Mentat'

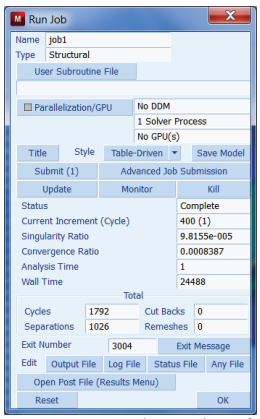

Figure 6.5: Job results of panel 1

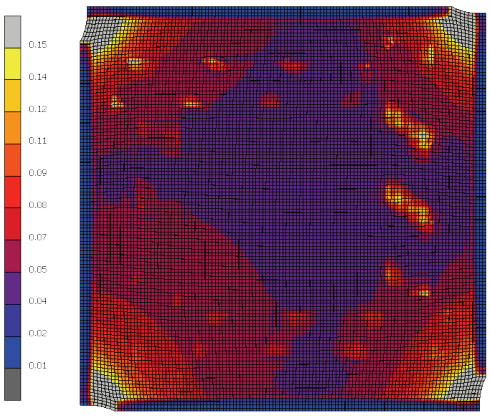

Figure 6.6: Equivalent of total strain

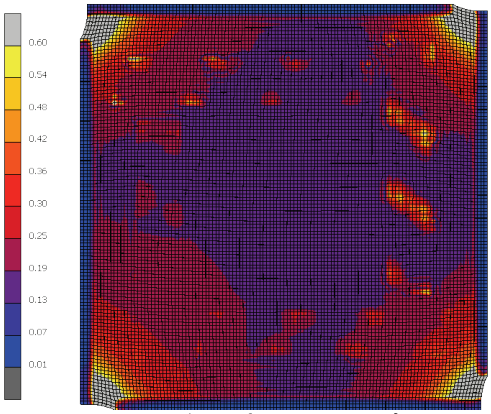

Figure 6.7: Equivalent of stress [N/mm^2]

The results shown in Figure 6.6 and Figure 6.7 provide an estimation of the equivalent of total strain and the equivalent of stress of the silicone flexible layer. In the simulation results can be seen most strain occurs in the corners. However, it is not possible to attach the corners of the flexible layer to the side rod of the Fluid Mould, because the L-shaped colums are positioned in the corners. The prevention of the relative high stresses is an additional advantage. It is decided to attach the corners of the flexible layer to the side rod to aviod loose hanging corners in the simulation model. The loose hanging layer would make the simulation model unnecessarily complex. This also implies to the other simulations of panel 2 and panel A.

It is clearly noticeable the maximum strain ratio of 3,5 will not be reached according this prediction, as can be seen in Figure 6.6. The strain ratio of 1,0 is not even reached, so the Mooney–Rivlin model should give a valid representation (chapter 3). As can be seen in Figure 6.7, the tensile strength of 6 N/mm^2 for silicone rubber will not be reached as well (the silicone rubber material properties are shown in Table 3.3.

6.5.2 Panel 2

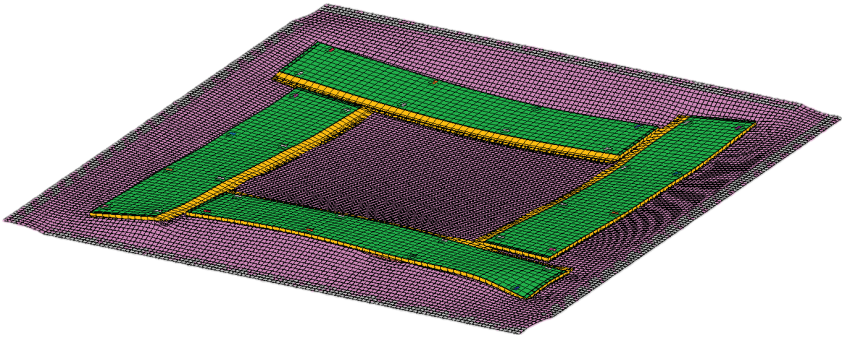

Figure 6.8: Visualization result of the panel 2 simulation by 'Marc Mentat'

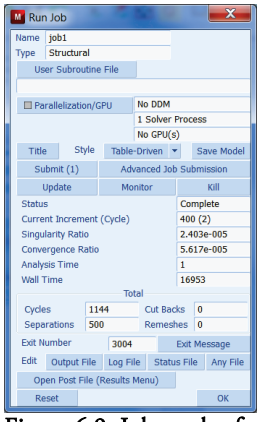

Figure 6.9: Job resuls of panel 2

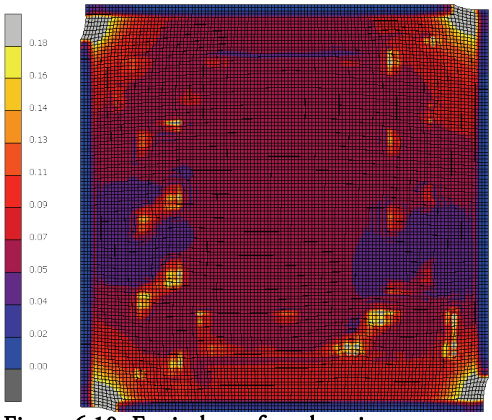

Figure 6.10: Equivalent of total strain

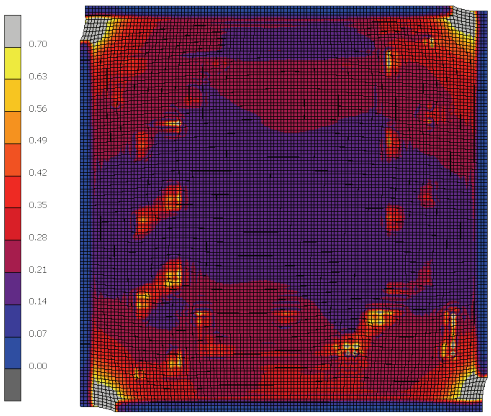

Figure 6.11: Equivalent of stress [N/mm^2]

The patterns of the actuators are visible in Figure 6.10 and Figure 6.11 (also present in the simulation model of panel 1). The upper and lower actuators are moved to the desired positions through the use of fixed displacements set in the boundary conditions of the simulation model. This implies when the desired positions of the actuators are achieved, the actuators are fixated at that exact position. The upper actuators of the Fluid Mould have the same principle. When the nuts are supported by the upper steel plate, the actuators should be fixated to the proper position due to the gravity load. However, the lower edges are always applying upward pressure due to the compression springs. The simulation represents therefore not a plausible estimation at the sections of the actuators. The simulation uses a fixed displacement of both upper and lower actuators, by which the clamping force which is applied by compression springs in the lower actuators is excluded.
Similar to the simulation of panel 1, the tensile strength and maximum strain are not reached. The simulation model should give an valid prediction.

6.5.3 Panel A

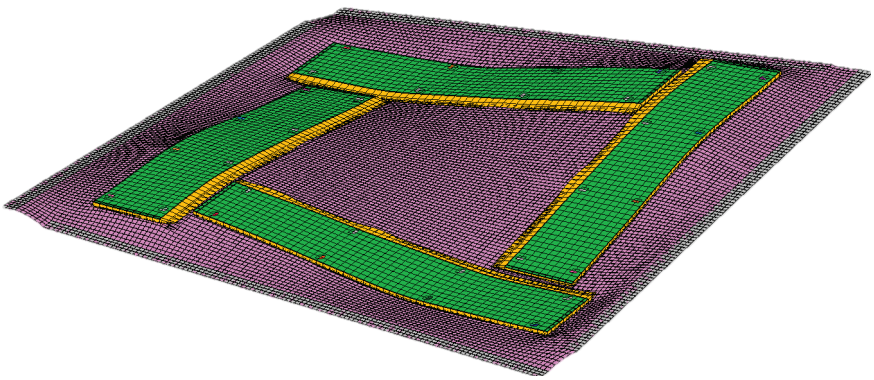

Figure 6.12: Visualization result of the panel A simulation by 'Marc Mentat'

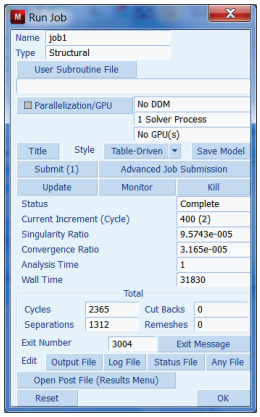

Figure 6.13: Job results of panel A

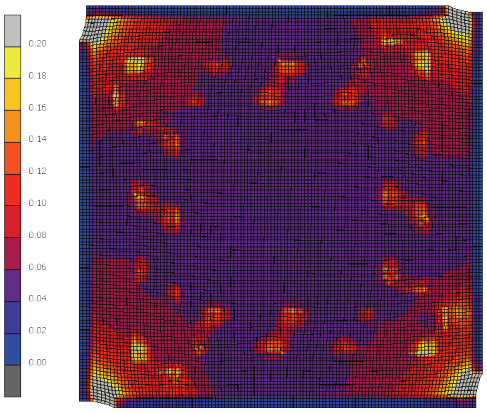

Figure 6.14: Equivalent of total strain

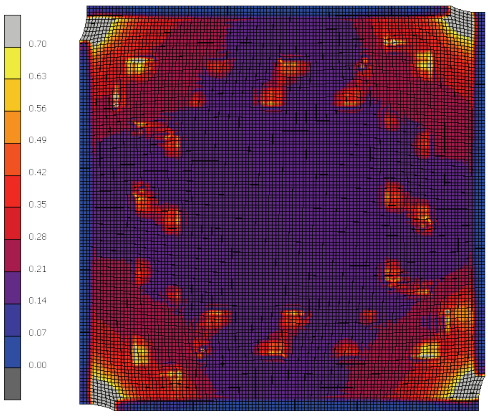

Figure 6.15: Equivalent of stress [N/mm²]

The symmetry of panel 'A' gives an approximately uniform distribution of stress and strain (Figure 6.14 and Figure 6.15). The tensile strength and maximum strain are not reached. The predicition should be valid.

6.5.4 Panel B

The simulation process of the panel B is the most complex calculation compared with the abovementioned simulations. This is due to the relative extreme curvatures of panel B. The mentioned structure of the simulation model in paragraph 6.2 was not able to generate a successful outcome of the simulation for Panel B. This is caused by excluding the pendulum rods in the simulation model. Each flexible edge is controlled by eight little surfaces. These surfaces move linear from the start position to the desired position while in reality these points because of the use of pendulum rods do not move linear, as can be seen in Figure 6.16. During the simulation process the flexible edges could not properly deform which causes an incorrect outcome. Noteworthy, the simulation models of the panels '1', '2' and 'A' did not have any struggle with the linear paths of movement of the actuators.

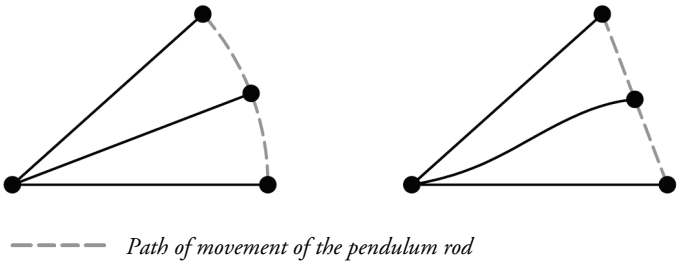

Figure 6.16: Movement pendulum rods. Left: The actual movement of points attached to a pendulum rod. Right: The simulated movement of these points.

If the pendulum rods would be modelled in the simulation model, the flexible edge should theoretically be able to deform smoothly during the simulation process. However, this will make the simulation model far more complex. Each flexible edge would consist of one fixed pendulum rod, four pendulum rods with planar degree of freedoms (clevis eye connections) and three pendulum rods with three-dimensional degree of freedoms (ball joint connections). Due to the degree of freedoms, the calculation becomes more complex and the risk of miscalculations will thereby be increased significantly.

6.5.5 Penetration failures

In some simulation models some penetration occurs between the flexible edges and flexible layer, as can be seen in Figure 6.17 and Figure 6.18. This can be reduced or even prevented through applying more calculation steps for a job and/or by subdividing the elements for a sufficient amount. Adding more steps to a simulation model is

a minor adjustment. The wall time of a job will not increase much while the simulation model will significantly improve, as can be seen in Figure 6.19 and Figure 6.20.

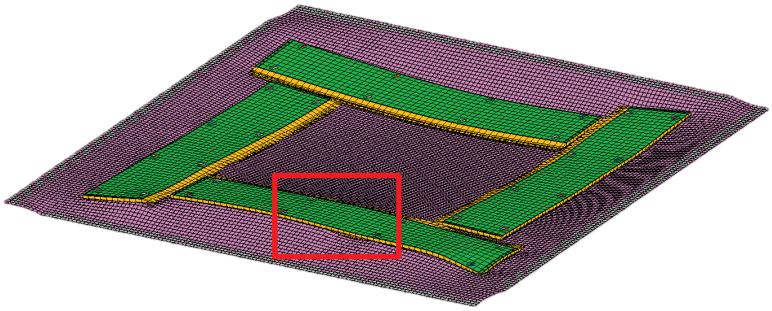

Figure 6.17: Penetration occurred in the simulation of panel 2 using 200 steps (Wall time 6:40h)

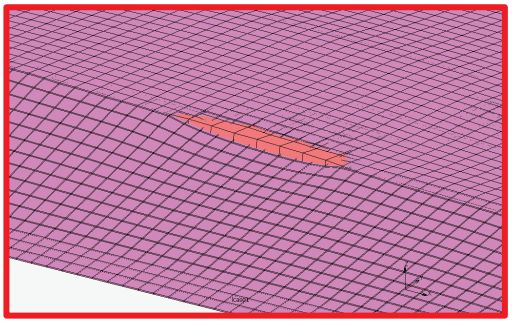

Figure 6.18: Detail view of penetration using 200 steps

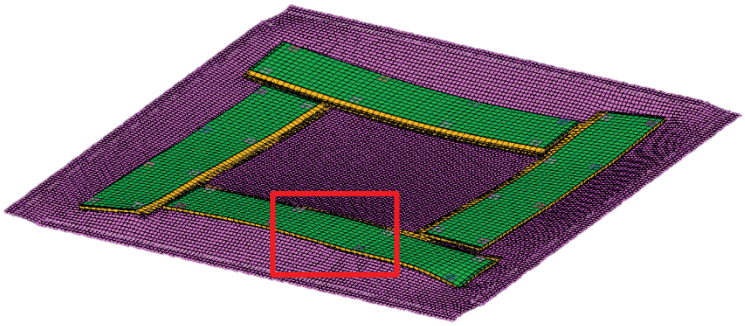

Figure 6.19: Penetration occurred in the simulation of panel 2 using 400 steps (Wall time 8:50h)

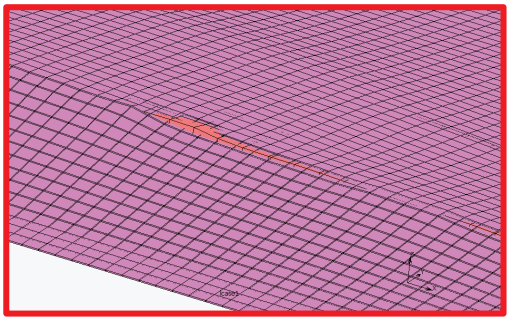

Figure 6.20: Detail view of penetration using 400 steps

The required amount of elements depends on the 'master-slave' ratio (Shetty, 2013). The 'master' component is the movable part which should have a less fine mesh than the 'slave' (static) component (Figure 6.21). Nevertheless, the calculation becomes more complex when the elements are subdivided and takes significantly more time. The used simulation model used a 'master-slave' ratio of 2:3.

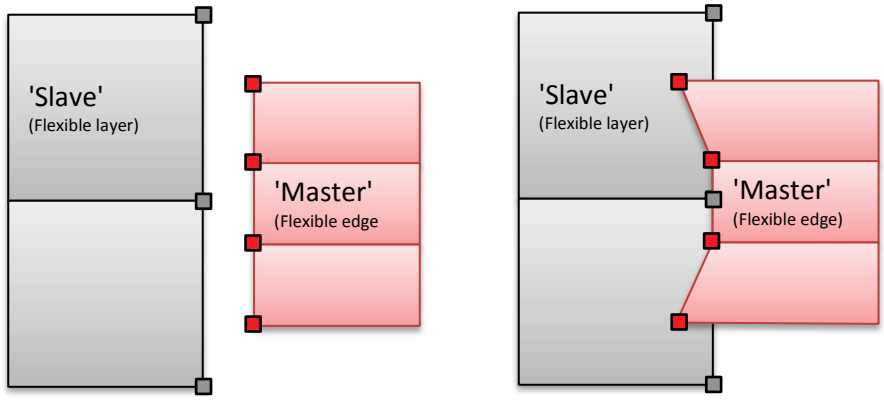

Figure 6.21: Penetration problem occurs when the 'master' components consist of a finer mesh than the slave component (replicated from Shetty)

6.6 Conclusions

The simulation model of the simplified representation of the Fluid Mould operates. The results of the simulation models '1', '2' and 'A' should provide a plausible prediction of the deformation behaviour of the flexible layer. However, the simulation model failures to more complex curvatures (panel 'B'), which is caused by excluding the pendulum rods in the simulation.

It has to be noted these simulations are only capable to predict the deformation behaviour of the silicone rubber layer. Thermoplastic properties such as thermal expansion and shrinkage could have a significant effect on the deformation behaviour of the thermoplastic sheet. However, these properties are not included in the simulation model. Thermal expansion of the Fluid Mould itself is also not included.

The first intension was to apply various tension settings in order to manipulate the flexible layer if the desired geometry was not approximated with sufficient accuracy. This would require a validation feedback to the design analysis. Unfortunately, it takes too much time and effort to iteratively validate the simulation model and to return a job. The wall time can take up to 8,5 hours. Eventually it is decided to use of one setting of tension; all edges of the flexible layer are stretched 10mm outwards. Consequently, the flexible layer of the Fluid Mould is stretched totally 20mm outwards.
In chapter 8 'Validation' the accuracy of the predicted deformation by the simulation models will be elaborated.

7 Mould Manufacture

7.1 Calibration and preparation Fluid Mould

For the production of thermoplastic moulds, the entire Fluid Mould is placed in a large oven. In this chapter the manufacturing procedure is elaborated.

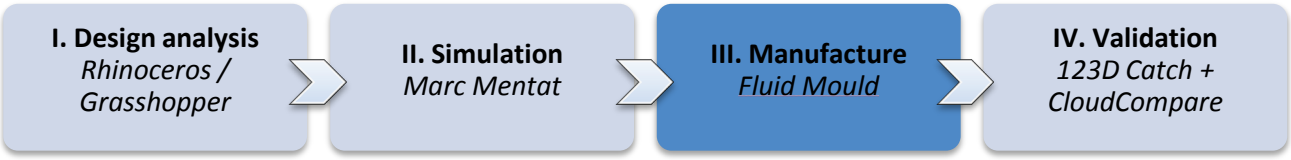

Figure 7.1: Overview of the production process

Before the actuators of the Fluid Mould can be set in the proper height, the actuator heights have to be calibrated. A zero level is required in order to set the actuators in the proper heights. To gain a zero level, each flexible edge is positioned on horizontally placed wooden laths, as can be seen in Figure 7.2. The laths are supported by the side rods, which are fixated horizontally to the Fluid Mould at a certain distance between the top of the side rod and the top of the L-shaped column (Figure 7.3).

Figure 7.2: Calibrating the flexible edge with the use of wooden laths supporting on the side rods

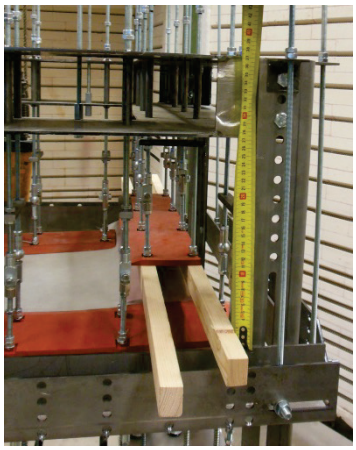

Figure 7.3: Fixating the side rod to obtain a zero level

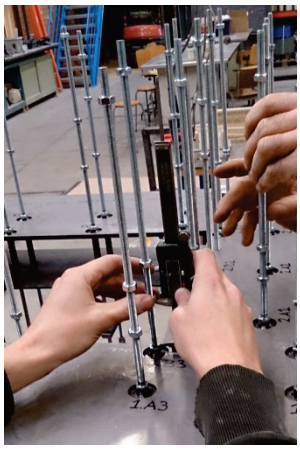

Figure 7.4: The top of the steel plate is taken as the measure point

Once the side rods are fixated and the flexible edge is completely supported by the wooden laths, the nuts can be set to the proper height. The top of the steel plate is taken as the measuring point, as can be seen in Figure 7.4. By the use of a digital calliper the nuts are set in the desired height. These height settings are obtained from the 'Excel' file created with the use of the Grasshopper analysis. Two nuts are tightened counter-wise to ensure a proper fixation.

After calibrating all flexible edges and setting all nuts to the proper height, the weights are fixated on top of the actuators. The next step is to lift the lifting plate so space between the flexible edges is created. This space is needed to place the thermoplastic sheet between the flexible edges, as can be seen in Figure 7.5. The lifting plate is eventually lowered to distance holders (Figure 7.6), so the upper flexible edges stay in horizontal position and leave some space between the flexible edges and thermoplastic sheet. This space ensures a more homogeneous heated thermoplastic sheet during the oven process. The Fluid Mould can now be placed in the oven, as can be seen in Figure 7.7.

Figure 7.5: Lifting up the lifting plate

Figure 7.6: Lifting plate supported by the distance holders

Figure 7.7: Fluid Mould ready to use

7.2 Setting the oven

The foundation 'Beeldenstorm' at Eindhoven is in possession of a 'Toma ceramic oven type 9512/100245' and is controlled by a 'Toma oven regulator type 914-01801'. With the use of this regulator, the oven is set step by step. The settings used for the first experiment to deform a polycarbonate sheet can be seen in Table 7.1.

Configuration of the 'Toma oven regulator type 914-01801'		
Step number	*Time [min]*	*Temperature (°C]*
13.1	0 (ASAP)	120
13.2	60	120
13.3	0 (ASAP)	180
13.4	15	180

Table 7.1: Oven set-up first experiment polycarbonate

Figure 7.8: Oven regulator

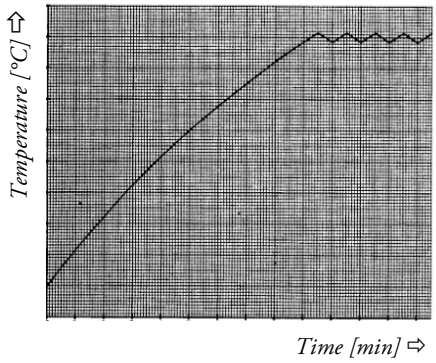

Figure 7.9: Schematic chart progress of the oven (adapted from natuurkunde.nl)

Once the regulator is set and started, the oven is heated approximately to the desired temperature. The oven will be turned off automatically when the temperature is ±6°C above the desired temperature. The oven will eventually heat again automatically if the temperature is ±6°C below the desired temperature. This procedure (Figure 7.9) continues during the entire process until the set time is reached and the oven will be finally turned off.

7.3 Manufacturing process

After placing the Fluid Mould in the oven (Figure 7.10) and setting the oven regulator, the oven is turned on. The Fluid Mould is ready to be pulled out of the oven after a period of approximately 85 minutes (Figure 7.11). The lifting plate is held at place by four people (Figure 7.12), which allows a fifth person to remove the distance holders (Figure 7.13). Now the lifting plate can be completely lowered and so the actuators are set to the proper height (Figure 7.14). It has to be noted safety clothing is required to prevent burning injuries. Now the contours

of the flexible edges can be drawn at the thermoplastic sheet, so it can later be cut to the proper dimensions (Figure 7.15). After cooling, the thermoplastic sheet can be removed from the Fluid Mould (Figure 7.16) and the same process can be repeated for the other thermoplastic sheets. The next step is to cut the thermoplastic sheet to size, this is done with the use of a band saw (Figure 7.17).
The thermoplastic moulds for panel 1, panel 2, panel A and panel B are produced by the described procedure.

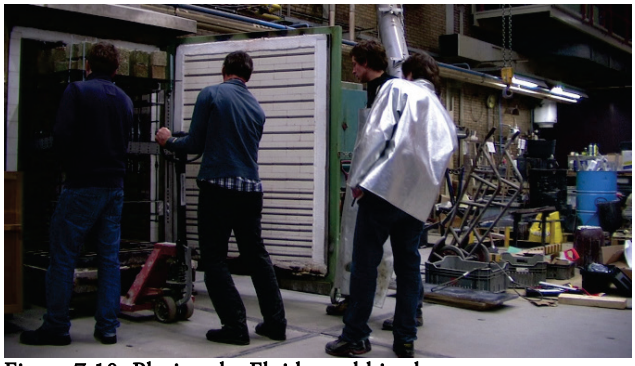
Figure 7.10: Placing the Fluid mould in the oven


Figure 7.11: Pulling out the Fluid Mould


Figure 7.12: Lifting the lifting plate


Figure 7.13: Removing the distance holders


Figure 7.14: Lowering the lifting plate


Figure 7.15: Drawing contours flexible edges and let the thermoplastic sheet cool

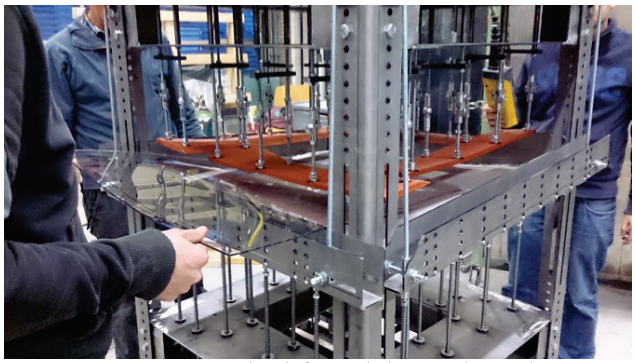

Figure 7.16: Removing the deformed thermoplastic sheet

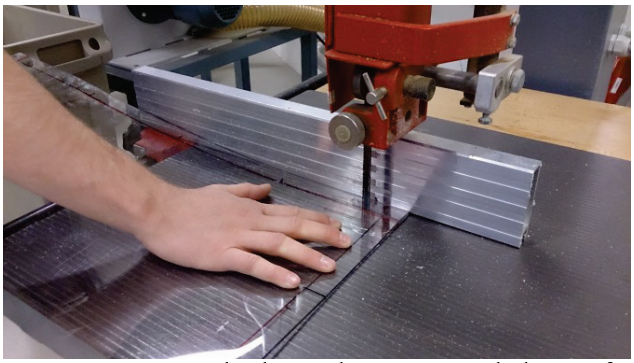

Figure 7.17: Cutting the thermoplastic to size with the use of a band saw

7.4 Concrete casting

Lightweight concrete (Beamix concrete 111) has been used to produce the double curved cladding panels. The required volume of concrete has been derived from the Grasshopper analysis.
To ensure a closed mould, the material XPS (Styrodur 2500 C) is chosen as a formwork. This allows slices to be cut in the formwork (Figure 7.18) so the thermoplastic sheets can be fixated by clamping the sheets in this seam. The thermoplastic sheets are placed at 50mm offset. The formwork is clamped with the use of threaded rods and the seams are sealed with the use of tape (Figure 7.19). To prevent the thermoplastic sheets to deform caused by the hydrostatic pressure of casted concrete, XPS blocks are fixated along the edges of the thermoplastic sheets. The middle sections of the thermoplastic sheets are supported by nine threaded rods on each side (Figure 7.20). These rods are used, so the thermoplastic sheets could be monitored while casting the concrete. The hydrostatic pressure of the concrete has been so large that the thermoplastic sheets at various locations at the threaded rods cracked (Figure 7.21 and Figure 7.22). These cracks could be observed at the concrete surface after removing the formwork (Figure 7.23). Figure 7.24 to Figure 7.27 show the results of the concrete casting of panel 1 and panel B. The surfaces of both panels are very glossy. However, many surface voids can be observed and the surface is not entirely smooth due to the point loads of the threaded rods.

Figure 7.18: Cutting slices in the XPS formwork

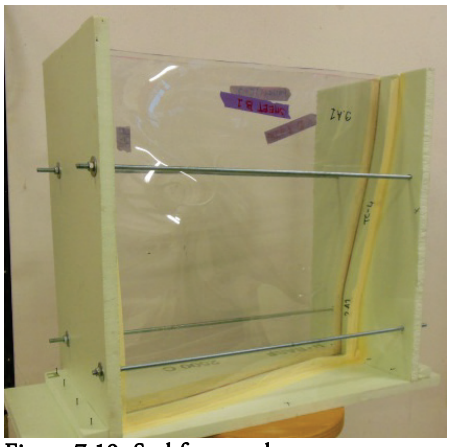

Figure 7.19: Seal formwork seams

Figure 7.20: Formwork supported with pins

Figure 7.21: Concrete casted

Figure 7.22: Cracks in thermoplastic sheet

Figure 7.23: Crack thermoplastic visible at concrete surface

Figure 7.24: Panel 1 front

Figure 7.25: Panel 1 back

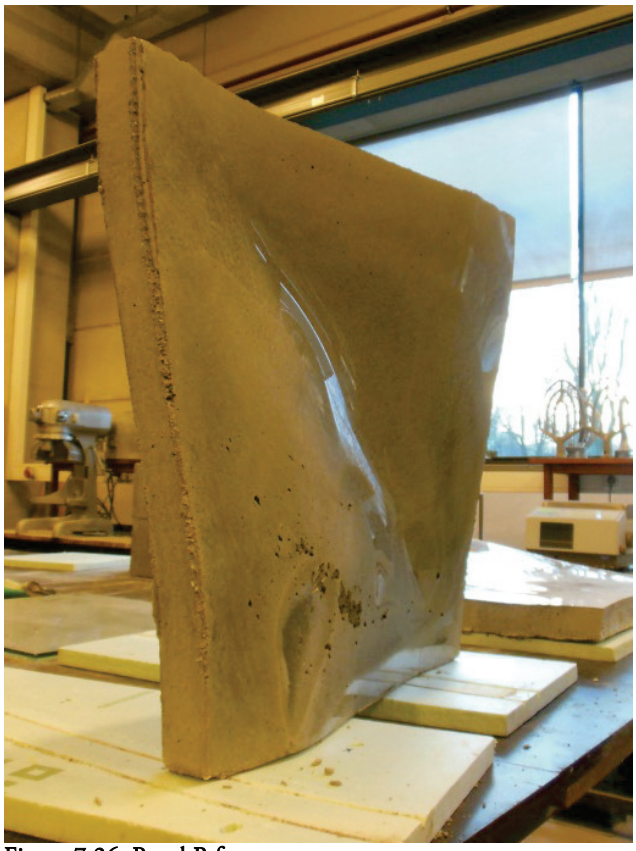

Figure 7.26: Panel B front

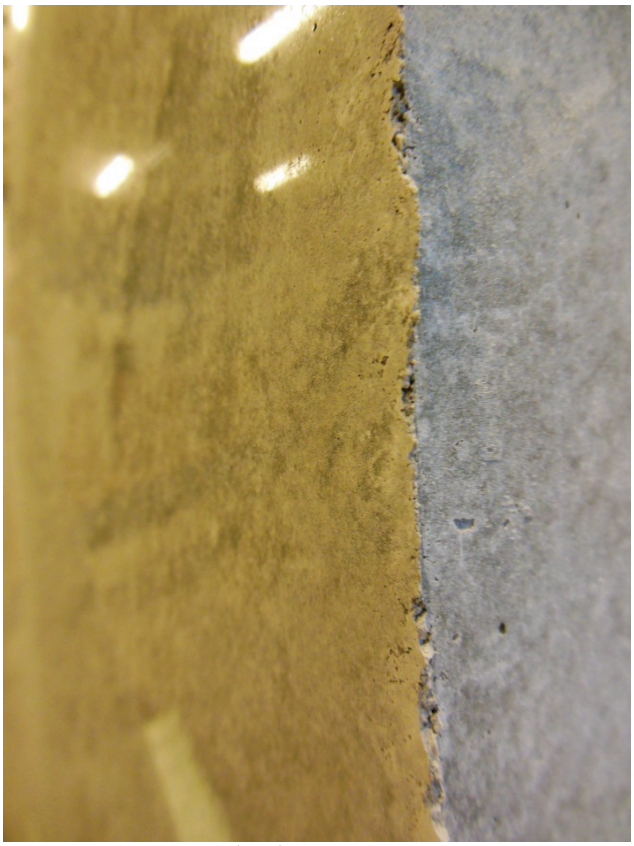

Figure 7.27: Concrete detail

Another cast has been done with the use of fine granules instead of threaded rods as counter pressure and stronger boards have been used as a formwork (Figure 7.28). This method uses a uniformly distributed load instead of point loads so the thermoplastic sheets do not crack. When the concrete is cured, the formwork can be removed (Figure 7.31). Although a uniformly distributed load was applied, one small crack could be observed in the thermoplastic sheet after removing the formwork. The resulting concrete panel can be seen in Figure 7.32 to Figure 7.35. This concrete panel is less glossy than the previous casted concrete panels, which is probably due to dust that came from the granules. The dust stuck to the release agent which had been applied to the thermoplastic sheet. However, the concrete surface has fewer surface voids and it is smoother. Also the edge of the panel obtained a higher aesthetical quality than the other concrete panels.

Figure 7.28: Granules used for counter pressure

Figure 7.29: After the concrete is cured the supporting material can be removed

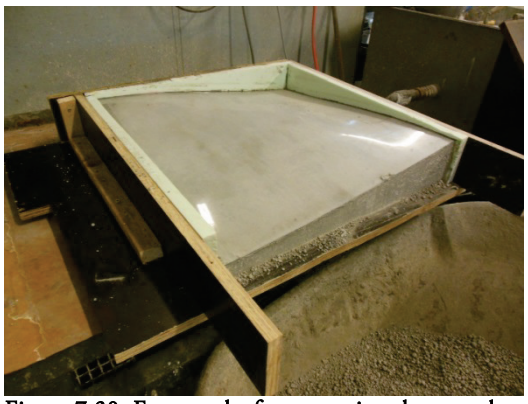

Figure 7.30: Formwork after removing the granules

Figure 7.31: Resulting concrete panel

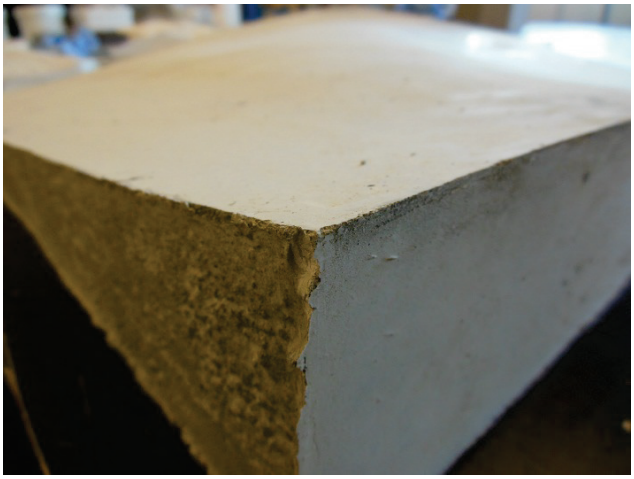

Figure 7.32: Detailed view of casting side and mould side

Figure 7.33: Resulting concrete panel

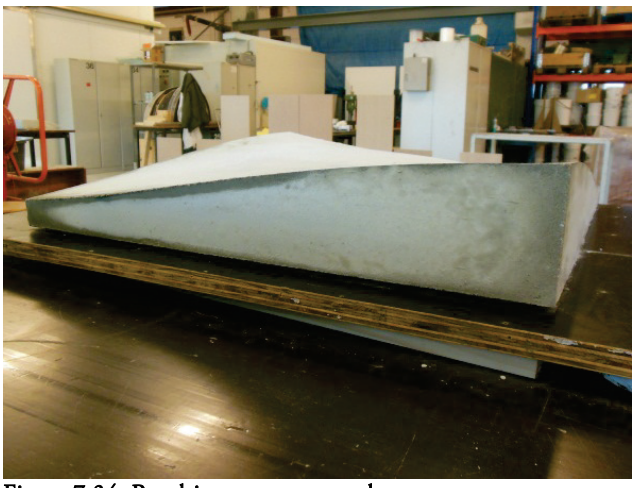

Figure 7.34: Resulting concrete panel

7.5 Conclusions

No major setbacks occurred during the manufacturing process. The discussed steps (Figure 7.10 to Figure 7.17) were done smoothly. However, some actuators jammed occasionally. The play of the actuators is more than expected. The main cause is the inner radius of the guide pipes is larger than was ordered. The play of guide pipes and the slightly bending actuators could cause jamming of the actuator. A little push was needed to lower the actuator in the end. The lower actuators jammed occasionally due to the compression springs. The end part of the springs could get stuck to the steel guide pipes. Bending the end of the spring and checking the springs before the Fluid Mould is placed the oven partially solved this problem.
The main issues are the labour-intensity of the lowering of the weights and the time-consuming calibration and preparation of Fluid Mould. An implementation of for example a heat resistant lifting jack into the Fluid Mould could solve the labour-intensive activity of lowering the weights. The calibration time and preparation time can relative easy be reduced with the use of stepper motors. As discussed before, the investment costs for this adjustment are too high and so the time consuming process is taken for granted. It does not have major influence of proving the concept of the Fluid Mould.

The use of a large oven could eventually affect the thermoplastic sheet of obtaining the desired shape. It took about 35 seconds from placing the Fluid Mould out of the oven to completely lowering the actuators. Within these 35 seconds the thermoplastic sheet could be already cooled for a certain amount.

It has been checked if the thermoplastic sheet shifts in x –and y-direction while setting the actuators at the proper heights. This is done by drawing contours of the flexible edge on the thermoplastic sheet before and after deforming. With regard to the relatively low curved sheets, both lines where at identical position, so no shifting occurred. This implies these thermoplastic sheets can be cut to the exact required size. However, for the relatively high curved sheets a minor shift to the centre could be observed and so oversized sheets are needed.
All deformed thermoplastic sheets obtain fluid shapes. Unfortunately little imprints by the flexible edges were still noticeable. However, the imprint at the surface is not always palpable.
The amount of curvature of the thermoplastic sheet influences the stiffness. The more curved sheets acquire more stiffness than the less curved sheets. During pouring of concrete the sheets must be supported.
A point of attention is the stiffness of the thermoplastic sheet. The first formwork used threaded rods for supporting the thermoplastic sheet. This leads to point loads by which the thermoplastic sheets cracked. The surface of both panels is very glossy. However, many surface voids can be observed and the surface is not entirely smooth due to the point loads of the threaded rods.
Another cast has been done with the use of fine granules instead of threaded rods as counter pressure so a uniformly distributed load is applied and stronger boards have been used as a formwork. This concrete panel is less glossy than the previous casted concrete panels, which is probably due to dust that came from the granules. However, the concrete surface has fewer voids in it and is smoother. Also the edge of the panel obtained a higher aesthetical quality than the other concrete panels.

8 Validation

8.1 Validation procedure

The end products of the third process 'manufacturing' are validated in this chapter to provide insight into the accuracy of the Fluid Mould.

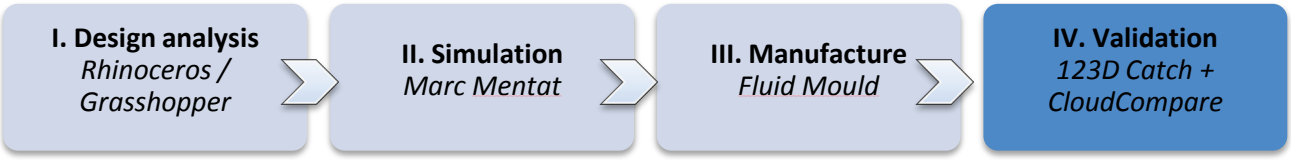

Figure 8.1: Overview of the production process

In order to validate the thermoplastic sheets, three-dimensional scans of the sheets are made with the use of 'Autodesk's 123D Catch'. The software application can be freely downloaded for the use for creating 3D meshes from digital photographs. The process to obtain accurate 3D scans with the use of the 'Autodesk's 123D Catch' application is explained in the appendix A.

The validations are done with the use of the software application 'CloudCompare', which is an open source 3D point cloud processing software application, which also can process triangular meshes. This software allows to align two geometries and to compute distances between those aligned geometries. In appendix B this process is described step by step. In the next paragraph the designed Rhinoceros model, simulation model and thermoplastic sheet are compared to each other.

The following inaccuracies are included in the validations:

- Exchange of data between various software applications;
- Simplified simulation model;
- Materials imperfections;
- Fluid Mould imperfections;
- Production process inaccuracy;
- 3D scan inaccuracy;
- Validation method inaccuracy.

8.2 Results

From the designed end product only the thermoplastic moulds for panel 1 (Figure 8.2) and panel 2 (Figure 8.3) have been produced with the use of the Fluid Mould. To show the maximum capacities of the Fluid Mould in combination with the large oven, thermoplastic moulds for panel A and panel B have also been produced (Figure 5.7 and Figure 5.8).

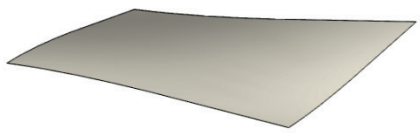

Figure 8.2: Panel 1

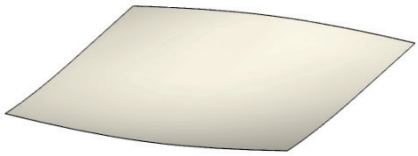

Figure 8.3: Panel 2

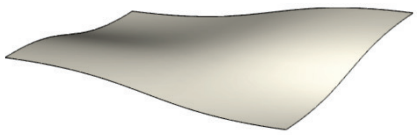

Figure 8.4: Panel A

Figure 8.5: Panel B

This has led to a total amount of six thermoformed sheets which will be discussed in this chapter. The sheets are validated using the previously discussed method in which the Marc Mentat model is created as a point cloud and both Rhinoceros model and 123D Catch model are created as a mesh. For all validations cloud to mesh distances are computed.
For each sheet the validation is done as follows:

- Marc Mentat model is aligned to the Rhinoceros model, with C2M distances computed on the Marc Mentat model
- 123D Catch model is aligned to the Marc Mentat model, with C2M distances computed on the Marc Mentat model
- 123D Catch model is aligned to the Rhinoceros model, with C2M distances computed on the Rhinoceros model

The validation figures illustrate the measured deviations in millimetres, which are represented by a colour gradient from blue, yellow to red. The yellow colour represents the most accurate areas, red shows the most positive deviations and blue shows the most negative deviations. A symmetrical colour scale is used, by which the gradient is fully extended to the deviation range. This has to be taken into account when comparing various figures. In order to obtain a more accurate validation, the middle section of the geometry is cut out prior to aligning so the inaccurate middle section is not included in the calculation. After aligning the edges, the resulting translation matrix is applied to the whole geometry.
A noticeable aspect of the validation is the deviation at the edge curves. This deviation is mainly a result of aligning two geometries. The 123D Catch model is often aligned using a slightly z-rotation, which leads the surface edges to be out of bound. The resulting deviations should not be considered as true deviations between the two geometries and are therefore neglected.

8.2.1 Panel 1

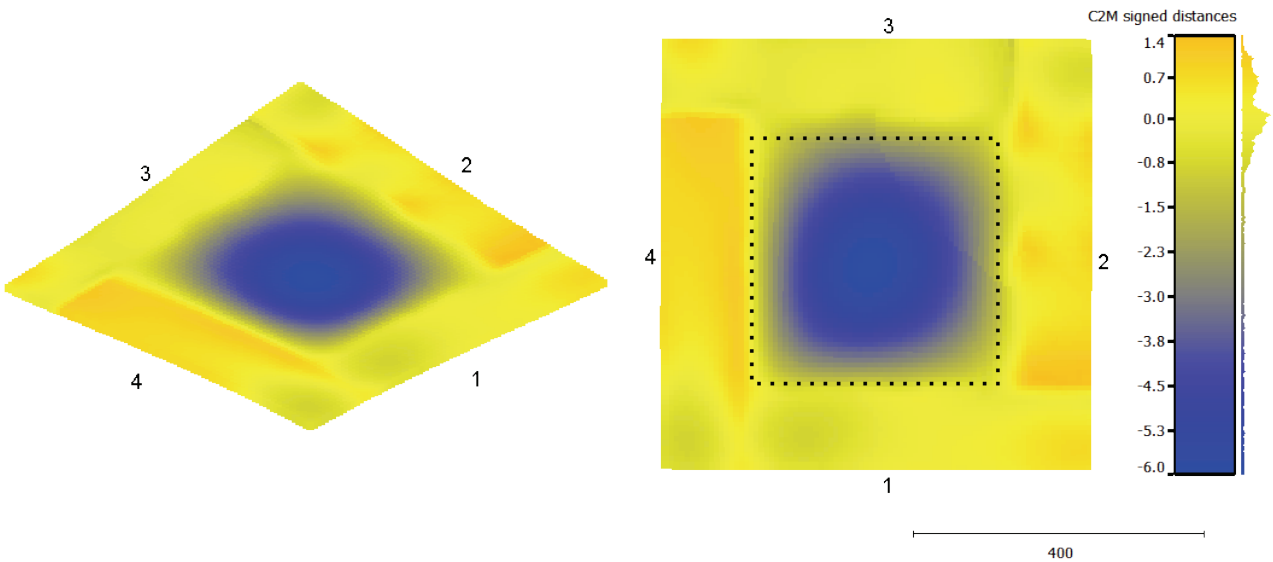

Figure 8.6: Rhinoceros model aligned to Marc Mentat model. Distances plotted to Marc Mentat model.

The prediction of the edge deformation of Marc Mentat is very accurate as can be seen in Figure 8.6. Locally small deviations can be observed, which are mainly due to inaccuracies of the simulation process. However, at the start of each flexible edge (at actuators 1.A1, 2.A1, 3.A1 and 4.A1), some larger deviations can be observed. This could be caused by the small extension of the flexible edge towards the adjacent edge, as can be seen in Figure 8.7. This extension of the flexible edge of 25 millimetres is designed to provide sufficient space to attach the actuators. Possibly a tapered extension would lead to smaller deviations/imprints in the simulation model.

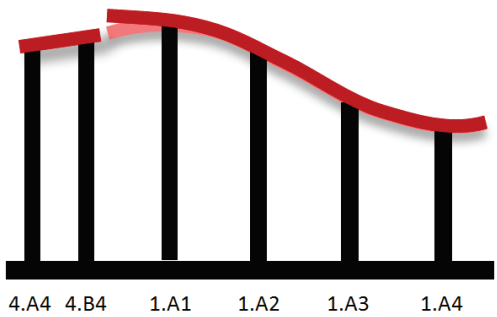

Figure 8.7: Effect extension of the flexible edge towards the adjacent edge

To produce a closed mould for panel 1, two polycarbonate sheets (sheet 1.1 and sheet 1.2) are deformed. For both sheets, the same settings of the oven are used (Table 8.1). The drying process of one hour was sufficient to prevent forming of gas bubbles in the polycarbonate sheets.

Settings oven for sheet 1.1 and sheet 1.2		
	Temperature	Time
Drying	15-120°C 120°C	±5 min 60 min
Heating	120-180°C 180°C	±5 min 15 min

Table 8.1: Used oven settings for sheet 1.1 and 1.2

Sheet 1.1

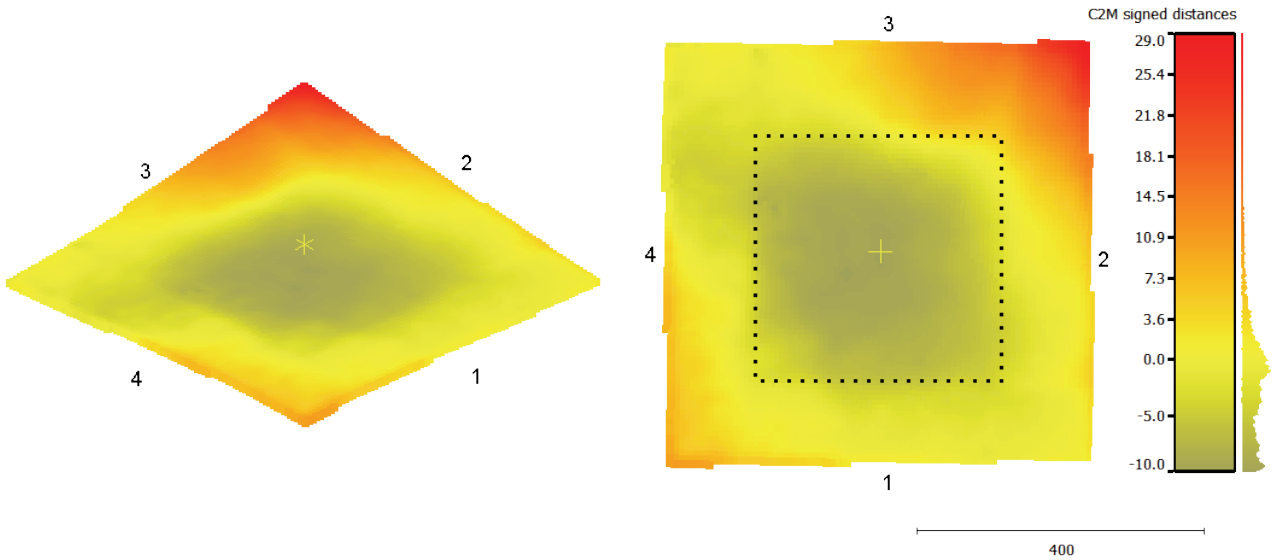

Figure 8.8: Sheet 1.1 - 123D Catch model aligned to Marc Mentat model. Distances plotted to Marc Mentat point cloud model.

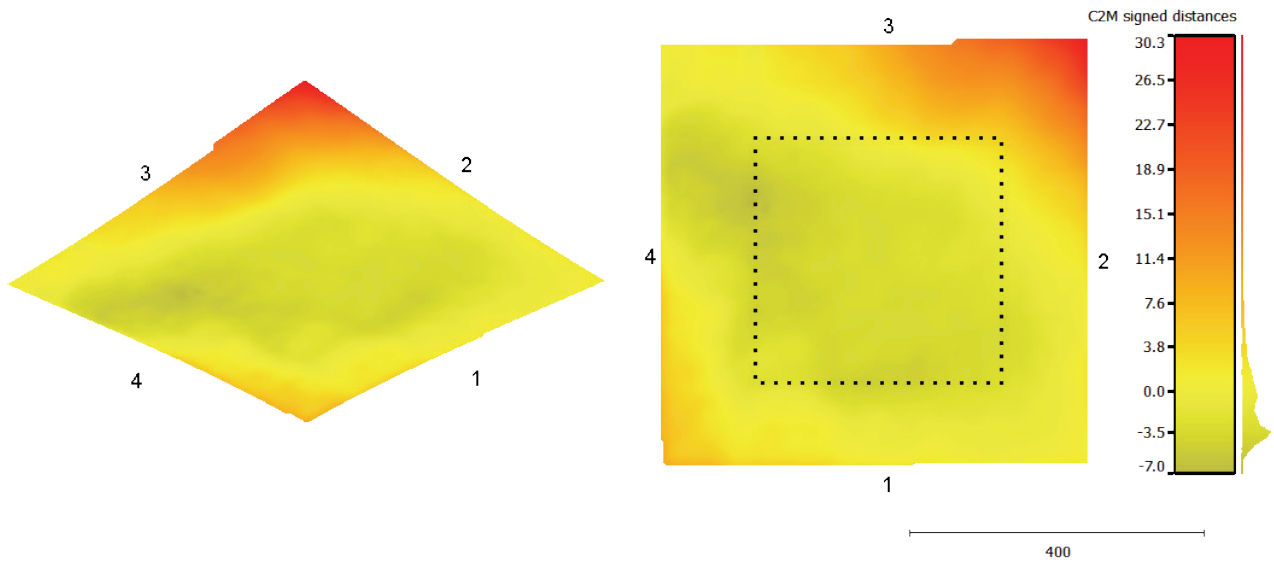

Figure 8.9: Sheet 1.1 - 123D Catch model aligned to Rhinoceros model. Distances plotted to Rhinoceros model.

According to the Marc Mentat simulation, the silicone rubber sheet for sheet 1.1 should have sagged more in the middle section. This corresponds to the observations during the production process; the PC sheet did not entirely made contact with the flexible layer during the deformation.

Problems occurred during the manufacturing process which causes the deviance of the corner 2-3. The lower flexible edge did not clamp to the upper flexible edge (as can be seen in Figure 8.11). Because of this deviation, the corner 2-3 is excluded in the alignment calculation in CloudCompare. It appears the majority of the amount of deviation is due to this corner. This problem is also noticeable in validation of sheet 1.2, as can be seen in Figure 8.14 and Figure 8.15.

As discussed the corner 2-3 does not match in both validations due to manufacturing problems. The other sections of the edges are more accurate, however e.g. edge 4 still obtains a deviation of approximate -7mm to +7mm.

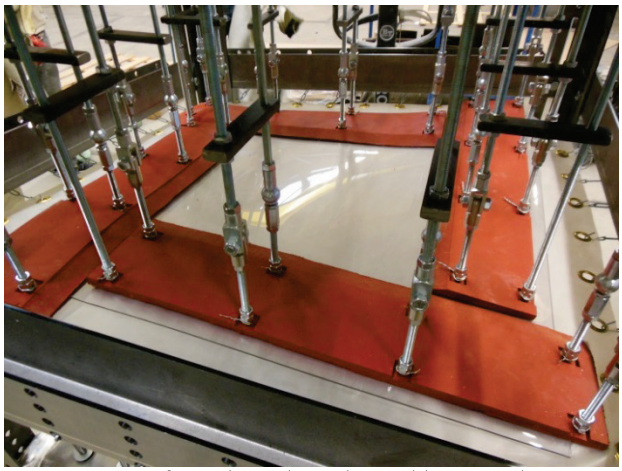

Figure 8.10: Deformed PC sheet clamped between the flexible edges

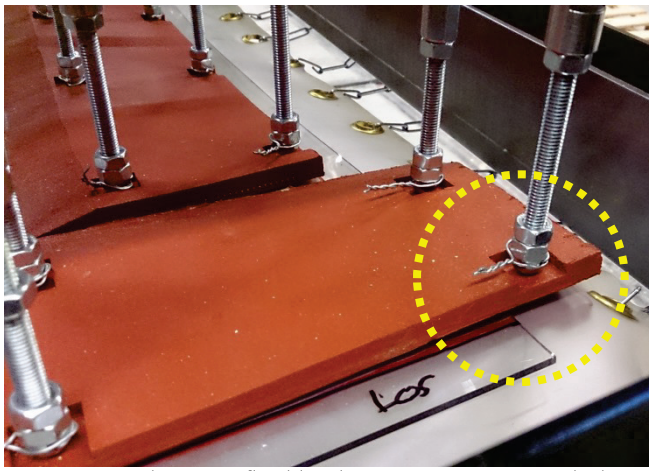

Figure 8.11: The upper flexible edge is not in contact with the PC sheet after lowering the lifting plate

Looking back at extension of flexible edge towards the adjacent edge (Figure 8.6), this phenomenon cannot be observed in validations of the 123D Catch model with the Rhinoceros model (Figure 8.12 and Figure 8.13).

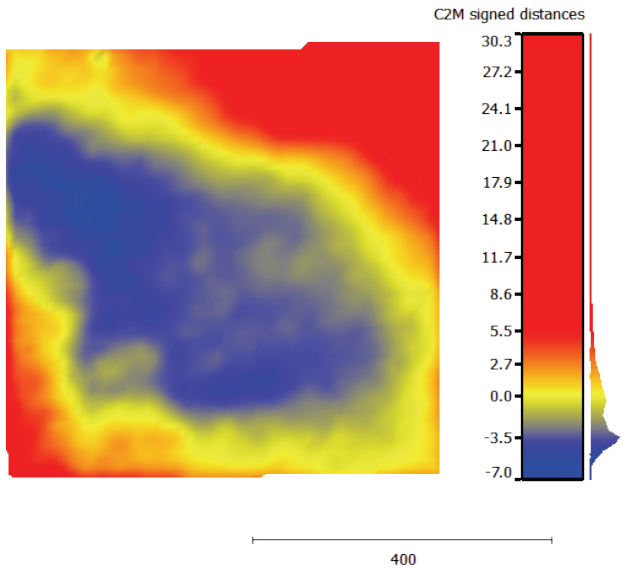

Figure 8.12: Effect flexible edge extension not visible at detailed level for 123D Catch of sheet 1.1 compared to Rhinoceros

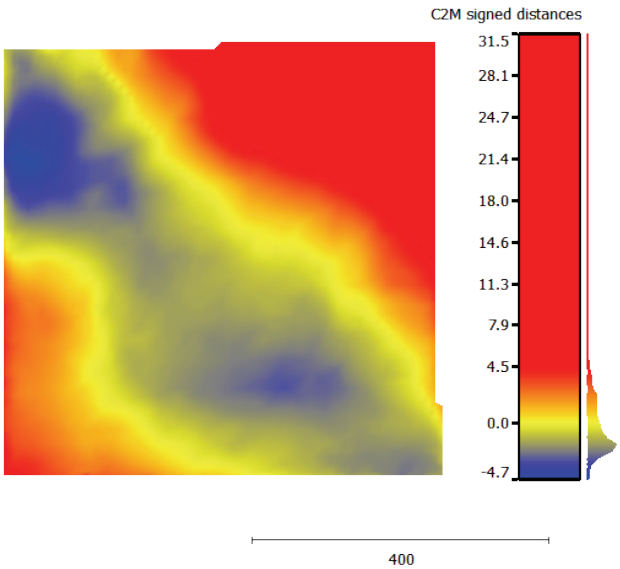

Figure 8.13: Effect flexible edge extension not visible at detailed level for 123D Catch of sheet 1.2 compared to Rhinoceros

Sheet 1.2

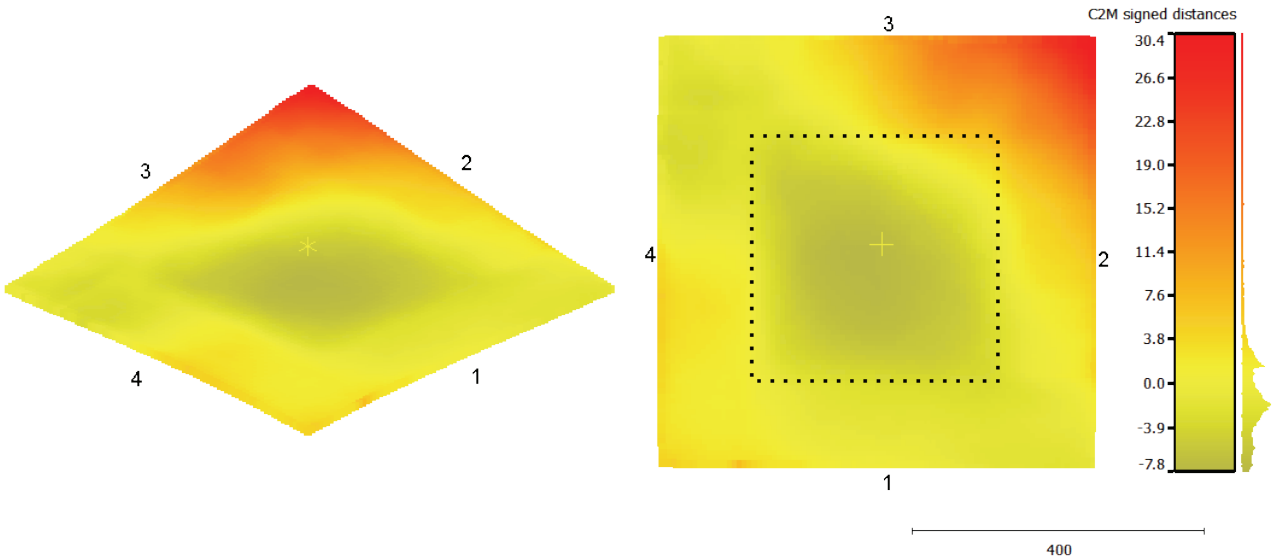

Figure 8.14: Sheet 1.2 - Marc Mentat model aligned to 123D Catch model. Distances plotted to Marc Mentat point cloud model.

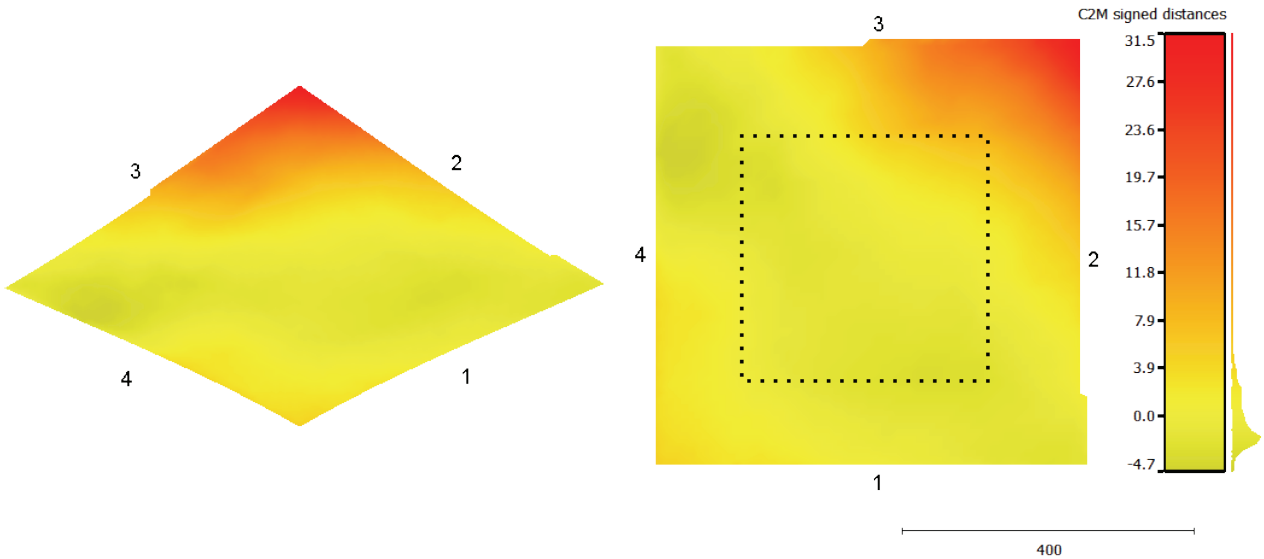

Figure 8.15: Sheet 1.2 – Rhinoceros model aligned to 123D Catch model. Distances plotted to Rhinoceros model.

The clamping problem which occurred was solved by tightening some springs of the lower actuators. However, the corner 2-3 has still the largest deviation. Thus the clamping problem did probably not cause this large amount of deviation. The PC sheet was probably too much cooled because of the time needed to take the Fluid Mould out of the oven.

Conclusion sheet 1.1 and 1.2

The resulting deviation is not entirely caused by the clamping problem, so corner 2-3 should probably not have been excluded for the alignment calculation. In Figure 8.16 and Figure 8.17 validations of the Rhinoceros model and 123D Catch model can be seen, in which the alignment is done by including the entire edge.

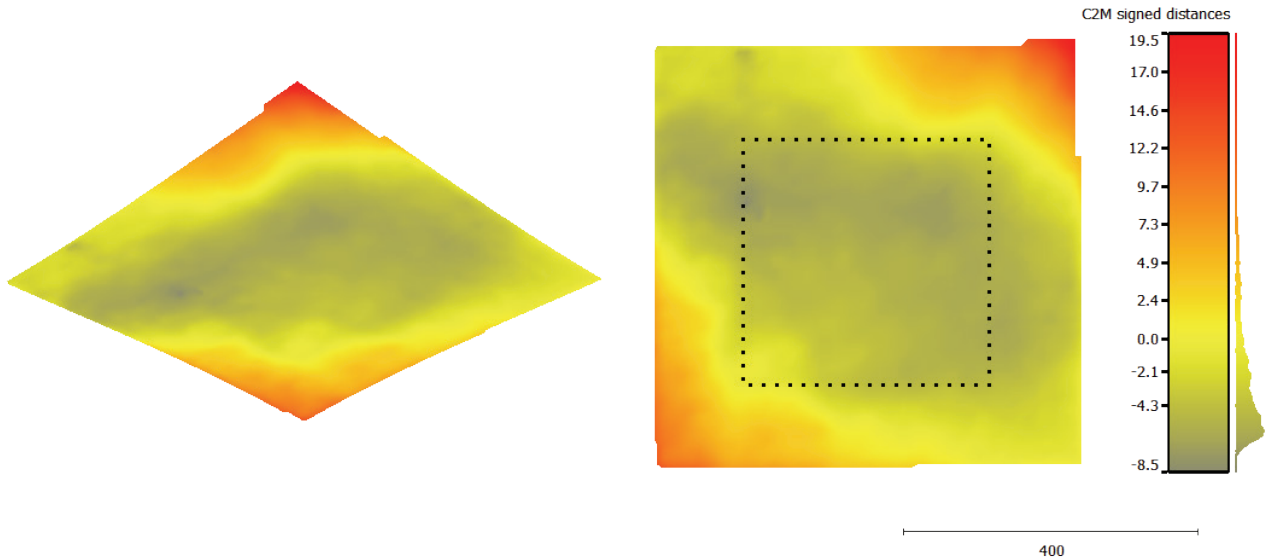

Figure 8.16: Sheet 1.1 – Rhinoceros model aligned to 123D Catch model. Distances plotted to Rhinoceros model.

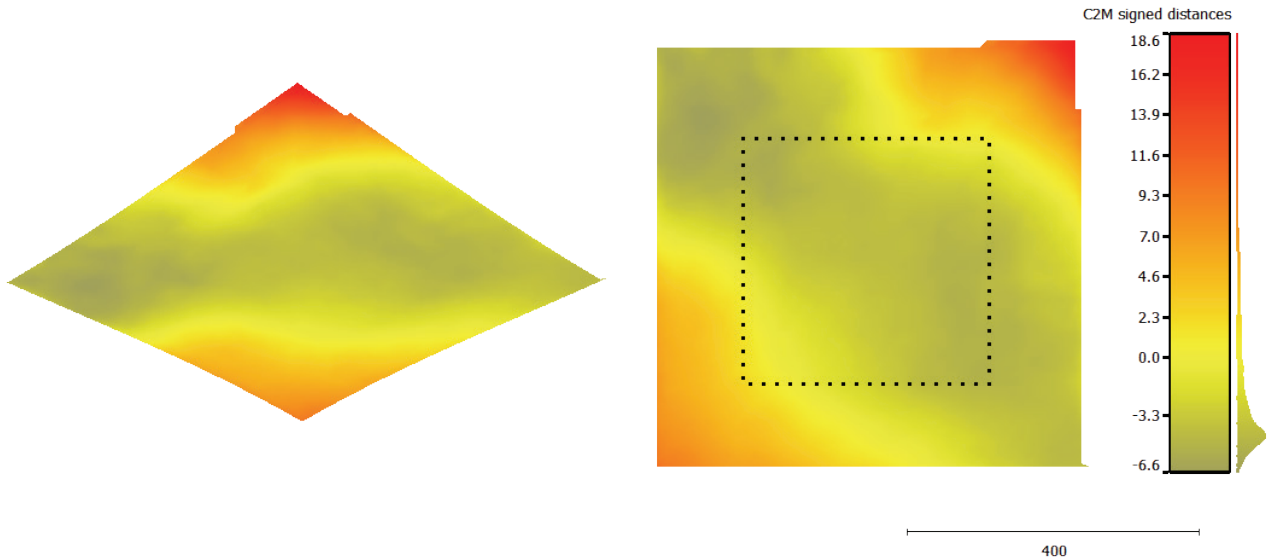

Figure 8.17: Sheet 1.2 – Rhinoceros model aligned to 123D Catch model. Distances plotted to Rhinoceros model.

For the sheets 1.1 and 1.2 the same settings of the oven were used (Table 8.1). Both sheets show similar deviation. The areas of positive and negative deviation show symmetry from which can be derived the sheets deform slightly back to its original flat shape. The PETG sheet was probably not sufficiently heated to be deformed into the desired shape. Most likely, a higher temperature is needed to achieve a more accurate panel.

8.2.2 Panel 2

Two PETG sheets (sheet 2.1 and sheet 2.2) are deformed to be used for a closed mould for panel 2. The production cycle of these sheets is faster because the drying time of one hour is no longer a necessity. Thereby more sheets could be produced per day. Different settings are used per sheet as can be seen in Table 8.2.

Settings oven for sheet 2.1	
Temperature	Time
15-90°C	±3 min
90°C	15 min

Settings oven for sheet 2.2	
Temperature	Time
15-100°C	±3 min
100°C	20 min

Table 8.2: Used oven settings for sheet 2.1 and 2.2

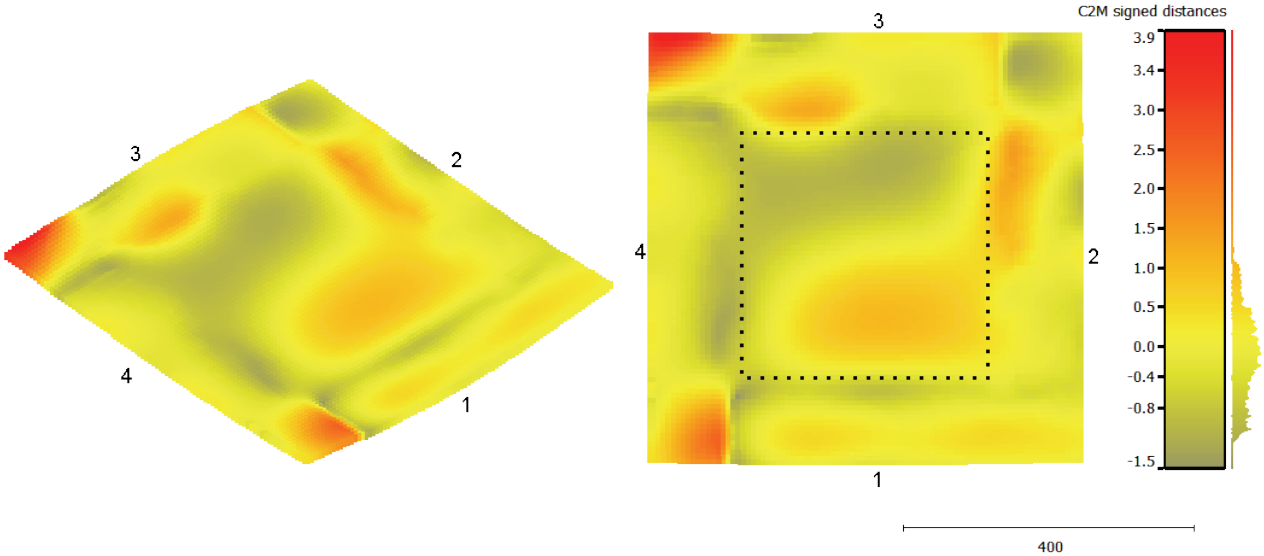

Figure 8.18: Sheet 2 –Rhinoceros model aligned to Marc Mentat model. Distances plotted to Marc Mentat.

Similar deviations as stated in the validation for sheet 1 can be observed. Unfortunately, this simulation also shows some inaccuracies of the contact bodies due to the simplification of the pendulum rods in the simulation model (chapter 6). This has led to large deviations as can be seen in Figure 8.18. The middle section of the silicone rubber forms the desired geometry very well with an accuracy of approximately -1,5mm to +1,5mm.

Sheet 2.1

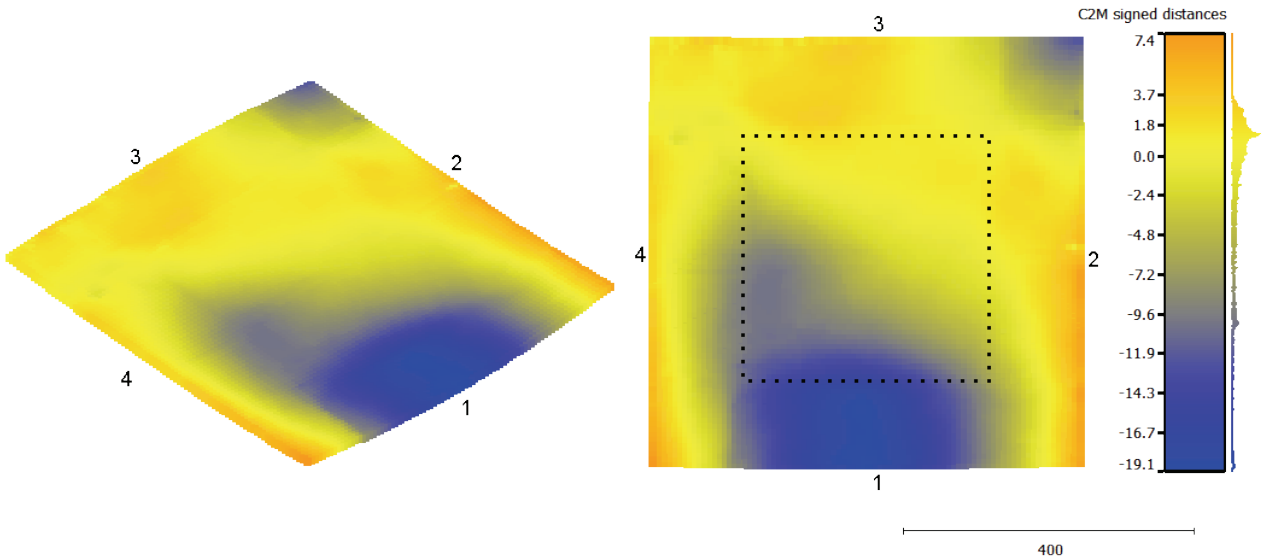

Figure 8.19: Sheet 2.1 - Marc Mentat model aligned to 123D Catch model. Distances plotted to Marc Mentat point cloud model.

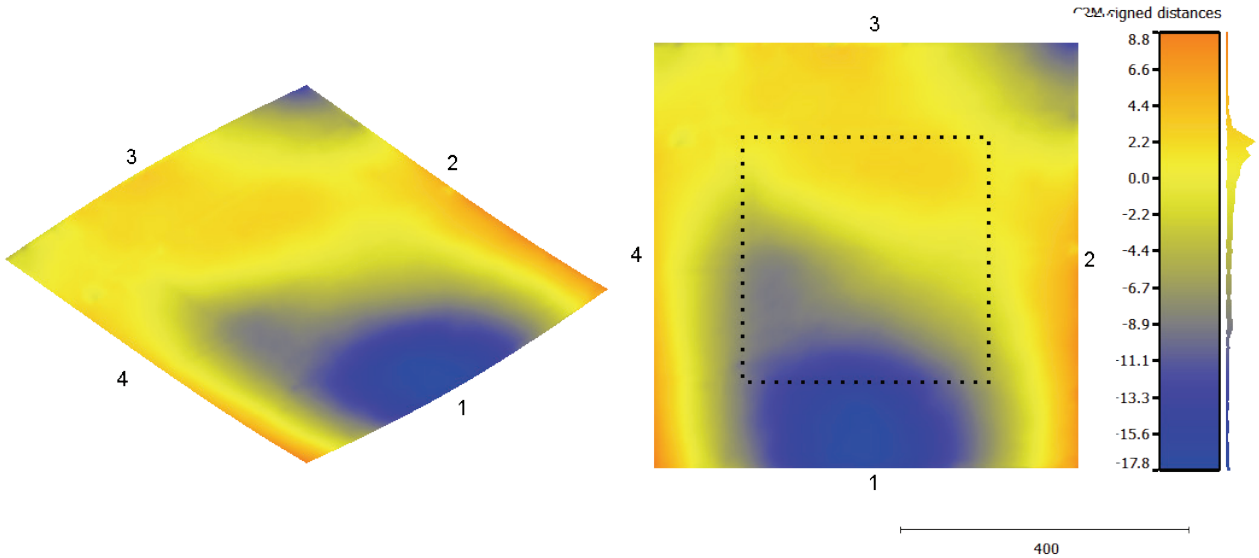

Figure 8.20: Sheet 2.1 – Rhinoceros model aligned to 123D Catch model. Distances plotted to Rhinoceros model.

In Figure 8.19 the Marc Mentat inaccuracy can clearly be seen in corner 3-4. The PETG sheet partially returned back into its original shape after lifting up the lifting plate of the Fluid Mould. This is clearly visible at the edge 1. This edge has an inverse curvature than the desired shape. This phenomenon could also be observed in the 123D Catch model and Rhinoceros model validation (Figure 8.20). Therefore edge 1 is excluded in the alignment calculation. For the sheet 2.2 a higher temperature for an extended period of time is used (Table 8.2).

Sheet 2.2

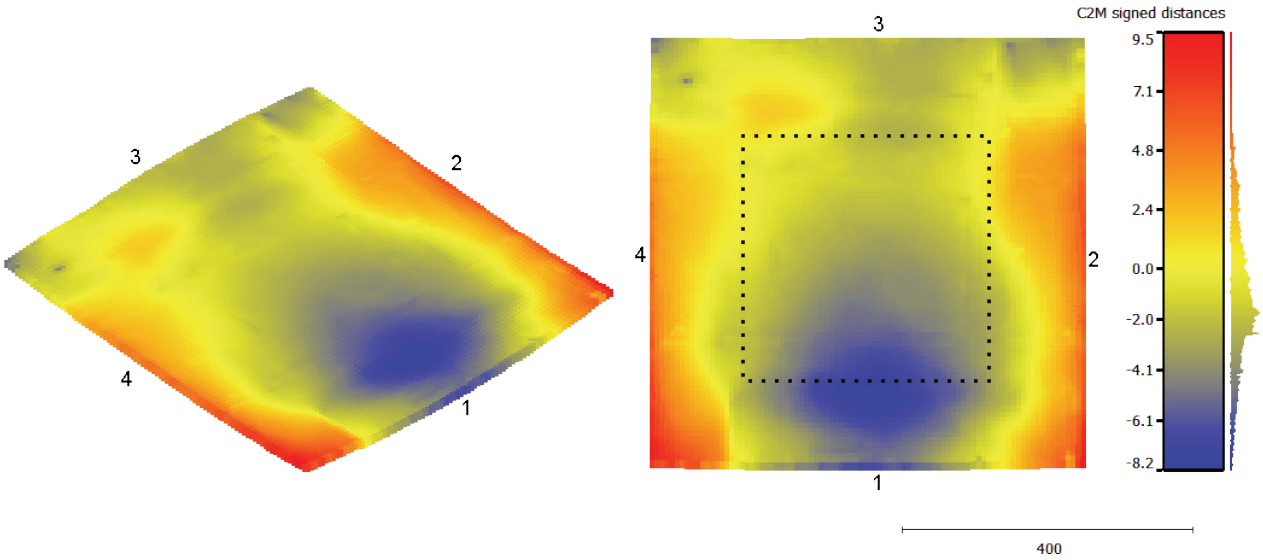

Figure 8.21: Sheet 2.2 - Marc Mentat model aligned to 123D Catch model. Distances plotted to Marc Mentat point cloud model.

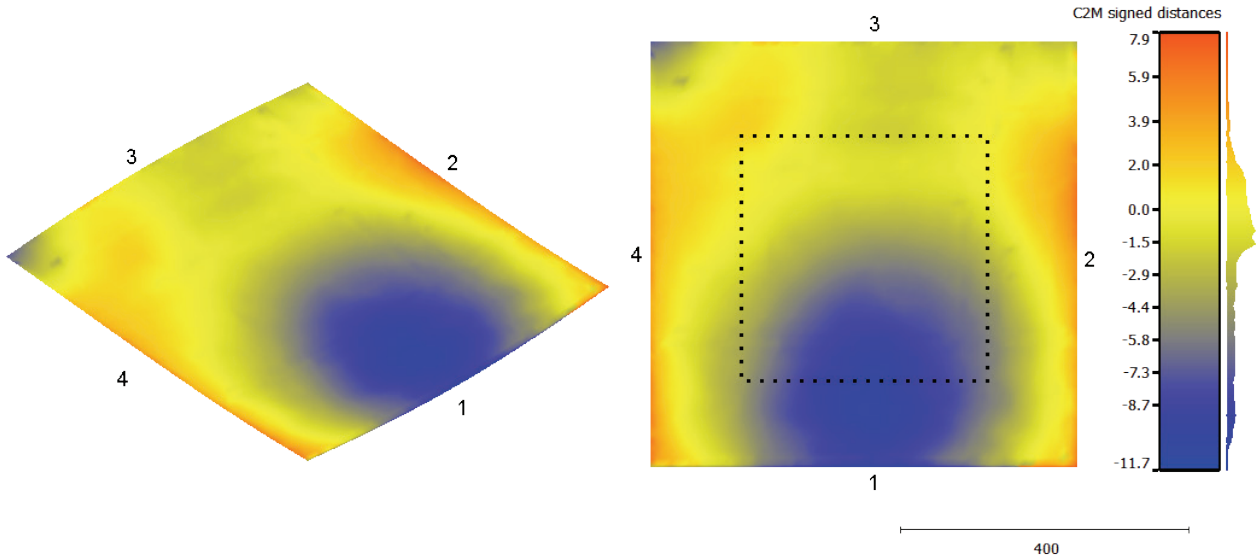

Figure 8.22: Sheet 2.2 – Rhinoceros model aligned to 123D Catch model. Distances plotted to Rhinoceros model.

The use of a higher temperature and an extended period of time are immediately noticeable; the variance is less and the inverse curvature of edge 1 as in sheet 2.1 cannot be observed. However, there can be seen edge 1 is more flat than it should be. Because of the better approximation of the shape, the entire edge is included in the alignment calculation. Aside from the improvements, the same pattern of deviation at the edges is still detectible.

Conclusion sheet 2.1 and 2.2

Sheet 2.2 achieves more accurately the desired shape than sheet 2.1. Nonetheless, the curvatures of the PETG sheets are still less extreme in comparison with the Rhinoceros model. The use of an even higher temperature is eventually not an alternative; the risk of obtaining wrinkles is too great (Table 8.4).

8.2.3 Panel A and Panel B

More extreme curvatures are made for panel A and B. Panel A and Panel B are comparable in terms of form, but panel B has larger curvatures. The sheets are produced with the use of the same oven settings (Table 8.3).

Settings oven for sheet A and B	
Temperature	Time
15-100°C	±3 min
100°C	20 min

Table 8.3: Used oven settings for sheet A and B

Sheet A

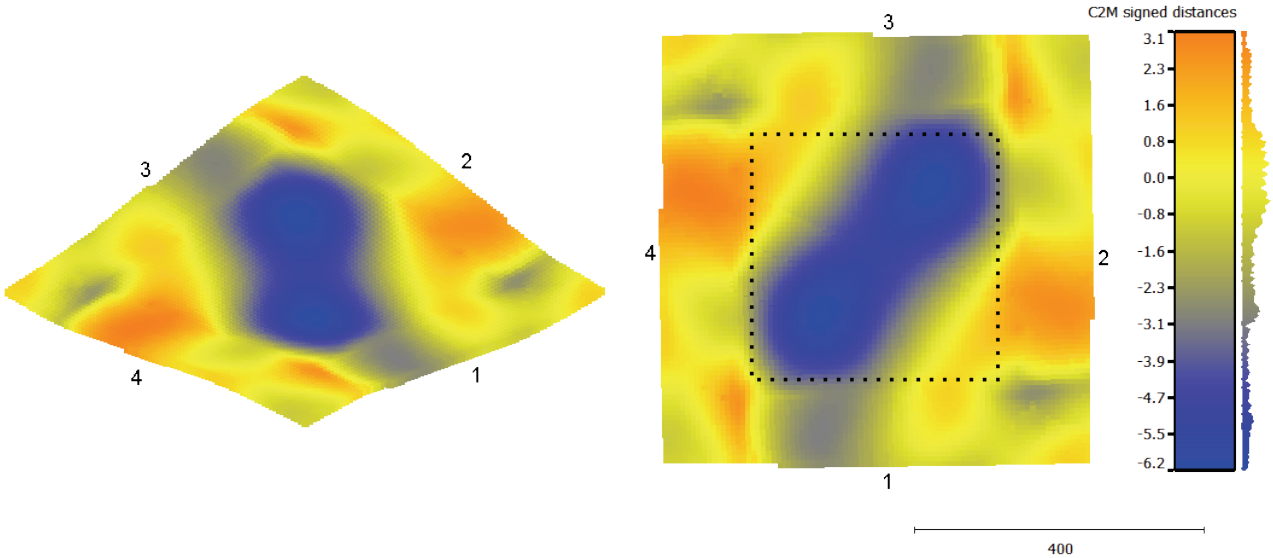

Figure 8.23: Sheet A – Rhinoceros model aligned to Marc Mentat model. Distances plotted to Marc Mentat point cloud model.

The edges are accurately deformed, however the deviations as stated in the validation for sheet 1 can be observed. The sag in the Marc Mentat model is approximately 6,2mm compared to the Rhinoceros model.

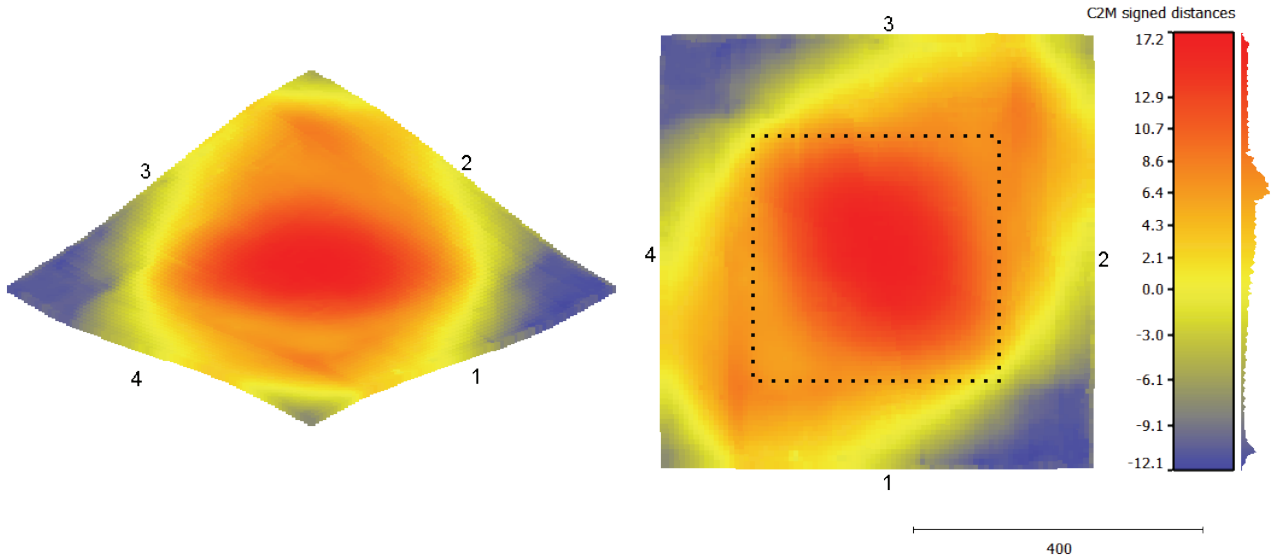

Figure 8.24: Sheet A - Marc Mentat model aligned to 123D Catch model. Distances plotted to Marc Mentat point cloud model.

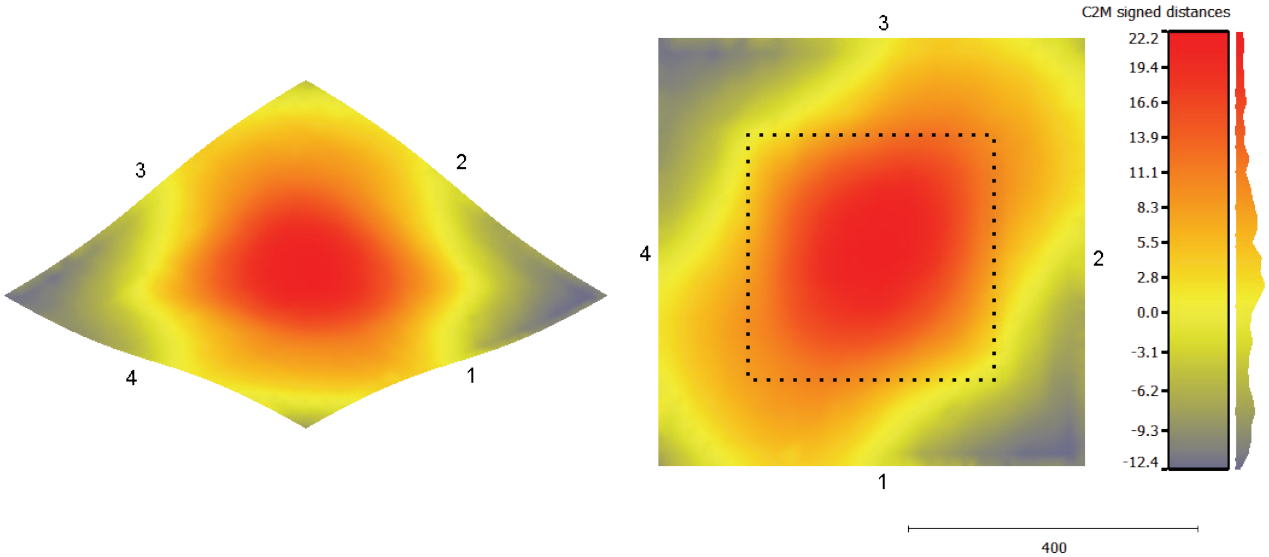

Figure 8.25: Sheet A – Rhinoceros model aligned to 123D Catch model. Distances plotted to Rhinoceros model.

More tension should be applied to the silicone layer according the prediction of the Marc Mentat model. There can again be observed the desired edge curvature is not acquired. A higher temperature could be required.

Sheet B

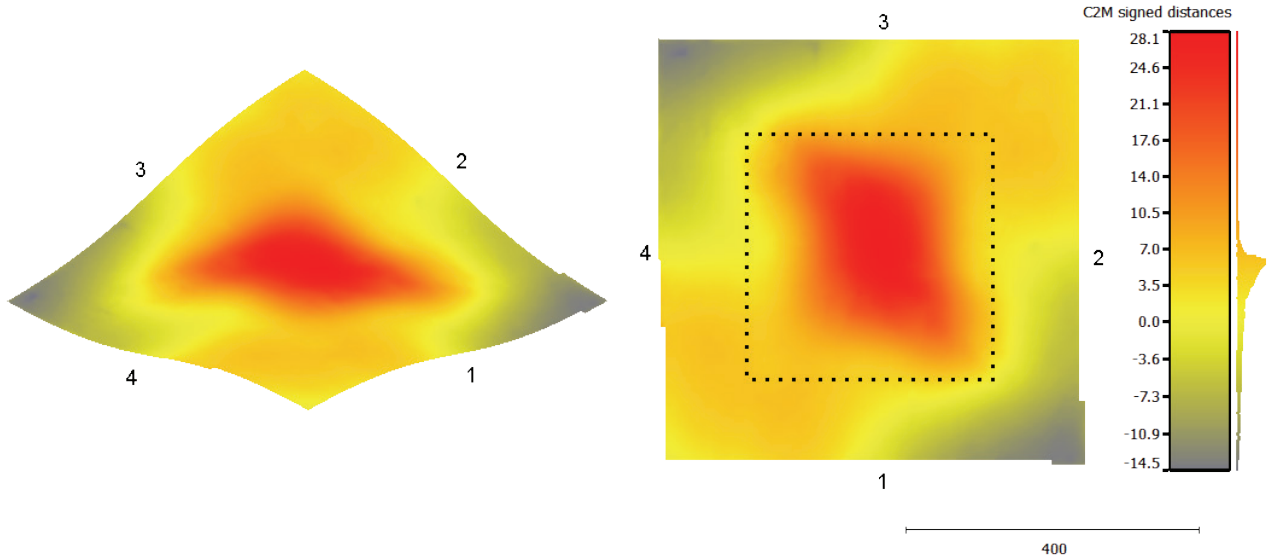

Figure 8.26: Sheet B – Rhinoceros model aligned to 123D Catch model. Distances plotted to Rhinoceros model.

Panel B consists of more extreme curvatures than panel A. Because panel A appeared to be successfully produces the same oven settings are used for panel B. During the manufacturing process of panel B, it became clear the Fluid Mould showed problems in producing of more extreme shapes. The Fluid Mould had trouble to lower the flexible edges. The weights did not lower the actuators sufficiently due to the greater upward force of the springs. Additionally, the relatively large forces that are needed had a negative effect to the M8 threaded rods. The rods were eventually out of plumb. Furthermore, the lower actuators occasionally jammed, because the end of the springs got stuck between the steel pipes. In order to obtain a more accurate sheet, non-uniform tension could be applied between corner 2-3 and 4-1.

Conclusions sheets A and B

For sheet A and B a higher temperature could be needed. Also non-uniform tension is required to obtain a more accurate sheet. The oven setting is adjusted for sheet B. Eventually, these used setting are not compatible for deforming the PETG sheets; wrinkles in the middle section of the sheets occurred.

Settings oven for failed sheet B	
Temperature	Time
15-100°C	±3 min
100°C	25 min

Table 8.4: Used oven settings for failed sheets B

Flexible edge set for panel B

The accuracy of the formed thermoplastic sheets depends among other things on the accuracy of the flexible edge. Therefore the upper flexible edge 4 for panel B is scanned by the use of 123D Catch and compared with the Rhinoceros model, as can be seen in Figure 8.27.

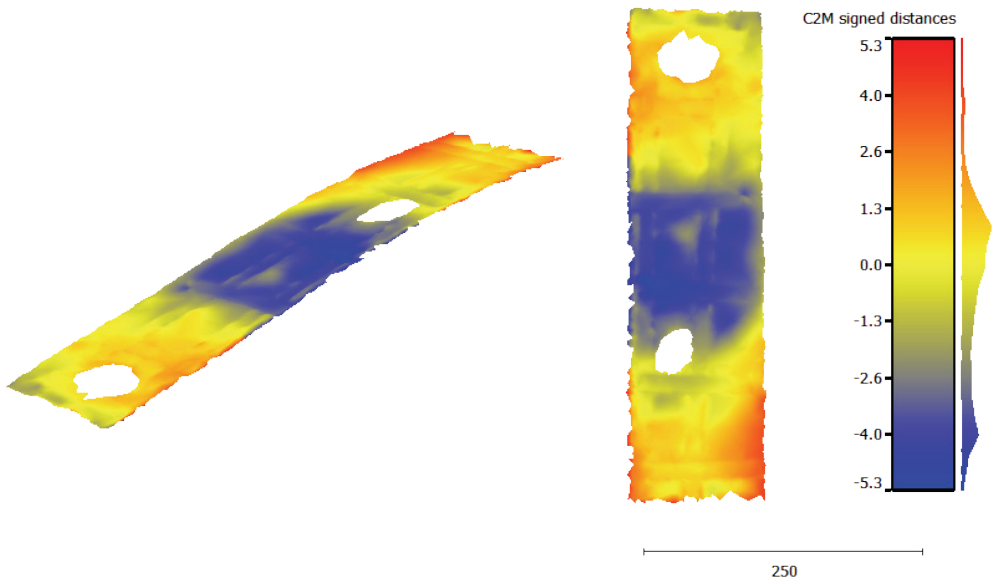

Figure 8.27: Flexible edge 4 is set for panel B. Rhinoceros model aligned to 123D Catch model. Distances plotted to 123D Catch model.

Some light reflection on the silicone rubber occurred while taking photos. This has led 123D Catch to generate two holes in the flexible edge. The remaining parts of the scan have been well managed.
The validation shows a fine match between the two models (Figure 8.28). As can be seen maximum deviations of -5,3mm to +5,3mm occur.

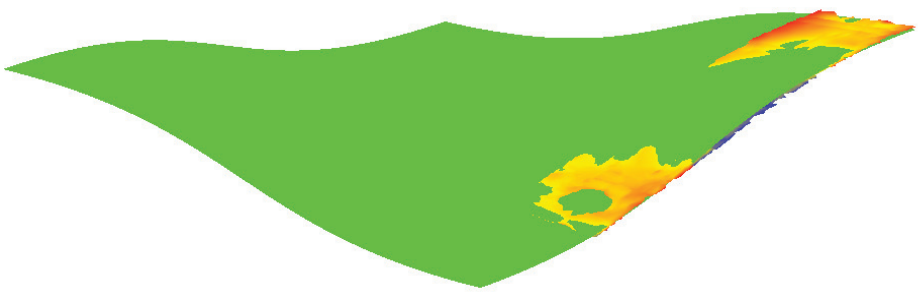

Figure 8.28: Flexible edge aligned to Rhinoceros model. Distances plotted to 123D Catch model.

8.3 Conclusions

An important aspect is that the required time to remove the Fluid Mould out of the oven is too long. If the Fluid Mould is removed from the oven too slowly, the viscoelastic material could become too rigid to be properly thermoformed. After forming the thermoplastic sheet it returns slightly back to its original shape. In addition, the edges of the thermoplastic sheets are probably more rapidly cooled than the middle section, so the edges are more difficult to deform. To better monitor the deformation process, the thermoforming process could be applied inside the oven, which is hard-to-reach. Another option is to develop a built-in heater element, as has been discussed in chapter 4.

The setting of the compression springs partially determines the accuracy of the deformed thermoplastic sheet. If the compression is too little, there is a risk the thermoplastic sheet is not clamped between the two flexible edges. If the compression is great, the risk of jamming of the actuators is too high. When the actuators jam, the actuators tend to bend instead of moving down.

The Fluid Mould was able to produce thermoplastic moulds with an absolute deviation varying from 11,7mm to 28,1mm. The maximum absolute deviation of 28,1mm occurs in the middle section of the extremely curved sheet B. The minimum absolute deviation of 11,7mm occurs in the middle of edge 1 of sheet 2.2.

The flexible edge is an accurate component of the Fluid Mould for the production of panel B. It can be assumed that the flexible edge can be set with a similar accuracy for the other panels. It can be concluded that the composite flexible edge which consists of silicone rubber casted in spring steel mesh is a success factor of the Fluid Mould because of its stiffness and smoothness which allows an accurate flexible edge setup.
Noteworthy, the flexible edge does tend to follow a slightly shorter and straighter curve than initially is intended. It also has to be noted the flexible edge surface acts like a ruled surface, because in one direction has only two actuators. With the use of two actuators the flexible edge cannot be bended in that direction. More accuracy can be achieved by inclusion of the material properties during the production process ‘design analysis’. In this way, the flexible edge deformation can be simulated and deviations in the flexible edge can be corrected be adjusting the actuator heights.

It has to be noted the alignment of geometries in CloudCompare determine in which area inaccuracies can be observed. Because the flexible edge is assumed to be very accurate, the edges are cut out and aligned. Therefore, more deviation will be noticeable in the middle section of the sheets. The scan of the flexible edge for sheet B proves this is probably a very feasible method. However, this scan is done for the upper flexible edge without any clamping force applied to it. This force could have an effect on the shape of the flexible edge.

9 Conclusions and Recommendations

9.1 SWOT-analysis

Thermoplastic moulds show great potential for casting concrete elements. With the use of thermoplastic moulds fluid concrete elements with an excellent aesthetic surface quality have been produced. The rapidly deformation process and the low-investment cost of the material offer great opportunities for the future of fluid architecture. In Table 9.1 the strengths, weaknesses, opportunities and threats are evaluated for the Fluid Mould prototype and will be elaborated in the following paragraphs.

		Helpful	Harmful
		To achieving the objective	*To achieving the objective*
Internal origin	*Attributes of the organization*	***Strengths*** - Fast production cycle - Relatively low-cost production method - Resulting aesthetical quality of the concrete surface - Accuracy flexible edge - Recyclable mould material - Simple manual configuration	***Weaknesses*** - Limited producible forms - Depending on simulations to predict the form of the mould - Only suitable for 'quadratic' panels - Large oven required - Energy use of oven - Limited accessibility in the oven in order to adjust the mould device - Manual configuration
External origin	*Attributes of the environment*	***Opportunities*** - Trends in fluid architecture - High costs of current moulding techniques - Scale up Fluid Mould for higher cost-effectiveness - Industrialize production process - Automatic configuration - Manipulate flexible layer by applying non-uniform tension - Additional manipulation methods - Iterative process between simulation and designed geometry for higher accuracy - Additional suitability for 'double curved' thermoplastic façades	***Threats*** - Jamming of actuators - Play in the actuators - Drying time polycarbonate - Required time to take the Fluid Mould out of the oven to lowering of the actuators - Deviation in deformed thermoplastic sheets - Imprints in thermoplastic sheet - Supporting of thermoplastic sheets for concrete casting - Correlation simulation with production process - Wall time simulations

Table 9.1: SWOT analysis of the Fluid Mould

9.2 Conclusions

In this research a 'Fluid Mould' prototype for the mass-production of non-repetitive double-curved concrete elements has been developed in order to contribute to the research in flexible moulds. The mould has used the 'tensioned flexible layer method' in combination with an intermediate thermoplastic sheet and has showed great potential for rapid production of non-repetitive moulds. The Fluid Mould prototype provides a solid base for many possibilities for further development.

Both PETG and PC have proven to be suitable mould materials. A supporting flexible layer for the thermoplastic was needed of which its behaviour is not time dependent. Silicone rubber proves to be a suitable flexible layer material. It has excellent stable properties, even at elevated temperatures, which allows the use of FEA software to predict the flexible layer deformation.

The production process consists of four steps i.e. design analysis, simulation, manufacture and validation. The mould settings have been successfully derived with the use of a developed Grasshopper component. The simulations were successfully performed by applying the Mooney-Rivlin hyper elasticity model in the software application 'MSC Marc Mentat'. The results of the simulation models of the panel '1', '2' and 'A' provide a plausible prediction of the deformation behaviour of the flexible layer. However, the simulation model fails with more complex curvatures (panel 'B'), which is caused by excluding the pendulum rods in the simulation.

No major setbacks occurred during the manufacturing process. Some actuators jammed occasionally, especially during the production of the more extremely curved panel B. The play of the actuators was more than expected. The main reason for this is that the inner radius of the guide pipes was larger than was ordered.
It took about 35 seconds from placing the Fluid Mould out of the oven to completely lowering the actuators. Within these 35 seconds the thermoplastic sheet was already partly cooled and therefore the viscoelastic material became too rigid to be properly thermoformed. After forming the thermoplastic sheet it slightly returned back to its original flat shape.
All deformed thermoplastic sheets obtained fluid shapes. Little imprints at the location of the flexible edges were noticeable. However, the imprint at the surface was not always palpable.
A point of attention is the low stiffness of the deformed thermoplastic sheet. Whilst pouring concrete, the thermoplastic sheets must be supported with a uniformly distributed load because of the low stiffness. The first formwork used threaded rods for supporting the thermoplastic sheet. This leads to point loads by which the thermoplastic sheets cracked. The surface of both panels is very glossy. However, many voids can be observed and the surface is not entirely smooth due to the point loads of the threaded rods. The second formwork used fine granules instead of threaded rods as counter pressure which acts as a uniformly distributed load. Also stronger boards have been used as a formwork. This concrete panel is less glossy than the previous casted concrete panels, which is probably due to dust that came from the granules. However, the concrete surface has fewer voids in it and is smoother. Also the edge of the panel obtained a higher aesthetical quality than the other concrete panels.
Excluding man-hours, the costs per deformed PC sheet is approximately € 58,25 and the costs per deformed PETG sheet is approximately € 37,42. Therefore the mentioned costs consist of material costs and rental charges of the oven. The PC sheets require a one hour drying period which make using this material more expensive.

The Fluid Mould was able to produce thermoplastic moulds with an absolute deviation varying from 11,7mm to 28,1mm. The maximum absolute deviation of 28,1mm occurred in the middle section of the extremely curved panel B. This panel has shown the limitations of the Fluid Mould in combination with the dimensions of the used oven, because larger height settings did not fit in the oven and the actuators tended to jam and bend during deforming the thermoplastic sheets for this panel. The minimum absolute deviation of 11,7mm occurred in the middle of edge 1 of panel 2.2.
The flexible edge is an accurate component of the Fluid Mould for the production of panel B. It can be assumed that the flexible edge can be set with a similar accuracy for the other panels. It can be concluded the composite

flexible edge which consists of silicone rubber casted in spring steel mesh is a success factor of the Fluid Mould because of its stiffness and smoothness which allows an accurate flexible edge setup.

The production process steps design analysis, simulation, manufacture and validation have successfully been completed. By validating the designed model, simulation model and manufactured thermoplastic sheet, a correlation between the processes is found. However, the results of each process are not identical due to various inaccuracies, simplifications and parameters of the production process.

9.3 Recommendations

The results of the validation process can be used as feedback to the simulation process and design analysis to improve the accuracy of these processes. When the manufactured thermoplastic sheets and the simulations accurately correlate, the simulations can be used in an iterative process to manipulate the flexible layer. This can be done by applying non-uniform tension in a way that the desired shape can be accurately approximated. The main issue of this iterative process is that the simulations take a long wall time. Simulations that were done for this research took a wall time of approximately 8,5 hours. The computing capacity of current computers is not capable to run such a simulation in a short period in order for these simulations to be used in an iterative process. For this reason the number of iterations would have to be limited in order to conduct the simulations in an iterative process. Another option would be to use less complex FEA software application which is better suited for 'quick checks'. An example is to use the software application 'GSA Suite' in combination with the 'GeometryGym' software tool as a FEA background solver for 'Grasshopper'. However, this software has limited possibilities in accurately simulating the true deformation behaviour of silicone rubber.

The Fluid Mould inaccuracies have to be solved in order to achieve an accurate correlation between the manufactured thermoplastic sheets and the simulations. For the Fluid Mould prototype developed for this research, relative low-cost materials were used which have had a negative influence to the accuracy of the flexible edges setup. It is recommended to improve the accuracy and capacities of the prototype with the use of robust materials, roller bearings and stepper motors.
The thermoforming process must take place in a better controlled environment in order to avoid sheets to cool down during this process. It is recommended for the thermoforming process either to be carried out inside the oven, which is hard-to-reach, or to be done with the use of a built-in heater element.
Further research has to be done to fine-tune the parameters of the deformation process. The weights and springs have to be adjusted to avoid jamming. Also the required temperature and time settings of the oven have to be tuned in combination with the abovementioned better controlled environment in order to obtain fluid curved sheets without any imprints.

The manufacturing procedure has to be industrialized in order to be able to rapidly and cost-effectively produce fluid thermoplastic sheets. The main issues of the prototype are the labour-intensity of the lowering of the weights and the time-consuming calibration and preparation of the Fluid Mould. An implementation of a heat resistant lifting jack in the Fluid Mould could solve the labour-intensive activity of lowering the weights. The calibration time and preparation time could significantly be reduced with the use of stepper motors.

A method has to be developed in order to systematically produce finished moulds. The two thermoplastic sheets of a mould have to be supported by a plane load such as sand, water or granules in order to provide counter pressure to the hydrostatic pressure of the casted concrete. The casting of the mould has to be done in a short production time of in order to maintain a fast production cycle.

The capacities of the Fluid Mould should be improved in order to produce more varieties of fluid shapes. The prototype consists of in-plane fixated flexible edges, in which only sheets for panels of a quadratic planar grid can be produced. If the flexible edges would be movable in the x- and y-axis, the range of producible fluid panels could be increased.
With simply the use of actuators at the flexible edges, the investment costs of a larger-scaled Fluid Mould would become relative lower. The ratio between the usable surface and the amount of actuators of the flexible layer becomes larger. The effect of the accuracy of a larger-scaled Fluid Mould must be examined. Due to the flexible edges, the middle section of the flexible layer could additionally be deformed in various ways which can be further examined with the use of the paper '85 ways to manipulate membranes'. This could also lead to an increased range of producible fluid panels.

In addition, the deformed thermoplastic sheets could be used as an end-product, for example as a replacement of double curved glass. However, this appliance of thermoplastic requires different properties than for the use as a mould and has not been elaborated in this research. Therefore, it is recommended for this application to be researched further.

It can be concluded that this research contributes to the research in flexible moulds, focussed on cost-effective production of double-curved non-repetitive concrete panels for fluid architectural designs. The Fluid Mould offers great opportunities for the future of fluid architecture because of the low-investment costs and the rapid production of intermediate thermoplastic moulds. The Fluid Mould prototype provides a solid base for many possibilities for further development.

Reference list of literature

1. Altidis, P., Warner, B. & Adams, V., 2005. *Analyzing Hyperelastic Materials.* s.l.:IMPACT Engineering Solutions, Inc. .
2. Bauman, J. T., 2008. *Fatigue, Stress, and Strain of Rubber Components - A Guide for Design Engineers.* s.l.:Carl Hanser Verlag GmbH & Co. KG.
3. Becerik-Gerber, B. & Rice, S., 2009. *An Assessment of Building Information Modeling Value and Use,* Los Angeles: Department of Civil and Environmental Engineering, University of Southern California.
4. Biron, M., 2013. *Thermoplastics and thermoplastic composites.* Oxford: Elsevier.
5. Boers, S., 2009. *OptiMal Forming Solutions - FlexiMold.* s.l.:s.n.
6. Brell-Çokcan, S. & Braumann, J., 2011. *Computer Numeric Controlled Manufacturing for Freeform Surfaces in Architecture.* Vienna: Vienna University of Technology.
7. Craven, J., n.d. *What Is Organic Architecture?.* [Online]
   Available at: http://architecture.about.com/od/periodsstyles/g/organic.htm
   [Accessed February 2014].
8. Curl, J. S., 2006. *A Dictionary of Architecture and Landscape Architecture.* 2nd ed. s.l.:Oxford University Press.
9. D2S-International, n.d. *Marc & Mentat : Geavanceerde Niet-lineaire Simulaties.* [Online]
   Available at: http://www.d2sint.com/Marc_n
   [Accessed September 2014].
10. Dow Corning Corporation, n.d. *About Silicone Rubber.* [Online]
    Available at: http://www.dowcorning.com/content/rubber/silicone-rubber.aspx?e=About+Silicone+Rubber
    [Accessed July 2014].
11. Eigensatz, M. et al., 2010. *Paneling Architectural Freeform Surfaces,* s.l.: s.n.
12. Eriks, n.d. *High Performance Silicone (technical documentation).* Hoboken, België: ERIKS BV.
13. Fimmtech inc., 2007. *Injection Molding Online.* [Online]
    Available at: http://www.injectionmoldingonline.com/Molding101/PolymerViscosity.aspx
    [Accessed April 2014].
14. Gard, F., 2013. *Flexible Mold - An innovative production method to produce double curved concrete panels.* Eindhoven: Eindhoven University of Technology.
15. Gelderman, S. & Homan, R., 2009. Dubbelgekromde betonmallen. *Cement,* Volume 2009-05, pp. 42-46.
16. Grünewald, S. et al., n.d. *Deliberate deformation of concrete after casting.* Delft: Delft University of Technology,.
17. Hamilton, J. R., 2003. An overview of silicone rubber. *Rubber World.*
18. Helvoirt, J. v., 2005. *Een 3D blob huid.* Eindhoven: Eindhoven University of Technology.
19. Heugten, R. v. & Huijben, F., 2012. 'Flexibel' bekisten met vacuumatics. *Cement,* Volume 2012-4, pp. 116-121.
20. HRS Silicone Corporation, n.d. *Silicone Rubber.* [Online]
    Available at: http://www.hrssilicone.com/eng/silicone/silicone-rubber.htm
21. Huijben, F., 2014. *Vacuumatics:3D Formwork system.* Eindhoven: Eindhoven University of Technology.
22. Iwamoto, L., 2009. *Digital Fabrications: Architectural and Material Techniques.* New York: Priceton Architectural Press.
23. Kaufmyn, W., n.d. *Polymeric materials (polymers).* [Online]
    Available at: http://fog.ccsf.cc.ca.us/~wkaufmyn/ENGN45/Course%20Handouts/Chap13_Polymers.doc.
    [Accessed May 2014].
24. Kaufmyn, W., n.d. *Polymeric materials (polymers).* [Online]
    Available at: http://fog.ccsf.cc.ca.us/~wkaufmyn/ENGN45/Course%20Handouts/Chap13_Polymers.doc.
25. Kazuli, 2003. *Lexan 940: Polymer Additives and Mechanical Properties.* [Online]
    Available at: http://www.kazuli.com/UW/4A/ME534/lexan2.htm
    [Accessed May 2014].

26. Kelly, P., 2013. *Solid Mechanics Lecture Notes - An Introduction to Solid Mechanics.* Auckland: The University of Auckland.
27. Kolarevic, B., 2001. *Digital Fabrication: Manufacturing Architecture in the Information Age.* Pennsylvania: University of Pennsylvania, USA.
28. Kolarevic, B., 2004. *Digital Praxis: From digital to material.* [Online]
    Available at: http://www.era21.cz/index.asp?page_id=98
    [Accessed February 2014].
29. Kutz, M., 2011. *Applied Plastics Engineering Handbook: Processing and Materials.* First edition ed. Oxford, UK: Elsevier.
30. Meunier, L. et al., 2008. Mechanical experimental characterisation and numerical modelling of an unfilled silicone rubber. In: *Polymer Testing.* Grenoble, France: Elsevier, pp. Volume 27, 765–777.
31. Meunier, L. et al., 2008. Mechanical experimental characterisation and numerical modelling of an unfilled silicone rubber. *Polymer Testing,* Volume 27, pp. 765-777.
32. Milev, I. & Gruendig, L., 2008. *Terrestrial laser scanning applied for reverse engineering and monitoring of historical buildings.* Berlin: Technical University of Berlin.
33. MSC Software, 2010. *Nonlinear Finite Element Analysis of Elastomers,* s.l.: MSC.Software Corporation.
34. MSC.Software, 2010. *Nonlinear Finite Element Analysis of Elastomers,* s.l.: MSC.Software Corporation.
35. Munro, C. & Walczyk, D., 2007. Reconfigurable Pin-Type Tooling: A Survey of Prior. *Journal of Manufacturing Science and Engineering,,* p. Vol 129/551.
36. Muzzy, J. D., n.d. *Thermoplastics – Properties.* Atlanta, GA, USA: Georgia Institute of Technology.
37. Oesterle, S., Vansteenkiste, A. & Mirjan, A., 2012. *Zero Waste Free-Form Formwork.* Zurich, icff2012.
38. Pahl, G. & Beitz, K., 1999. *Engineering Design: A systematic approach.* 2nd ed. s.l.:Springer.
39. Polyservice BV, 2009. *Siliconenrubber HB 1 kg set.* [Online]
    Available at: http://www.polyservice.nl/Siliconenrubber-HB-1-kg-set-p-16269.html
    [Accessed October 2014].
40. Pottmann, H., Schiftner, A. & Johannes, W., 2008. *Geometry of Architectural Freeform Freeform Structures.* s.l.:Osterr. Math. Gesellschaft.
41. Princeton University, n.d. *What is viscosity?.* [Online]
    Available at: https://www.princeton.edu/~gasdyn/Research/T-C_Research_Folder/Viscosity_def.html
    [Accessed April 2014].
42. Pronk, A. & Dominicus, M., 2011. *85 Ways To Make A Membrane Mould.* Barcelona, Spain, International Center for Numerical Methods in Engineering (CIMNE), pp. 28-54.
43. Raun, C., 2013. *Adaptive Moulds.* [Online]
    Available at: http://adapa.dk/products/adaptive-moulds/
    [Accessed April 2014].
44. Rietbergen, B. v., 2011. *FE-analysis of the 3-point bending experiment, using MARC/MENTAT 2010,* Eindhoven: Eindhoven University of Technology.
45. Rooy, I. van; Schinkel, P.; Pronk, A., 2009. *Dubbel gekromde oppervlaktes met behulp van een textiele mal.* Eindhoven: Eindhoven University of Technology.
46. RTP Company, n.d. *Amorphous Polymers.* [Online]
    Available at: http://www.rtpcompany.com/products/high-temperature/amorphous-polymers/
    [Accessed March 2014].
47. Schipper, R., 2015. *PhD-Thesis.* Delft: Delft University of Technology.
48. Schipper, R. & Grünewald, S., 2014. *Efficient material use through smart flexible formwork method.* Delft: Delft University of Technology.
49. Schipper, R. et al., 2014. *Optimization of the Flexible Mould Process for the production of double-curved concrete elements.* Oslo, Norway, CIC2014.
50. Schipper, R. & Janssen, B., 2011. *Manufacturing double-curved elements in precast concrete using a flexible mould - First experimental results.* Prague, fib Symposium.
51. Shetty, K., 2013. *SimAcademy webinar: Segment to Segment Contact in Marc.* s.l.:MSC.Software Corporation.
52. Spuybroek, L., 2004. *NOX: Machine Architecture.* New York: Thames & Hudson.

53. Steel, J., Drogemuller, R. & Toth, B., 2010. *Model interoperability in building information modelling,* Brisbane: Springer.
54. Throne, J., 2011. Thermoforming. In: *Applied Plastics Engineering Handbook.* Dunedin, Florida, USA: Elsevier Inc., pp. 333-358.
55. University of Cambridge, 2008. *Polymer stress-strain curve.* [Online] Available at: www.doitpoms.ac.uk/tlplib/polymers/stress-strain.php
56. Utrecht University, 2014. *Morfologische analyse.* [Online] Available at: http://www.uu.nl/SiteCollectionDocuments/DGK/morfologische%20analyse.pdf [Accessed October 2014].
57. Vegt, A. v. d., 1999. *Polymeren van keten tot kunststof.* Delft: Delft University Press.
58. Vegt, A. v. d. & Govaert, L., 2003. *Polymeren: van keten tot kunststof.* Delft: DUP Blue Print.
59. Vree, J. d., 2014. *Mal.* [Online] Available at: http://www.joostdevree.nl/shtmls/mal.shtml [Accessed October 2014].
60. Wapperom, H., 2004. Volautomatisch 3D-frezen in polystyreen. *Cement,* Volume 2004-8, pp. 71-73.
61. Way, S. & Regis, B., 2001. *Mechanical Properties of Thermoplastics - An Introduction.* [Online] Available at: http://www.azom.com/article.aspx?ArticleID=510# [Accessed June 2014].
62. Wenstop, F., 2008. *Rhino Basics.* [Online] Available at: http://cadcam.ctw.utwente.nl/downloads/Rhino/rhino_basics.pdf [Accessed September 2014].

Reference list of figures

Figures produced by the authors are not listed.

Figure 1.1 Hagens, W., n.d. *Philips Pavilion.* [Online]
Available at: http://architectuul.com/architecture/view_image/philips-pavilion/1528
[Accessed March 2014]

Figure 1.2 Franken\Architekten, n.d. *Bubble.* [Online]
Available at: http://www.franken-architekten.de/index.php?pagetype=projectdetail&lang=de&cat=-1&param=overview&param2=21&param3=0&
[Accessed March 2014].

Figure 1.3 Salamone, F., 2007. *Wikipedia.* [Online]
Available at:
http://en.wikipedia.org/wiki/Neuer_Zollhof#mediaviewer/File:D%C3%BCsseldorf,_Medienhafen.jpg
[Accessed March 2014].

Figure 1.4 austria.info, 2012. *Kunsthaus Graz.* [Online]
Available at: http://www.austria.info/nl/cultuur-steden/kunsthaus-graz-1139489.html
[Accessed March 2014].

Figure 1.5 Kolarevic, B., 2005. Designing and Manufacturing Architecture in the Digital Age. *Architectural Information Management,* p. 121.

Figure 1.6 Eigensatz, M. et al., 2010. *Paneling Architectural Freeform Surfaces,* s.l.: s.n.

Figure 1.7 Eigensatz, M. et al., 2010. *Paneling Architectural Freeform Surfaces,* s.l.: s.n.

Figure 1.9 Pahl, G. & Beitz, K., 1999. *Engineering Design: A systematic approach.* 2nd ed. s.l.:Springer.

Figure 2.1 Foamlinx, n.d. *Small Hot Wire CNC Foam Cutters.* [Online]
Available at: http://www.foamlinx.com/foamlinx_small_hot_wire_cnc_foam_cutters.html
[Accessed Apil 2014].

Figure 2.2 Foamlinx, sd *EPS lathe cut with router and hot wire.* [Online]
Available at:
http://www.foamlinx.com/images/foamlinx_eps_lathe_cut_with_router_and_hot_wire.jpg
[Accessed April 2014].

Figure 2.3 Gard, F., 2013. *Flexible Mold - An innovative production method to produce double curved concrete panels.* Eindhoven: Eindhoven University of Technology.

Figure 2.4 Gard, F., 2013. *Flexible Mold - An innovative production method to produce double curved concrete panels.* Eindhoven: Eindhoven University of Technology.

Figure 2.5 Nedcam, 2009. *Auditorium Mahler 4 Amsterdam: 3D interieurbekleding van "The Rock".* [Online]
Available at: http://www.nedcam.com/auditorium-mahler-4-amsterdam.htm
[Accessed June 2014].

Figure 2.6 Hout, W. V., 2009. *De duurste rijwielstalling van de stad.* [Online]
Available at: http://www.eindhoven-in-beeld.nl/picture/show/20356/De-duurste-rijwielstalling-van-de-stad
[Accessed May 2015].

Figure 2.7 Meijden, D. v. d., 2014. *Stalen bekisting voor brug Parallelweg Den Bosch.* [Online]
Available at: http://www.bd.nl/regio/den-bosch-en-omgeving/s-hertogenbosch/stalen-bekisting-voor-brug-parallelweg-den-bosch-1.4216723
[Accessed April 2014].

Figure 2.8 University of Manitoba, n.d. *Fabric formwork.* [Online]
Available at: http://www.umanitoba.ca/cast_building/research/fabric_formwork/
[Accessed May 2014].

Figure 2.11 Schipper, R., 2012. *Flexible Mould Project.* [Online]

Available at:
http://homepage.tudelft.nl/6w3a0/images/HTML%20gallery/casting%20specimens%20batch%2011/content/_7088623587_large.html
[Accessed June 2014].

Figure 2.12 arch.mcgill.ca, n.d. *The Philips pavilion at the Brussels Expo '58 (The first effort at panelization of large double curved surfaces).* [Online]
Available at: http://www.arch.mcgill.ca/prof/sijpkes/Downloads/proposal-htmlonly.html
[Accessed March 2014].

Figure 2.13 Boers, S., 2012. *OptiMal Forming Solutions.* s.l.:s.n.

Figure 2.14 Oesterle, S., Vansteenkiste, A. & Mirjan, A., 2012. *Zero Waste Free-Form Formwork.* Zurich: icff2012.

Figure 2.15 Gard, F., 2013. *Flexible Mold - An innovative production method to produce double curved concrete panels.* Eindhoven: Eindhoven University of Technology.

Figure 2.16 Boers, S., 2012. *OptiMal Forming Solutions.* s.l.:s.n.

Figure 2.17 Vollers, K. & Rietbergen, D., 2013. *Shaping Building Surfaces.* [Online]
Available at: http://www.praktijkverenigingbout.nl/article-rectification-rumoer-56-shaping-building-surfaces-roel-schipper/
[Accessed May 2014].

Figure 2.18 Oesterle, S., Vansteenkiste, A. & Mirjan, A., 2012. *Zero Waste Free-Form Formwork.* Zurich: icff2012.

Figure 2.19 Raun, C., 2013. *Adaptive Moulds.* [Online]
Available at: http://adapa.dk/products/adaptive-moulds/
[Accessed April 2014].

Figure 2.20 Schipper, R., 2013. *Flexible Mould Project.* [Online]
Available at: http://homepage.tudelft.nl/6w3a0/FlexibleMouldProject.htm
[Accessed May 2014].

Figure 2.21 I. van Rooy, P. Schinkel, A. Pronk, 2009. *Dubbel gekromde oppervlaktes met behulp van een textiele mal.* Eindhoven: Eindhoven University of Technology.

Figure 2.22 Gard, F., 2013. *Flexible Mold - An innovative production method to produce double curved concrete panels.* Eindhoven: Eindhoven University of Technology.

Figure 2.23 Huijben, F., 2014. *Vacuumatics:3D Formwork system.* Eindhoven: Eindhoven University of Technology.

Figure 2.24 Gard, F., 2013. *Flexible Mold - An innovative production method to produce double curved concrete panels.* Eindhoven: Eindhoven University of Technology.

Figure 2.25 Gaba, E., 2006. *Minimal surface curvature planes.* [Online]
Available at: http://en.wikipedia.org/wiki/File:Minimal_surface_curvature_planes-en.svg
[Accessed November 2014].

Figure 2.26 Pronk, A. & Dominicus, M., 2011. *85 Ways To Make A Membrane Mould.* Barcelona, Spain, International Center for Numerical Methods in Engineering (CIMNE), pp. 28-54.

Figure 3.1 Kaufmyn, W., n.d. *Polymeric materials (polymers).* [Online]
Available at:
http://fog.ccsf.cc.ca.us/~wkaufmyn/ENGN45/Course%20Handouts/Chap13_Polymers.doc.

Figure 3.2 Kaufmyn, W., n.d. *Polymeric materials (polymers).* [Online]
Available at:
http://fog.ccsf.cc.ca.us/~wkaufmyn/ENGN45/Course%20Handouts/Chap13_Polymers.doc.

Figure 3.3 Kazuli, 2003. *Lexan 940: Polymer Additives and Mechanical Properties.* [Online]
Available at: http://www.kazuli.com/UW/4A/ME534/lexan2.htm
[Accessed May 2014].

Figure 3.4 Kazuli, 2003. *Lexan 940: Polymer Additives and Mechanical Properties.* [Online]

Available at: http://www.kazuli.com/UW/4A/ME534/lexan2.htm
[Accessed May 2014].

Figure 3.5 Schultz, J., 1974. *Polymer Materials Science.* sl:Prentice-Hal.

Figure 3.6 Vegt, A. v. d. & Govaert, L., 2003. *Polymeren: van keten tot kunststof.* Delft: DUP Blue Print.

Figure 3.7 Muzzy, J. D., n.d. *Thermoplastics – Properties.* Atlanta, GA, USA: Georgia Institute of Technology.

Figure 3.8 Muzzy, J. D., n.d. *Thermoplastics – Properties.* Atlanta, GA, USA: Georgia Institute of Technology.

Figure 3.9 Vegt, A. v. d., 1999. *Polymeren van keten tot kunststof.* Delft: Delft University Press.

Figure 3.10 Vegt, A. v. d., 1999. *Polymeren van keten tot kunststof.* Delft: Delft University Press.

Figure 3.11 Vegt, A. v. d., 1999. *Polymeren van keten tot kunststof.* Delft: Delft University Press.

Figure 3.33 Richeton, J. et al., 2005. *Influence of temperature and strain rate on the mechanical behavior of three amorphous polymers: Characterization and modeling of the compressive yield stress,* sl: Elsevier.

Figure 3.40 Bauman, J. T., 2008. *Fatigue, Stress, and Strain of Rubber Components - A Guide for Design Engineers.* sl:Carl Hanser Verlag GmbH & Co. KG.

Figure 3.41 MSC Software, 2010. *Nonlinear Finite Element Analysis of Elastomers,* sl: MSC.Software Corporation.

Figure 3.42 MSC Software, 2010. *Nonlinear Finite Element Analysis of Elastomers,* sl: MSC.Software Corporation.

Figure 3.43 MSC Software, 2010. *Nonlinear Finite Element Analysis of Elastomers,* sl: MSC.Software Corporation.

Figure 3.44 MSC Software, 2010. *Nonlinear Finite Element Analysis of Elastomers,* sl: MSC.Software Corporation.

Figure 3.45 MSC Software, 2010. *Nonlinear Finite Element Analysis of Elastomers,* sl: MSC.Software Corporation.

Figure 4.7 Gard, F., 2013. *Flexible Mold - An innovative production method to produce double curved concrete panels.* Eindhoven: Eindhoven University of Technology.

Figure 4.8 Gard, F., 2013. *Flexible Mold - An innovative production method to produce double curved concrete panels.* Eindhoven: Eindhoven University of Technology.

Figure 4.19 DTV Springs, n.d. *Drukveer 1000 mm.* [Online]
Available at: http://www.dtvsprings.nl/winkel/index.php?target=categories&category_id=56
[Accessed October 2014].

Figure 4.23 Lieshout, L. v., 2014. *Thermovormen.* [Online]
Available at: http://nl.wikipedia.org/wiki/Thermovormen
[Accessed December 2014].

Figure 4.24 Lieshout, L. v., 2014. *Thermovormen.* [Online]
Available at: http://nl.wikipedia.org/wiki/Thermovormen
[Accessed December 2014].

Figure 4.28 National University of Singapore, 2009. *Vacuum Forming: Vacuum Former 1820.* Singapore: National University of Singapore.

Figure 4.29 National University of Singapore, 2009. *Vacuum Forming: Vacuum Former 1820.* Singapore: National University of Singapore.

Figure 4.30 National University of Singapore, 2009. *Vacuum Forming: Vacuum Former 1820.* Singapore: National University of Singapore.

Figure 4.31 ASB Heating Elements Ltd., n.d. *Silicone rubber heaters.* [Online]
Available at:
http://www.asbheat.com/01_html/products/16_silicone_rubber_heaters.shtml#mounting
[Accessed January 2015].

Figure 4.37 Groneman, n.d. *Elso kogel- en kruiskoppelingen.* [Online]
Available at: http://www.groneman.nl/aandrijftechniek/cardanassen/elso_koppelingen
[Accessed September 2014]

Figure 6.2 Rietbergen, B. v., 2011. *FE-analysis of the 3-point bending experiment, using MARC/MENTAT 2010,* Eindhoven: Eindhoven University of Technology.

Figure 6.21 Shetty, K., 2013. *SimAcademy webinar: Segment to Segment Contact in Marc.* sl:MSC.Software Corporation.

Figure 7.9 natuurkunde.nl, n.d. *Oven.* [Online]
Available at: http://www.natuurkunde.nl/opdrachten/1120/oven
[Accessed January 2015].

Reference list of tables

Tables produced by the authors are not listed.

Table 2.3 Gard, F., 2013. *Flexible Mold - An innovative production method to produce double curved concrete panels.* Eindhoven: Eindhoven University of Technology.

Table 3.1 Eriks, n.d. *High Performance Silicone (technical documentation).* Hoboken, België: ERIKS nv.

Table 3.3 Eriks, 2014. *RX® Silicone Si- (of MVQ-)rubber,* Alkmaar: ERIKS BV.

Table 4.1 DTV Springs, n.d. *Drukveer 1000 mm.* [Online]
Available at: http://www.dtvsprings.nl/winkel/index.php?target=categories&category_id=56
[Accessed October 2014].

Appendix

Appendix A: Autodesk's 123D Catch

Autodesk's 123D Catch

Autodesk 123D Catch is an open source software package which can be freely downloaded for the use for creating 3D meshes from digital photographs. Image-based modeling is for some known as "photogrammetry". It simply requires the user to supply a minimum of three to a maximum of 70 images of an object acquired from various viewpoints, which are then uploaded to a server for processing. However, exact details are not provided by Autodesk.
An algorithm (scale invariant feature transform) is used which identifies common image features across images. The processing method involves the SfM (Structure from Motion) method. After that, adjustment are used to compute the parameters to represent the inner and exterior camera geometry. To represent the object, these parameters will be combined with a dense point cloud. (Chandler & Fryer, 2013). The photogrammetry technique is an interesting technique because there is no need for expensive 3D scanner and specific expertise. Furthermore, lasers scanners and structured lighting systems are not portable, time consuming and not flexible to use. (Santagati & Inzerillo, 2013)

Accuracy of 123D Catch

The main issue of the software package is how accurate is it. Some research has been done in order to determine the accuracy of 123D Catch. Below the studies are reviewed.

- "AutoDesk 123D Catch: How accurate is it?" (Chandler & Fryer, 2013):

A past project of Chandler and Fryer conducted to record an aboriginal cave (9 m in length) site was reprocessed. *"In 2004, this processing stage had required four days' work, with a high level of user input and experience past project conducted to record an aboriginal cave site was reprocessed. For this latest test, the sixteen original images were uploaded to the 123D Catch server and were processed successfully and automatically within just fifteen minutes.*
The 123D Catch control points and original control coordinates derived from the reflectorless total station were then used in a 3D similarity transformation to determine the optimum rigid body transform between the two coordinate systems. Seven parameters were estimated: 3 translation, 3 rotation and 1 scale.
As the overall standard deviations suggest, the fit to the original control is just 12 mm, 11 mm and 4 mm in XYZ respectively. Although such accuracy is comparatively low (1:600) compared to normal stereo close-range photogrammetry (1:1,000-1:10,000), but a significantly greater effort had been required! Also if more imagery at a diverse range of scales had been acquired originally and used to provide a stronger configuration, accuracies would certainly have been improved". (Chandler & Fryer, 2013)

- '123D Catch: Efficiency, Accuracy, Constraints and Limitations in Architectural' (Santagati & Inzerillo, 2013)

"The researchers investigated on the metric reliability of the 123D Catch models comparing them with terrestrial laser scanner acquisitions or reliable Ground Control Points (GCP), on the surfaces reconstruction quality and on the detail quality in relation with the number of images and their resolution. The main fundamental aspects to investigate are two:

1. *the mesh visual accuracy: we obtain a 3D model that reproduces reality;*
2. *the mesh metric accuracy: we obtain a 3D model that is metrically close to reality.*

Several tests have been carried out both on the small, the medium and large scale". (Santagati & Inzerillo, 2013)

For the purpose of the double curved concrete elements only the small scale element are of interest. Figure A.1 shows the small scaled architectural elements that were photographed. The comparison of the 3D models is done with the use of 'Meshlab', which is an open source software that is able to scale, align and process both point clouds and meshes, see Table A.1 and Table A.2

Figure A.1: Architectural elements of the Auteri Chapel, Cantania (adapter from Santagati, C. & Inzerillo, L., 2013. *123D Catch: Efficiency,Accuracy, Constraints and Limitations in Architectural Heritage Field.* Catania, Italy: International Journal of Heritage in the Digital Era)

Architectural element 1	Part of the base	Photo of the element
Dimension of the object	1.50x1.50 m	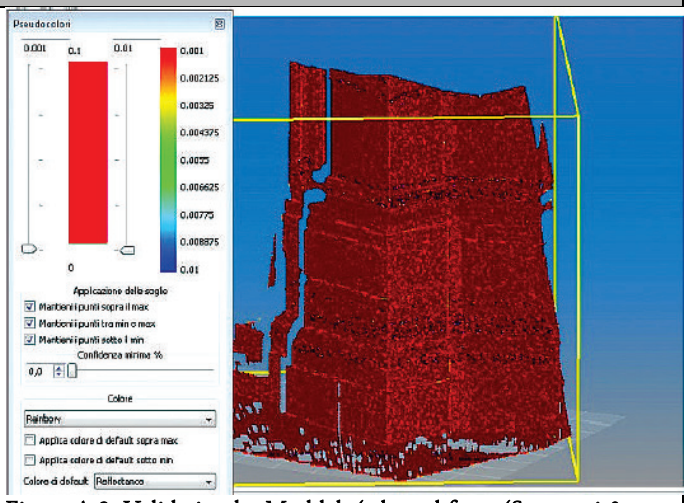
Number of images	14	
Resolution	8.5 Mpixel	
123D Catch mesh	693,736 triangles 368,357 vertices	
Laser scan point cloud	154,901 vertices	
Average error	0.0025-0.001m	Figure A.2: Validation by Meshlab (adapted from (Santagati & Inzerillo, 2013)

Table A.1: Validition of the first Architectural elements of the Auteri Chapel, Cantania (adapted from Santagati, C. & Inzerillo, L., 2013. *123D Catch: Efficiency,Accuracy, Constraints and Limitations in Architectural Heritage Field.* Catania, Italy: International Journal of Heritage in the Digital Era)

Architectural element 2	Part of the base	Photo of the element
Dimension of the object	1.50x1.50 m	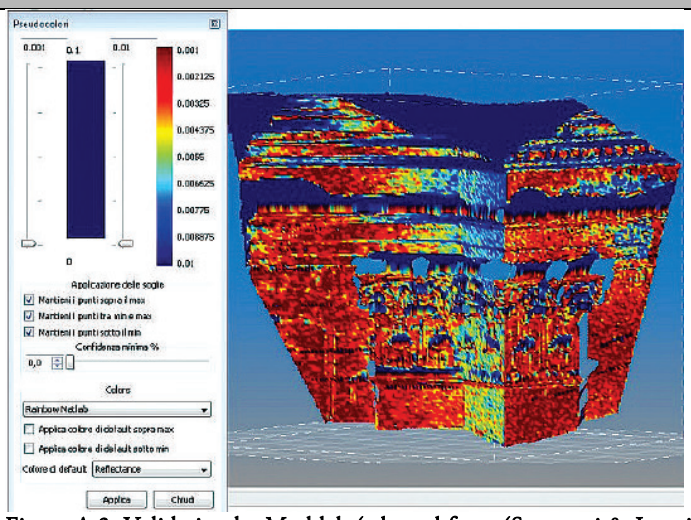
Number of images	11	
Resolution	8.5 Mpixel	
123D Catch mesh	872.000 triangles 438.845 vertices	
Laser scan point cloud	179.784 vertices	
Average error	0.0010-0.001m	

Figure A.3: Validation by Meshlab (adapted from (Santagati & Inzerillo, 2013)

Table A.2: Validition of the second Architectural elements of the Auteri Chapel, Cantania (adapted from Santagati, C. & Inzerillo, L., 2013. *123D Catch: Efficiency,Accuracy, Constraints and Limitations in Architectural Heritage Field.* Catania, Italy: International Journal of Heritage in the Digital Era)

Considering the results of Meshlab, the scans are reliable as much as a time-of-flight (TOF) 3D laser scanner (accuracy 0.006m) (Santagati & Inzerillo, 2013). However, the amount of used images is still limited. Additionally, the scans can be more accurate when some guidelines are used (Autodesk, 2011).

Advantages	Disadvantages
Low processing times;	The uploaded dataset of the taken photos has to be organized.
Processing on cloud;	The intended object to scan should be photographed in its entireness. The software is not able to manage the overlapping between two frames in height
Accuracies in the order of millimetres are feasible for statues, work of arts, archeological and architectural details	
Accuracies in the order of 1-2 centimetres are feasible for large scale architectural buildings	
To achieve accurate scans it is necessary to use a camera with a resolution between 6-12 megapixels. The use professional cameras with specific lenses is unnecessary.	

Table A.3: Advantages and disadvantages of 123D Catch (adapted from Santagati, C. & Inzerillo, L., 2013. *123D Catch: Efficiency,Accuracy, Constraints and Limitations in Architectural Heritage Field.* Catania, Italy: International Journal of Heritage in the Digital Era)

Planning guidelines

Autodesk has given guidelines to obtain an accurate 3D model. These guidelines are divided and are further discussed below. Eventually a 3D-scan set up is made on the basis of the guidelines (Autodesk, 2011).

Accessibility

It is important planning how to attend to move above the scene and shoot the subject before shooting the photos. To get the whole object in frame first, take photos in a row sequentially around the object. Details

photos can be shoot next. In general all surfaces which will be modelled should be visible in 3 to 4 photos from different angles.
Implementations for the 3D scan setup:

- Take photos in two different rows/heights;
- Each row exists of maximum 35 photos;
- Detail shots are unnecessary for the thermoplastic –and concrete panels

Occlusions and number of photos to shoot
Some objects can be self-concluding. Views of parts can be blocked by other parts of an object. These occlusions can be solved by planning the shots. It will require tighter intervals between your photos and object. Five to ten degree intervals are necessary instead of 20 degree intervals with non-self-concluding subject. To avoid less accuracy, plan the photos wisely if the project should contain up to around 50 photos and should not exceed 70 photos.
Implementations for the 3D scan setup:

- Marks of every 5 degree intervals will be made.

Photographs need features
Laborious manually stitching process can be avoided by creating features on objects such as a white wall or a fabric couch is necessary. To create identifiable feature, e.g. painter tape or variety cloth on or near the subject can be used. In some cases the features are symmetrical, repetitive or identical such as a fabric, repetitive windows of a modern building. The automatic stitching process of the software may mistake one part of the subject with another part. Keep this in mind during shooting the photos.
Implementations for the 3D scan setup:

- Manually stitching must be avoid;
- Colored squared papers are used to create identifiable features.

Transparent, reflective or glossy subjects
Transparent, reflective or glossy subjects cannot be scanned. Features on these types of subjects are difficult to mesh among the photos as the viewpoint changes around the subject. Even if the photos can be stitched, it is still difficult to determine a 3D surface.
Implementations for the 3D scan setup:

- By the use of painter tape, the transparent and reflective surfaces of thermoplastics will be prevented.

Subjects cannot move
The only thing that is allowed to move about the scene is the position of the camera. During shooting an object, the object should not move. Features are attracted of the whole photograph and not just the subject.
Implementations for the 3D scan setup:

- Static environment around the object;
- Position of the camera rotates around the object
- Distance of camera to the object will be same.

Consistent lighting
Overexposed and underexposed images often cause more damages than good for the 3D model. Consequent light conditions of the environment ensure a better 3D model. The photos will match better. During the shooting of the subject, using a flash is not acceptable. The flash of the camera creates a unique lighting situation with each photograph.
Implementations for the 3D scan setup:

- Avoid daylight
- Using a static lightning source above the set-up

3D scan setup

Through these guidelines from Autodesk and the papers, the following setup has been developed in order to photograph the objects, see Figure A.4.

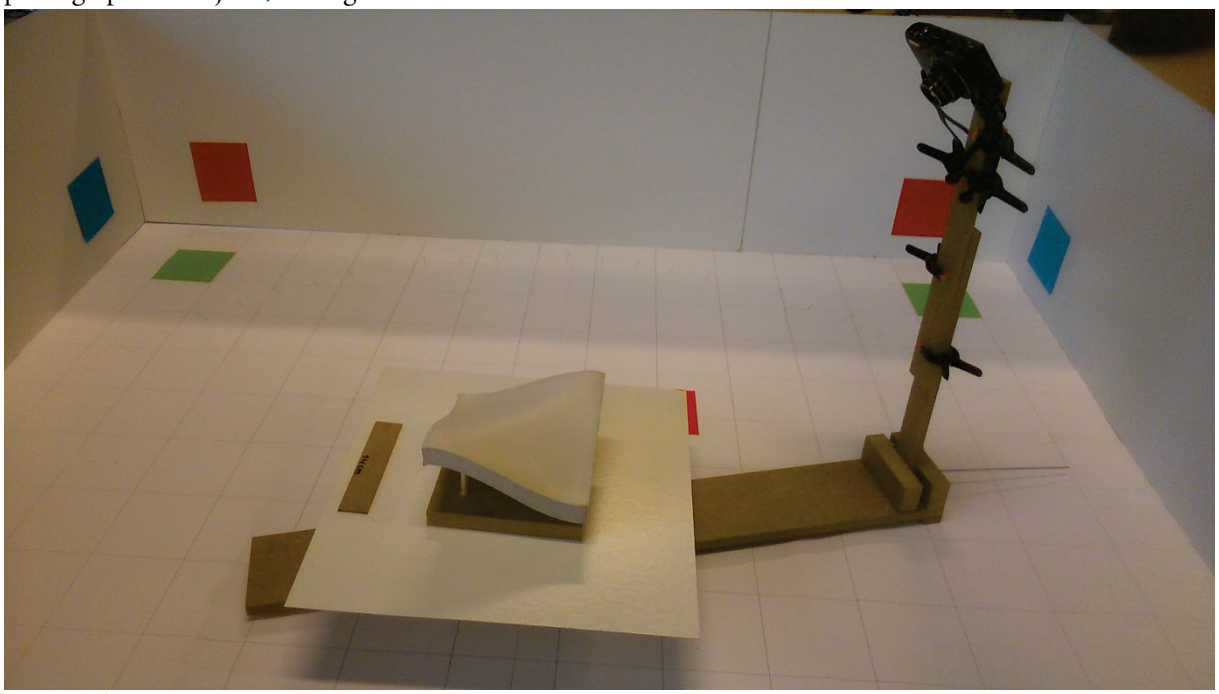

Figure A.4: 3D scan setup

The camera moves around the object while it is maintaining the same distance to the object. The height of the camera is adjustable. Pictures will be taken of two heights. For each height 35 pictures maximum can be taken to not exceed the maximum of 70 photos.

The red, blue and green surfaces in the corners are reference points. A grid of 100x100mm is projected on the ground surface, the lines of this pattern displays the depth and acts as a reference. Every 5 degrees, marks are projected onto the ground surface in order to indicate the camera positions. This is necessary to prevent stitching. Eventually a reference distance is needed to scale the scan to the right dimensions.

It is important the scan setup is not placed nearby daylight. Lighting conditions of daylight are not constant. A static light source is needed above the setup. The brightness of the light source should be sufficient to make clear pictures.

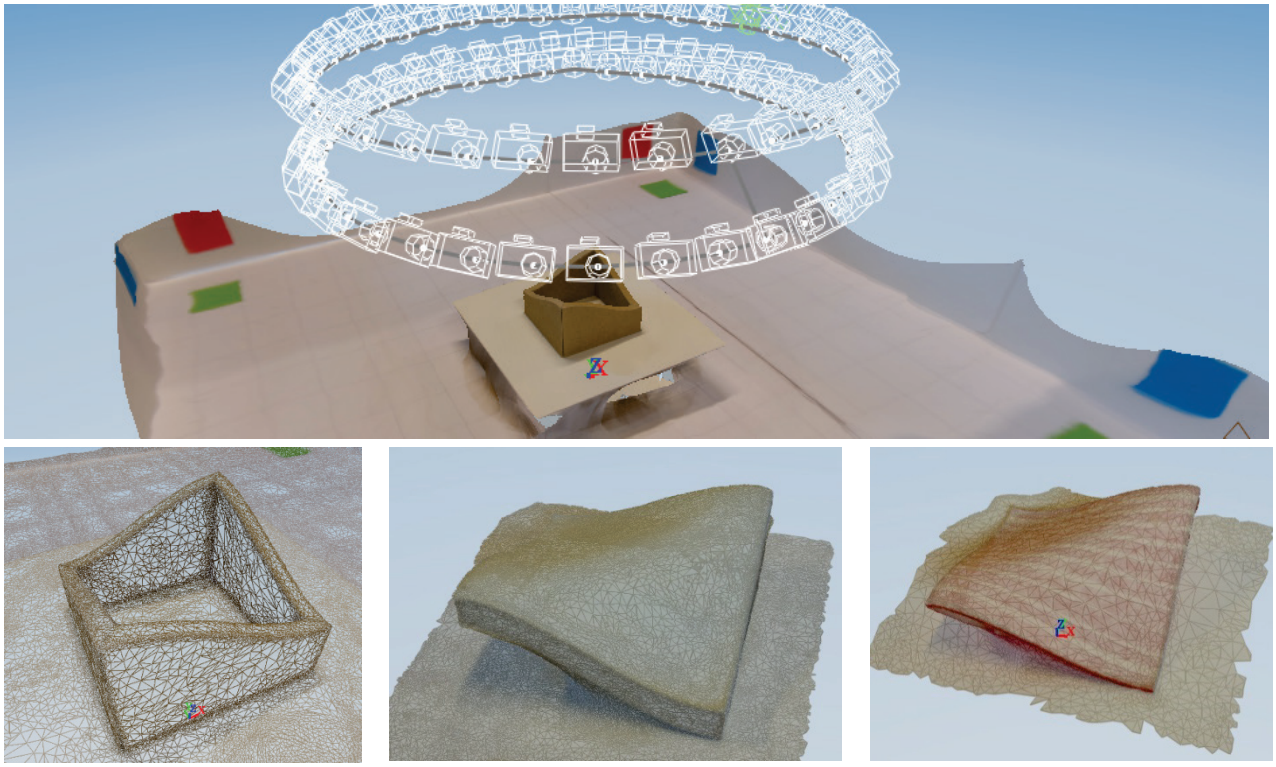

Figure A.5: Scanned object of the static edge mould method

After uploading the photos to 123D catch, 3D meshes will be generated automatically (Figure A.5). After scaling the scanned object, it can be exported to a validation software package.

The accuracy of 123D Catch in cooperation with the 3D scan setup has been tested based on a scan of a wooden panel, as shown in Table A.4. The panel is measured with a digital caliper (Topcraft DMV-SL05). According to the manufacturer with the caliper tolerance is 0.02 mm +/- for measurements less than 100mm and 0.03 mm +/- for measurements between 100-150mm (Teknihall, 2010). In Table A.4 the specifications of scanned object are shown. The result of the verification test can be seen in Table A.5 and Table A.6.

Scan specifications		Photo of the element
Dimension of the object	150x140mm	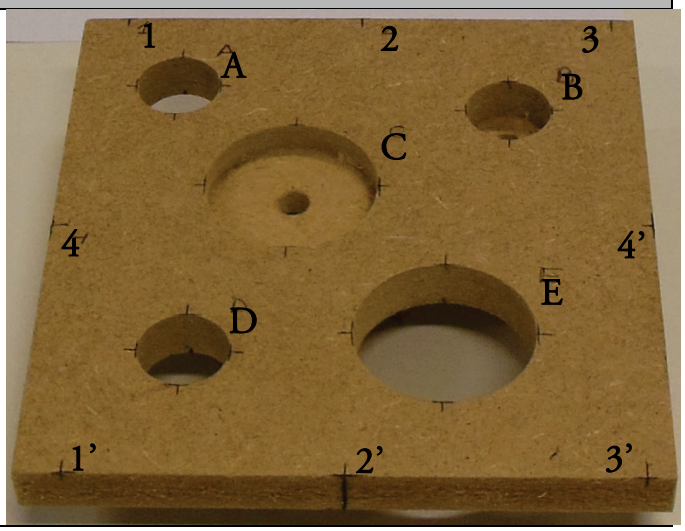
Number of images	70	
Camera	Nikon Coolpix S6300	
Resolution	4608x3456 pixels	
Exposure time	1/50s	
f-stop	f/3.2	
ISO-speed	ISO-125	
Exposure bias	0-step	
Focal length	4mm	
Max. aperture	3.3	

Table A.4: Scan specifications

	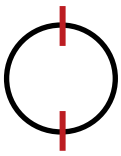		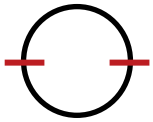		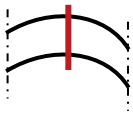	
	Measured distance [mm]	Distance in 123D Catch [mm]	Measured distance [mm]	Distance in 123D Catch [mm]	Measured thickness [mm]	Thickness in 123D Catch[mm]
A	20,45	22,00	20,49	20,81	12,20	10,62
B	20,44	21,32	20,45	21,36	-	
C	40,40	41,64	40,40	41,31	-	
D	20,46	21,63	20,43	20,89	12,18	11,33
E	40,44	41,52	40,42	41,13	12,16	10,72
Error range [mm]	0,88-1,55		0,32-0,91		0,58-1,58	

Table A.5: Accuracy test 123D Catch, measurement range ±12-40mm

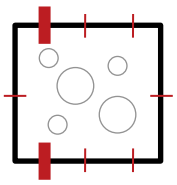 1		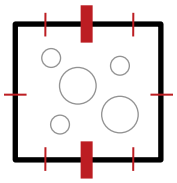 2		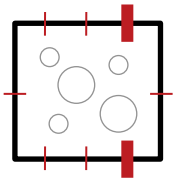 3		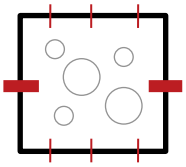 4	
Measured distance [mm]	Distance in 123D Catch [mm]	Measured distance [mm]	Distance in 123D Catch [mm]	Measured distance [mm]	Distance in 123D Catch [mm]	Measured distance [mm]	Distance in 123D Catch [mm]
147,86	147,41	147,72	147,52	147,32	146,87	138,67	138,52
Error range [mm]		0,15 - 0,45					
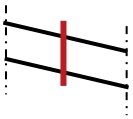 1		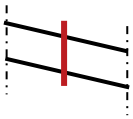 2		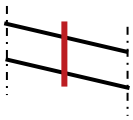 3		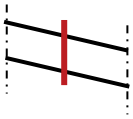 4	
Measured thickness [mm]	Thickness in 123D Catch [mm]	Measured distance [mm]	Thickness in 123D Catch [mm]	Measured thickness [mm]	Thickness in 123D Catch [mm]	Measured thickness [mm]	Thickness in 123D Catch [mm]
12,05	11,11	12,04	11,46	12,14	11,51	12,08	11,87
Error range [mm]		0,21 - 0,94					

Table A.6: Accuracy test 123D Catch, measurement range ±12mm and ±130-150mm

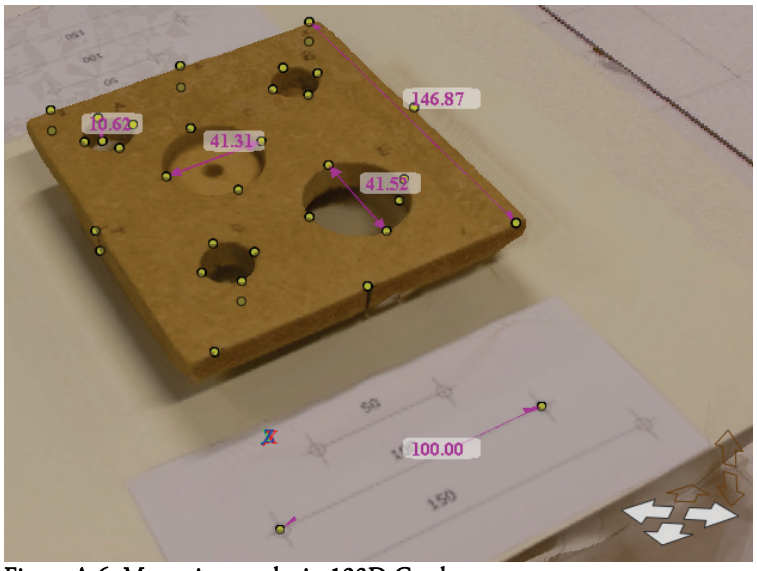

Figure A.6: Measuring results in 123D Catch

In this verification method the following inaccuracies occur:

- Selecting the 'reference points' in 123D Catch (see Figure A.6)
- Accuracy of the algorithm of 123D Catch
- Printing accuracy of the reference distance on paper
- Digital caliper accuracy
- Manually measuring with the caliper

As can be seen in the results, error in the x and y-direction varies between the 0.2 and 1.6 mm, with an average error of 0.8 mm. In the z-direction the error varies between the 0.2 and 1.6 mm, with an average error of 0.9 mm. Noteworthy, this is not a fixed error for all future scans. This value is only the error of this measurement and gives an insight of what the error is approximately.
Finally, the wooden panel is modelled in CAD with the use of the digital caliper. This CAD model is compared with the 123D Catch model in CloudCompare, see Figure A.7.

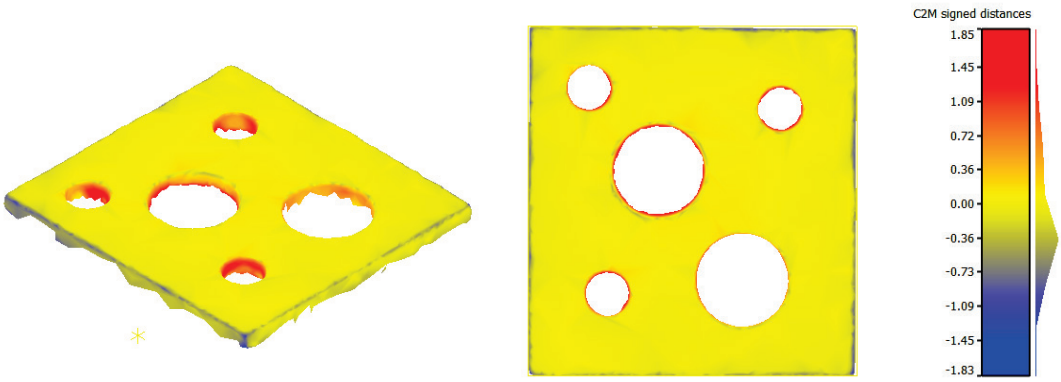

Figure A.7: Scanned model compared to the CAD model by CloudCompare

References

Autodesk, 2011. *123D Catch - Create Your Own 3D model: Planning your shoot.* [Online]
Available at: https://www.youtube.com/watch?v=7TfXXJxDsXw
[Accessed June 2014].

Chandler, J. & Fryer, J., 2013. AutoDesk 123D Catch: How accurate is it?. *Geomatics World*, February, p. 32.

Santagati, C. & Inzerillo, L., 2013. *123D Catch: Efficiency,Accuracy, Constraints and Limitations in Architectural Heritage Field.* Catania, Italy: International Journal of Heritage in the Digital Era.

Teknihall, 2010. *Topcraft GT-DC-02.* [Online]
Available at: http://www.teknihall.be/index.php?id=1339&L=1
[Accessed July 2014].

Appendix B: CloudCompare

CloudCompare validation process

The validations are done by the software CloudCompare. CloudCompare is a free 3D point cloud processing software application, which also can handle triangular meshes. This software is used for aligning the two geometries and for computing the distance between the geometries. The validation process is described step by step.

First, the scanned geometry will be inserted first to CloudCompare, the geometry has to be modified. The mesh of the scanned object has to be cleaned in order to obtain only the surface of the desired object itself. This object then can be exported to .obj format. The designed geometry from Rhinoceros also has to be exported to an .obj format, see Figure B.1. Then the geometries can be manually rotated and aligned in CloudCompare.

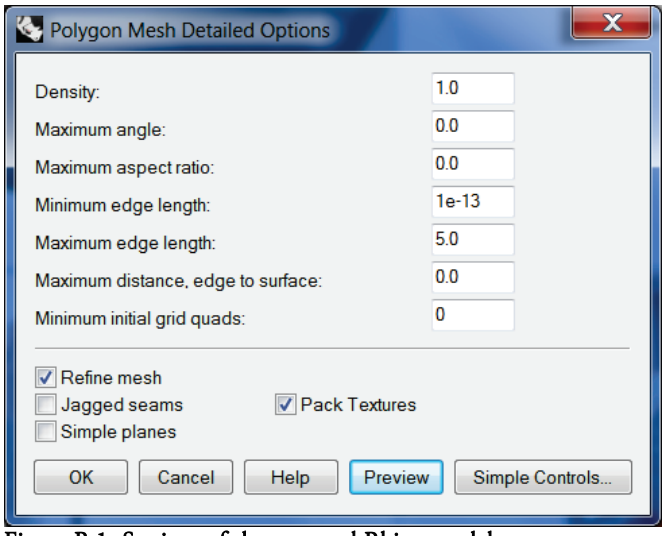

Figure B.1: Settings of the exported Rhino model

The edges of the panels are theoretical the most accurate through the use of the flexible edges of the Fluid Mould device. The panels edges should be aligned with the reference geometry/model (designed Rhinoceros surface) so the larger inaccuracies in the middle part of the panel can be calculated. Therefore the middle section of the mesh has to be cut out. Then the remaining geometry, which is the panels edge, can be aligned by using the align tool. The parameters error difference and random sampling limit have to be set (which settings?). As a result, the scanned geometry will be translated so the mean square errors between the two geometries will be minimal. The translation is given in a translation matrix, which has to be copied to the whole scanned geometry. Now the cloud/mesh distance between those geometries can be computed to a geometry. For clarification, the visible cloud/mesh distances and colour scale can be adjusted. The last step is to export and save all data. As an example, the validation process of the static edge mould method is elaborated, see Figure B.2 up to Figure B.7.

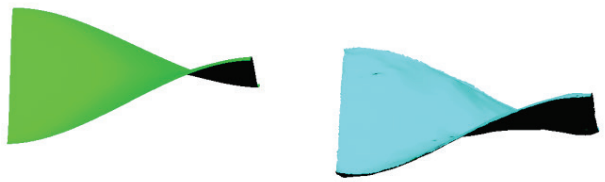

Figure B.2: Import objects in CloudCompare

Figure B.3: Manually rotate and align objects

Figure B.4: Cut out inner section of the scanned geometry

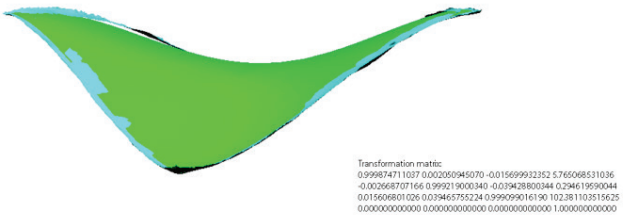

Figure B.5: Align outer section of the scanned geometry with the reference surface (designed panel from Rhinoceros) and copy the resulting translation matrix

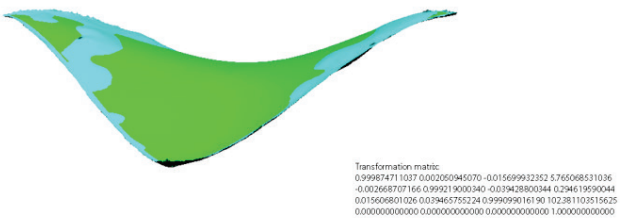

Figure B.6: Paste translation matrix to the whole scanned geometry

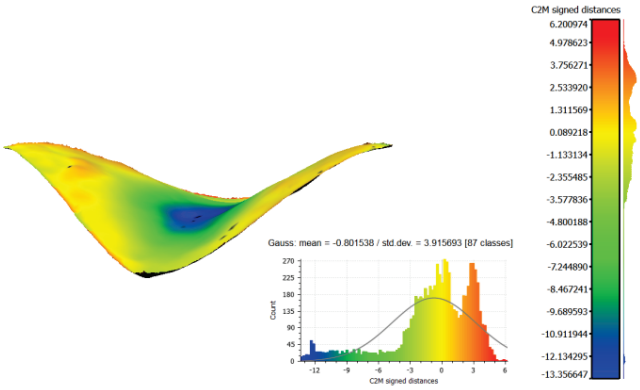

Figure B.7: Compute cloud to mesh distance on the scanned geometry and turn off the Rhinoceros geometry layer. Adjust visible distances and color scale if necessary and export data (.bmp, .ASCII and .BIN)

Appendix C: Morphological Matrix

Morphological Matrix - Fluid Mould

				1	2	3	4	5	6
A	Mould technique			A1  Static mould	A2  Re-formable mould	A3  Flexible mould			
B	Flexible mould method			B1  Pin-bed surface	B2  Supported flexible layer	B3  Tensioned flexible layer	B4  Pressurized flexible layer		
C	Tensioned flexible layer			C1  Thermoplastic layer	C2 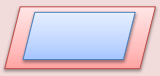 Elastomer support layer for the thermoplastic sheet				
D	Actuators	D1	Amount of actuators	D11 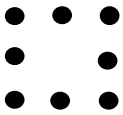 4x3	D12 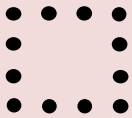 4x4	D13 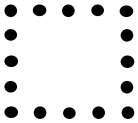 4x5	D14 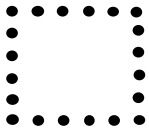 4x6	D15  Pin-bed edge	
		D2	Determine actuator heights	D21  Analytical determination	D22 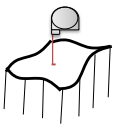 Experimental determination				
		D3	Set actuator height	D31  Nuts	D32 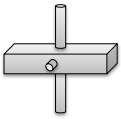 Clamping the actuators	D33 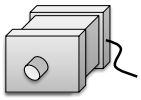 Step motor			
		D4	Set actuator angle	D41 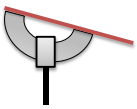 Rotation plate	D42  Use of two actuators	D43 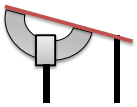 Use of rotation plate and two actuators			
		D5	Lowering of actuators	D51 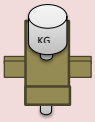 Use of rods and weights	D52 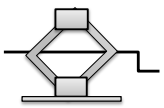 Use of a lifting jack	D53 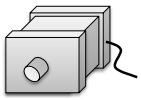 Use of step motor			
		D6	Allow length variations in flexible edge	D61 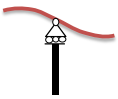 Roller support	D62  Pendulum rod	D63 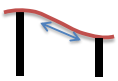 Allow strain in flexible layer			
		D7	Prevent axial rotation actuators	D71  Squared actuator	D72 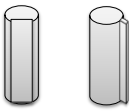 Modified threated rods	D73 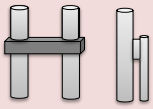 Support actuator			

E	Flexible edge	E1	Material	E11 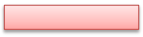 Silicone rubber	E12  Silicone rubber stiffened by a thin steel stroke	E13 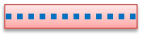 Silicone rubber reinforced by glass fibers	E14  Silicone rubber reinforced by a spring steel wire mesh		
		E2	Form	E21 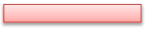 Rectangular strip	E22  Tapered edge				
		E3	Single / dual flexible edge(s)	E31  Single flexible edge	E32  Dual flexible edges				
		E4	Joint actuator and flexible edge	E41 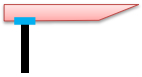 Glue actuator to flexible edge	E42 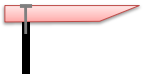 Srew actuator to flexible edge	E43  Attach actuator to reinforcement			
		E5	Clamping system	E51 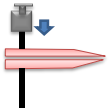 Use of weights	E52 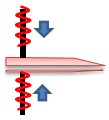 Use of springs	E53 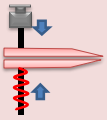 Use of weights and springs	E54 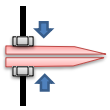 Use of nuts	E55 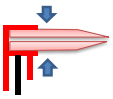 Screw clamp	
		E6	Corner solution	E61  Single frame	E62  Windmill blade formation				

F	Flexible layer	F1	Apply tension to flexible layer	F11 Uniform	F12 Non-uniform				
		F2	Fixation frame flexible layer	F21 Planar frame	F22 Deformable frame	F23			
		F3	When to approximate deformation to flexible layer	F31 Before deforming flexible edges	F32 After deforming flexible edges	F33 During deforming flexible edges			
		F4	Move flexible layer edge	F41 Side rod	F42 Actuators	F43 Side rod attached to actuators			
		F5	Fixation flexible layer	F51 Steel cable	F52 Cable with flexible rod	F53 Folded flexible layer	F54 Clamp between profiles	F55 Shoelace' with gommets/eyelets	F56 Steel cables with fixation openings
		F6	Apply/adjust tension to the flexible layer	F61 Use 'shoelace'	F62 Use cables with hooks and eyes	F63 Use turnbuckles	F64 Use an inflatable		
G	Thermoforming procedure			G1 Use of a large oven	G2 Use of a small oven	G3 Build-in heater element	G4 Silicone rubber heater		
H	Customize thermoplastic sheet			H1 Band saw	H2 Hand held cutting	H3 Hand held router	H4 CNC cutting		
I	Casting concrete panel			I1 Thermoplastic sheets between frames	I2 Visco casting on open mould				

Appendix D: Technical drawings

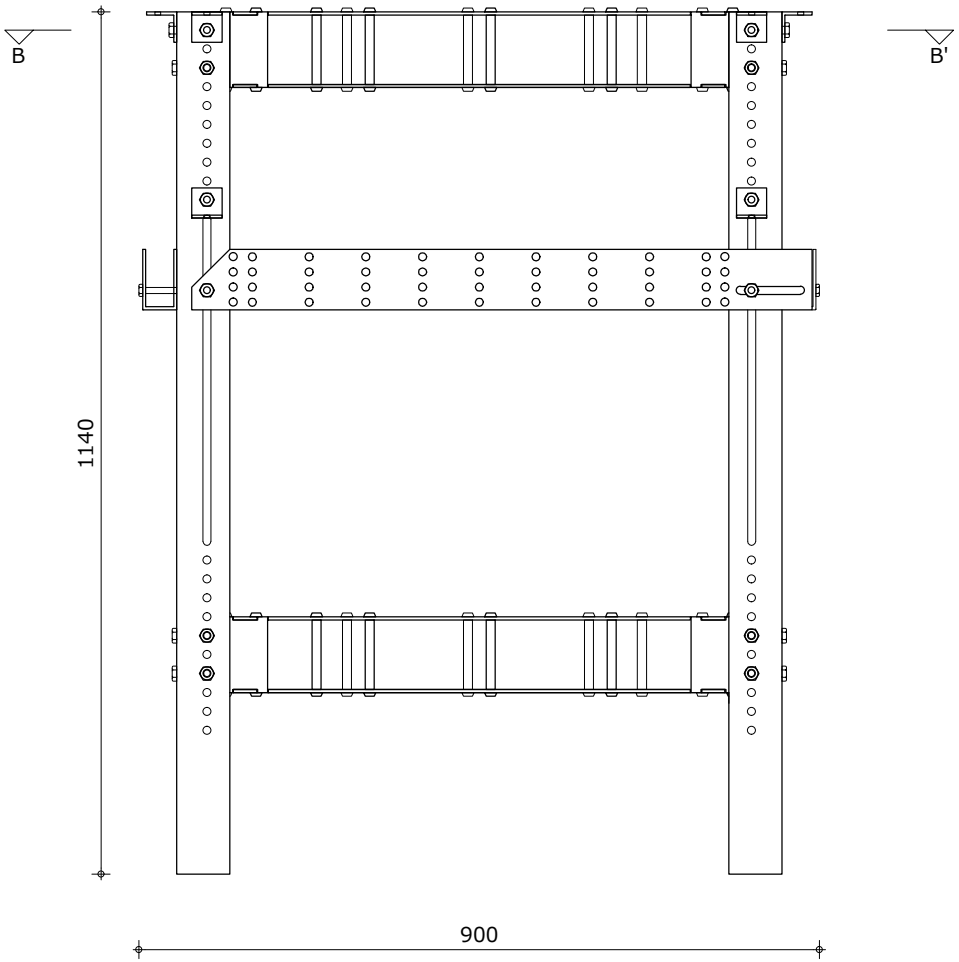

Front view
1:10

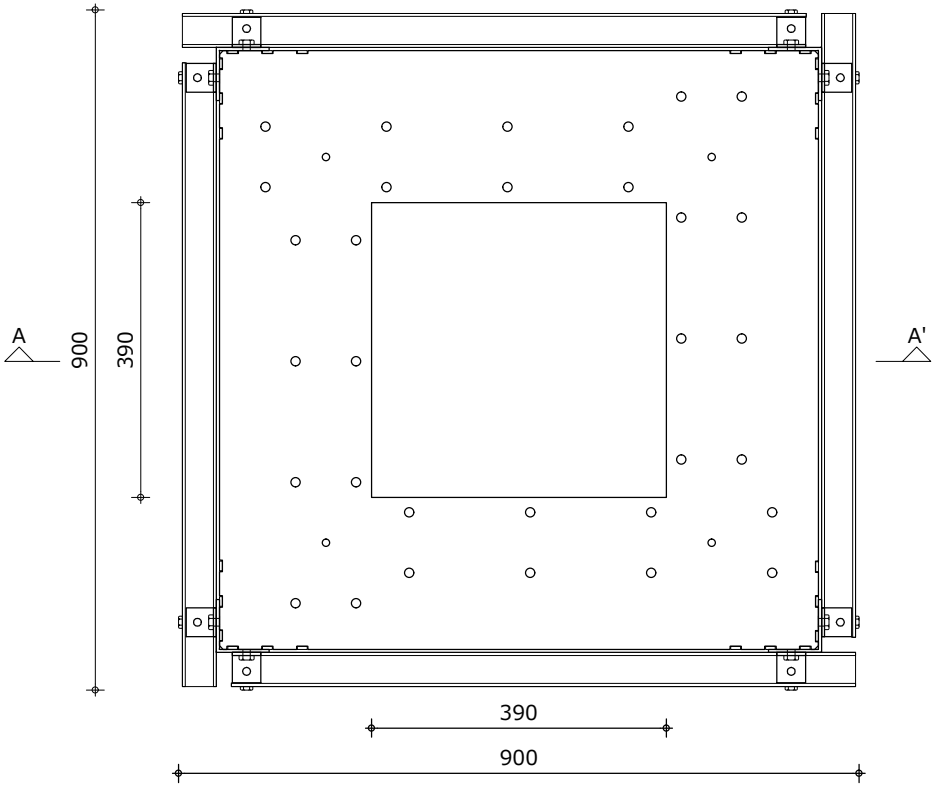

Top view
1:10

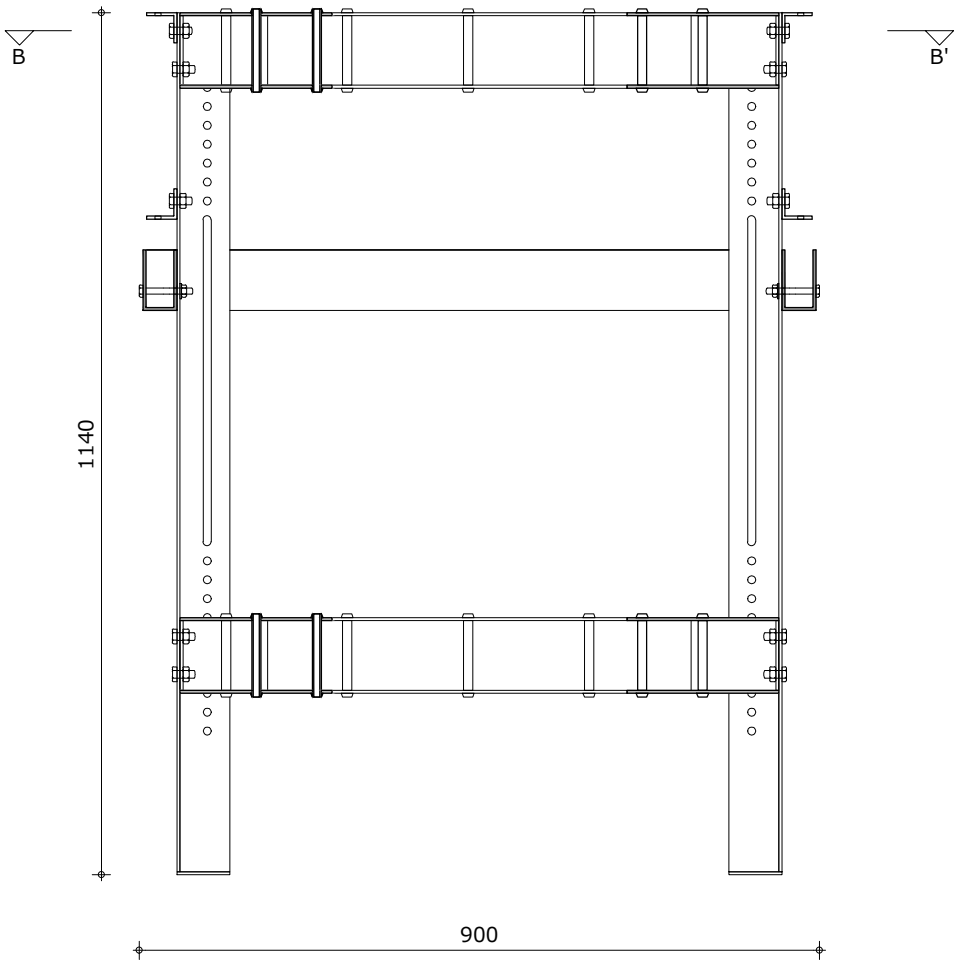

Section A-A'
1:10

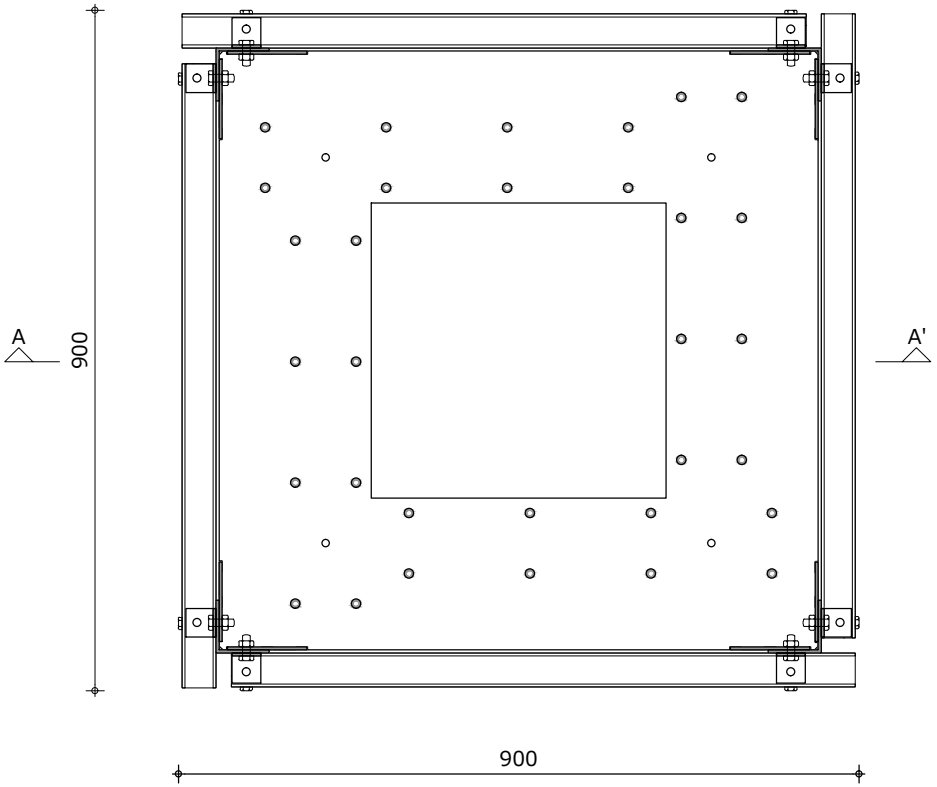

Section B-B'
1:10

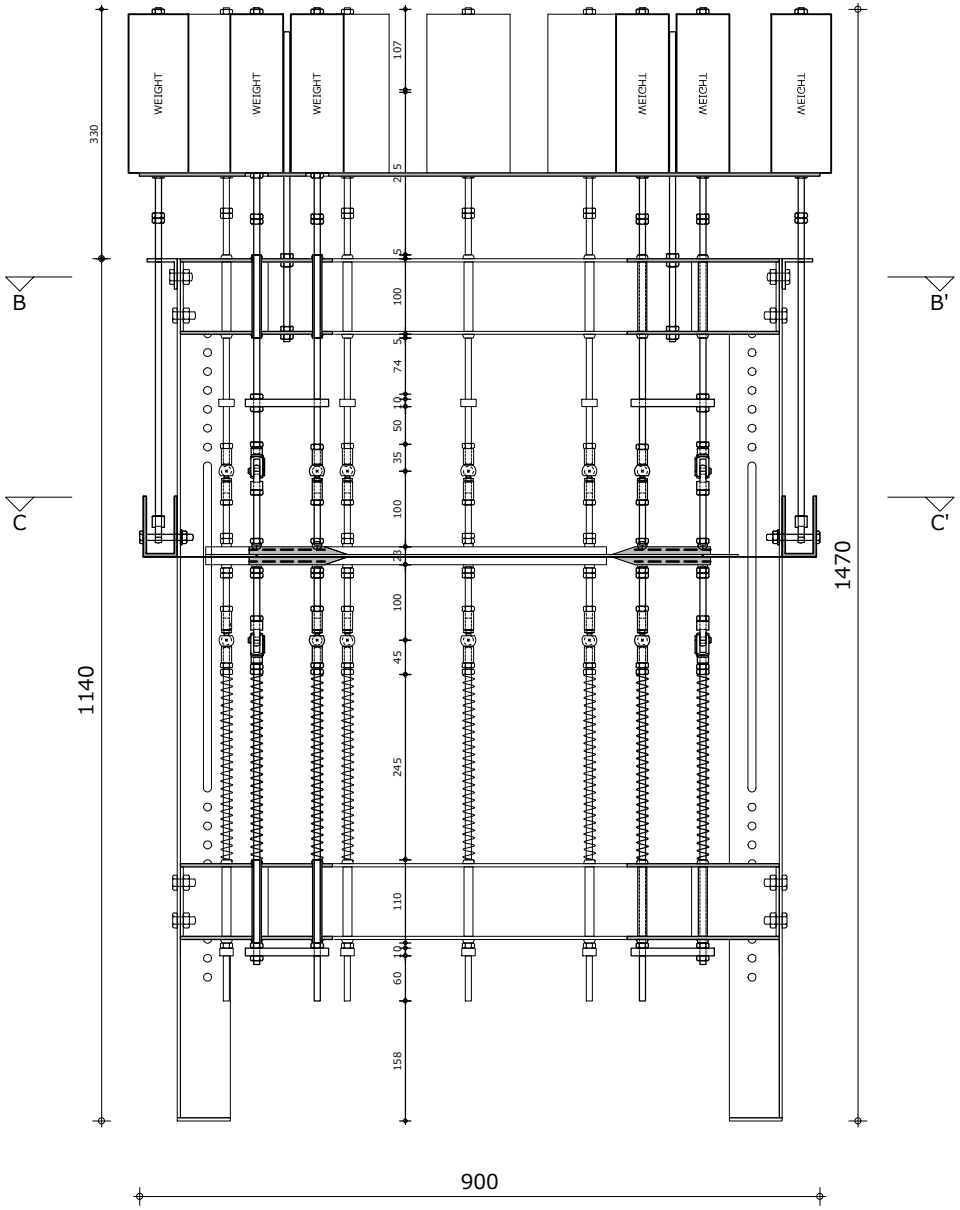

Section C-C'2
1:10

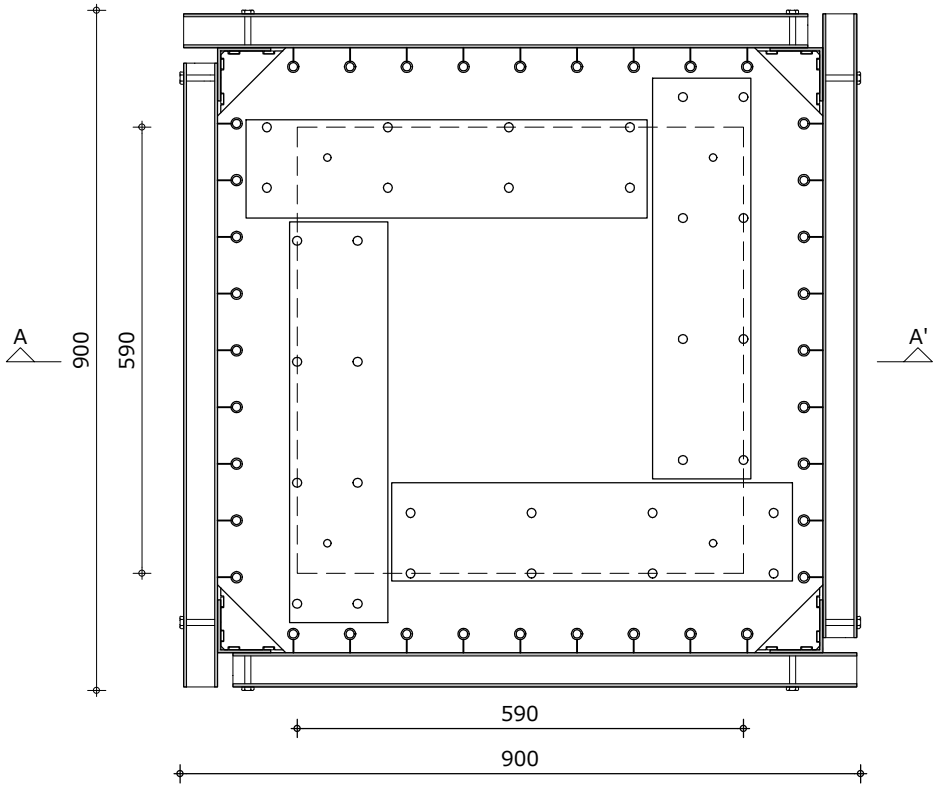

Section D-D'
1:10

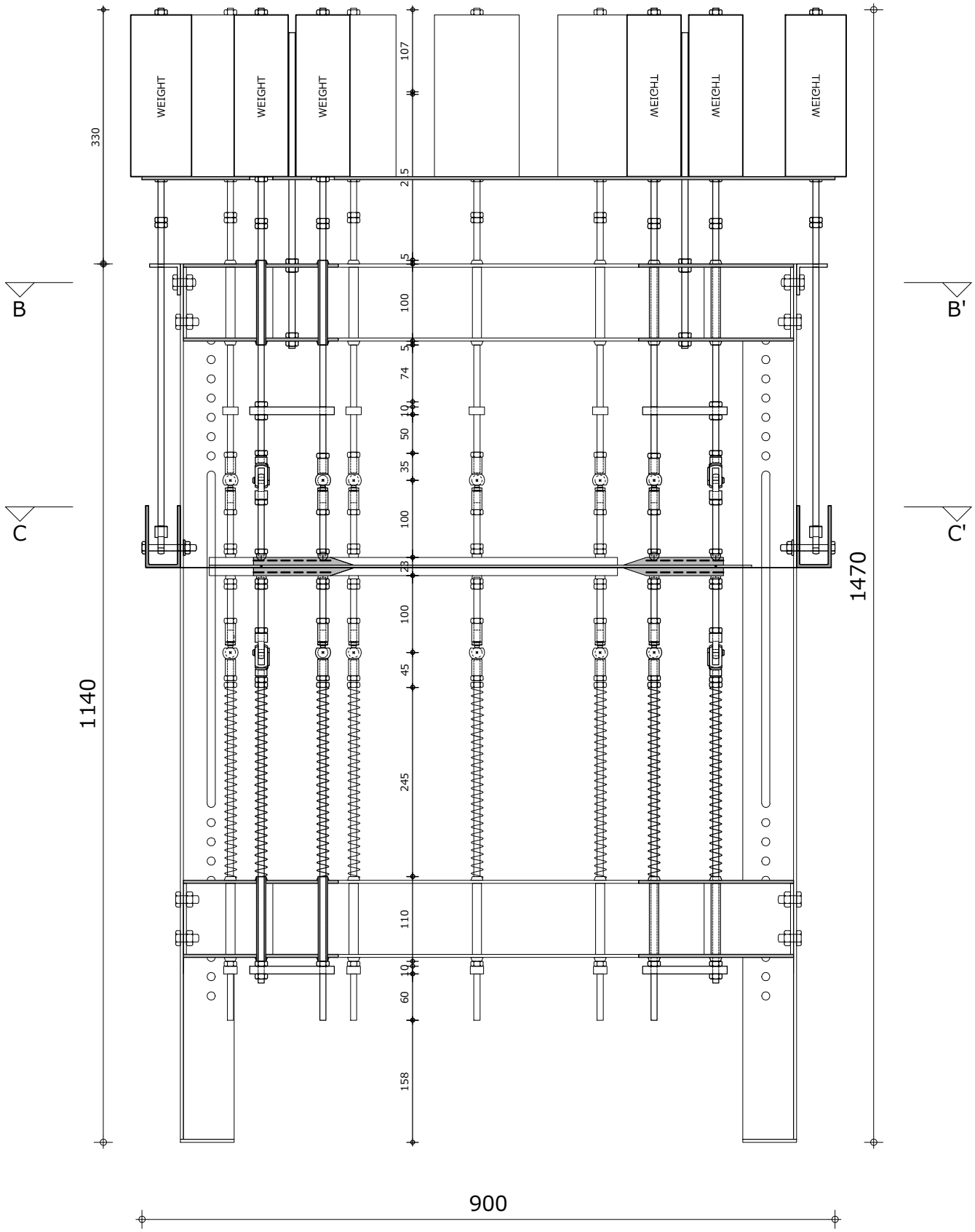

Section A-A'
1:7

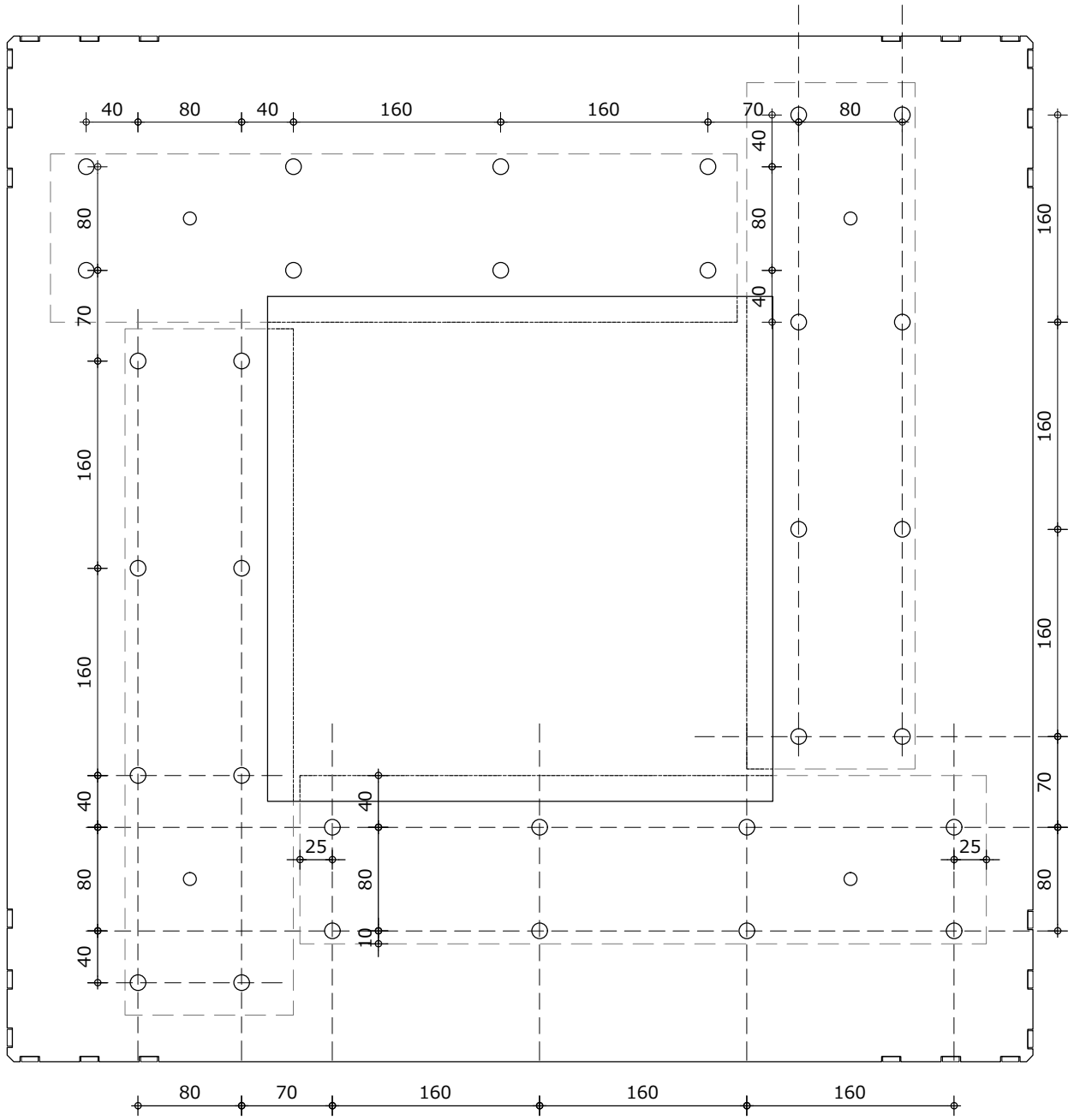

Actuators
1:5

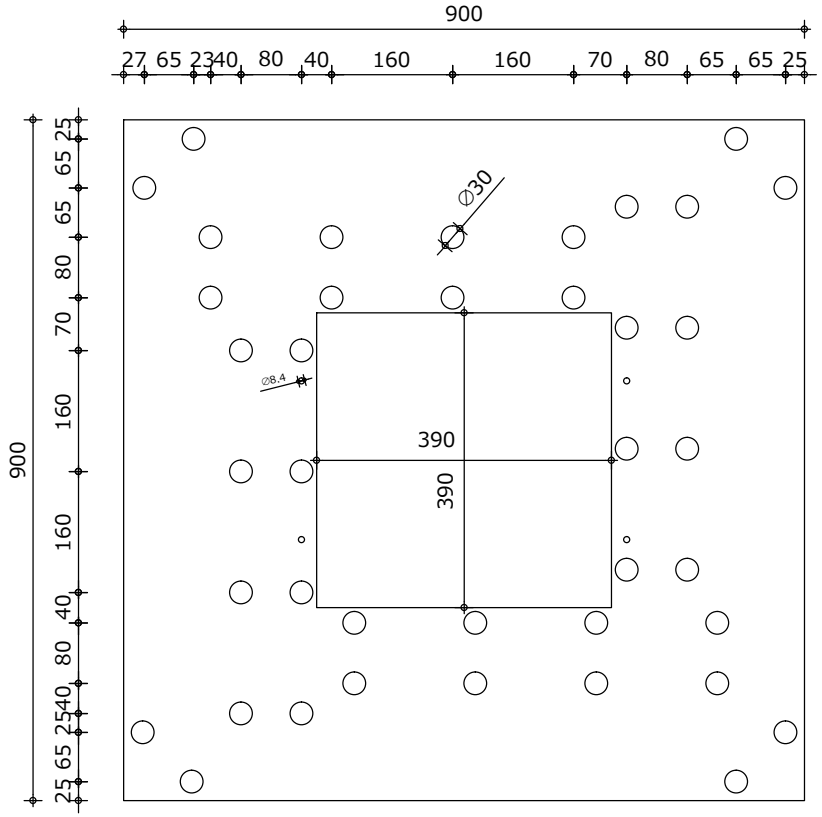

Steel plate, thickness: 4mm
1X

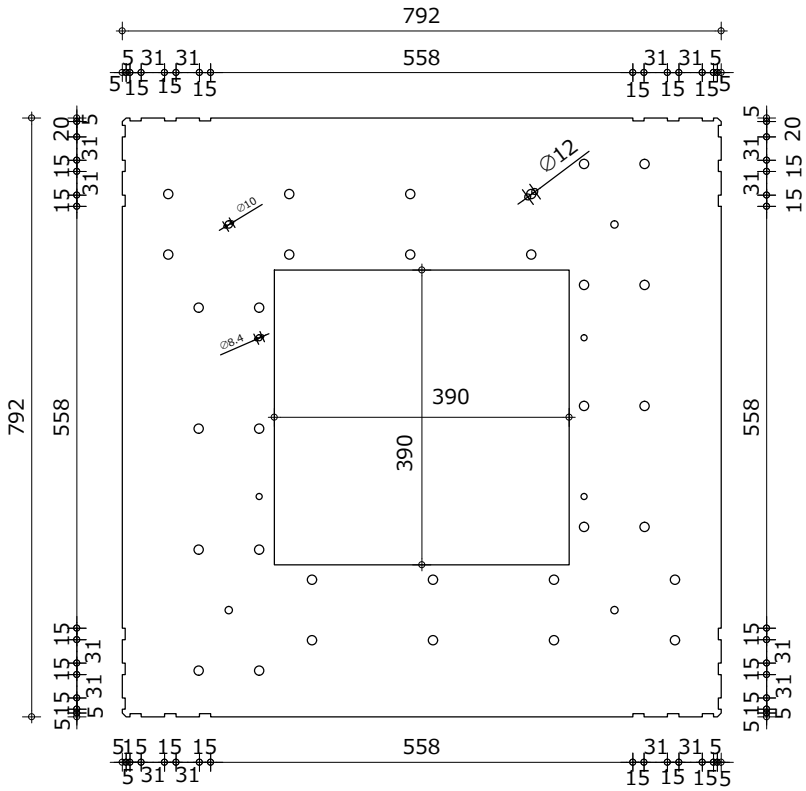

Steel plate, thickness: 4mm
4X

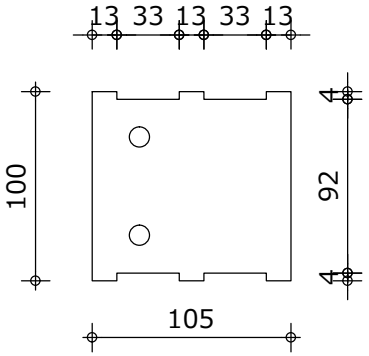

Steel plate, thickness: 4mm
16X

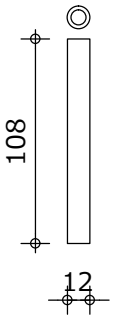

Steel pipe, ∅2x12mm
64X

Steel plates, thickness: 4mm

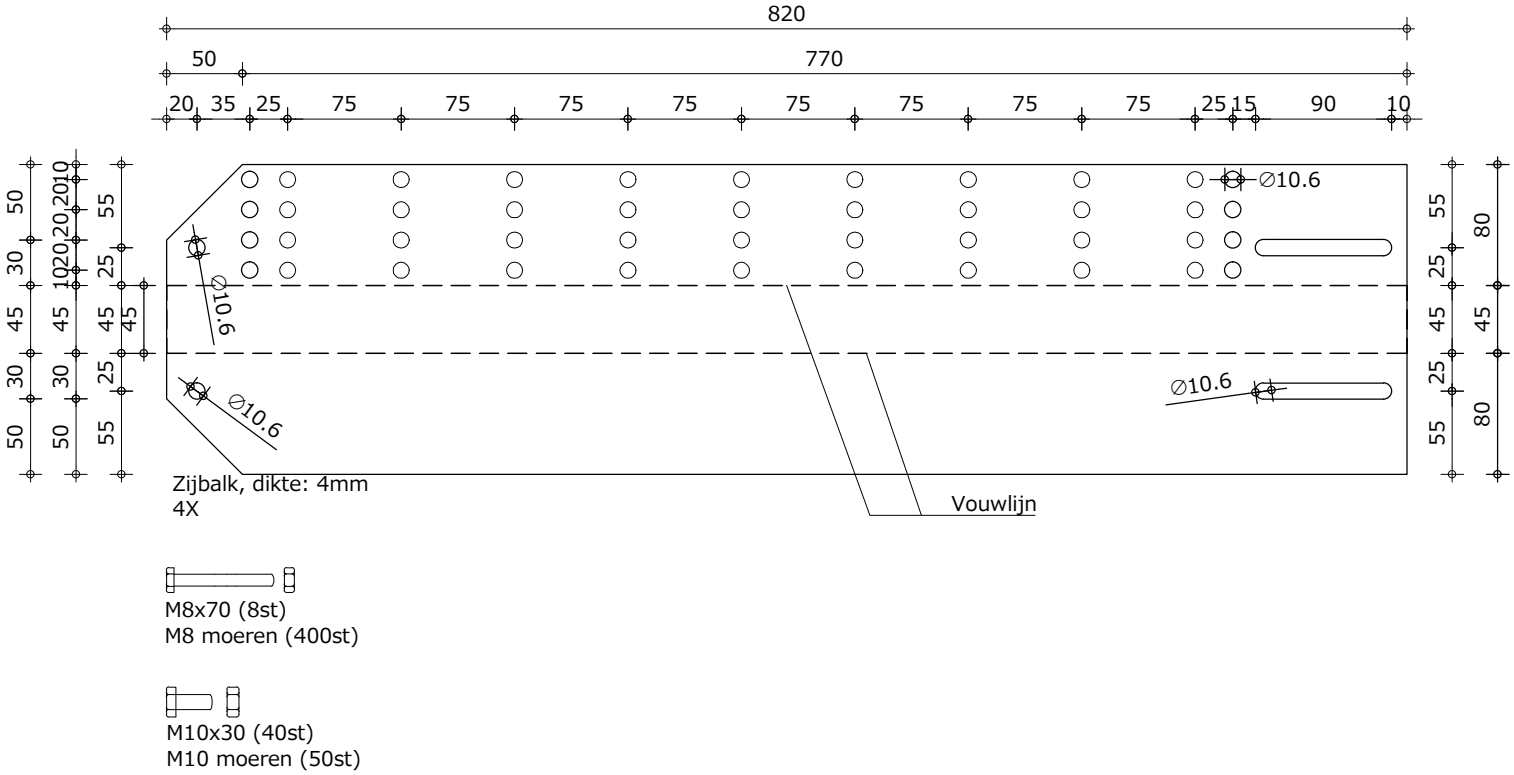

M8x70 (8st)
M8 moeren (400st)

M10x30 (40st)
M10 moeren (50st)

Side rod, thickness: 4mm

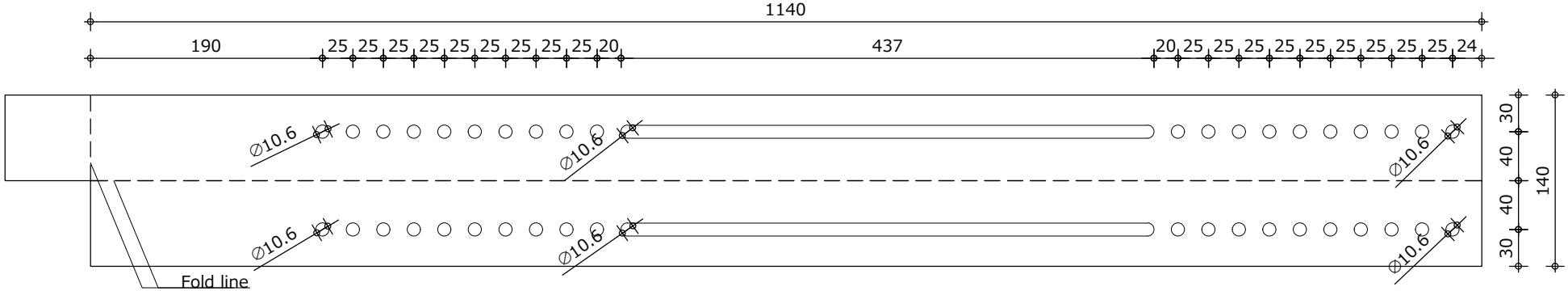

Corner colum, tickness: 4mm
4X

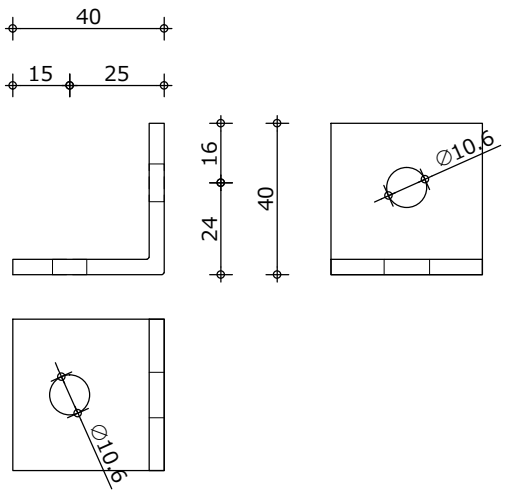

Angled steel, thickness:4mm
16X

Corner column and angled steel, thickness:4mm

Appendix E: Rhinoceros / Grasshopper

Design Analysis structure

Figure E.1: Selected panel

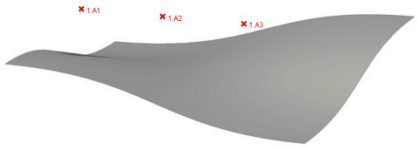

Figure E.2: Draw grid actuators A1 to A3

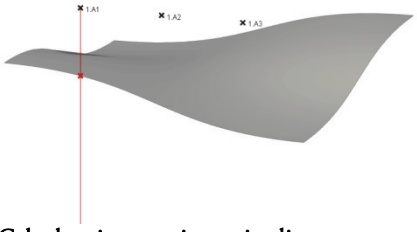

Figure E.3: Calculate intersection point linear actuator A1 with surface edge curve

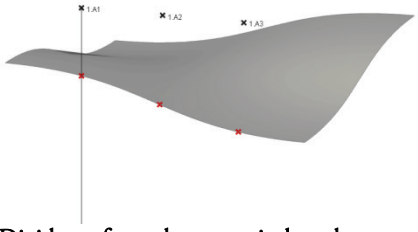

Figure E.4: Divide surface edge curve in length segments (similar lengths as actuator distance)

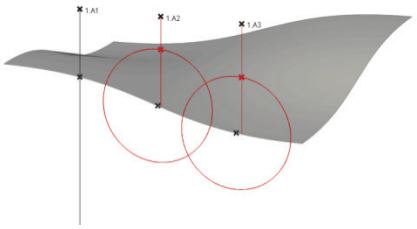

Figure E.5: Draw planar circles at segment points and calculate intersection points with vertical lines from Actuator A2 and A3

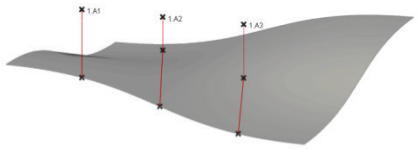

Figure E.6: Draw actuator heights from the grid and pendulum rods

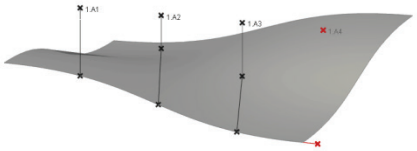

Figure E.7: Draw actuator A4 grid and extend surface edge curve with proper tangent to 160mm

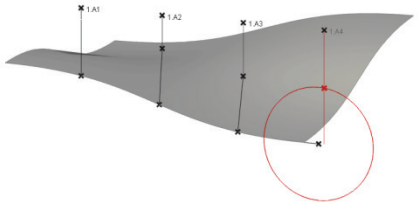

Figure E.8: Draw planar circle at segment point and calculate intersection point with vertical line from Actuator A4

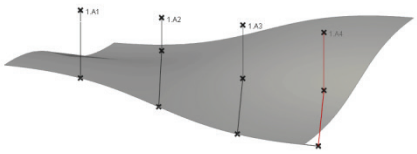

Figure E.9: Draw actuator height from grid and pendulum rod

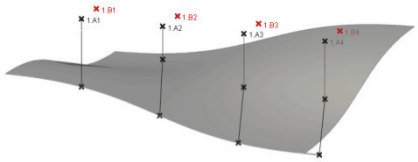

Figure E.10: Draw grid actuators B1 to B4

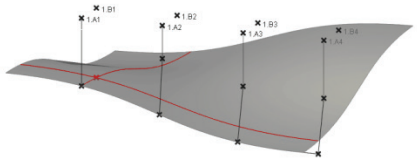

Figure E.11: Draw uv curves at 80mm distance from actuator A1

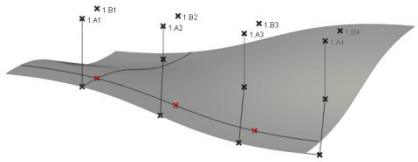

Figure E.12: Divide curve in length segments (similar lengths as actuator distance)

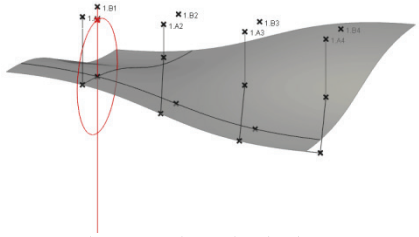

Figure E.13: Draw planar circle and calculate intersection point with vertical line from Actuator B1

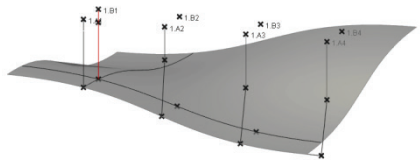

Figure E.14: Draw actuator height from grid and pendulum rod

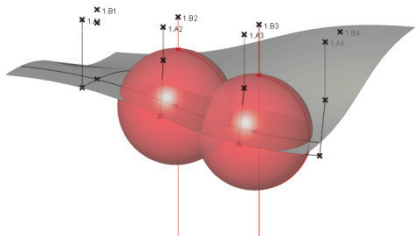

Figure E.15: Draw spheres from segment points and calculate intersection points with vertical lines from actuators B2 and B3

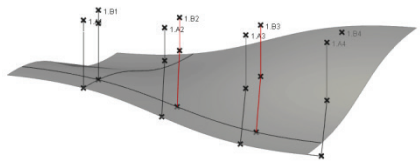

Figure E.16: Draw actuator heights from grid and pendulum rods

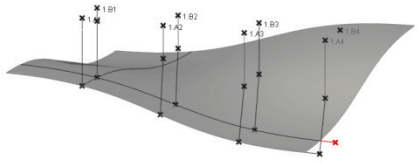

Figure E.17: Extend uv curve to 160mm

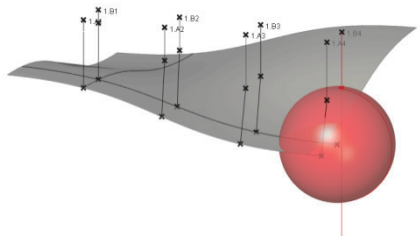

Figure E.18: Draw sphere from segment point and calculate intersection point with vertical line from actuator B4

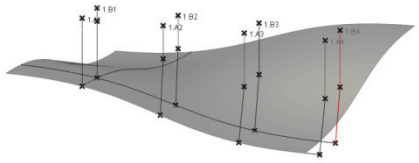

Figure E.19: Draw actuator height from grid and pendulum rod

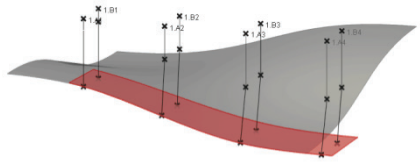

Figure E.20: Draw flexible edge geometry visualization

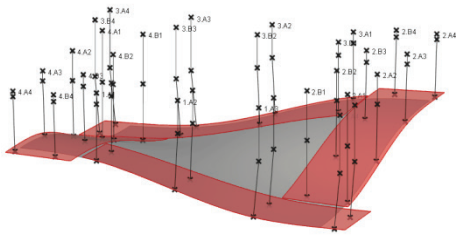

Figure E.21: Apply calculations for all four surface edges

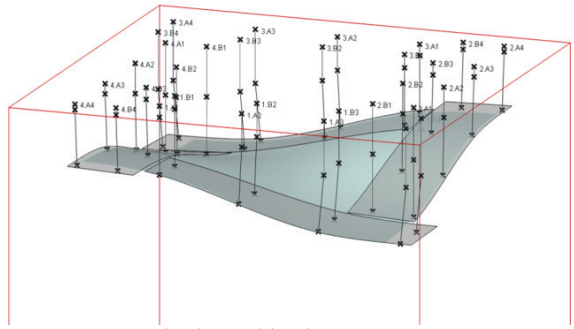

Figure E.22: Draw Fluid Mould column corners

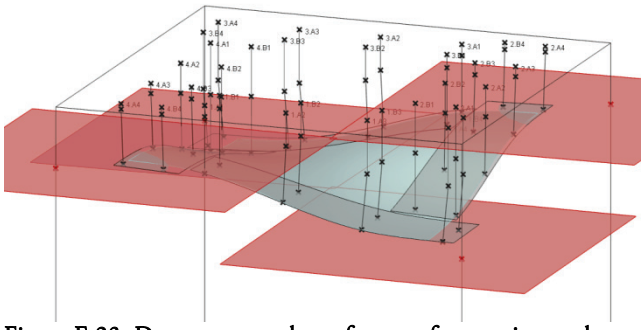

Figure E.23: Draw tangent planes from surface vertices and calculate intersection point with column corners

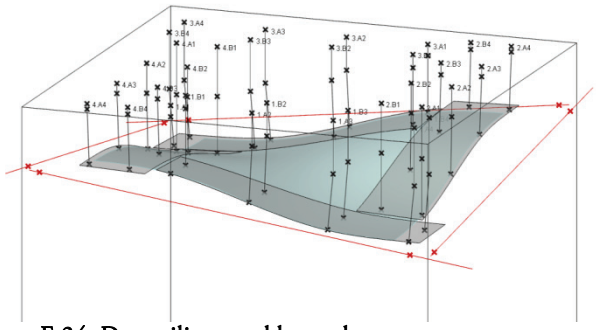

Figure E.24: Draw silicone rubber rods

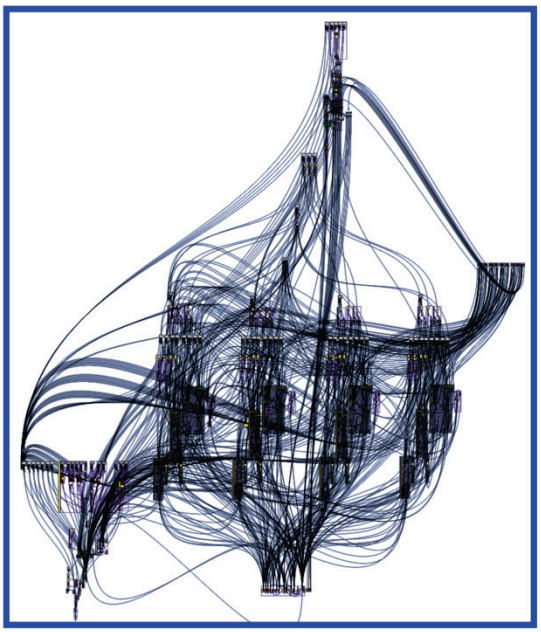

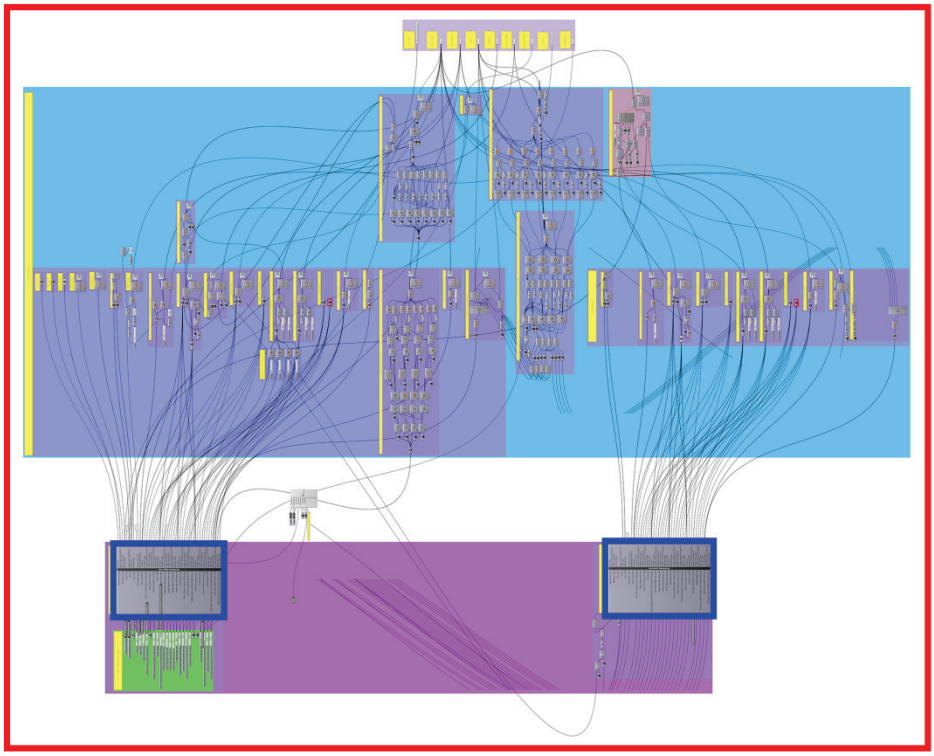

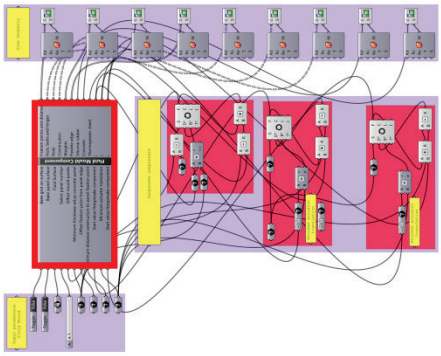

Figure E.25: Grasshopper clusters

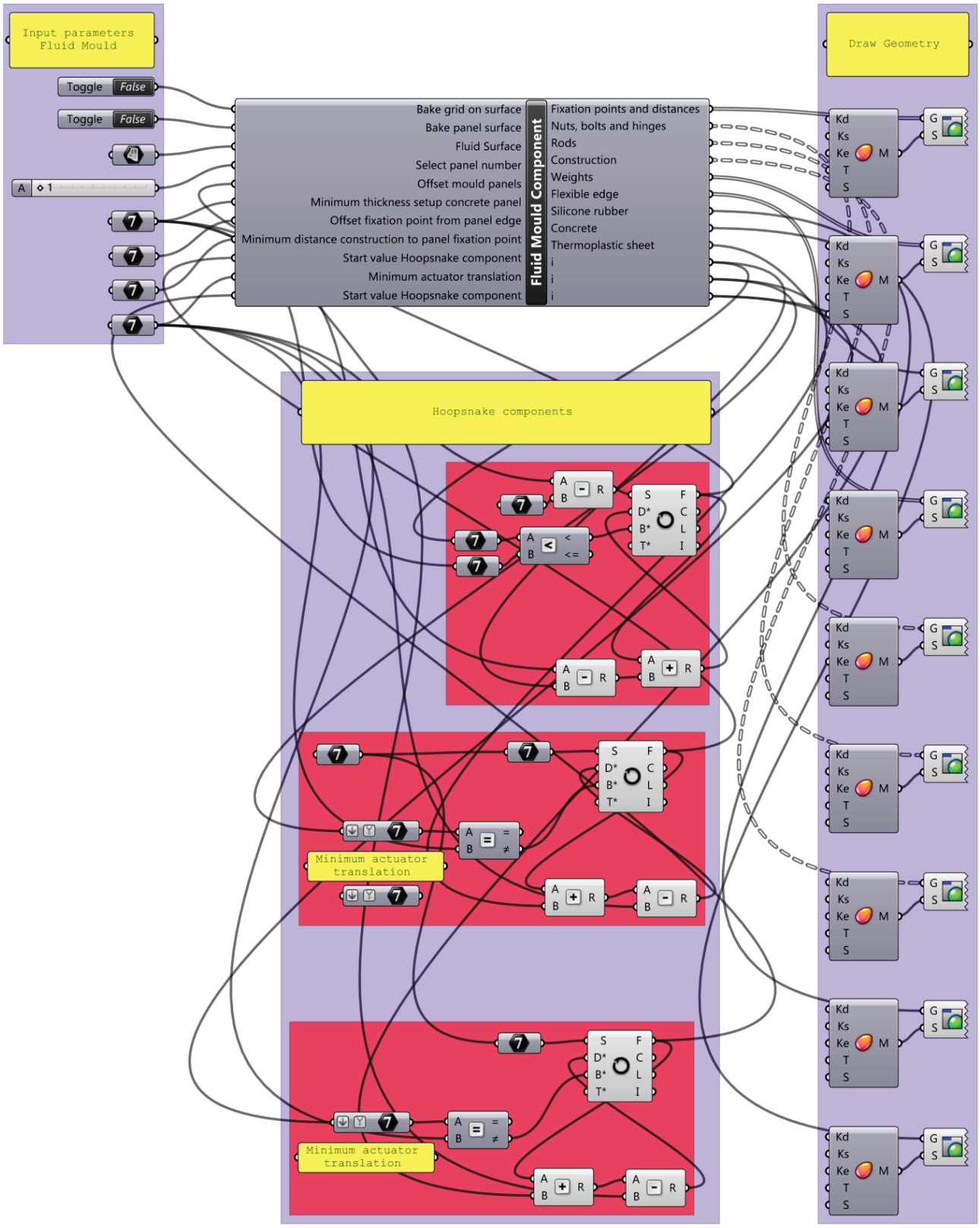

Figure E.26: Fluid Mould Grasshopper component

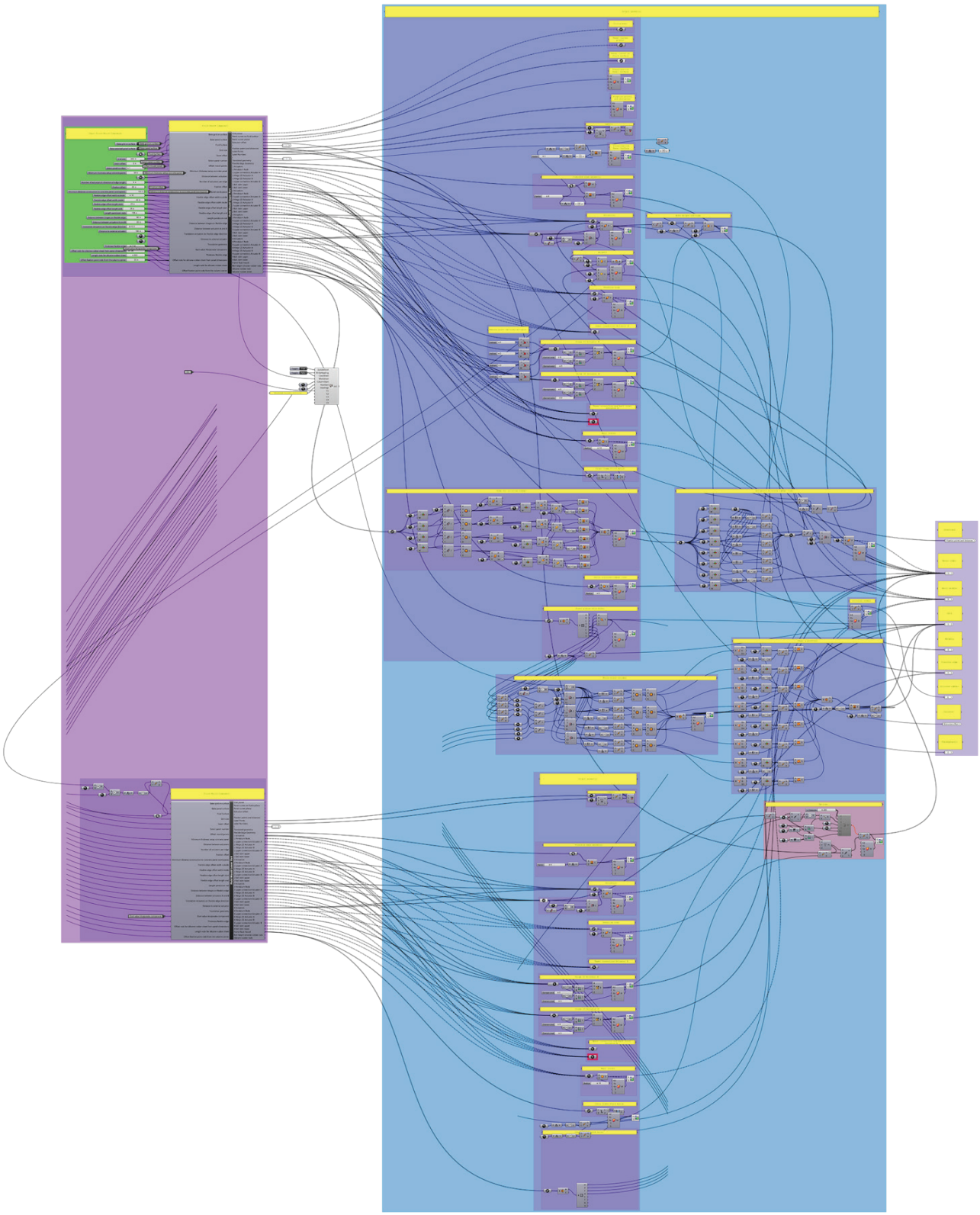

Figure E.27: Fluid Mould Grasshopper component Cluster 1

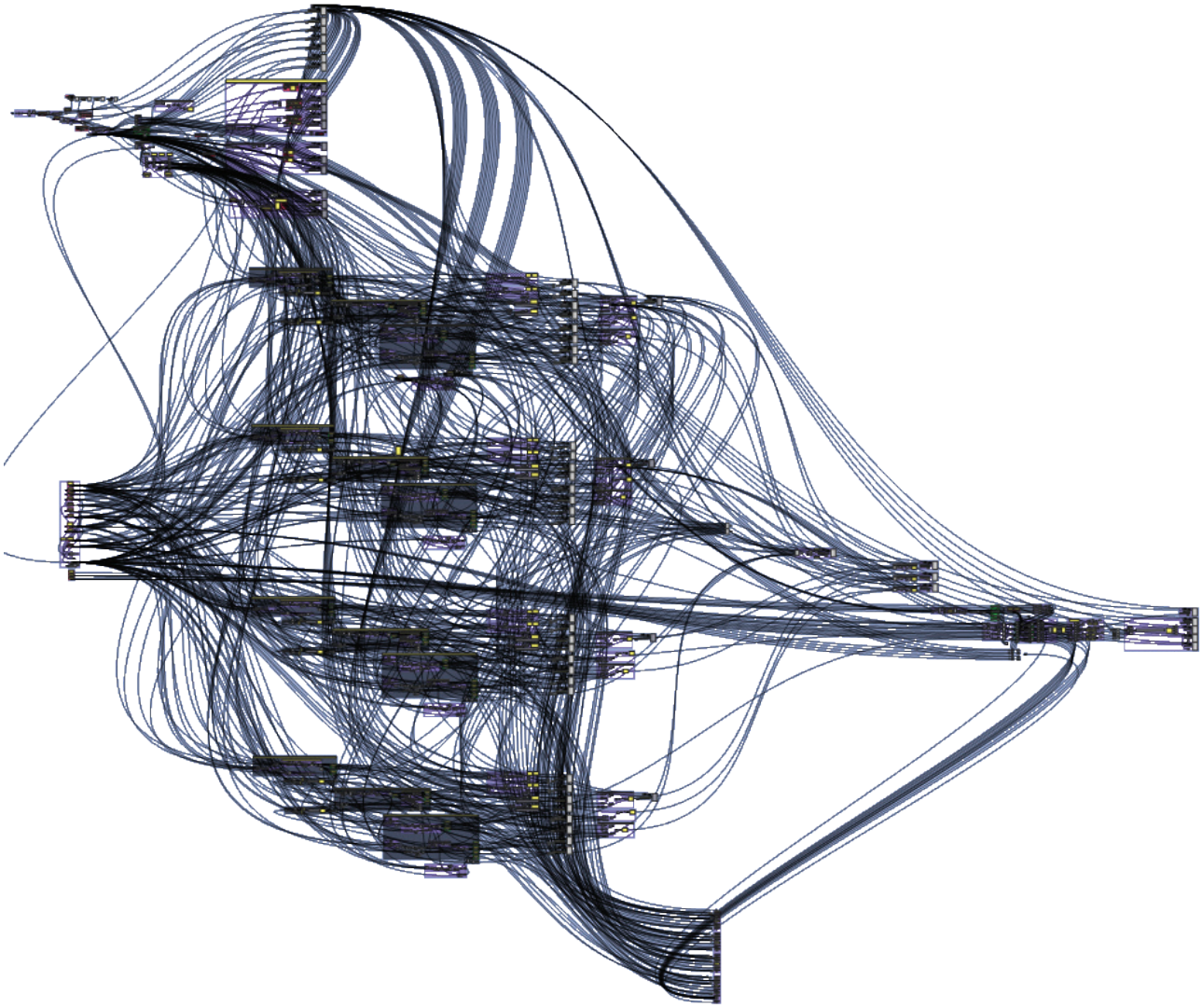

Figure E.28: Fluid Mould Grasshopper component Cluster 2

Excel sheets panel 1

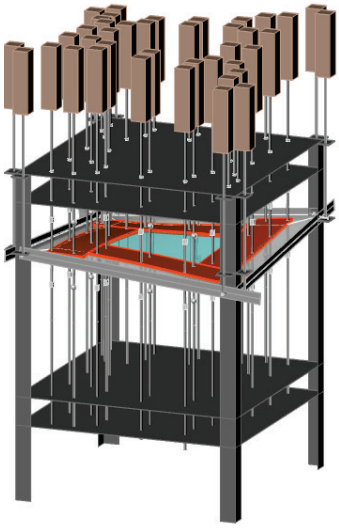

Figure E.29: Visualisation panel 1

Design info	
Number of actuators	64
Distance between actuators [mm]	160
Planar grid size [mm]	600
Panel size [mm]	590
Seam size [mm]	10
Number of panels	9
Panel number	1
Maximum radius of curvature [mm]	10096000,0
Minimum radius of curvature [mm]	10790,4
Maximum absolute principal curvature	5,82E-04
Minimum absolute principal curvature	6,22E-07
Minimum thickness set-up [mm]	50
Mould panel offset [mm]	50,0
Minimum thickness in panel [mm]	50
Volume [dm³]	17,4
Fixation point offset from the panels edge [mm]	50
Minimum distance between frame and panel/fixation point [mm]	20
Distance frame and fixation point 0 (inc min distance) [mm]	93,4
Distance frame and fixation point 1 (inc min distance) [mm]	46,4
Distance frame and fixation point 2 (inc min distance) [mm]	79,5
Distance frame and fixation point 3 (inc min distance) [mm]	46,4
Maximum actuator height setting [mm]	125,2
Maximum absolute angle ball joint actuator B [degrees]	1,4
Minimum height setting from zero point [mm]	66,0

Actuator number	Height	Corrected Height	Translation points Marc Mentat
1.A1	71,9	71,9	0, 0, -71.92
1.A2	87,1	87,0	-0.73, 0, -87.06
1.A3	106,4	106,3	-1.9, 0, -106.39
1.A4	125,2	125,1	-3.01, 0, -125.14
2.A1	115,8	115,7	0, 0, -115.78
2.A2	102,4	102,3	-0.01, -0.57, -102.37
2.A3	85,2	85,2	-0.01, -1.49, -85.24
2.A4	68,7	68,6	-0.01, -2.36, -68.63
3.A1	88,4	88,3	0, 0, -88.39
3.A2	105,2	105,1	0.88, 0, -105.18
3.A3	117,5	117,4	1.37, 0, -117.45
3.A4	121,1	121,1	1.43, 0, -121.09
4.A1	102,9	102,8	0, 0, -102.88
4.A2	83,9	83,9	0, 1.13, -83.93
4.A3	70,1	70,1	0, 1.75, -70.06
4.A4	65,9	65,9	0, 1.83, -65.92

Actuator number	Height	Corrected Height	Translation points Marc Mentat
1.B1	73,4	73,4	0, -0.01, -73.42
1.B2	87,6	87,5	-0.64, -0.01, -87.59
1.B3	105,7	105,7	-1.67, -0.01, -105.7
1.B4	123,3	123,2	-2.64, -0.01, -123.26
2.B1	108,3	108,3	0.35, 0, -108.29
2.B2	99,7	99,7	0.35, -0.23, -99.74
2.B3	88,8	88,8	0.35, -0.61, -88.79
2.B4	78,2	78,2	0.35, -0.96, -78.2
3.B1	90,9	90,8	0, 0.04, -90.87
3.B2	101,6	101,5	0.36, 0.04, -101.56
3.B3	109,4	109,3	0.55, 0.04, -109.35
3.B4	111,6	111,6	0.58, 0.04, -111.64
4.B1	102,4	102,3	0, 0, -102.39
4.B2	84,6	84,6	0, 0.99, -84.64
4.B3	71,7	71,7	0, 1.53, -71.66
4.B4	67,8	67,8	0, 1.6, -67.8

Actuator number silicone rubber rods	Height	Translation/rotation points Marc Mentat
1	-176,40	0, 0, -68.4, -0.08
2	-238,06	
3	-237,45	0, 0, -129.45, -0.1
4	-163,11	
5	-163,11	0, 0, -55.11, 0.1
6	-237,45	
7	-238,06	0, 0, -130.06, 0.08
8	-176,40	

Excel sheets panel 2

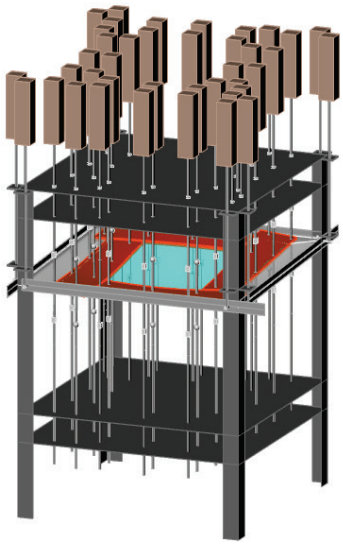

Figure E.30: Visualisation panel 2

Design info	
Number of actuators	64
Distance between actuators [mm]	160
Planar grid size [mm]	600
Panel size [mm]	590
Seam size [mm]	10
Number of panels	9
Panel number	2
Maximum radius of curvature [mm]	8339300,0
Minimum radius of curvature [mm]	10,0
Maximum absolute principal curvature	8,37E-04
Minimum absolute principal curvature	0,00E+00
Minimum thickness set-up [mm]	50
Mould panel offset [mm]	51,0
Minimum thickness in panel [mm]	50
Volume [dm^3]	17,8
Fixation point offset from the panels edge [mm]	50
Minimum distance between frame and panel/fixation point [mm]	20
Distance frame and fixation point 0 (inc min distance) [mm]	34,5
Distance frame and fixation point 1 (inc min distance) [mm]	34,5
Distance frame and fixation point 2 (inc min distance) [mm]	87,9
Distance frame and fixation point 3 (inc min distance) [mm]	87,9
Maximum actuator height setting [mm]	151,9
Maximum absolute angle ball joint actuator B [degrees]	2,3
Minimum height setting from zero point [mm]	66,0

Actuator number	Height	Corrected Height	Translation points Marc Mentat
1.A1	146,8	146,8	0, 0, -146.79
1.A2	151,9	151,9	-0.12, 0, -151.94
1.A3	144,6	144,6	-0.32, 0, -144.62
1.A4	128,8	128,8	-1.11, 0, -128.83
2.A1	127,7	127,6	-0.01, 0, -127.67
2.A2	113,7	113,6	0, -0.62, -113.69
2.A3	95,8	95,8	0, -1.62, -95.83
2.A4	78,5	78,5	0, -2.56, -78.51
3.A1	70,3	70,2	0, 0, -70.28
3.A2	65,7	65,6	0.1, 0, -65.72
3.A3	72,2	72,1	0.25, 0, -72.2
3.A4	86,2	86,1	0.87, 0, -86.19
4.A1	99,1	99,0	0, 0, -99.1
4.A2	116,6	116,6	0, 0.96, -116.6
4.A3	129,4	129,4	0, 1.49, -129.4
4.A4	133,2	133,2	0, 1.56, -133.21

Actuator number	Height	Corrected Height	Translation points Marc Mentat
1.B1	144,2	144,2	0, -0.04, -144.18
1.B2	149,0	149,0	-0.11, -0.04, -149
1.B3	142,2	142,1	-0.28, -0.04, -142.15
1.B4	127,4	127,3	-0.97, -0.04, -127.36
2.B1	134,1	134,1	0.25, 0, -134.11
2.B2	116,0	115,9	0.25, -1.05, -115.99
2.B3	92,9	92,8	0.25, -2.73, -92.88
2.B4	70,5	70,4	0.25, -4.31, -70.44
3.B1	83,2	83,1	0, 1.05, -83.22
3.B2	80,3	80,2	0.04, 1.05, -80.3
3.B3	84,5	84,3	0.1, 1.05, -84.45
3.B4	93,4	93,3	0.36, 1.05, -93.43
4.B1	97,0	96,9	-0.03, 0, -96.96
4.B2	119,7	119,6	-0.03, 1.62, -119.64
4.B3	136,3	136,3	-0.03, 2.51, -136.31
4.B4	141,4	141,3	-0.03, 2.63, -141.33

Actuator number silicone rubber rods	Height	Translation/rotation points Marc Mentat
1	-229,82	0, 0, -121.82, 0
2	-229,82	
3	-228,06	0, 0, -120.06, -0.05
4	-191,51	
5	-189,76	0, 0, -81.76, 0
6	-189,76	
7	-191,51	0, 0, -83.51, -0.05
8	-228,06	

Excel sheet panel 3

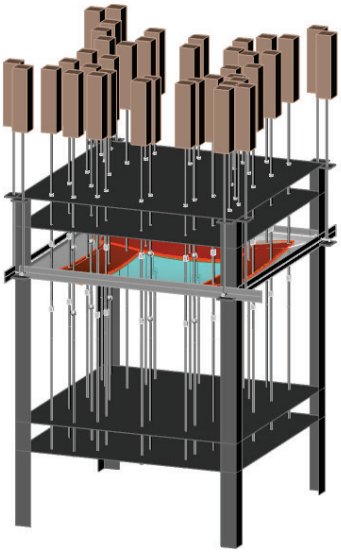

Figure E.31: Visualisation panel 3

Design info	
Number of actuators	64
Distance between actuators [mm]	160
Planar grid size [mm]	600
Panel size [mm]	590
Seam size [mm]	10
Number of panels	9
Panel number	5
Maximum radius of curvature [mm]	585592,9
Minimum radius of curvature [mm]	7203,7
Maximum absolute principal curvature	8,72E-04
Minimum absolute principal curvature	1,10E-05
Minimum thickness set-up [mm]	50
Mould panel offset [mm]	51,0
Minimum thickness in panel [mm]	50
Volume [dm³]	17,8
Fixation point offset from the panels edge [mm]	50
Minimum distance between frame and panel/fixation point [mm]	20
Distance frame and fixation point 0 (inc min distance) [mm]	56,5
Distance frame and fixation point 1 (inc min distance) [mm]	56,5
Distance frame and fixation point 2 (inc min distance) [mm]	56,5
Distance frame and fixation point 3 (inc min distance) [mm]	56,5
Maximum actuator height setting [mm]	99,5
Maximum absolute angle ball joint actuator B [degrees]	0,9
Minimum height setting from zero point [mm]	66,0

Actuator number	Height	Corrected Height	Translation points Marc Mentat
1.A1	82,2	82,1	0, 0, -82.19
1.A2	86,9	86,8	-0.1, 0, -86.94
1.A3	80,2	80,1	-0.27, 0, -80.19
1.A4	65,6	65,5	-0.95, 0, -65.6
2.A1	82,2	82,1	0, 0, -82.19
2.A2	86,9	86,8	0, -0.1, -86.94
2.A3	80,2	80,1	0, -0.27, -80.19
2.A4	65,6	65,5	0, -0.95, -65.6
3.A1	82,2	82,1	0, -0.01, -82.19
3.A2	86,9	86,8	0.1, 0, -86.94
3.A3	80,2	80,1	0.27, 0, -80.19
3.A4	65,6	65,5	0.95, 0, -65.6
4.A1	82,2	82,1	0, 0, -82.19
4.A2	86,9	86,8	0, 0.1, -86.94
4.A3	80,2	80,1	0, 0.27, -80.19
4.A4	65,6	65,5	0, 0.95, -65.6

Actuator number	Height	Corrected Height	Translation points Marc Mentat
1.B1	93,4	93,3	0, -0.78, -93.35
1.B2	99,5	99,4	-0.17, -0.78, -99.53
1.B3	90,8	90,7	-0.46, -0.78, -90.77
1.B4	71,9	71,8	-1.59, -0.78, -71.9
2.B1	93,4	93,3	0.78, 0, -93.35
2.B2	99,5	99,4	0.78, -0.17, -99.53
2.B3	90,8	90,7	0.78, -0.46, -90.77
2.B4	71,9	71,8	0.78, -1.59, -71.9
3.B1	93,4	93,3	0, 0.78, -93.36
3.B2	99,5	99,4	0.17, 0.78, -99.53
3.B3	90,8	90,7	0.46, 0.78, -90.77
3.B4	71,9	71,8	1.59, 0.78, -71.91
4.B1	93,4	93,3	-0.78, 0, -93.35
4.B2	99,5	99,4	-0.78, 0.17, -99.53
4.B3	90,8	90,7	-0.78, 0.46, -90.77
4.B4	71,9	71,8	-0.78, 1.59, -71.9

Actuator number silicone rubber rods	Height	Translation/rotation points Marc Mentat
1	-156,22	0, 0, -48.22, 0
2	-156,22	
3	-156,22	0, 0, -48.22, 0
4	-156,22	
5	-156,22	0, 0, -48.22, 0
6	-156,22	
7	-156,22	0, 0, -48.22, 0
8	-156,22	

Excel sheet Panel A

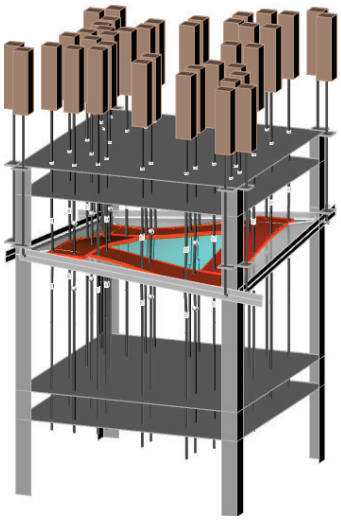

Figure E.32: Visualisation panel A

Design info	
Number of actuators	64
Distance between actuators [mm]	160
Planar grid size [mm]	600
Panel size [mm]	590
Seam size [mm]	10
Number of panels	1
Panel number	1
Maximum radius of curvature [mm]	8290200,0
Minimum radius of curvature [mm]	4544,1
Maximum absolute principal curvature	1,38E-03
Minimum absolute principal curvature	7,58E-07
Minimum thickness set-up [mm]	50
Mould panel offset [mm]	51,0
Minimum thickness in panel [mm]	50
Volume [dm³]	17,8
Fixation point offset from the panels edge [mm]	50
Minimum distance between frame and panel/fixation point [mm]	20
Distance frame and fixation point 0 (inc min distance) [mm]	87,9
Distance frame and fixation point 1 (inc min distance) [mm]	22,1
Distance frame and fixation point 2 (inc min distance) [mm]	87,9
Distance frame and fixation point 3 (inc min distance) [mm]	22,1
Maximum actuator height setting [mm]	136,3
Maximum absolute angle ball joint actuator B [degrees]	2,4
Minimum height setting from zero point [mm]	66,0

Actuator number	Height	Corrected Height	Translation points Marc Mentat
1.A1	74,1	74,0	0, 0, -74.08
1.A2	103,9	103,7	-2.9, 0, -103.83
1.A3	130,7	130,6	-5.28, 0, -130.53
1.A4	136,3	136,2	-5.44, 0, -136.12
2.A1	128,0	127,9	0, 0, -127.96
2.A2	98,2	98,0	0, -2.9, -98.21
2.A3	71,6	71,6	0, -5.28, -71.51
2.A4	66,1	66,0	0, -5.44, -65.92
3.A1	74,1	74,0	0, 0, -74.08
3.A2	103,9	103,7	2.9, 0, -103.83
3.A3	130,7	130,6	5.28, 0, -130.53
3.A4	136,3	136,2	5.44, 0, -136.12
4.A1	128,0	127,9	0, 0, -127.96
4.A2	98,2	98,0	0, 2.9, -98.21
4.A3	71,6	71,6	0, 5.28, -71.51
4.A4	66,1	66,0	0, 5.44, -65.92

Actuator number	Height	Corrected Height	Translation points Marc Mentat
1.B1	76,6	76,6	0, -0.04, -76.64
1.B2	103,7	103,5	-2.37, -0.04, -103.63
1.B3	128,0	128,0	-4.33, -0.04, -127.92
1.B4	134,4	134,4	-4.5, -0.04, -134.31
2.B1	125,4	125,3	0.04, 0, -125.39
2.B2	98,4	98,3	0.04, -2.37, -98.4
2.B3	74,2	74,2	0.04, -4.33, -74.12
2.B4	67,8	67,8	0.04, -4.5, -67.73
3.B1	76,6	76,6	0, 0.04, -76.64
3.B2	103,7	103,5	2.37, 0.04, -103.63
3.B3	128,0	128,0	4.33, 0.04, -127.92
3.B4	134,4	134,4	4.5, 0.04, -134.31
4.B1	125,4	125,3	-0.04, 0, -125.39
4.B2	98,4	98,3	-0.04, 2.37, -98.4
4.B3	74,2	74,2	-0.04, 4.33, -74.12
4.B4	67,8	67,8	-0.04, 4.5, -67.73

Actuator number silicone rubber rods	Height	Translation/rotation points Marc Mentat
1	-176,43	0, 0, -68.43, -0.09
2	-241,60	
3	-241,60	0, 0, -133.6, -0.09
4	-176,43	
5	-176,43	0, 0, -68.43, 0.09
6	-241,60	
7	-241,60	0, 0, -133.6, 0.09
8	-176,43	

Excel sheet panel B

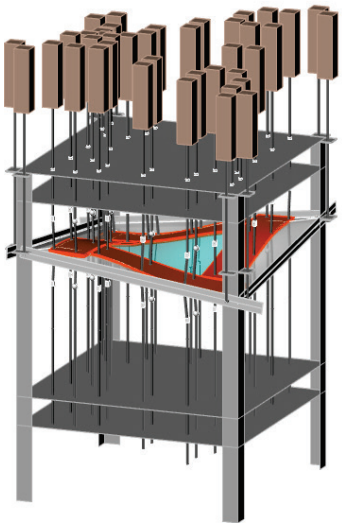

Figure E.33: Visualisation panel B

Design info	
Number of actuators	64
Distance between actuators [mm]	160
Planar grid size [mm]	600
Panel size [mm]	590
Seam size [mm]	10
Number of panels	1
Panel number	1
Maximum radius of curvature [mm]	5968400,0
Minimum radius of curvature [mm]	3180,9
Maximum absolute principal curvature	1,98E-03
Minimum absolute principal curvature	1,05E-06
Minimum thickness set-up [mm]	50
Mould panel offset [mm]	53,0
Minimum thickness in panel [mm]	50
Volume [dm^3]	18,4
Fixation point offset from the panels edge [mm]	50
Minimum distance between frame and panel/fixation point [mm]	20
Distance frame and fixation point 0 (inc min distance) [mm]	117,0
Distance frame and fixation point 1 (inc min distance) [mm]	23,0
Distance frame and fixation point 2 (inc min distance) [mm]	117,0
Distance frame and fixation point 3 (inc min distance) [mm]	23,0
Maximum actuator height setting [mm]	166,7
Maximum absolute angle ball joint actuator B [degrees]	4,8
Minimum height setting from zero point [mm]	66,0

Actuator number	Height	Corrected Height	Translation points Marc Mentat
1.A1	77,5	77,4	0, 0, -77.54
1.A2	119,3	118,8	-5.7, 0, -119.11
1.A3	158,0	157,9	-10.63, 0, -157.46
1.A4	166,7	166,6	-11, 0, -166.14
2.A1	154,5	154,4	0, 0, -154.51
2.A2	113,1	112,7	0, -5.7, -112.94
2.A3	75,1	75,0	0, -10.63, -74.59
2.A4	66,5	66,4	0, -11, -65.91
3.A1	77,5	77,4	0, 0, -77.54
3.A2	119,3	118,8	5.7, 0, -119.11
3.A3	158,0	157,9	10.63, 0, -157.46
3.A4	166,7	166,6	11, 0, -166.14
4.A1	154,5	154,4	0, 0, -154.51
4.A2	113,1	112,7	0, 5.7, -112.94
4.A3	75,1	75,0	0, 10.63, -74.59
4.A4	66,5	66,4	0, 11, -65.91

Actuator number	Height	Corrected Height	Translation points Marc Mentat
1.B1	81,2	81,1	0, -0.08, -81.2
1.B2	119,2	118,8	-4.7, -0.08, -119.08
1.B3	154,2	154,2	-8.73, -0.08, -153.89
1.B4	163,9	163,8	-9.11, -0.08, -163.49
2.B1	150,8	150,7	0.08, 0, -150.85
2.B2	113,1	112,7	0.08, -4.7, -112.97
2.B3	78,5	78,4	0.08, -8.73, -78.16
2.B4	68,9	68,9	0.08, -9.11, -68.56
3.B1	81,2	81,1	0, 0.08, -81.2
3.B2	119,2	118,8	4.7, 0.08, -119.08
3.B3	154,2	154,2	8.73, 0.08, -153.89
3.B4	163,9	163,8	9.11, 0.08, -163.49
4.B1	150,8	150,7	-0.08, 0, -150.85
4.B2	113,1	112,7	-0.08, 4.7, -112.97
4.B3	78,5	78,4	-0.08, 8.73, -78.16
4.B4	68,9	68,9	-0.08, 9.11, -68.56

Actuator number silicone rubber rods	Height	Translation/rotation points Marc Mentat
1	-177,48	0, 0, -69.48, -0.13
2	-270,57	
3	-270,57	0, 0, -162.57, -0.13
4	-177,48	
5	-177,48	0, 0, -69.48, 0.13
6	-270,57	
7	-270,57	0, 0, -162.57, 0.13
8	-177,48	

Appendix F: DVD